

Higher order QCD corrections and resummation effects to the Drell-Yan process in the Standard Model and beyond

By
PULAK BANERJEE
PHYS10201304002

The Institute of Mathematical Sciences, Chennai

A thesis submitted to the
Board of Studies in Physical Sciences
In partial fulfilment of requirements
For the Degree of
DOCTOR OF PHILOSOPHY
of
HOMI BHABHA NATIONAL INSTITUTE



May, 2018

Homi Bhabha National Institute

Recommendations of the Viva Voce Board

As members of the Viva Voce Board, we certify that we have read the dissertation prepared by Mr. Pulak Banerjee entitled “Higher order QCD corrections and resummation effects to the Drell-Yan process in the Standard Model and beyond” and recommend that it maybe accepted as fulfilling the dissertation requirement for the Degree of Doctor of Philosophy.

_____ Date:

Chair - Prof. Rahul Sinha

_____ Date:

Guide/Convener - Prof. V. Ravindran

_____ Date:

Member 1 - Prof. D. Indumathi

_____ Date:

Member 2 - Prof. Nita Sinha

_____ Date:

Member 3 - Prof. Syed R. Hassan

_____ Date:

External Examiner - Prof. P. Poulose

Final approval and acceptance of this dissertation is contingent upon the candidate's submission of the final copies of the dissertation to HBNI.

I hereby certify that I have read this dissertation prepared under my direction and recommend that it may be accepted as fulfilling the dissertation requirement.

Date:

Place: IMSc, Chennai

Guide - Prof. V. Ravindran

STATEMENT BY AUTHOR

This dissertation has been submitted in partial fulfilment of requirements for an advanced degree at Homi Bhabha National Institute (HBNI) and is deposited in the Library to be made available to borrowers under rules of the HBNI.

Brief quotations from this dissertation are allowable without special permission, provided that accurate acknowledgement of source is made. Requests for permission for extended quotation from or reproduction of this manuscript in whole or in part may be granted by the Competent Authority of HBNI when in his or her judgment the proposed use of the material is in the interests of scholarship. In all other instances, however, permission must be obtained from the author.

Pulak Banerjee

DECLARATION

I, hereby declare that the investigation presented in the thesis has been carried out by me.
The work is original and has not been submitted earlier as a whole or in part for a degree
/ diploma at this or any other Institution / University.

Pulak Banerjee

List of Publications arising from the thesis

Journal

1. **NNLO QCD corrections to the Drell-Yan Cross Section in Models of TeV-Scale Gravity**

Taushif Ahmed, Pulak Banerjee, Prasanna K. Dhani, M.C. Kumar, Prakash Mathews, Narayan Rana, V. Ravindran

Eur.Phys.J. C77 (2017) no.1, 22

2. **Three loop form factors of a massive spin-2 particle with nonuniversal coupling**

Taushif Ahmed, Pulak Banerjee, Prasanna K. Dhani, Prakash Mathews, Narayan Rana, V. Ravindran

Phys.Rev. D95 (2017) no.3, 034035

3. **NNLO QCD corrections to production of a spin-2 particle with nonuniversal couplings in the Drell-Yan process**

Pulak Banerjee, Prasanna K. Dhani, M.C.Kumar, Prakash Mathews, V. Ravindran

Phys.Rev. D97 (2018) no.9, 094028

4. **Threshold resummation of the rapidity distribution for Drell-Yan production at NNLO+NNLL**

Pulak Banerjee, Goutam Das, Prasanna K. Dhani, V. Ravindran

Phys.Rev. D98 (2018) 054018

List of other Publications, Not included in the thesis

Journal

1. Konishi form factor at three loops in $\mathcal{N} = 4$ supersymmetric Yang-Mills theory

Taushif Ahmed, Pulak Banerjee, Prasanna K. Dhani, Narayan Rana, V. Ravindran,
Satyajit Seth

Phys.Rev. D95 (2017) no.8, 085019

2. Finite remainders of the Konishi at two loops in $\mathcal{N} = 4$ SYM

Pulak Banerjee, Prasanna K. Dhani, Maguni Mahakhud, V. Ravindran, Satyajit Seth

JHEP 1705 (2017) 085

3. Two loop QCD corrections for the process pseudo-scalar Higgs \rightarrow 3 partons

Pulak Banerjee, Prasanna K. Dhani, V. Ravindran

JHEP 1710 (2017) 067

4. Threshold resummation of the rapidity distribution for Higgs production at NNLO+NNLL

Pulak Banerjee, Goutam Das, Prasanna K. Dhani, V. Ravindran

Phys. Rev. D 97, 054024

Preprint

1. The gluon jet function at three loops in QCD

Pulak Banerjee, Prasanna K. Dhani, V. Ravindran

arXiv:1805.02637

Seminars presented

1. “Threshold resummation of the rapidity distribution in two dimensional Mellin space”

presented at the Institute for Theoretical Physics, Bern, Switzerland, 27th October, 2017

based on ‘Threshold resummation of the rapidity distribution for Higgs production at NNLO+NNLL”

Pulak Banerjee, Goutam Das, Prasanna K. Dhani and V. Ravindran

Phys. Rev. D **97** (2018) 054024

2. “Higher order corrections in QCD”

presented at the Department of Physical Sciences, IISER Kolkata, 27th January, 2018

Pulak Banerjee

To my family and friends

ACKNOWLEDGEMENTS

I would like to express my deepest gratitude to my supervisor, Prof. V. Ravindran for constantly motivating me to complete the journey of my Ph.D. life. His thorough knowledge and understanding of physics has helped me to gain a better perspective of the subject. Working with him was a rewarding experience, both at professional as well as personal level, that I will always cherish.

I would also like to thank Prof. Prakash Mathews for his guidance during various projects that I worked with him over these years. It has been an enriching experience to work with him.

The journey of my Ph.D. life would have been difficult without the support from my friend, Prasanna Kumar Dhani. It has been a lovely journey together, both professionally and personally; I extend my gratitude for the rich experience that I gained over all these years. I would also sincerely thank Goutam Das for being such a wonderful person to work as well as discuss about physics and other subjects during my Ph.D. life. Thanks to Taushif Ahmed and Narayan Rana for their guidance and support. I had spent some good moments with them in IMSc. I also thank M. C. Kumar, Maguni Mahakahud and Satyajit Seth for successful collaborations and useful discussions about physics. I express my gratitude to Thomas Gehrmann and Sophia Borowka for our recent collaboration. It was a really nice time to spend with my new friends, Amlan Chakraborty, Ajjath A H and Pooja Mukherjee; I enjoyed the fruitful interactions and useful discussions. Thanks to all of them for the successful collaborations over the past few months. I enjoyed the musical performances that I had with Pooja and Ajjath!

I would also like to thank my teachers Prof. Debashis Ghoshal, Prof. Rupamanjari Ghosh, Prof. Ramakrishna Ramaswamy, Anjan sir, Rajarshi sir, Sourav sir for helping me reach where I am now. I take this opportunity to convey my heartfelt thanks to all of them.

Starting from my BSc. till the end of Ph.D. I got the opportunity to have many friends.

I have spent some good years of my life with Rajarshi, Madhurima Nath, Soumen, Subhayan, Rituporno, Kazi, Avik, Robi, Rajat, Deeproda. I was fortunate to have some really good company at IMSc from Sagnik, Sanjay, Dipanjan, Arindam, Arnab, Anirban and Abinash. Thanks to my friends with whom I regularly go for the evening walk! I enjoyed a lot the musical collaboration I had with Aritra during all these years at IMSc. I also want to thank all my other friends and colleagues at IMSc: Ankit, Arghya, Tanmay, Ria Ghosh, Ria Sain, Shibasis, Rusa, Shilpa, Jilmy, Atanu, Dheerej, Madhusudhan, Rathul, Anvy, Anand, Ankita, Prafulla.

I would also like to thank several members of the non-academic staff at IMSc for their help throughout all these years.

Finally I would like to express my heartfelt gratitude and love to my parents and my sister, whose unconditional love and support has helped me to move past the difficulties during all these years. A special thanks to my brother-in-law Souvik for providing support and encouragement. Last but not the least, lots of love for my nephew Sounivo.

Contents

Synopsis

1	Introduction	1
1.1	The Standard Model	1
1.1.1	Spontaneous symmetry breaking	2
1.1.2	The Higgs Mechanism	5
2	Quantum Chromodynamics	9
2.1	Quarks and gluons	9
2.2	Basics of QCD	11
2.3	Asymptotic freedom	13
3	The parton model and its application to the Drell-Yan process	17
3.1	The Drell-Yan process	19
4	Beyond the Standard Model	25
4.1	Field theories with extra dimension	26

4.1.1	Kaluza Klein reduction	26
4.1.2	The ADD model	28
4.2	Theoretical Framework	29
4.2.1	The effective action	29
4.2.2	Invariant Lepton Pair Mass Distribution $d\sigma/dQ^2$	30
4.3	Outline of the thesis	42
5	Second order QCD corrections in models of TeV scale gravity: Universal coupling	43
5.1	Introduction	43
5.2	Computation	46
5.3	Phenomenology	52
5.4	Conclusion	62
6	Form factors with nonuniversal coupling	63
6.1	Introduction	63
6.2	Theoretical Framework	66
6.2.1	The Effective Action	66
6.2.2	Ultraviolet renormalization	67
6.3	Form factors and its infrared structure	69
6.4	Computation and results	72
6.5	Leading Transcendentality principle	76

6.6	Conclusion	77
7	Second order QCD corrections in models of gravity with nonuniversal coupling	79
7.1	Introduction	79
7.2	Phenomenology	82
7.3	Conclusion	92
8	Soft gluon resummation in two dimensional Mellin space	94
8.1	Introduction	94
8.2	Theoretical framework	95
8.2.1	The Soft-virtual cross section	95
8.2.2	Solution of the form factor	100
8.2.3	Solution of the soft distribution function	104
8.3	The resummation formula in double Mellin space	109
9	Threshold resummation of the rapidity distribution in the DY process	113
9.1	Introduction	113
9.2	Theoretical framework	116
9.3	Phenomenology	118
9.4	Conclusion	130
10	Conclusion	132

11 Appendix	134
11.1 Feynman rules for spin-2 particle	134
11.2 Computation of the integrals in double Mellin space	137
11.2.1 I_A	138
11.2.2 I_B	139
11.2.3 I_C	140
11.3 Unrenormalized form factors	141
11.4 Results of the partonic cross sections: universal coupling	148
11.5 Results of the partonic cross sections: nonuniversal coupling	169

Synopsis

The Standard Model (SM) of particle physics is a gauge quantum field theory, containing the unitary product group $SU(3) \times SU(2) \times U(1)$. The gauge field particles of the $SU(3)$ group are the eight massless gluons, whose interactions with each other as well as with the matter fields are described by Quantum Chromodynamics (QCD). The dynamics of electroweak theory is described by $SU(2) \times U(1)$ gauge group. One of the important processes in the SM is the Drell-Yan (DY) [1] production of a lepton pair. According to the parton model picture, this process takes place through the annihilation of a quark-antiquark pair, giving rise to a photon or a Z boson in the intermediate state, which then decays to a lepton pair. At the Large Hadron Collider (LHC), the typical scales at which the interactions take place during particle collisions is of the order of TeV. At such high energy scales, QCD effects become an important part of the DY process. One of the ways of computing such contributions is by expanding in a perturbative series of the strong coupling constant. According to the powers in coupling constant, they are known as the Leading Order (LO), next-to-leading order (NLO), next-to-next-to-leading order (NNLO) etc.. Beyond LO such expansions gives rise to divergences which can be categorized under two types: ultraviolet divergences (UV) and infrared divergences (IR). The UV singularities arise when the momentum of the particles in the virtual loops go to infinity. This divergence can be removed by regularizing the theory and then renormalizing the strong coupling constant. The IR divergences are of two types: soft and collinear. The soft singularities can be removed by adding the virtual diagrams and the real radiation processes that yield the same observable final state; the initial state collinear divergences

are removed by mass factorization. As a result, two unphysical scales μ_R and μ_F enter into computations of perturbative QCD. It is thus of utmost importance to calculate higher orders in perturbative expansion so that the effect of unphysical scales on observable reduces. *This thesis arises exactly in the context of calculating higher order radiative corrections for different processes in QCD.*

Despite the enormous success of the SM, it is still unable to incorporate properly the fourth force of nature: gravity. There are enormous efforts that are underway to formulate a concrete theory of all the four forces. One of the ways in which the unification of gauge fields with general relativity can be achieved is through Kaluza-Klein reduction. This describes the dynamics of (3+1) dimensional SM fields coupled to (4+n) gravity. Performing a mode expansion, we get a massive spin-2 particle, (n-1) massive vector bosons and $n(n-1)/2$ massive scalars. The spin-2 particle has tensorial nature of interactions with the SM fields. *In this thesis, we have considered the production of a spin-2 particle as an intermediate state in the DY type process and computed the higher order QCD corrections in a model independent way.* The phenomenological impact of these corrections can then be studied in different extra dimensional models. The contributions of the higher order radiative corrections with respect to LO can be expressed in terms of K factors, which is important to constrain the parameters from different extra-dimensional models in a more precise way.

1. NNLO QCD corrections in models of TeV scale Gravity with universal coupling

Production of a spin-2 particle at LO takes place through the DY process, with both gluons and quarks as the initial states. In the effective theory, the couplings of the gluon and quark to the massive spin-2 particle are assumed to be same. At LO there is no strong coupling constant dependency; at NLO level the coupling constant first enters into the calculation. The result at NLO thus becomes sensitive to μ_R and higher order corrections are needed to reduce this dependence. It is necessary to perform NNLO corrections in order to stabilize the cross section against scale variations. Often it is not easy to perform such higher order

corrections; increase in number external particles in real emission processes make phase space integration too complicated and challenging. In addition, the increase in number of scales that accompany a NNLO computation makes the problem worse. This makes it difficult to compute real emission processes. However, in contrast to real emission process, there have been lots of development in computing the virtual corrections. It will be less taxing if we can compute the real emission processes similarly like the virtual diagrams. The goal of this section is to briefly describe the method adopted for calculating the real processes and also state the phenomenological impact of the NNLO corrections for the Arkani-Dimopoulos-Dvali (ADD) model.

Using the state-of-the-art method of reverse unitarity [2], the real emission phase space diagrams were converted to loop integrals; the corresponding loop matrix elements were computed by standard techniques. At the end of our computations, we have to reinstate the loop propagators to final state real particles and use the available Master integrals to compute the partonic cross sections. The real-virtual processes were also handled in identical manner. The resulting partonic cross sections contains UV and IR divergences. To eliminate these singularities it is needed to introduce two unphysical renormalization and factorization scales. It is important to study the dependence of these scales on the cross section to asses the need for further higher order computations. We find [3] that the inclusion of NNLO corrections indeed reduce the dependence on these unphysical scales and provides a more reliable theoretical prediction. In addition, the cross section increases as we incorporate these radiative corrections; the NLO QCD corrections increase the LO cross section by 68%; the NNLO corrections increase an additional 12%. These reduced scale uncertainties and increase in perturbative convergence highlights the importance of the NNLO corrections. Our predictions of differential distributions will undoubtedly play very important role at the LHC.

2. Three loop form factors of spin-2 particle with non-universal coupling

In many extra dimensional models the coupling of a spin-2 particle to gluon pairs and

photon pairs are assumed to be equal. However analysis has shown that this universal nature of coupling may not be the favorable scenario. A model which incorporates a RS Graviton with a mass of 125 GeV and universal couplings has been excluded from experimental measurements at the Tevatron [4]. Drawing conclusions from the above, it is important to study the effects of setting the couplings of spin-2 with SM fields to non-equal values. For such a non-universal scenario, we can investigate the stability of effective field theory with respect to higher order corrections. *This is the motivation for the study of three loop form factors for a massive spin-2 production, where the SM gauge bosons and fermions couple to the massive particle through different coupling strengths.* Although the EM tensor of the SM is not conserved any more, the gauge symmetries are not affected. We have considered [5] a minimal effective action that consists of two gauge invariant operators: one containing pure gauge fields and another operator has gauge and fermionic fields. To use the form factors for further phenomenological studies, we have to renormalize the UV divergences that arise from the two composite operators. This is achieved by multiplying overall operator renormalization constants. Computation of these renormalization constants is non-trivial: the operators have same quantum numbers and hence mix under renormalization. However we have computed these anomalous dimensions by exploiting the universal IR structure of the on-shell form factors. These bare form factors satisfy an integro-differential equation, the K+G equation, which follows from gauge and renormalization group invariances. By using the predictive power of the solution of form factors, we determine the anomalous dimensions up to third order in the perturbation theory. This will be important for our phenomenological studies of NNLO QCD corrections for models with non-universal coupling.

3. NNLO QCD corrections to production of a spin-2 particle with non-universal coupling

In our study of form factors with non-universal coupling, we have seen that the nature of IR singularities of amplitudes remain unaffected. It is also of interest to investigate whether the same property holds for real emission processes. *This work achieves the above mentioned goal; the universal nature of IR divergences were found to hold true*

for purely real emission as well as real-virtual processes, leading to an extensive and thorough study of the phenomenology of models with non-universal coupling. In addition non-universal models have been used to distinguish a spin-0 from a spin-2, to characterize the 125 GeV boson as the Higgs boson [6]. The ATLAS collaboration have also used non-universal models to exclude several non SM spin hypothesis. It is thus important to compute NNLO corrections for such a model and study its phenomenology, which will be useful at the LHC.

We have computed [7] the higher order QCD contributions from various subprocesses and presented its impact for a resonance production of a spin-2 particle of mass 500 GeV. At the energies of LHC we find that the gg subprocess dominates over the rest. However the total NNLO correction is smaller than gg channel due to the negative contribution from the qg channel. At the resonance, the K-factor both for NLO as well as NNLO is different for different choice of coupling strengths. We also find that the uncertainties coming from factorization and renormalization scale dependencies, for LO, NLO and NNLO are 49%, 52%, 30% respectively.

4. Threshold resummation of rapidity distribution in the DY process at NNLO+NNLL

Any computation of fixed order partonic cross section result in polynomials, plus distributions and other logarithms, all expressed in terms of some dimensionless variable z , where the latter is the ratio of invariant mass of the final state and the partonic centre of mass energy. It is to be noted that the plus distributions are the result of soft and/or collinear gluon emissions from the final state. In the kinematical limit (threshold limit) $z \rightarrow 1$, the contributions to the UV and IR finite cross section can be divided into two parts : Soft virtual (SV) or threshold and hard part. At any order α_s^k , plus distributions like $\left[\frac{\ln^{m-1}(1-z)}{1-z} \right]_+$ ($m \leq 2k$) and delta functions fall under the SV category; while the polynomials and other logarithms like $\ln(1-z)$ can be listed under the hard contributions. It is to be remembered that the plus distributions are integrable. However in the threshold limit $z \rightarrow 1$, these SV terms give dominant contributions as compared to the hard part. The

product $\alpha_s^k \left[\frac{\ln^{m-1}(1-z)}{1-z} \right]_+$ becomes comparable to similar contributions from $k + 1$ th order, which spoils the reliability of perturbative expansion. In order to obtain a sensible result for inclusive and differential cross sections, we have to resum to all orders in perturbation theory. *This is called threshold resummation.*

It is challenging task to compute the SV cross section that contain the resummed contributions due to soft gluon emissions to all orders in perturbation expansion. There have been huge amount of works in the past to obtain such all order results. *In our recent work we have followed a completely different methodology to obtain the SV cross section in z space.* In a work by one of the author of this paper [8], it was shown that the SV rapidity distribution in z_1, z_2 space can be factorized in terms of purely form factor contributions and soft distribution functions. Here z_1, z_2 are related to the inclusive variable z and rapidity y . Often it is easier to work in Mellin space as compared to z_1, z_2 space; such a transformation converts the convolutions into normal products. Performing a double Mellin (N_1, N_2) transformation of the soft distribution function, we obtain a compact form of the all order resummation formula; then return back to z_1, z_2 space to get the resummation improved rapidity distribution. *This is the first time where a completely general, double variable resummation is performed, taking into account all the deltas and plus distributions.* In addition our method is applicable for production of any colorless final state particle. In this work, we have studied the phenomenology for DY production of a lepton pair up to NNLO+NNLL accuracy. Our result shows improved perturbative convergence as compared to the existing fixed order result. In addition the scale uncertainties reduce at NNLO+NNLL level. This is the most accurate result for soft gluon resummation of DY rapidity distribution, which will play an important role in the upcoming runs at the LHC.

List of Figures

1.1	Spontaneous symmetry breaking.	4
2.1	Higher order QCD correction to the process $gg \rightarrow H$	13
3.1	Deep inelastic scattering process	18
3.2	The Drell-Yan process	20
3.3	Lowest order DY process	21
3.4	Sample diagrams contributing to $O(a_s)$ QCD corrections	23
3.5	Gluon emitted at an angle θ in center of mass frame of the quark-antiquark system.	24
4.1	Leading order processes for the DY	35
5.1	Leading order processes for the DY	46
5.2	Interference of two loop with Born	47
5.3	self interference of double real emission	48
5.4	Effective two loop diagram with three cut propagators	49
5.5	Interference of real-virtual with single real emission	50

5.6	Various sub-process contributions to the di-lepton production computed at $\mathcal{O}(\alpha_s^2)$ QCD in ADD model. The SM background contains the full α_s^2 correction.	53
5.7	Pure graviton contribution to the Drell-Yan production cross section (left panel) up to NNLO QCD in the ADD model for LHC13 and the corresponding K-factors (right panel).	54
5.8	Drell-Yan production cross section (left panel) for SM, GR and the signal in the ADD model for LHC13 along with the corresponding K-factors (right panel). Here, $M_s = 4$ TeV and $d = 3$	55
5.9	Drell-Yan production cross section (left panel) for SM as well as the signal in the ADD model for LHC13 along with the corresponding K-factors (right panel).	56
5.10	Dependence of the signal production cross sections at NNLO on the the scale of the ADD model M_s (left panel) and the corresponding signal K-factors(right panel) for d=3.	57
5.11	Dependence of the signal production cross sections at NNLO on the the scale of the ADD model M_s (left panel) and the corresponding signal K-factors(right panel).	57
5.12	Dependence of the signal production cross sections at NNLO on the number of extra dimensions d (left panel) and the corresponding K-factors (right panel).	58
5.13	Uncertainties in the signal production cross section due to the choice of renormalisation scale μ_R (left panel) and factorization scale μ_F (right panel).	58

5.14	Uncertainties in the signal production cross section due to the choice of the scale $\mu = \mu_R = \mu_F$	59
5.15	Dependence of the signal production cross sections at NNLO on the center of mass energy at LHC (left panel) and the corresponding K-factors (right panel).	59
5.16	Dependence of the signal production cross sections at NNLO on the choice of PDFs (left panel). Signal K-factors at NNLO for different PDFs (right panel).	60
5.17	NLO and NNLO predictions obtained from modified SV approximation for the signal only with the gg subprocess contribution.	61
7.1	First order QCD corrections from different subprocesses to di-lepton production. The choice of the model parameters is as mentioned in the text.	82
7.2	Di-lepton invariant mass distributions are presented to NLO QCD for different choice of couplings (k_q, k_g) in the left panel. The corresponding K-factors are presented in the right panel.	83
7.3	Percentage of qg subprocess contribution $R_{qg}^{(1)}$ as defined in the text for different choice of nonuniversal couplings.	84
7.4	Second order QCD corrections from various subprocess to the di-lepton invariant mass distribution.	85
7.5	Percentage of qg contribution $R_{qg}^{(2)}$ as defined in the text.	86
7.6	Cross sections at different orders (left panel) and the corresponding K-factors K_1 and K_2 (right panel) are presented for different couplings.	86
7.7	Same as fig. 7.6 but for a different set of couplings.	87

7.8	Di-lepton invariant mass distributions to NNLO for different choice of couplings (left panel) and the corresponding K-factors (right panel) are presented.	87
7.9	Same as fig. 7.8 but for a different set of couplings.	88
7.10	Same as fig. 7.8 but for a different set of couplings.	88
7.11	Dependence of cross sections on the di-lepton invariant mass distribution for universal couplings (1.0, 1.0).	89
7.12	Same as fig. 7.11 but for the default choice of nonuniversal couplings (0.5, 1.0).	89
7.13	Renormalization (left) and factorization (right) scale dependence of the di-lepton invariant mass distribution at LO, NLO and NNLO.	90
7.14	Same as fig. 7.13 but with $\mu_R = \mu_F = \mu$	90
7.15	Di-lepton invariant mass distributions for different choice parton distribution functions (PDFs).	91
9.1	Cross sections against μ_F (left), μ_R (middle) and μ (right) variations at NNLO+NNLL for 14 TeV LHC. The bands are obtained by using 7 point scale variation (see text for more details).	119
9.2	Resummed rapidity distribution in Drell-Yan production for the two sets of central scale choices (M_Z, M_Z) and $(M_Z/2, M_Z)$ using MMHT PDFs at 14 TeV LHC. Corresponding bands are obtained using 7-point scale variation around the central scale. The lower panel represents the corresponding K-factors.	120

- 9.3 Fixed order predictions with the central scale $\mu_R = M_Z, \mu_F = M_Z$ and resummed prediction with the central scale $\mu_R = M_Z/2, \mu_F = M_Z$ for rapidity $y=0$ and $y=2.4$ using MMHT2014 PDF at each order. The uncertainties are obtained by using 7 point scale variation around the central scale (see text for more details). 121
- 9.4 Drell-Yan rapidity distribution for 14 TeV LHC at $q = M_Z$ using MMHT PDFs. The fixed order results are plotted in the left panel and the resummed results in the right panel. Central scale is chosen as $\mu_R = \mu_F = M_Z$ for both and the corresponding bands are obtained using 7-point scale variation (see text for more details) around the central scale. The lower panel represents the corresponding K-factors. 123
- 9.5 Drell-Yan rapidity distribution for 14 TeV LHC at $y = 0$ using MMHT PDFs. The variation of fixed order and resummed results as a function of μ_R are shown separately for $q\bar{q}$ channel and also for all the channels added together. 124
- 9.6 Same as fig. 9.4 but for $q = 1$ TeV. 124
- 9.7 PDF variation at NNLO+NNLL using various sets. The y-axis represents the ratio of extremum variation over the central PDF set. 127
- 9.8 Rapidity distribution at NNLO+NNLL for 8 TeV LHC in the invariant mass range $60 < q < 120$ GeV. The dotted line is the fixed order NNLO contribution, the dashed line represents NNLO+NNLL result and the solid line includes electro-weak corrections. 128
- 9.9 Comparison of resummed results with the CDF data [246] at $\sqrt{s} = 1.8$ TeV and [247] at $\sqrt{s} = 1.96$ TeV in the invariant mass range $66 < q < 116$ GeV for two different PDF sets. 129

List of Tables

9.1	Comparison of resummed results for Mellin-Fourier space (M-F) and double Mellin space (M-M) approach in the minimal prescription scheme at $y = 0$ for various choices of scales.	122
9.2	Fixed order and the resummed cross sections with % scale uncertainties along with the K-factors at the central scale $\mu_R = \mu_F = M_Z$	126
9.3	Cross sections at NNLO+NNLL using different PDF sets along with percentage uncertainties for $y = 0, 0.8, 1.6, 2.4$	127

1

Introduction

1.1 The Standard Model

The quest for understanding the basic constituents of matter that exists in the world around us has fascinated human minds for a long time. It goes back to the era when the atomic theory was developed through the relentless pursuit of Leucippus and Democritus. The modern theory of atoms started from the nineteenth century with the help of John Dalton and other scientists. The discovery of the protons, neutrons and other subatomic particles paved a new way to understand the physics of the universe. Gradually our understanding of the world became more precise, thanks to the several experimental and theoretical endeavor that followed in the mid nineteenth century. All these efforts resulted in a concrete theory in particle physics : The Standard Model (SM). It is a gauge quantum field theory containing the unitary product group $SU(3)_C \otimes SU(2)_L \otimes U(1)_Y$. Each of these group in the SM contain gauge particle/particles which mediate the interaction in different collision processes. The strong interactions are described by the gauge group $SU(3)_C$ which consists of eight gluons. Their interactions with each other as well as with the quarks are explained in the theory of Quantum chromodynamics (QCD). The weak and the electromagnetic interactions are encapsulated together in the electroweak theory, described by the gauge group $SU(2)_L \otimes U(1)_Y$. In this section we shall briefly describe the theory of electroweak interactions; we will elaborate on the strong interactions in the next chapter.

The simplest gauge theory in nature is quantum electrodynamics(QED), described by the group $U(1)$. Electromagnetic interactions take place via the exchange of photons, which are massless spin-1 bosons. There is only one photon (γ) which acts as the generator of the group, it has no charge but can mediate in the interaction between two charged particles like the electrons. During 1950's, questions were being raised as to whether weak interactions can be thought along the similar lines of electromagnetic theory. This led to the $V - A$ theory [9, 10], where the weak interactions were thought to be taking place via the exchange of spin-1 W^\pm bosons. In the work [11] Schwinger developed the theory of weak interactions into a gauge theory, where the mediators were the W^\pm bosons. He also suggested about the possibility of a combined theory of the weak and electromagnetic interactions, where the gauge bosons would be W^\pm and γ . However the idea of combining the electromagnetic and weak interactions faced stiff problems: the W^\pm particles were massive due to the short range nature of weak interactions, whereas the photons were massless. In addition the symmetry of such a theory needed to be broken due to the mass difference between these gauge particles. Later on in 1961 Glashow gave a combined theory of the weak and electromagnetic interactions [12] comprising of a bigger symmetry group $SU(2) \otimes U(1)$. The generators of the group were three parity violating, massive W^\pm and Z_0 particles and one parity conserving particle, the massless photon. But there were still difficulties in assigning mass to these gauge bosons by breaking the symmetry, particularly, the theory became unrenormalizable. This problem was solved by introducing the concept of spontaneous symmetry breaking.

1.1.1 Spontaneous symmetry breaking

The concept of spontaneous symmetry breaking appears in condensed matter physics associated with phase transitions. It happens when the Hamiltonian of the system has a symmetry, hence a conserved quantity, but the ground state of the system does not respect that symmetry. One of the most common example is the ferromagnet. Above the Curie

temperature (T_C), all the electron's spin in a ferromagnet are randomly oriented resulting in no overall magnetization. But below T_C , there happens to be a preferred direction of magnetization and the rotational invariance property is broken. It cannot be predicted in advance in which direction the ferromagnet will acquire a magnetization when cooled below T_C , hence the symmetry broken is spontaneous. This phenomenon can also be observed in particle physics. We take the example of complex scalar field with a ϕ^4 interaction term in quantum field theory and illustrate the phenomenon of spontaneous symmetry breaking. The Lagrangian is

$$\mathcal{L} = (\partial_\mu \phi)^* (\partial^\mu \phi) - \mu^2 \phi^* \phi - \lambda (\phi^* \phi)^2. \quad (1.1)$$

where $\lambda > 0$. This Lagrangian has a global U(1) symmetry; under the transformation $\phi \rightarrow \exp(-i\theta) \phi$ the Lagrangian remains invariant. The first piece of the Lagrangian represents the kinetic term. Here μ is the mass term and λ is the coupling strength of interacting scalar fields. The potential term of the Lagrangian, $V(\phi)$, consists of the mass and the interaction term. For $\mu^2 > 0$, there is a unique minimum at $\phi = 0$ and no spontaneous symmetry breaking is observed. In other words, there is a unique vacuum at $\phi = 0$. However if $\mu^2 < 0$ the minimum of the potential in eq. 1.1 is not anymore at $\phi = 0$. The U(1) symmetry is broken by a vacuum expectation value of ϕ , which at the classical level is the minimum of the potential. We write $\phi = \frac{1}{\sqrt{2}} (\phi_1 + i \phi_2)$ and put it in the Lagrangian. Choosing a value $\langle \phi_2 \rangle = 0$, we get

$$\langle \phi_1 \rangle = \pm \sqrt{\frac{-\mu^2}{\lambda}} = \pm v \quad (1.2)$$

Thus there are two values of ϕ_1 for which the potential acquires a minimum value. This is shown below in fig. 1.1

Out of these two symmetric ground states we can choose arbitrarily any one of them. This choice spontaneously breaks the symmetry of the vacuum. Although the ground

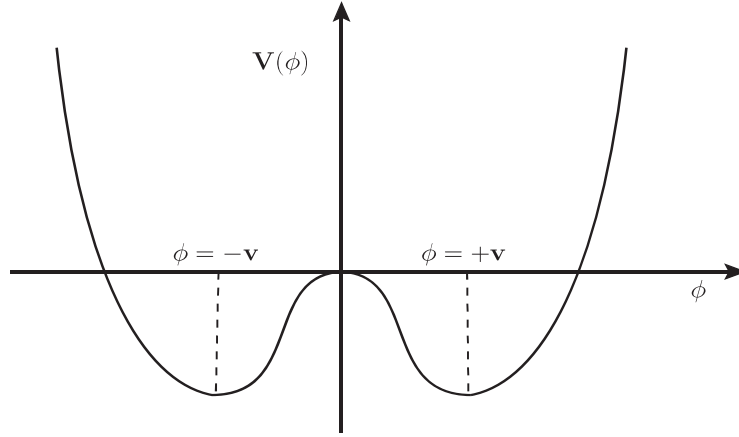


Figure 1.1: Spontaneous symmetry breaking.

state does not respect anymore the symmetry of the theory, the Lagrangian still remains invariant under the global U(1) symmetry.

Introducing two real scalar fields σ and η , we can reparametrize ϕ as

$$\phi(x) = \frac{1}{\sqrt{2}} [v + \sigma(x) + i\eta(x)] \quad (1.3)$$

and putting them back into eq. 1.1 we get,

$$\begin{aligned} \mathcal{L} = & \frac{1}{2}(\partial_\mu \sigma)(\partial^\mu \sigma) + \frac{1}{2}(\partial_\eta \sigma)(\partial^\eta \sigma) - \frac{1}{2}(2\lambda v^2)\sigma^2 \\ & - \lambda v \sigma^3 - \lambda v \sigma \eta^2 - \frac{1}{4}\lambda \sigma^4 - \frac{1}{4}\lambda \eta^4 - \frac{1}{2}\lambda \sigma^2 \eta^2 \end{aligned} \quad (1.4)$$

In above the particle σ acquires a mass $= \sqrt{2\lambda v^2}$; while η remains massless. This massless particle is called a Goldstone boson. In other words, if a Lagrangian having continuous symmetry is spontaneously broken then there will be massless particles which are the Goldstone bosons [13]; the number of such particle(s) will be same as the number of broken generator(s) of the symmetry group.

However these massless particles are not seen in nature. This puzzle was resolved by Englert, Brout, Higgs, Guralnik, Hagen and Kibble. The mechanism is popularly known as the Higgs mechanism. In the next section we shall see how this concept plays an

important role in generating the masses of W^\pm and Z bosons.

1.1.2 The Higgs Mechanism

We consider the Abelian example where a complex scalar field couples to itself as well as to an electromagnetic field :

$$\mathcal{L} = -\frac{1}{4}F^{\mu\nu}F_{\mu\nu} + \left|D_\mu\phi\right|^2 + \mu^2\phi^*\phi - \lambda(\phi^*\phi)^2 \quad (1.5)$$

where $D_\mu = \partial_\mu + ie A_\mu$. The Lagrangian has a local $U(1)$ symmetry, $\phi \rightarrow \exp(i\theta(x))\phi$, and the gauge field transforms as $A_\mu \rightarrow A_\mu - \frac{1}{e}\partial_\mu\theta(x)$. The sign of the mass term is opposite to that of the example considered in previous section.

We follow the arguments along the line of the previous section, except that for $\mu^2 > 0$, the field ϕ will acquire a vacuum expectation value through spontaneous breaking of the local $U(1)$ symmetry. Considering the minimum as ϕ_0 we can expand the Lagrangian about the vacuum state with

$$\phi(x) = \phi_0 + \frac{1}{\sqrt{2}}[\phi_1 + i\phi_2]. \quad (1.6)$$

On putting the above expression for ϕ in eq. 1.5 we find that the field ϕ_1 acquires a mass $m_{\phi_1} = \sqrt{2}\mu$ and the field ϕ_2 turns out to be the Goldstone boson. From the kinetic term of the Lagrangian we find that the field A_μ acquires a mass $m_A = 2e^2\phi_0^2$. Thus spontaneous symmetry breaking generates mass for the gauge boson. The Goldstone boson does not appear as an independent particle of the theory; if we work in unitarity gauge the terms corresponding to ϕ_2 in the Lagrangian vanishes. This can be physically interpreted by considering that the vector boson has acquired its mass by eating up the Goldstone boson.

This phenomenon of mass generation for gauge bosons through spontaneous breaking of local gauge symmetry paved the way for unification of the electromagnetism and weak interaction [14]. To generate masses for W^\pm and Z bosons, it is necessary to break the

$SU(2)_L \otimes U(1)_Y$ symmetry. The Lagrangian containing the scalar field reads as

$$\mathcal{L}_{scalar} = (D_\mu \phi)^\dagger (D^\mu \phi) + \mu^2 (\phi^\dagger \phi) - \lambda (\phi^\dagger \phi)^2, \quad (1.7)$$

where D_μ is the covariant derivative corresponding to the gauge group $SU(2)_L \otimes U(1)_Y$

$$D_\mu = \partial_\mu + \frac{1}{2} i g_1 \vec{\tau} \cdot \vec{W}_\mu + \frac{1}{2} i g_2 Y B_\mu. \quad (1.8)$$

The $SU(2)$ group has three generators, the Pauli matrices, denoted by $\vec{\tau}$. The three vector fields are denoted by \vec{W}_μ . Y is the hypercharge and B_μ is the field corresponding to group $U(1)$. g_1, g_2 are the couplings of W_μ and B_μ to the scalar field ϕ respectively; the latter is a doublet under $SU(2)$

$$\phi = \begin{bmatrix} \phi^+(x) \\ \phi^0(x) \end{bmatrix}. \quad (1.9)$$

This is a left handed doublet with weak Isospin $= \frac{1}{2}$. The upper component has charge $+1$ while the lower one has charge 0 . Each component is a complex scalar field which can be written as

$$\phi^+ = \frac{1}{\sqrt{2}}(\phi_1 + i \phi_2), \quad \phi^0 = \frac{1}{\sqrt{2}}(\phi_3 + i \phi_4). \quad (1.10)$$

There is a $O(4)$ symmetry associated with ϕ . The potential in eq. 1.5 has a minimum for $\mu^2 > 0$ at

$$\phi^\dagger \phi = \frac{\mu^2}{2\lambda} = \frac{v^2}{2} \quad (1.11)$$

In order to generate masses we have to choose a vacuum; a gauge transformation with $\phi_1 = \phi_2 = \phi_4 = 0$ and $\phi_3 = v$ allows us to write the field ϕ in eq. 1.9 as

$$\phi = \frac{1}{\sqrt{2}} \begin{bmatrix} 0 \\ v + h(x) \end{bmatrix} \quad (1.12)$$

where v = vacuum expectation value = $\sqrt{\frac{\mu^2}{\lambda}}$ and $h(x)$ is a scalar field, with $\langle h(x) \rangle = 0$. This results in breaking of three local symmetries which generates the three massless Goldstone bosons. These Goldstone bosons are eaten up by the three gauge bosons and thus they become massive; however the photon still remains massless. From the Lagrangian the masses of the gauge bosons are found out to be

$$M_W = \frac{v g_1}{2} \quad M_Z = \frac{v}{2} \sqrt{g_1^2 + g_2^2}. \quad (1.13)$$

The massive vector bosons were experimentally discovered at CERN [15, 16]. Precise measurement of their mass gives: $M_W = 80.385 \pm 0.015$ GeV and $M_Z = 91.1876 \pm 0.0021$ GeV. Thus the unification of $SU(2)_L \otimes U(1)_Y$ was achieved and it has been one of the greatest achievement in the history of the particle physics.

The term $h(x)$ in the doublet structure of ϕ_0 is the scalar Higgs field of the SM. The quanta corresponding to this field is the Higgs particle, whose mass can be derived from the Abelian example we have considered at the start of this section. It reads as

$$m_h = \sqrt{2 \lambda} v. \quad (1.14)$$

The Higgs particle remained elusive in high energy experiments for quite a long time. In 2012 [17, 18], a resonance of 125 GeV was discovered at the CERN's Large Hadron Collider (LHC) and it was confirmed to be the Higgs particle.

We have seen how the dream of unifying the weak and electromagnetic interactions culminated in the discovery of the electroweak theory. The theory of spontaneous symmetry breaking was introduced to generate masses for gauge bosons and fermions. The only scalar particle of the SM, the Higgs boson, was finally found out at the LHC. It is important to mention that the energies at which the LHC operates is of the order of TeV, where protons moving at velocities close to speed of light collide with one another. As we shall see in the next chapter the proton is made up of large number of gluons and quarks and

these constituents contribute significantly at such high energies. The gluons and quarks are held together by strong interactions described by the gauge group $SU(3)_C$. In other words, at such high energies the effect of strong interactions cannot be neglected in observables like the inclusive and differential cross section. In fact at the LHC the dominant channel for production of Higgs boson is the gluon fusion channel, which gets radiative corrections due to the strong interactions. One of the reasons for the precise measurement of the mass of the Higgs boson was due to the spectacular higher order corrections that resulted from QCD [2, 8, 19–30]. We shall briefly discuss in the next chapter how this theory was developed over the years of intense effort from physicists all over the world.

2 Quantum Chromodynamics

2.1 Quarks and gluons

In the previous chapter we have briefly described the theoretical endeavor that went on to formulate the electroweak theory, described by the gauge group $SU(2)_L \otimes U(1)_Y$. In addition the SM also contains the gauge group that describes the strong interactions namely $SU(3)_C$. The strong interaction is the force that binds the protons and neutrons together inside the nucleus of an atom. At the scale of 10^{-15} m the strong force dominates over the other two forces, namely the electromagnetic and weak force. The study of strong force began with the endeavor to understand the hadrons and its properties, which has been an area of interest for quite a long time. The most famous example of a hadron is a proton, a name given to the hydrogen nucleus by Ernest Rutherford in 1920. The subsequent discoveries of neutron, kaon, pion etc. increased the list of the hadrons and as more and more new particles emerged from experiments during 1950's, it became necessary to find a way to categorize the particles and also to understand their spectrum. The brilliant analysis by M.Gell-Mann [31] and Y. Ne'eman [32] helped to categorize the hadrons into representation of the symmetry group $SU(3)$: the octets of baryons and mesons. While protons, neutrons, Λ , Σ and Ξ belonged to baryons, the family of meson comprised of the pions, k-mesons and η mesons. In 1964 Gell-Mann [33] and Zweig [34] independently proposed that the hadrons are made up of quarks. The mesons are formed of one quark

and one anti-quark; on the other hand the baryons were composed of three quarks. Subsequently three flavor of quarks: up, down and strange were discovered but to explain the quantum numbers of hadrons, quarks were assigned fractional electric charge. The action of the $SU(3)_{\text{flavor}}$ group on the three flavors led to the mass formulas for the hadrons. Later on Gürsey and Radicati [35] introduced the symmetry group $SU(2)_{\text{spin}}$ and thus the quarks were identified as spin $\frac{1}{2}$ particles. The $SU(2)_{\text{spin}}$ and $SU(3)_{\text{flavour}}$ group were combined into a larger $SU(6)_{\text{spin-flavor}}$ symmetry. Following this unification and in order to explain the bound state of baryons, it was necessary that the low-lying baryons were in a symmetric state under permutations. This contradicted the Pauli's spin-statistics theorem [36], which requires that the spin $\frac{1}{2}$ quarks to be in an anti-symmetric state under permutations.

To resolve this tension, Greenberg [37] proposed that the quarks had an additional symmetry, the color, along with the the flavor, spin and space degrees of freedom. Now the quarks could be in an anti-symmetric configuration corresponding to the color degree of freedom and in a symmetric state in terms of the other three degrees of freedom. The color symmetry remains unbroken and all the hadrons are color singlets. While measurement of properties of excited baryons served as evidence for the existence of color, measuring the ratio of annihilation cross section for $e^+e^- \rightarrow \text{hadrons}$ to that of $e^+e^- \rightarrow \mu^+\mu^-$ established color as a degree of freedom.

The quarks inside the hadrons are bound together by the strong force. Drawing analogy from QED, we can imagine that the mediators of the strong force can only be gauge particles, owing to the $SU(3)$ nature of the quarks. In addition, these mediators should interact with the color charge analogously as the photon responds to the electric charge. It was found that the interaction between the quarks are generated by massless gauge bosons known as gluons. We have seen earlier how the electromagnetic and weak interactions were unified into the electroweak theory, a non-Abelian gauge theory. To construct a gauge theory of strong interactions, it was necessary to explain a phenomenon called Bjorken scaling (we shall discuss about it in the next chapter). This required the theory of

the quarks and the gluons to be a non-Abelian gauge theory. All these efforts gave rise to the theory of strong interactions: QCD. There are some fundamental differences between QED and QCD: in contrast to one photon in QED, there are eight gluons in QCD; gluons carry color charge while photons have no charge. In the next section, we give a brief description of the Lagrangian of QCD.

2.2 Basics of QCD

The Lagrangian density of QCD is as follows :

$$\mathcal{L} = -\frac{1}{4}G_{\mu\nu}^a G^{\mu\nu,a} + \sum_{f=1}^{n_f} \bar{\psi}_i^f (i\gamma^\mu D_\mu^{ij} - m \delta_{ij}) \psi_j^f - \frac{1}{2\zeta} (\partial^\mu A_\mu^a)^2 + \bar{\omega}^d (-\partial^\mu \mathcal{D}_\mu^{de}) \omega^e. \quad (2.1)$$

In above the field tensor $G_{\mu\nu}^a$, the covariant derivative in fundamental representation D_μ^{ij} and the covariant derivative in adjoint representation \mathcal{D}_μ^{de} are given by

$$\begin{aligned} G_{\mu\nu}^a &= \partial_\mu A_\nu^a - \partial_\nu A_\mu^a + g_s f^{abc} A_\mu^b A_\nu^c, \\ D_\mu^{ij} &= \delta^{ij} \partial_\mu - i g_s A_\mu^a (T^a)^{ij}, \\ \mathcal{D}_\mu^{de} &= \delta^{de} \partial_\mu + g_s f^{deg} A_\mu^g. \end{aligned} \quad (2.2)$$

The other quantities appearing in the Lagrangian are as follows

A_μ^a = gluon field,

$\bar{\psi}_i^f$ = quark field,

ω^d = ghost field,

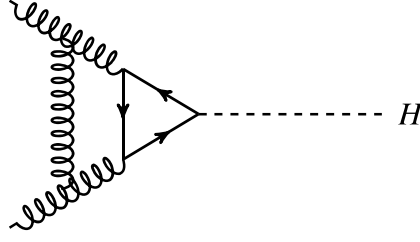
a, d, e = color indices in the adjoint representation,

i, j = color indices in the fundamental representation,

f^{abc} = structure constants of SU(3),

$$\begin{aligned}
(T^a)^{ij} &= \text{Gell-Mann matrices} , \\
g_s &= \text{strong coupling constant} , \\
m &= \text{mass of the quark} , \\
\zeta &= \text{gauge fixing parameter} , \\
n_f &= \text{number of fermion species} .
\end{aligned} \tag{2.3}$$

The first term and second term in eq. 2.1 represents the kinetic term for the gauge field and the fermionic field respectively. The non-abelian nature of the Lagrangian is reflected through f^{abc} in the kinetic term of gauge field, which is absent in QED. This term is responsible for three-point and four point vertices in QCD. The third term denotes the gauge fixing term which is needed to properly define the gluon propagator. The last term represents the kinetic term for the ghost field. The ghosts are unphysical as they violate the spin-statistics theorem. The gluons appearing in loops can have four degrees of freedom but a physical gluon can have only two degrees of freedom. The ghosts cancel the two extra unphysical degrees of freedom coming from the gluons appearing in the loops.

Figure 2.1: Higher order QCD correction to the process $gg \rightarrow H$

2.3 Asymptotic freedom

The QCD Lagrangian discussed in the previous section describes how the gluons interact with themselves as well as with the matter fields. The millions and millions of quarks and gluons in a proton are held together by the strong force. In high energy collision processes at the LHC, where the centre of mass energy of the colliding protons is of the order of TeV, the strong force dominates over the electromagnetic and the weak force. QCD corrections to the signal and the background processes become important; it is necessary to compute these contributions for precisely predicting observables such as inclusive and differential cross sections. For example at the LHC the production of Higgs boson is dominated by the gluon fusion process. The virtual QCD correction at the signal is shown in fig. 2.1. The coupling of fermions to the Higgs boson is proportional to the mass of the fermions; hence the dominant contribution in the fermion loop in the fig. 2.1 is from the top quark. Also we observe that there is a gluon loop between the two incoming particles; this is an example of higher order QCD correction for processes at the LHC. One of the ways to compute such contributions is to expand in a perturbative series of the strong coupling constant :

$$\mathcal{A} = \sum_{j=0}^{\infty} \hat{a}_s^j \hat{\mathcal{A}}^j \quad (2.4)$$

where $\hat{a}_s \equiv \frac{\hat{g}_s^2}{16\pi^2}$. The observables, $\hat{\mathcal{A}}^j$ are computed by writing down the Feynman rules from the Lagrangian 2.1 and then evaluating the amplitudes by summing over Dirac in-

dices, color indices and expressing them in terms of dot products of external momentum of particles. The contribution at \hat{a}_s^0 is called Leading order (LO); the \hat{a}_s order is called next-to-leading order (NLO); $O(\hat{a}_s^2)$ level is called next-to-next-to-leading order (NNLO) and so on. For example the diagram in fig. 2.1 illustrates NNLO correction to the process $gg \rightarrow H$. Such kind of diagrams are divergent due to high momentum particles moving in the virtual loops. More precisely while evaluating this diagram there will be integrals with the four-momentum of the massless virtual particles running from 0 to ∞ . In the limit of the momentum $\rightarrow \infty$, the divergence that arise is called ultraviolet (UV) singularity. To eliminate the divergence we have to regularize the theory in dimensional regularization, by going to $n = 4 + \epsilon$ dimension and then renormalize the coupling constant of the theory. This renormalization is done by choosing a scheme; for us we choose $\overline{\text{MS}}$ such that :

$$\hat{a}_s = \left(\frac{\mu}{\mu_R} \right)^\epsilon S_\epsilon^{-1} Z(a_s(\mu_R^2)) a_s(\mu_R^2) \quad (2.5)$$

where μ is the scale introduced to keep the unrenormalized strong coupling constant \hat{a}_s dimensionless in n -dimensions and μ_R is the renormalization scale.

$S_\epsilon = \exp [(\gamma_E - \ln 4\pi)\epsilon/2]$, $\gamma_E = 0.5772 \dots$. The coupling constant renormalization term $Z(a_s(\mu_R^2))$ reads as :

$$\begin{aligned} Z_{a_s} = 1 &+ a_s \left[\frac{2}{\epsilon} \beta_0 \right] + a_s^2 \left[\frac{4}{\epsilon^2} \beta_0^2 + \frac{1}{\epsilon} \beta_1 \right] + a_s^3 \left[\frac{8}{\epsilon^3} \beta_0^3 + \frac{14}{3\epsilon^2} \beta_0 \beta_1 + \frac{2}{3\epsilon} \beta_2 \right] \\ &+ a_s^4 \left[\frac{16}{\epsilon^4} \beta_0^4 + \frac{46}{3\epsilon^3} \beta_0^2 \beta_1 + \frac{3}{2\epsilon^2} \beta_1^2 + \frac{10}{3\epsilon^2} \beta_0 \beta_2 + \frac{1}{2\epsilon} \beta_3 \right] \\ &+ a_s^5 \left[\frac{32}{\epsilon^5} \beta_0^5 + \frac{652}{15\epsilon^4} \beta_0^3 \beta_1 + \frac{157}{15\epsilon^3} \beta_0 \beta_1^2 + \frac{172}{15} \epsilon^3 \beta_0^2 \beta_2 + \frac{34}{15\epsilon^2} \beta_1 \beta_2 \right. \\ &\left. + \frac{13}{5\epsilon^2} \beta_0 \beta_3 + \frac{2}{5\epsilon} \beta_4 \right]. \end{aligned} \quad (2.6)$$

The renormalization group equation (RGE) satisfied by the renormalized coupling $a_s(\mu_R^2)$ is

$$\mu_R^2 \frac{da_s(\mu_R^2)}{d\mu_R^2} = \frac{\epsilon a_s(\mu_R^2)}{2} + \beta(a_s(\mu_R^2)), \quad (2.7)$$

with

$$\beta(a_s(\mu_R^2)) = a_s(\mu_R^2) \mu_R^2 \frac{d \ln Z(\mu_R^2)}{d \mu_R^2} = - \sum_{k=0}^{\infty} a_s(\mu_R^2)^{k+2} \beta_k. \quad (2.8)$$

β_k is the beta function of QCD. The one loop QCD beta function was computed independently by Gross and Wilczek [38] and by Politzer [39]. For SU(N) theory it's value is: $\beta_0 = -(\frac{11}{3}N - \frac{2}{3}n_f)$, where n_f are the number of fermion species. This negative value of beta function in QCD is in contrast to the corresponding value in QED.

The RGE in 2.7 can be solved with the initial scale as μ^2 and final scale Q^2 (can represent momentum transfer in a particular process)

$$a_s(Q^2) = \frac{a_s(\mu^2)}{1 - \frac{\beta_0}{4\pi} a_s(\mu^2) \ln(Q^2/\mu^2)}. \quad (2.9)$$

The above solution implies that the coupling constants are not truly 'constants'; their strength depends on the energy scale at which the interaction takes place. For $\beta_0 < 0$ (as in QCD) the coupling $a_s(Q^2)$ decreases as Q^2 increases and in the limit of very high Q^2 *i.e.*

$$a_s(Q^2) \rightarrow 0 \quad \text{as} \quad Q^2 \rightarrow \infty. \quad (2.10)$$

Thus in processes where a large momentum transfer Q^2 is involved, we can explain the dynamics of QCD in the light of free behavior of quarks and gluons. This reduction of strong coupling constant at high energies is called asymptotic freedom, discovered independently by Gross, Wilczek [38] and Politzer [39]. At low energies the coupling is not small, which explains the binding of quarks in the hadrons. As the distance decreases, the ratio $\alpha_s(Q^2)/\alpha_{em}(Q^2)$ decreases, where $\alpha_{em}(Q^2)$ is the fine structure constant in QED. This is the conceptualization of the asymptotic freedom. One of the consequences of the asymptotic freedom observed in high energy experiments are formation of jets, where the later is a collection of energetic quarks and gluons moving in a common direction. As the quarks and gluons evolve to form hadrons, in order to conserve energy and momentum, they interact weakly with highly virtual particles. Therefore detection of these jets and

measuring their properties in experiments like CERN and SLAC serves as confirmation of asymptotic freedom and also solidifies the framework of perturbative QCD (pQCD).

Asymptotic freedom is an important property of non-abelian gauge theories. It allows us to compute QCD effects at high energies as corrections to the free quark behavior. In the next chapter we shall see how the pQCD corrections can be computed in the framework of parton model.

3

The parton model and its application to the Drell-Yan process

In the previous chapter we saw how the concept of asymptotic freedom makes QCD effects an important component of high energy colliders like the LHC. Hence it is of utmost importance to compute the higher order QCD corrections for making accurate predictions about observables like the inclusive and differential cross sections. QCD interactions involve quarks and gluons and they are described by the Lagrangian in eq. 2.1. These elementary particles are the constituents of hadrons; the former does not exist in free state whereas in experiments, hadrons are the ones that take part in the collision. Thus from theoretical side it is important to connect the hadronic picture with that of the elementary ones to enable us perform calculations in pQCD. In this chapter we shall see how this was possible after the discovery of the parton model.

While there were great developments in search for a unified theory of QED and weak interactions, there was also considerable progress to understand the nature of strong interactions. In the previous chapter we have seen how the understanding of quarks and gluons eventually led to the theory of QCD. Subsequently there were advancements made by Gell-Mann to derive the current algebras, the commutation relations for the vector and axial vector currents [40]. These current algebras were used to derive sum rules [41] which helped to understand the scattering processes of highly energetic neutrino and anti-neutrino. Bjorken [42] applied these sum rules to high energy electron nucleon scattering

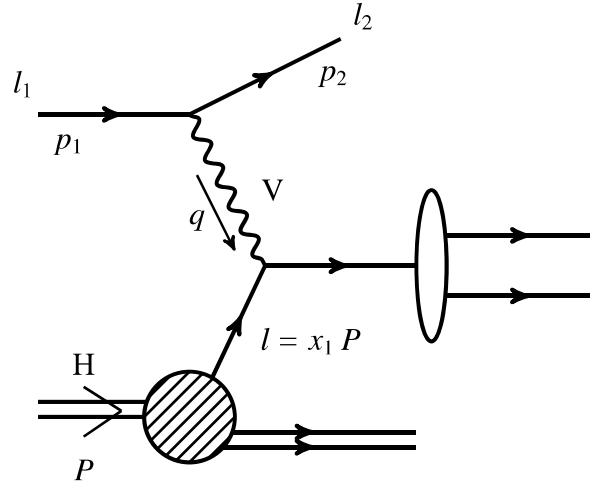


Figure 3.1: Deep inelastic scattering process

and showed that the cross section of such a scattering process can be thought of as a point like target. This subsequently led to the concept of Bjorken scaling [43], which was confirmed by the experiments at the SLAC. Bjorken scaling was explained by Feynman [44] as incoherent scattering of point like constituents of nucleon by the incident electron. These point like constituents were named as partons; this was the advent of the parton model. In the language of QCD, partons are quarks, antiquarks and gluons. The deep inelastic lepton-hadron scattering (DIS) process could be explained in terms of parton model with some corrections, thanks to the asymptotic nature of QCD. The DIS process is

$$l_1(p_1) + H(P) \rightarrow l_2(p_2) + X \quad (3.1)$$

where P is the momentum of the hadron H , p_1, p_2 are the momentum of leptons and X is some hadronic state. Fig 3.1 shows the DIS process as realized through the parton model. The interaction of a lepton and a parton of momentum l takes place through an intermediate vector boson (V), having momentum q . The differential cross section is

$$\frac{d^2\sigma}{dQ^2 d\nu}(\tau, Q^2) = \sum_{i=q,\bar{q},g} \int_0^1 dx_1 \int_0^1 dz \delta(\tau - x_1 z) x_1 f_i^H(x_1) \frac{d^2\sigma^i}{dQ^2 d\nu}(z, Q^2), \quad (3.2)$$

where $Q^2 = -q^2$, the scaling variable $\tau = -q^2/2P \cdot q$ and $\nu = \frac{P \cdot q}{M}$ where M is the mass

of the hadron. x_1 is the fraction of hadron's momentum carried by the parton i i.e., $l = x_1 P$ and $0 \leq x_1 \leq 1$. The scaling variable at parton level is $z = \frac{-q^2}{2p \cdot q}$. $f_i^H(x_1)$ is the parton distribution function (PDF), which is the probability of finding a parton i in H with momentum fraction between x and $x + dx$. PDF satisfy the following properties :

$$\int_0^1 dx [f_u(x) - f_{\bar{u}}(x)] = 2, \quad \int_0^1 dx [f_d(x) - f_{\bar{d}}(x)] = 1, \quad (3.3)$$

which says that the integral of the difference between quarks and anti-quarks equals the number of quarks in proton. Conservation of momenta implies

$$\sum_i \int_0^1 dx x f_i(x) = 1. \quad (3.4)$$

The parton level cross section in eq. 3.2 is $\frac{d^2\sigma^i}{dQ^2 dv}(z, Q^2)$ and it can be expanded in a power series of the strong coupling constant to compute the higher order QCD corrections.

3.1 The Drell-Yan process

In 1970 hadron-hadron collision was being studied at BNL [45], where the process investigated was collision of protons of energies 22-29 GeV giving rise to muon pair of mass 1-6.7 GeV. One of the interesting features of the data was the rapid fall-off of the cross section with muon-pair mass. Drell and Yan [1] explained this fall based on a hadron-hadron collision process giving rise to massive lepton pairs; this process is now popularly known as the Drell-Yan (DY) process. It takes place as:

$$H_1(P_1) + H_2(P_2) \rightarrow l^+(l_1) + l^-(l_2) + X(P_X). \quad (3.5)$$

P_1, P_2 are the momentum of the hadrons and l_1, l_2 are the momentum of the leptons. X denotes any final inclusive state which is allowed by the conservation of quantum numbers.

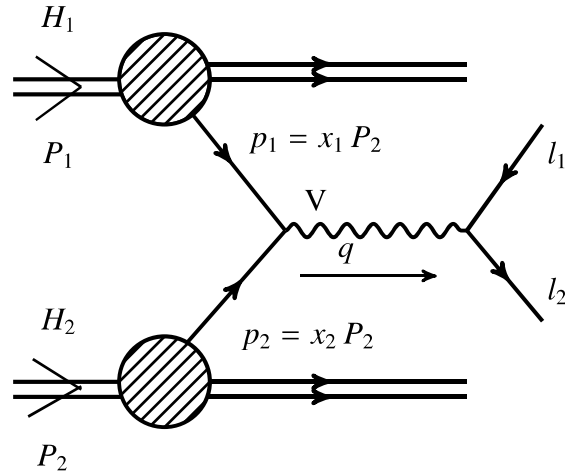


Figure 3.2: The Drell-Yan process

Fig. 3.2 depicts the DY process as realized through parton model picture. According to the parton model, a quark from one hadron annihilates an antiquark from another hadron, giving rise to a vector boson (V), which subsequently decays to a lepton pair. The differential cross section for the DY process in terms of the parton model can be quantified in the following way: We consider the hadronic collision process in eq. 3.5 with a virtual photon ($V = \gamma$) of momentum q in the intermediate state. The invariant mass squared of the final state lepton pair is Q^2 and the centre of mass energy of the colliding protons is \sqrt{S} . These variables are related to one another in the following way

$$S = (P_1 + P_2)^2, \quad \tau = \frac{Q^2}{S}, \quad Q^2 = q^2. \quad (3.6)$$

The DY cross section reads as follows

$$\begin{aligned} \frac{d\sigma}{dQ^2}(\tau, Q^2) = & \sum_{i,j} \int_0^1 dx_1 \int_0^1 dx_2 \int_0^1 dz \delta(\tau - z x_1 x_2) \\ & x_1 f_i^{H_1}(x_1) x_2 f_j^{H_2}(x_2) \frac{d\sigma^{i,j}}{dQ^2}(z, Q^2) \end{aligned} \quad (3.7)$$

where we have two PDF's coming due to two partons taking part in the collision; $z = \frac{Q^2}{S}$ and \sqrt{S} are the scaling variable and the center of mass energy at the partonic level respectively. The partonic cross section is represented by $\frac{d\sigma^{i,j}}{dQ^2}(z, Q^2)$. If Q^2 is large, then

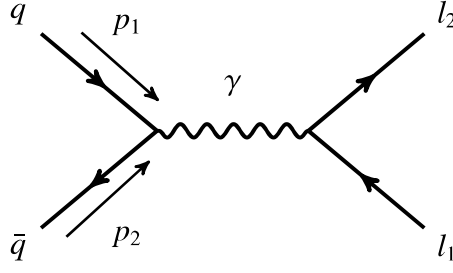


Figure 3.3: Lowest order DY process

by Heisenberg uncertainty principle, the time of interaction of the quark and the anti-quark is short and the partons participating in the reaction cannot interact with the other partons present in the proton. The light quarks and the gluons which do not take part in the reaction come out as final state hadrons. While measuring the cross section of the DY process, we sum over all these final state hadrons, denoted by X in eq. 3.5.

A number of predictions can be made from the DY formalism, which includes a) scaling behavior of the differential cross sections *w.r.t* the Feynman variable x_F or rapidity y , b) dependence of cross section on atomic number, c) angular distribution of the decay products. There have been large number of experimental measurements conducted over all these years and fair consistency with the predictions have been reported.

In addition to photon, W and Z ($V = W, Z$) boson can also appear in the intermediate stage of the DY process. The processes take place as follows

$$p\bar{p} \rightarrow W \rightarrow l\bar{\nu}_l + X, \quad p\bar{p} \rightarrow Z \rightarrow f\bar{f} + X. \quad (3.8)$$

The experimental signatures involve two high p_T leptons as a result of the decay of Z boson or a single high p_T lepton and missing transverse energy in the case of W boson. The W and Z bosons were discovered in the UA1 and UA2 collaborations at the CERN [15, 16]. The DY process is a very important experimental tool due to its high production rate and clean experimental final state, which lead to the determination the electroweak model parameters. Measurements of the W boson production at the Tevatron [46] resulted

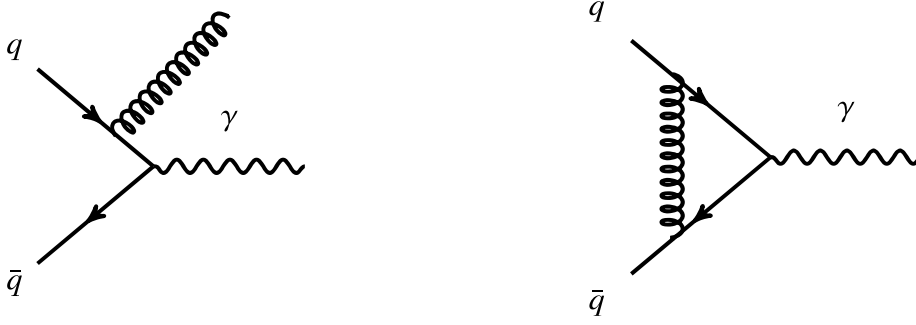
in an accurate determination of the W mass and width.

The partonic cross section in eq. 3.7 can be realized through fig. 3.3 with $V = \gamma$. We call it as a leading order process ($O(\alpha_{em}^2)$) as we shall see later that this is lowest order diagram that appears when the cross section is expanded in a perturbative series of the strong coupling constant a_s . The value of the cross section is [47]

$$\begin{aligned} \frac{d\sigma}{dQ^2} \Big|_{\gamma}(\tau, Q^2) = & \tau \frac{4\pi\alpha_{em}^2}{3Q^4N} \sum_q e_q^2 \int_0^1 dx_1 \int_0^1 dx_2 \int_0^1 dz \delta(\tau - z x_1 x_2) \\ & \left\{ f_q^{H_1}(x_1) f_{\bar{q}}^{H_2}(x_2) + f_{\bar{q}}^{H_1}(x_1) f_q^{H_2}(x_2) \right\} \delta(1 - z) \end{aligned} \quad (3.9)$$

where N is the number of colors in QCD, α_{em} is the fine structure constant. The charge of quark is denoted by e_q . The term $1/Q^4$ on the right hand side explains the rapid fall of cross section with the increase in invariant mass of the lepton pair.

However the leading order computation of the DY process is not a good approximation, due to the discrepancy reported between the theoretical predictions and the experimental data; namely the NA3 group [48] found it in 1979 and this was also concluded by other fixed target experiments. The experimental result for cross section was larger by a factor of 2.3 ± 0.5 than the theoretical prediction [48]. Around that time the spectacular one loop QCD ($O(a_s)$) corrections to the DY process were being performed by different groups [49–53]. The $O(a_s)$ corrected cross section of the DY process was then compared against the data from the CERN and the FERMILAB and it was concluded that the discrepancy seen before was due to the unavailable one loop QCD corrections. This highlights the necessity of higher order QCD corrections in process like the DY. Some of the diagrams contributing to one loop are shown in fig. 3.4. We shall elaborate on these diagrams and the associated divergences in the next paragraph. However the one loop corrections turned out to be large, $\sim 70\%$ for fixed target energies, which questioned the reliability of the perturbative series. Therefore to strengthen the one loop corrections it was necessary to compute the two loop (NNLO) corrections to the DY process [54]. The NNLO cross

Figure 3.4: Sample diagrams contributing to $O(a_s)$ QCD corrections

section for Z boson production was found to be in good agreement with the existing UA2 [55] experimental data. For W boson production, the theoretical predictions were found to lie systematically above the UA2 data. There have been attempts to go beyond NNLO; the NNLL resummation was reported in [56]. Using Sudakov resummation of QCD amplitudes, RG invariance and mass factorization theorem, the $N^3\text{LO}$ soft virtual QCD corrections for the DY was finally achieved; for inclusive production see [57, 58] for rapidity distribution see [30].

Finally we describe the type of divergences that appear beyond the leading order in the DY process. As we can see from fig. 3.4 there are two classes of diagrams that can appear. One of them contain a virtual gluon loop, the type we encountered in sec. 2.3. This gives rise to the UV divergences and to eliminate them we have to renormalize the strong coupling constant after regulating the theory in dimensional regularization ($d = 4 + \epsilon$). As a result a unphysical renormalization scale, μ_R enters into pQCD calculations. There are two more singularities that can arise from the loop diagram. The momentum of the massless virtual particle in the loop runs from 0 to ∞ and in the limit when the momentum $\rightarrow 0$, there are divergences which are known as soft singularities. In other words soft singularities arise due to massless gauge particles. In addition the particle in the loop can become parallel to one of the external massless partons, which can give rise collinear singularity. As shown in fig. 3.5 in the center of mass frame of the quark-antiquark system, the gluon is emitted at an angle θ with respect to the quark. Collinear singularity arises when $\theta \rightarrow 0$. These two singularities, the soft and collinear, together are called infrared (IR) divergences.

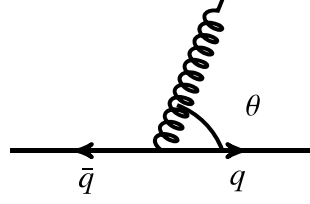


Figure 3.5: Gluon emitted at an angle θ in center of mass frame of the quark-antiquark system.

The second class of diagram consist of one real emission from the initial state as shown in fig. 3.4. When multiplied by its own conjugate it will contribute to $O(a_s)$. This diagram can give rise to both soft and collinear singularities. According to the KLN theorem [59, 60] the soft and collinear singularities from virtual diagrams cancel against the soft divergences from the real emission ones, when the two classes of diagram are added together. To cancel the initial state collinear divergence, we have to perform mass factorization [61]. The process of mass factorization introduces an additional scale into the computation, μ_F ; hence the UV and IR finite result contains two unphysical scale dependencies: μ_R and μ_F . At a particular fixed order in the perturbative expansion, if the cross section varies considerably *w.r.t* to these scales, then it indicates the need for higher order QCD radiative corrections. As we saw before, this was one of the reason that prompted the NNLO corrections to the DY cross section.

The DY process in the SM is now one of the widely studied and understood areas in particle physics. It has established itself as one of the benchmark processes to probe physics at TeV energies at the colliders, namely earlier at the Tevatron and now at the LHC. Because of its large cross-section and small systematic uncertainties, DY production also serves as luminosity monitor [62] at the LHC. Its clean electromagnetic probe is best suited for the search of any new physics beyond the SM (BSM). An excess rate over the SM in this channel will potentially indicate the signature of BSM physics. Drell-Yan is the potential background for processes involving Z' or W' and also for spin-2/graviton searches. In this thesis using the DY process, we shall study the scenario where a massive spin-2 particle can appear in the intermediate stages, which then subsequently decays to a lepton pair.

4 Beyond the Standard Model

The SM of particle physics has been very successful in explaining the phenomenon that take place at the subatomic level. We saw in the previous chapters how the theory was built over years of perseverance of physicists from all over the world. The final milestone was achieved in 2012 when the Higgs boson was discovered at the LHC [17, 18]. However the theory has many limitations: it does not have dark matter candidate to explain the relic abundance in the early universe; it fails to explain the observed baryon asymmetry in our universe; it lacks a proper description of the phenomenon of neutrino oscillations. In addition the theory cannot incorporate properly the fourth force of nature: gravitational force. These above mentioned evidences served as compelling reasons to construct theories beyond the SM. In the next section we shall concentrate on how extra-dimensional models incorporate gravity and thereby allow it to interact with the SM fields which can lead to observable signatures at the colliders. We shall concentrate on the DY production of a massive spin-2 particle which subsequently decays to a lepton pair. We have seen earlier that QCD corrections play an important role in the SM DY process; hence we shall compute second order QCD corrections in models of TeV scale gravity. We describe them in details in the next two sections.

4.1 Field theories with extra dimension

Unification of all the four forces that exist in nature has been a dream of physicists for quite a long time. Although the strong, weak and electromagnetic forces have been combined together and they are explained by the SM, there is still no successful theory in which gravity can be described at par with the three forces. This inability arises due to the huge difference between the two fundamental energy scales in nature: electroweak scale (m_W) $\sim 10^3$ GeV and the Plank scale (M_P) $\sim 10^{19}$ GeV. In other words at the subatomic scales, gravitational force is weaker compared to other three forces in the SM. In order to explain this hierarchy, proposals of extra-dimensional models have been made with the aim to allow gravity interact with the SM fields. The idea to unify the forces in nature dates back to early nineteenth century when Kaluza [63] and Klein [64] tried to combine electromagnetism with general relativity by proposing a 5-d model, where one spatial dimension was compactified on a circle. A higher-dimensional field theory can be reduced to 4-dimension after the extra dimensions are compactified. This is called Kaluza-Klein reduction. We illustrate this in the next section with an example of a free scalar field.

4.1.1 Kaluza Klein reduction

The action representing a free massless scalar field in 5-d reads as follow [65]

$$S = \int d^5x \frac{1}{2} \partial_M \phi(x^\mu, z) \partial^M \phi(x^\mu, z). \quad (4.1)$$

In above, z is the extra dimension compactified on a circle of radius R , $M = 0, 1, 2, 3, 5$ and $\mu \in [0, 3]$. The measure of the integral is $d^5x = d^4x dz$. The field ϕ is periodic along z with $\phi(x^\mu, z + 2\pi R) = \phi(x^\mu, z)$. We perform a Fourier expansion of the scalar field along

the extra dimension,

$$\phi(x^\mu, z) = \frac{1}{\sqrt{2\pi R}} \sum_{l=-\infty}^{\infty} \phi^{(l)}(x^\mu) e^{i \frac{l}{R} z} \quad (4.2)$$

where the field is subjected to the constraint $(\phi^{(l)})^\dagger = \phi^{(-l)}$. Putting the expansion in the above equation into the action in eq. 4.1 and performing the z integration we get:

$$S = \int d^4x \left(\frac{1}{2} \partial_\mu \phi^{(0)} \partial^\mu \phi^{(0)} + \sum_{l=1}^{\infty} \left[\partial_\mu \phi^{(l)\dagger} \partial^\mu \phi^{(l)} - \frac{l^2}{R^2} \phi^{(l)\dagger} \phi^{(l)} \right] \right). \quad (4.3)$$

Thus by compactifying the extra dimension and then performing a Fourier expansion along it, we notice that a 5-d theory has been reduced to 4 dimensions. The first term represents the 0'th mode of the Fourier expansion, which remains massless in 4 dimension. The second term describes an infinite series of states, popularly called the Kaluza-Klein (KK) tower of states, with each state having a mass $m = l/R$. For higher dimension compactified on a torus, the generalization is straightforward and the masses of the KK states are as follows:

$$m_{l_5, l_6, \dots}^2 = \frac{l_5^2}{R_5^2} + \frac{l_6^2}{R_6^2} + \frac{l_7^2}{R_7^2} + \dots \quad (4.4)$$

with R_i is the radius of the i 'th compact dimension.

The KK reduction can be similarly carried out for a gauge field in 5-d as well as gravitational field in $d = n + 4$ dimensions. To describe KK reduction for gravitational scenario, we consider an action describing coupled gravity + gauge + matter systems in $d = 4 + n$ dimensions. Since gravity is a non-renormalizable theory, an UV cut-off has to be chosen, which can be related to the compactification radius of the extra dimensions. On performing a mode expansion, the $l = 0$ mode correspond to m massless vectors, $m(m + 1)/2$ massless scalars and one massless graviton. On the other hand for the mode $l \neq 0$, we get for each KK level, one massive spin-2 tensor, $m - 1$ massive vectors and $m(m - 1)/2$ massive scalars.

In the next section we shall describe how extra-dimensional models try to solve the hierarchy problem and try to unify SM with gravity.

4.1.2 The ADD model

One of the extra dimensional models addressing the problem of hierarchy was given by Arkani-Hamed, Dimopoulos and Dvali (ADD), popularly called the ADD model [66]. Here the authors consider the experimentally determined electroweak scale as the mass scale of their model and the UV cutoff was set equal to m_W . In order to reduce the huge energy gap between the scales M_P and m_W , n extra spatial dimensions were introduced which were compactified in a torus of radius R . Denoting the Planck scale in the $4 + n$ dimensional theory as M_S , the following relation between M_P and M_S was shown to hold:

$$M_P^2 \sim M_S^{n+2} R^n \quad (4.5)$$

By taking R to be large the scale M_S can be lowered down to a few TeV and the hierarchy problem can be avoided.

In the ADD model the SM fields are constrained to a 3-brane while the gravitons propagate in the $4 + n$ dimensional bulk. Then the size of the extra dimensions is only constrained by the length scales to which the gravitational inverse square law has been experimentally tested, which are currently probing the sub-millimeter range. To reduce the higher dimensional theory to four dimensions, KK reduction is performed which results in a tower of KK modes. Among these, the zeroth mode gives rise to massless particles, while the rest of the modes, which are infinite in number gives rise to massive particles. The KK modes interact with the SM fields through the energy momentum tensor, $T^{\mu\nu}$, with coupling strength of each interaction being proportional to $1/M_P$ (we consider this as κ). In the effective theory all the KK modes are summed over and due to high multiplicity of these modes, the effective coupling becomes of the order of $1/M_S$. This enhanced coupling provides viable signatures of the graviton KK modes at colliders.

Most of the extra-dimensional models assume the coupling of the spin-2 particle to the

SM fields to be same. In other words the gauge and fermionic fields couple to the spin-2 particle with an universal coupling strength. In the next chapter we shall study the phenomenology of such a scenario in great details. However this is not the most general way in which the spin-2 can interact to the SM particles. There can be a generic massive spin-2 particle coupling differently to the fermionic and gauge fields. We shall also investigate such a scenario and present the phenomenological impact up to NNLO level in QCD.

In the next section we describe the general theoretical concepts required for computing the differential distribution of a lepton pair production from the decay of a massive spin-2 particle, where the latter appears in the intermediate stages in DY type of process. We describe the universal coupling scenario in the next section; the theory for non-universal case will be presented later in chapter 6.

4.2 Theoretical Framework

4.2.1 The effective action

We assume the massive spin-2 particle interacts universally with the SM fields. Since we are interested in the QCD regime of the SM we shall consider the coupling of the QCD energy-momentum tensor to the spin-2 field. The action describing such an interaction is

$$S = S_{\text{SM}} + S_h - \frac{\kappa}{2} \int d^4x T_{\mu\nu}^{\text{QCD}}(x) h^{\mu\nu}(x) \quad (4.6)$$

where, S_{SM} and S_h represent the actions of the SM and spin-2 fields, respectively. $T_{\mu\nu}^{\text{QCD}}$ is the conserved energy momentum tensor of QCD which is given by

$$T_{\mu\nu}^{\text{QCD}} = -g_{\mu\nu} \mathcal{L}_{\text{QCD}} - F_{\mu\rho}^a F_{\nu}^{a\rho} - \frac{1}{\xi} g_{\mu\nu} \partial^\rho (A_\rho^a \partial^\sigma A_\sigma^a) + \frac{1}{\xi} (A_\nu^a \partial_\mu (\partial^\sigma A_\sigma^a) + A_\mu^a \partial_\nu (\partial^\sigma A_\sigma^a))$$

$$\begin{aligned}
& + \frac{i}{4} \left[\bar{\psi} \gamma_\mu (\vec{\partial}_\nu - ig_s T^a A_\nu^a) \psi - \bar{\psi} (\vec{\partial}_\nu + ig_s T^a A_\nu^a) \gamma_\mu \psi + \bar{\psi} \gamma_\nu (\vec{\partial}_\mu - ig_s T^a A_\mu^a) \psi \right. \\
& \left. - \bar{\psi} (\vec{\partial}_\mu + ig_s T^a A_\mu^a) \gamma_\nu \psi \right] + \partial_\mu \bar{\omega}^a (\partial_\nu \omega^a - g_s f^{abc} A_\nu^c \omega^b) \\
& + \partial_\nu \bar{\omega}^a (\partial_\mu \omega^a - g_s f^{abc} A_\mu^c \omega^b). \tag{4.7}
\end{aligned}$$

In above g_s is the strong coupling constant and T^a , f^{abc} are the Gell-Mann matrices and structure constants of SU(N) gauge theory respectively. ξ is the gauge fixing parameter which is set to 1 as we have performed our computation in the Feynman gauge. The Feynman rules of the theory are presented in Appendix 11.1.

4.2.2 Invariant Lepton Pair Mass Distribution $d\sigma/dQ^2$

We consider the DY production of a lepton pair, l^+ and l^- , given by

$$H_1(P_1) + H_2(P_2) \rightarrow l^+(l_1) + l^-(l_2) + X(P_X), \tag{4.8}$$

where H_1 and H_2 are the two incoming hadrons and X takes into account all possible partonic emissions in the initial state. The four momenta of the corresponding particles are represented inside the parenthesis. In the QCD improved parton model we can express the hadronic cross section in terms of the partonic one in the following way:

$$\begin{aligned}
2S \frac{d\sigma^{H_1 H_2}}{dQ^2}(\tau, Q^2) &= \sum_{ab=q, \bar{q}, g} \int_0^1 dx_1 \int_0^1 dx_2 f_a^{H_1}(x_1) f_b^{H_2}(x_2) \\
&\times \int_0^1 dz \, 2\hat{s} \frac{d\hat{\sigma}^{ab}}{dQ^2}(z, Q^2) \delta(\tau - zx_1 x_2). \tag{4.9}
\end{aligned}$$

In the above equation S is the square of the hadronic center of mass energy which can be related to the corresponding partonic one, \hat{s} , through $\hat{s} = x_1 x_2 S$. Q^2 is the invariant mass of the final state leptonic pair *i.e.* $m_{l^+ l^-}^2 = Q^2$. f_a and f_b are the parton distribution functions

of the initial state partons a and b , respectively. The other parameters are defined as

$$\tau \equiv \frac{Q^2}{S}, \quad z \equiv \frac{Q^2}{\hat{s}} \quad \text{and} \quad \tau = x_1 x_2 z. \quad (4.10)$$

The underlying partonic process corresponding to the hadronic one (4.8) is

$$a(p_1) + b(p_2) \rightarrow j(q) + \sum_{i=1}^m X_i(q_i) \rightarrow l^+(l_1) + l^-(l_2) + \sum_{i=1}^m X_i(q_i)$$

where, j can be photon (γ^*), Z-boson (Z) or spin-2 particle. The DY cross section can be factorized in terms of partonic ($ab \rightarrow j$) and leptonic ($j \rightarrow l^+ l^-$) parts as follows:

$$\begin{aligned} 2\hat{s} \frac{d\hat{\sigma}^{ab}}{dQ^2} = & \left(\int \prod_i^m \frac{d^n q_i}{(2\pi)^n} 2\pi \delta^+(q_i^2) \right) \left(\int \frac{d^n l_1}{(2\pi)^n} 2\pi \delta^+(l_1^2) \right) \times \left(\int \frac{d^n l_2}{(2\pi)^n} 2\pi \delta^+(l_2^2) \right) \\ & (2\pi)^n \times \delta^{(n)} \left(p_1 + p_2 - q - \sum_{i=1}^m q_i \right) 2\pi \delta^+(q^2 - Q^2) \\ & \left(\frac{1}{2\pi} \sum_{j,j'=\gamma^*,Z,h} |\mathcal{M}^{ab \rightarrow jj' + \sum_{i=1}^m q_i}|^2 \cdot P_j(q) \cdot P_{j'}^*(q) \cdot |\mathcal{M}_L^{jj' \rightarrow l^+ l^-}|^2 \right) \end{aligned} \quad (4.11)$$

where in above $|\mathcal{M}^{ab \rightarrow jj' + \sum_{i=1}^m q_i}|^2$ is the partonic cross section while $|\mathcal{M}_L^{jj' \rightarrow l^+ l^-}|^2$ is the leptonic contribution. $j \neq j'$ reflects the interference terms between the channel j and j' . In the above equation, the sum over Lorentz indices between matrix element squared and the propagators is implicit through a symbol ‘dot product’. Introducing the identity

$$\int \frac{d^n q}{(2\pi)^n} \times (2\pi)^n \delta^n(q - l_1 - l_2) = 1 \quad (4.12)$$

and noting that

$$\begin{aligned} \int dPS_m &= \int \prod_i^m \frac{d^n q_i}{(2\pi)^n} 2\pi \delta^+(q_i^2) \\ \int dPS_m &\times \int \frac{d^n q}{(2\pi)^n} 2\pi \delta^+(q^2 - Q^2) (2\pi)^n \times \delta^{(n)} \left(p_1 + p_2 - q - \sum_{i=1}^m q_i \right) \\ &= \int dPS_{m+1} \end{aligned} \quad (4.13)$$

Thus we arrive at the following formula for partonic cross section

$$2\hat{s}\frac{d\hat{\sigma}^{ab}}{dQ^2} = \frac{1}{2\pi} \sum_{j,j'=\gamma^*,Z,h} \int dPS_{m+1} |\mathcal{M}^{ab \rightarrow jj'}|^2 \cdot P_j(q) \cdot P_{j'}^*(q) \cdot \mathcal{L}^{jj' \rightarrow l^+ l^-}(q) \quad (4.14)$$

with $\mathcal{L}^{jj' \rightarrow l^+ l^-}$ is given by

$$\mathcal{L}^{jj' \rightarrow l^+ l^-}(q) = \prod_{i=1}^2 \left(\frac{d^n l_i}{(2\pi)^n} 2\pi \delta^+(l_i^2) \right) \times (2\pi)^n \delta^n(q - l_1 - l_2) |\mathcal{M}^{jj' \rightarrow l^+ l^-}|^2. \quad (4.15)$$

In eq. 4.11 the propagators are

$$\begin{aligned} P_{\gamma,\mu\nu}(q) &= -\frac{i}{Q^2} \eta_{\mu\nu} \equiv \eta_{\mu\nu} \tilde{P}_\gamma(Q^2), \\ P_{Z,\mu\nu}(q) &= -\frac{i}{(Q^2 - M_Z^2 - iM_Z \Gamma_Z)} \eta_{\mu\nu} \equiv \eta_{\mu\nu} \tilde{P}_Z(Q^2), \\ P_{h,\mu\nu\rho\sigma}(q) &= \mathcal{D}(Q^2) B_{\mu\nu\rho\sigma}(q) \equiv B_{\mu\nu\rho\sigma}(q) \tilde{P}_h(Q^2) \end{aligned} \quad (4.16)$$

where

$$\begin{aligned} B_{\mu\nu\rho\sigma}(q) &= \left(\eta_{\mu\rho} - \frac{q_\mu q_\rho}{q \cdot q} \right) \left(\eta_{\nu\sigma} - \frac{q_\nu q_\sigma}{q \cdot q} \right) + \left(\eta_{\mu\sigma} - \frac{q_\mu q_\sigma}{q \cdot q} \right) \left(\eta_{\nu\rho} - \frac{q_\nu q_\rho}{q \cdot q} \right) \\ &\quad - \frac{2}{n-1} \left(\eta_{\mu\nu} - \frac{q_\mu q_\nu}{q \cdot q} \right) \left(\eta_{\rho\sigma} - \frac{q_\rho q_\sigma}{q \cdot q} \right), \end{aligned} \quad (4.17)$$

$\eta_{\mu\nu} = \text{diag}[1, -1, -1, -1, \dots]$ and $\mathcal{D}(Q^2)$, the summation over the virtual Kaluza-Klein (KK) modes in the time like propagators [67] in $(4+d)$ -dimensions, is

$$\mathcal{D}(Q^2) = 16\pi \left(\frac{Q^{d-2}}{\kappa^2 M_s^{d+2}} \right) I \left(\frac{M_s}{Q} \right). \quad (4.18)$$

In the UV region the integral I is regulated by a cutoff which is of the order of M_s [67]. This cutoff sets the limit on the applicability of the effective theory. For the DY process,

this implies $Q < M_S$. The summation over the non-resonant KK modes yields

$$I(\omega) = - \sum_{k=1}^{d/2-1} \frac{1}{2k} \omega^{2k} - \frac{1}{2} \log(\omega^2 - 1), \quad d = \text{even}, \quad (4.19)$$

$$I(\omega) = - \sum_{k=1}^{(d-1)/2} \frac{1}{2k-1} \omega^{2k-1} + \frac{1}{2} \log\left(\frac{\omega+1}{\omega-1}\right), \quad d = \text{odd}, \quad (4.20)$$

where $\omega = M_S/Q$.

In order to compute the hadronic cross section in eq. 4.9 we have to compute the leptonic part and partonic part separately and then fold the resulting partonic cross section in eq. 4.14 with the appropriate PDF's. The leptonic part turns out to be

$$\begin{aligned} \mathcal{L}^{jj' \rightarrow l^+ l^-}(q) &= g_{\mu\nu}(q) L_{jj'}(Q^2), \quad jj' = \{\gamma\gamma, ZZ, \gamma Z\}, \\ \mathcal{L}^{hh \rightarrow l^+ l^-}(q) &= B_{\mu\nu\rho\sigma}(q) L_{hh}(Q^2), \end{aligned} \quad (4.21)$$

where

$$\begin{aligned} L_{hh}(Q^2) &= Q^4 \frac{\kappa^2}{640\pi}, & L_{ZZ}(Q^2) &= Q^2 \frac{2\alpha}{3c_w^2 s_w^2} \left((g_e^V)^2 + (g_e^A)^2 \right), \\ L_{\gamma Z}(Q^2) &= -Q^2 \frac{2\alpha g_e^V}{3c_w s_w}, & L_{\gamma\gamma}(Q^2) &= Q^2 \frac{2\alpha}{3}, \\ \text{and } g_{\mu\nu}(q) &\equiv \eta_{\mu\nu} - \frac{q_\mu q_\nu}{q \cdot q}. \end{aligned} \quad (4.22)$$

In the above equation, α is the fine structure constant, $c_w \equiv \cos \theta_w$, $s_w \equiv \sin \theta_w$ and θ_w is the weak mixing angle. g_f^V and g_f^A can be expressed in terms of charge Q_f of the fermions (f) i.e. quarks, leptons and weak isospin T_f^3 :

$$g_f^V = \frac{1}{2} T_f^3 - s_w^2 Q_f, \quad g_f^A = -\frac{1}{2} T_f^3. \quad (4.23)$$

Hence, the hadronic cross section in eq. 4.9 can be rewritten as

$$2S \frac{d\sigma^{H_1 H_2}}{dQ^2} = \frac{1}{2\pi} \sum_{j,j'=\{\gamma^*, Z, h\}} \tilde{P}_j(Q^2) \tilde{P}_{j'}^*(Q^2) L_{jj'}(Q^2) W_{jj'}^{H_1 H_2}(\tau, Q^2) \quad (4.24)$$

where, the hadronic structure function W is

$$W_{jj'}^{H_1 H_2}(\tau, Q^2) = \sum_{a,b,j,j'} \int dx_1 \int dx_2 f_a^{H_1}(x_1) f_b^{H_2}(x_2) \int dz \delta(\tau - zx_1 x_2) \\ \times \int dPS_{m+1} |\mathcal{M}^{ab \rightarrow jj'}|^2 T_{jj'}(q) \quad (4.25)$$

with

$$T_{jj'}(q) = \begin{cases} g_{\mu\nu}(q), & jj' = \gamma\gamma, \gamma Z, ZZ \\ B_{\mu\nu\rho\sigma}(q), & jj' = hh. \end{cases} \quad (4.26)$$

To obtain the differential distribution in eq. 4.24 we need to compute the hadronic structure function $W_{jj'}$ in eq. 4.25 which further requires evaluation of the integrals in a suitable frame over dPS_{m+1} and dz after substituting the matrix element squared $|\mathcal{M}^{ab \rightarrow jj'}|^2 T_{jj'}(q)$. We define the bare partonic coefficient function $\hat{\mathcal{A}}_{ab}^{jj'}(z, Q^2, 1/\epsilon)$ as following

$$\hat{\mathcal{A}}_{ab}^{jj'}(z, Q^2, 1/\epsilon) = C_{jj'} \int dPS_{m+1} |\mathcal{M}^{ab \rightarrow jj'}|^2 T_{jj'}(q) \quad (4.27)$$

where

$$C_{jj'} = \begin{cases} \frac{1}{e^2} & jj' = \gamma\gamma, ZZ, \gamma Z, \\ \frac{1}{Q^2 \kappa^2} & jj' = hh. \end{cases} \quad (4.28)$$

There are two different class of processes which contributes to the partonic cross section: first one happens through a virtual photon (γ^*) or a Z-boson whereas the second one contains a spin-2 particle in the intermediate state. Interestingly, on performing the phase space integration, the interference term between the two classes of diagrams up to NNLO

identically vanishes, this was earlier noted to NLO [68]. This can be realized as follows: We consider the partonic processes where 1. a massive spin-2 particle is produced and 2. a photon/Z boson is produced and take the interference between these two processes. Then after the phase space integrations, the resulting expression will be a third rank tensor say $P^{\mu\nu\sigma}$. Now the only quantities available from which we can construct such a third rank tensor are $\eta_{\mu\nu}$ and q_σ ($q \cdot q \neq 0$). There can be no such $P^{\mu\nu\sigma}$ constructed out of $\eta_{\mu\nu}$ and q_σ which satisfies $q_\mu P^{\mu\nu\sigma} = 0$. This is also true for Levi-Civita tensor which appears in the case of the electro-weak vertices. This can also be checked by explicit computation. Therefore, our result contains no contribution from the interference terms.

In order to compute the matrix elements in eq. 4.25 we have to expand the amplitudes in a perturbative series of the strong coupling constant. For a spin-2 particle appearing as an intermediate state, at LO we can have gluon initiated process as well as quark initiated one. Thus at LO (see fig. 4.1)

$$q + \bar{q} \rightarrow \gamma^*/Z/h, \quad g + g \rightarrow h. \quad (4.29)$$

Beyond LO, the contributions arise from virtual as well as real emission diagrams. At



Figure 4.1: Leading order processes for the DY

NLO in QCD, we have

$$\begin{aligned}
q + \bar{q} &\rightarrow \gamma^*/Z/h + \text{one loop}, \\
q + \bar{q} &\rightarrow \gamma^*/Z/h + g, \\
g + g &\rightarrow h + g, \\
g + q &\rightarrow \gamma^*/Z/h + q, \\
g + g &\rightarrow h + \text{one loop}, \\
g + \bar{q} &\rightarrow \gamma^*/Z/h + \bar{q}.
\end{aligned} \tag{4.30}$$

Similarly at NNLO in QCD, the contributions can arise from three different categories: double-real emissions, real-virtual and double virtual diagrams. The processes which belong to the double-real emissions are

$$\begin{aligned}
q + \bar{q} &\rightarrow \gamma^*/Z^*/h + q + \bar{q}, & q + \bar{q} &\rightarrow \gamma^*/Z/h + g + g, \\
g + g &\rightarrow h + g + g, & g + g &\rightarrow \gamma^*/Z/h + q + \bar{q}, \\
g + q &\rightarrow \gamma^*/Z/h + g + q, & g + \bar{q} &\rightarrow \gamma^*/Z/h + g + \bar{q}, \\
q + q &\rightarrow \gamma^*/Z/h + q + q, & q_1 + q_2 &\rightarrow \gamma^*/Z/h + q_1 + q_2, \\
q_1 + \bar{q}_2 &\rightarrow \gamma^*/Z/h + q_1 + \bar{q}_2.
\end{aligned} \tag{4.31}$$

The processes which contribute in real-virtual are

$$\begin{aligned}
q + \bar{q} &\rightarrow \gamma^*/Z/h + g + \text{one loop}, & g + g &\rightarrow h + g + \text{one loop}, \\
g + q &\rightarrow \gamma^*/Z/h + q + \text{one loop}, & g + \bar{q} &\rightarrow \gamma^*/Z/h + \bar{q} + \text{one loop}
\end{aligned} \tag{4.32}$$

and the pure double virtual diagrams are

$$\begin{aligned}
q + \bar{q} &\rightarrow \gamma^*/Z/h + \text{two loop}, \\
g + g &\rightarrow h + \text{two loop}.
\end{aligned} \tag{4.33}$$

As we have discussed earlier in section 2.3 the evaluation of virtual diagrams give rise

to UV divergences. In addition IR singularities also arises from loop diagrams, when the virtual particle can become soft or parallel to one of the external particles. Moreover IR singularities also arise from real emission diagrams which we already discussed in section 3.1. We regulate the UV as well as IR divergences using dimensional regularisation where the space-time dimensions n is chosen to be equal to $4 + \epsilon$. All the singularities manifest themselves as the poles in dimensional regularization parameter ϵ : $1/\epsilon^\alpha$ with $\alpha \in [1, 4]$ up to NNLO. As we have already seen through eq. 2.5 and 2.6 in $\overline{\text{MS}}$, the UV poles are removed through strong coupling constant renormalisation using

$$\hat{a}_s S_\epsilon = \left(\frac{\mu^2}{\mu_R^2} \right)^{\epsilon/2} Z_{a_s} a_s \quad (4.34)$$

where, the renormalization constant Z_{a_s} up to $O(a_s^5)$ is given by

$$\begin{aligned} Z_{a_s} = & 1 + a_s \left[\frac{2}{\epsilon} \beta_0 \right] + a_s^2 \left[\frac{4}{\epsilon^2} \beta_0^2 + \frac{1}{\epsilon} \beta_1 \right] + a_s^3 \left[\frac{8}{\epsilon^3} \beta_0^3 + \frac{14}{3\epsilon^2} \beta_0 \beta_1 + \frac{2}{3\epsilon} \beta_2 \right] \\ & + a_s^4 \left[16 \frac{1}{\epsilon^4} \beta_0^4 + \frac{46}{3\epsilon^3} \beta_0^2 \beta_1 + \frac{3}{2\epsilon^2} \beta_1^2 + \frac{10}{3\epsilon^2} \beta_0 \beta_2 + \frac{1}{2\epsilon} \beta_3 \right] \\ & + a_s^5 \left[\frac{32}{\epsilon^5} \beta_0^5 + \frac{652}{15\epsilon^4} \beta_0^3 \beta_1 + \frac{157}{15\epsilon^3} \beta_0 \beta_1^2 + \frac{172}{15} \epsilon^3 \beta_0^2 \beta_2 + \frac{34}{15\epsilon^2} \beta_1 \beta_2 \right. \\ & \left. + \frac{13}{5\epsilon^2} \beta_0 \beta_3 + \frac{2}{5\epsilon} \beta_4 \right], \end{aligned} \quad (4.35)$$

and

$$\begin{aligned} S_\epsilon &= \exp [(\gamma_E - \ln 4\pi)\epsilon/2], \quad \gamma_E = 0.5772 \dots, \\ a_s &\equiv a_s(\mu_R^2) \equiv \frac{g_s^2}{16\pi^2}. \end{aligned} \quad (4.36)$$

μ is the scale introduced to keep the unrenormalized strong coupling constant \hat{a}_s dimensionless in n -dimensions. The corresponding renormalization scale is denoted by μ_R . β_i 's are the coefficients of QCD β -function [38, 39, 69–71]. The spin-2 particles couple to the SM ones via $T_{\mu\nu}^{\text{QCD}}$ which is conserved, hence κ is protected from any UV renormalisation. The soft divergences arising from virtual diagrams cancel exactly against the same coming

from real emission ones, thanks to the Kinoshita-Lee-Nauenberg (KLN) theorem [59, 60]. The initial state collinear divergences are removed through mass factorization, performed at the factorization scale μ_F :

$$\hat{\Delta}_{ab}^i(z, Q^2, 1/\epsilon) = \sum_{c,d=q,\bar{q},g} \Gamma_{ca}(z, \mu_F^2, 1/\epsilon) \otimes \Gamma_{db}(z, \mu_F^2, 1/\epsilon) \otimes \Delta_{cd}^i(z, Q^2, \mu_F^2). \quad (4.37)$$

The symbol \otimes stands for the convolution:

$$(f \otimes g)(z) \equiv \int_z^1 \frac{dx}{x} f(x) g\left(\frac{z}{x}\right). \quad (4.38)$$

In eq. 4.37, $\hat{\Delta} \equiv \hat{\sigma}/z$ is the bare partonic coefficient function and the corresponding one after performing the mass factorization is denoted by Δ . Further we have dropped the double index jj' from the partonic coefficient function (see eq. 4.27) because of the vanishing interference terms between the two classes of diagrams and replace it by the single index i instead. The mass factorization kernel in the $\overline{\text{MS}}$ scheme is given by

$$\Gamma_{ab}(z, \mu_F^2, 1/\epsilon) = \sum_{k=0}^{\infty} a_s^k(\mu_F^2) \Gamma_{ab}^{(k)}(z, \mu_F^2, 1/\epsilon)$$

with

$$\begin{aligned} \Gamma_{ab}^{(0)} &= \delta_{ab} \delta(1-z), \\ \Gamma_{ab}^{(1)} &= \frac{1}{\epsilon} P_{ab}^{(0)}(z), \\ \Gamma_{ab}^{(2)} &= \frac{1}{\epsilon^2} \left(\frac{1}{2} P_{ac}^{(0)} \otimes P_{cb}^{(0)} + \beta_0 P_{ab}^{(0)} \right) + \frac{1}{\epsilon} \left(\frac{1}{2} P_{ab}^{(1)} \right). \end{aligned} \quad (4.39)$$

$P_{ab}^{(i)}$ are the Altarelli-Parisi splitting functions [72–76].

Expanding the unrenormalised coefficient function in eq. 4.27 and the mass factorized

one in eq. 4.37 in powers of strong coupling constant as

$$\begin{aligned}\hat{\Delta}_{ab}^i &= \sum_{k=0}^{\infty} \hat{a}_s^k S_{\epsilon}^k \left(\frac{Q^2}{\mu^2} \right)^{k \frac{\epsilon}{2}} \hat{\Delta}_{ab}^{i,(k)}, \\ \Delta_{ab}^i &= \sum_{k=0}^{\infty} a_s^k (\mu_F^2) \Delta_{ab}^{i,(k)}\end{aligned}\quad (4.40)$$

and using eq. 4.39, we can get all the contributions to NNLO arising from all the subprocesses:

$$\begin{aligned}\Delta_{gg}^{i,(0)} &= \hat{\Delta}_{gg}^{i,(0)}, \\ \Delta_{gg}^{i,(1)} &= \hat{\Delta}_{gg}^{i,(1)} - 2\hat{\Delta}_{gg}^{i,(0)} \otimes \Gamma_{gg}^{(1)}, \\ \Delta_{gg}^{i,(2)} &= \hat{\Delta}_{gg}^{i,(2)} + 3\hat{\Delta}_{gg}^{i,(0)} \otimes \Gamma_{gg}^{(1)} \otimes \Gamma_{gg}^{(1)} + 4n_f \hat{\Delta}_{gg}^{i,(0)} \otimes \Gamma_{gq}^{(1)} \otimes \Gamma_{qg}^{(1)} \\ &\quad + 2n_f \hat{\Delta}_{q\bar{q}}^{i,(0)} \otimes \Gamma_{qg}^{(1)} \otimes \Gamma_{\bar{q}g}^{(1)} - 2\hat{\Delta}_{gg}^{i,(1)} \otimes \Gamma_{gg}^{(1)} - 4n_f \hat{\Delta}_{gq}^{i,(1)} \otimes \Gamma_{qg}^{(1)} - 2\hat{\Delta}_{gg}^{i,(0)} \otimes \Gamma_{gg}^{(2)}, \\ \Delta_{q\bar{q}}^{i,(0)} &= \hat{\Delta}_{q\bar{q}}^{i,(0)}, \\ \Delta_{q\bar{q}}^{i,(1)} &= \hat{\Delta}_{q\bar{q}}^{i,(1)} - 2\hat{\Delta}_{q\bar{q}}^{i,(0)} \otimes \Gamma_{q\bar{q}}^{(1)}, \\ \Delta_{q\bar{q}}^{i,(2)} &= \hat{\Delta}_{q\bar{q}}^{i,(2)} + \hat{\Delta}_{gg}^{i,(0)} \otimes \Gamma_{gq}^{(1)} \otimes \Gamma_{g\bar{q}}^{(1)} + 2\hat{\Delta}_{q\bar{q}}^{i,(0)} \otimes \Gamma_{qg}^{(1)} \otimes \Gamma_{g\bar{q}}^{(1)} + 3\hat{\Delta}_{q\bar{q}}^{i,(0)} \otimes \Gamma_{qq}^{(1)} \otimes \Gamma_{\bar{q}\bar{q}}^{(1)} \\ &\quad - 2\hat{\Delta}_{gq}^{i,(1)} \otimes \Gamma_{g\bar{q}}^{(1)} - 2\hat{\Delta}_{q\bar{q}}^{i,(0)} \otimes \Gamma_{qq}^{(2)} - 2\hat{\Delta}_{q\bar{q}}^{i,(1)} \otimes \Gamma_{qq}^{(1)}, \\ \Delta_{gq}^{i,(1)} &= \hat{\Delta}_{gq}^{i,(1)} - \hat{\Delta}_{gg}^{i,(0)} \otimes \Gamma_{gq}^{(1)} - \hat{\Delta}_{q\bar{q}}^{i,(0)} \otimes \Gamma_{\bar{q}g}^{(1)}, \\ \Delta_{gq}^{i,(2)} &= \hat{\Delta}_{gq}^{i,(2)} + 2\hat{\Delta}_{gg}^{i,(0)} \otimes \Gamma_{gg}^{(1)} \otimes \Gamma_{gq}^{(1)} + \hat{\Delta}_{gg}^{i,(0)} \otimes \Gamma_{gq}^{(1)} \otimes \Gamma_{qq}^{(1)} + \hat{\Delta}_{q\bar{q}}^{i,(0)} \otimes \Gamma_{\bar{q}g}^{(1)} \otimes \Gamma_{gg}^{(1)} \\ &\quad + 2\hat{\Delta}_{q\bar{q}}^{i,(0)} \otimes \Gamma_{qq}^{(1)} \otimes \Gamma_{\bar{q}g}^{(1)} - \hat{\Delta}_{gg}^{i,(0)} \otimes \Gamma_{gg}^{(2)} - \hat{\Delta}_{gg}^{i,(1)} \otimes \Gamma_{gq}^{(1)} - \hat{\Delta}_{gq}^{i,(1)} \otimes \Gamma_{gg}^{(1)} \\ &\quad - \hat{\Delta}_{gq}^{i,(1)} \otimes \Gamma_{qq}^{(1)} - \hat{\Delta}_{q\bar{q}}^{i,(0)} \otimes \Gamma_{\bar{q}g}^{(2)} - \hat{\Delta}_{q\bar{q}}^{i,(1)} \otimes \Gamma_{\bar{q}g}^{(1)}, \\ \Delta_{q\bar{q}}^{i,(2)} &= \hat{\Delta}_{q\bar{q}}^{i,(2)} + \hat{\Delta}_{gg}^{i,(0)} \otimes \Gamma_{gq}^{(1)} \otimes \Gamma_{g\bar{q}}^{(1)} + 2\hat{\Delta}_{q\bar{q}}^{i,(0)} \otimes \Gamma_{\bar{q}g}^{(1)} \otimes \Gamma_{gq}^{(1)} - 2\hat{\Delta}_{gq}^{i,(1)} \otimes \Gamma_{g\bar{q}}^{(1)} \\ &\quad - 2\hat{\Delta}_{q\bar{q}}^{i,(0)} \otimes \Gamma_{\bar{q}q}^{(2)}, \\ \Delta_{q_1 q_2}^{i,(2)} &= \hat{\Delta}_{q_1 q_2}^{i,(2)} \otimes \Gamma_{q_1 q_1}^{(0)} + \hat{\Delta}_{gg}^{i,(0)} \otimes \Gamma_{g q_1}^{(1)} \otimes \Gamma_{g q_2}^{(1)} + 2\hat{\Delta}_{q_1 \bar{q}_1}^{i,(0)} \otimes \Gamma_{\bar{q}_1 g}^{(1)} \otimes \Gamma_{g q_2}^{(1)}\end{aligned}$$

$$\begin{aligned}
& -2\hat{\Delta}_{gq_1}^{i,(1)} \otimes \Gamma_{gq_2}^{(1)} - 2\hat{\Delta}_{q_1\bar{q}_1}^{i,(0)} \otimes \Gamma_{\bar{q}_1q_2}^{S,(2)}, \\
\Delta_{q_1\bar{q}_2}^{i,(2)} &= \hat{\Delta}_{q_1\bar{q}_2}^{i,(2)} + \hat{\Delta}_{gq}^{i,(0)} \otimes \Gamma_{gq_1}^{(1)} \otimes \Gamma_{g\bar{q}_2}^{(1)} + 2\hat{\Delta}_{q_1\bar{q}_1}^{i,(0)} \otimes \Gamma_{q_1g}^{(1)} \otimes \Gamma_{g\bar{q}_2}^{(1)} - 2\hat{\Delta}_{gq_1}^{i,(1)} \otimes \Gamma_{g\bar{q}_2}^{(1)} \\
& - 2\hat{\Delta}_{q_1\bar{q}_1}^{i,(0)} \otimes \Gamma_{q_1q_1}^{S,(2)}.
\end{aligned} \tag{4.41}$$

To arrive at the above set of results 4.41, we have made use of

$$\begin{aligned}
\Gamma_{qg} &= \Gamma_{\bar{q}g}, \quad \Gamma_{gq} = \Gamma_{g\bar{q}} \\
\text{and } \Delta_{gq}^i &= \Delta_{g\bar{q}}^i = \Delta_{qg}^i = \Delta_{\bar{q}g}^i
\end{aligned} \tag{4.42}$$

and the presence of the n_f in RHS comes from the sum over flavors. The superscript S in the last two equations of 4.41 denotes the flavour singlet part of the AP kernel. From the results of the bare coefficient functions and the known splitting functions, we can obtain the finite Δ_{ab}^i using the above eq. 4.41. This in turn gives us the Q^2 distribution of the leptonic pair in the DY process:

$$\begin{aligned}
2S \frac{d\sigma^{H_1H_2}}{dQ^2}(\tau, Q^2) &= 2S \frac{d\sigma_{\text{SM}}^{H_1H_2}}{dQ^2}(\tau, Q^2) \\
&+ \sum \mathcal{F}_h \int_0^1 dx_1 \int_0^1 dx_2 \int_0^1 dz \delta(\tau - zx_1x_2) \\
&\times \left[H_{q\bar{q}} \sum_{k=0}^2 a_s^k \Delta_{q\bar{q}}^{h,(k)} + H_{gq} \sum_{k=0}^2 a_s^k \Delta_{gq}^{h,(k)} + (H_{gq} + H_{qg}) \sum_{k=1}^2 a_s^k \Delta_{gq}^{h,(k)} \right. \\
&\left. + H_{qg} \sum_{k=2}^2 a_s^k \Delta_{qg}^{h,(k)} + H_{q_1q_2} \sum_{k=2}^2 a_s^k \Delta_{q_1q_2}^{h,(k)} \right],
\end{aligned} \tag{4.43}$$

where the contribution from SM [54, 77–79] reads as follows:

$$\begin{aligned}
2S \frac{d\sigma_{\text{SM}}^{H_1H_2}}{dQ^2}(\tau, Q^2) &= \sum_q \mathcal{F}_{SM,q} \int_0^1 dx_1 \int_0^1 dx_2 \int_0^1 dz \delta(\tau - zx_1x_2) \\
&\times \left[H_{q\bar{q}} \sum_{k=0}^2 a_s^k \Delta_{q\bar{q}}^{h,(k)} + (H_{gq} + H_{qg}) \sum_{k=1}^2 a_s^k \Delta_{gq}^{h,(k)} \right]
\end{aligned}$$

$$+ H_{qq} \sum_{k=2}^2 a_s^k \mathcal{A}_{qq}^{h,(k)} + H_{q_1 q_2} \sum_{k=2}^2 a_s^k \mathcal{A}_{q_1 q_2}^{h,(k)} + H_{gg} \sum_{k=2}^2 a_s^k \mathcal{A}_{gg}^{h,(k)} \Big]. \quad (4.44)$$

In the above expression

$$\begin{aligned} \mathcal{F}_{SM,q} &= \frac{4\alpha_{em}^2}{3Q^2} \left[Q_q^2 - \frac{2Q^2(Q^2 - M_Z^2)}{((Q^2 - M_Z^2)^2 + M_Z^2 \Gamma_Z^2) c_w^2 s_w^2} Q_q g_e^V g_q^V \right. \\ &\quad \left. + \frac{Q^4}{((Q^2 - M_Z^2)^2 + M_Z^2 \Gamma_Z^2) c_w^4 s_w^4} ((g_e^V)^2 + (g_e^A)^2)((g_q^V)^2 + (g_q^A)^2) \right], \\ \mathcal{F}_h &= \frac{\kappa^4 Q^6}{320\pi^2} |\mathcal{D}(Q^2)|^2, \\ \mathcal{A}_{ab}^{i,(k)} &= \mathcal{A}_{ab}^{i,(k)}(z, \mu_F^2) \end{aligned} \quad (4.45)$$

and the renormalised partonic distributions are

$$\begin{aligned} H_{q\bar{q}}(x_1, x_2, \mu_F^2) &= f_q^{H_1}(x_1, \mu_F^2) f_{\bar{q}}^{H_2}(x_2, \mu_F^2) + f_{\bar{q}}^{H_1}(x_1, \mu_F^2) f_q^{H_2}(x_2, \mu_F^2), \\ H_{qq}(x_1, x_2, \mu_F^2) &= f_q^{H_1}(x_1, \mu_F^2) f_q^{H_2}(x_2, \mu_F^2) + f_{\bar{q}}^{H_1}(x_1, \mu_F^2) f_{\bar{q}}^{H_2}(x_2, \mu_F^2), \\ H_{q_1 q_2}(x_1, x_2, \mu_F^2) &= f_{q_1}^{H_1}(x_1, \mu_F^2) (f_{q_2}^{H_2}(x_2, \mu_F^2) + f_{\bar{q}_2}^{H_2}(x_2, \mu_F^2)) \\ &\quad + f_{\bar{q}_1}^{H_1}(x_1, \mu_F^2) (f_{q_2}^{H_2}(x_2, \mu_F^2) + f_{\bar{q}_2}^{H_2}(x_2, \mu_F^2)), \\ H_{gq}(x_1, x_2, \mu_F^2) &= f_g^{H_1}(x_1, \mu_F^2) (f_q^{H_2}(x_2, \mu_F^2) + f_{\bar{q}}^{H_2}(x_2, \mu_F^2)), \\ H_{qg}(x_1, x_2, \mu_F^2) &= H_{gq}(x_2, x_1, \mu_F^2), \\ H_{gg}(x_1, x_2, \mu_F^2) &= f_g^{H_1}(x_1, \mu_F^2) f_g^{H_2}(x_2, \mu_F^2). \end{aligned} \quad (4.46)$$

The differential distribution of the DY pair produced from a spin-2 particle already exists up to NLO QCD in the literature [68]; in this thesis we extend it up to NNLO. We discuss about the methodology to compute the finite partonic cross sections $\mathcal{A}_{ab}^{h,(2)}$ in the next chapter.

4.3 Outline of the thesis

This thesis contains both fixed order computations as well as resummation. It is divided into four parts : in chapter 5 we shall discuss the NNLO QCD corrections to production of a lepton pair where the latter is produced from an intermediate spin-2 particle which couples universally to the SM fields. We discuss the method of reverse unitarity that we employ to achieve the above computation. In chapter 6 we discuss the theoretical aspects where the spin-2 particle interacts with the SM fields with non-universal coupling. We compute the form factors and derive the anomalous dimensions up to three loop order in the perturbation theory, using the universal IR structure of the QCD amplitudes. Using the results of the form factor computed in chapter 6 and employing the reverse unitarity for computing the real emission processes, we compute the NNLO QCD corrections for such a nonuniversal model in chapter 7. The fixed order partonic cross sections receive large contributions from some regions of phase space, due to the emission of soft gluons. When these cross sections are multiplied by the PDF's, there can be large contributions at the hadronic level, which spoils the reliability of the perturbation theory. To resolve this issue we have to perform resummation to all orders in the perturbation theory. In chapter 8 we describe the formalism to obtain the soft-virtual cross section in z_i space ($i = 1, 2$), which we use to compute the resummed exponents in double Mellin space. In chapter 9 we apply the formalism to perform threshold resummation of the rapidity distribution in two dimensional Mellin space for the DY process. Finally we conclude in chapter 10.

5

Second order QCD corrections in models of TeV scale gravity: Universal coupling

In this chapter we discuss the next-to-next-to-leading order (NNLO) QCD corrections to production of di-leptons at the hadron colliders in large extra dimensional models with spin-2 particle produced in the intermediate stages. The spin-2 particle couples to the energy momentum tensor of the SM with the universal coupling strength κ . We present the numerical impact of the higher order corrections and demonstrate the reduction of scale uncertainty at NNLO level.

5.1 Introduction

The Run-1 at the LHC culminated in the discovery of the Higgs boson [17, 18], Run-II is currently in operation and the SM is being scrutinized at unprecedented levels of accuracy. From the theoretical perspective, precise predictions for both signals of new physics and the SM background are very essential. Computation of observables in QCD involve expansion in strong coupling constant and calculating the contributions coming from LO, NLO etc. The LO predictions are often very crude at the colliders due to miss-

ing higher order effects and the presence of unphysical scales resulting from ultraviolet renormalization and mass factorization. The predictions based on LO results are unreliable and they cannot constrain the model parameters stringently. At the energies of the LHC, the dominant corrections to LO DY result come from QCD; hence NLO corrections are large. For the DY process, the NNLO corrections in QCD are available for inclusive cross section [54], rapidity distributions [80, 81], fully exclusive distributions including γ -Z interference, the leptonic decay of gauge bosons and finite width effects are also included [82–84]. The current accuracy of the DY process is next-to-next-to-next-to-leading order (N^3 LO) corrections to the production cross section near the partonic threshold [57, 58, 85].

The SM of particle physics explains the dynamics of three forces: electromagnetic, weak and strong force. However it cannot successfully explain the phenomenon associated with gravity. Although both electromagnetic and gravitational force have interactions ranging up to infinity, yet at the subatomic scale, gravity is much weaker compared to electromagnetic force. There are two different fundamental energy scales in nature: the electroweak scale (10^3 GeV) and the Planck scale (10^{18}) GeV. Gravitational force is comparable to the gauge interactions at the Planck scale but not at the electroweak scale. In order to explain this huge difference between two scales in nature, many extra-dimensional models have been proposed involving a massive spin-2 particle interacting with the Standard Model fields through the conserved energy-momentum tensor. To achieve this, we have to go beyond the SM (BSM). In this context, massive spin-2 particle have been phenomenologically well studied in the context of models with extra spatial dimensions which could be flat as in the large extra dimension model, namely ADD [66, 86, 87], or warped as in the RS model [88] or any other new physics scenario with spin-2. They couple to all the SM particles through the energy-momentum tensor of the SM. A generic spin-2 particle can also contribute to other production channels, namely di-lepton or di-vector boson productions at the LHC. In this chapter, we will restrict ourselves to study the invariant mass of di-lepton pair in the ADD model with spin-2 particle. To match the theoretical accuracy of

the SM DY process, the di-lepton final states including a spin-2 intermediate state should also be calculated to the same order of accuracy in QCD. The present accuracy of fixed order computation for ADD and RS model is NLO QCD corrections, which are available for most of the di-final state process with a trivial color flow *viz.*: di-lepton [68, 89, 90], di-photon [91, 92], ZZ [93, 94] and W^+W^- [95, 96]. In addition, these processes have been extended to NLO+Parton Shower accuracy [97–100]. These corrections are found to be large i.e K-factors are turned out to be order of 1.6. For most of these processes the renormalisation scale (μ_R) dependence begins at the NLO level, which implies that we have to compute NNLO corrections. Only at NNLO the renormalisation scale dependence starts getting compensated. To go from NLO to NNLO it is prudent to take incremental steps. For large invariant mass systems threshold contributions play an important role as they capture the dominant part of the cross section. The form factors such as gluon-gluon \rightarrow spin-2 and quark-antiquark \rightarrow spin-2 at two-loop level in QCD [101, 102] were computed to obtain threshold corrections at NNLO in QCD for production of di-leptons at the hadron colliders in ADD model and resonant production of a spin-2 particle in RS model. The three loop QCD corrections for these form factors were computed in [103], the two loop corrections for a massive spin-2 decaying to 3 gluons was achieved in [104].

It is also necessary to go beyond threshold contributions and compute the hard part of the cross section, which may contribute significantly. In this chapter we shall describe the methodology to perform a full NNLO computation in a model independent way and study the impact of these higher order corrections for the ADD model. The theoretical background required to compute the differential cross section has been elaborated in section 4.2.1. In the next section we describe the methodology to compute the NNLO corrections.

5.2 Computation

We are interested to compute the partonic cross section $\mathcal{A}_{ab}^{h,(2)}$, which consists of the evaluation of the loop integrals arising from the virtual diagrams and the phase space integrals. For a spin-2 production, at LO we can have both gluon and quark initiated processes (see fig. 5.1)

$$q + \bar{q} \rightarrow \gamma^*/Z/h, \quad g + g \rightarrow h. \quad (5.1)$$



Figure 5.1: Leading order processes for the DY

Although we have already discussed about the type of processes that can appear up to NNLO while describing the theory part of spin-2, yet we list the processes again before moving on to describe the methodology to compute the partonic contributions. Beyond LO, contributions arise from virtual as well as real emission diagrams. At NLO in QCD, we have

$$\begin{aligned} q + \bar{q} &\rightarrow \gamma^*/Z/h + g, & q + \bar{q} &\rightarrow \gamma^*/Z/h + \text{one loop}, \\ g + g &\rightarrow h + g, & g + g &\rightarrow h + \text{one loop}, \\ g + q &\rightarrow \gamma^*/Z/h + q, & g + \bar{q} &\rightarrow \gamma^*/Z/h + \bar{q}. \end{aligned} \quad (5.2)$$

At the NNLO in QCD, the contributions can come from: double-real emissions, real-virtual and double virtual diagrams. The processes which belong to the double-real emissions are

$$\begin{aligned}
q + \bar{q} &\rightarrow \gamma^*/Z^*/h + q + \bar{q}, & q + \bar{q} &\rightarrow \gamma^*/Z/h + g + g, \\
g + g &\rightarrow h + g + g, & g + g &\rightarrow \gamma^*/Z/h + q + \bar{q}, \\
g + q &\rightarrow \gamma^*/Z/h + g + q, & g + \bar{q} &\rightarrow \gamma^*/Z/h + g + \bar{q}, \\
q + q &\rightarrow \gamma^*/Z/h + q + q, & q_1 + q_2 &\rightarrow \gamma^*/Z/h + q_1 + q_2, \\
q_1 + \bar{q}_2 &\rightarrow \gamma^*/Z/h + q_1 + \bar{q}_2.
\end{aligned} \tag{5.3}$$

The processes which contribute in real-virtual are

$$\begin{aligned}
q + \bar{q} &\rightarrow \gamma^*/Z/h + g + \text{one loop}, & g + g &\rightarrow h + g + \text{one loop}, \\
g + q &\rightarrow \gamma^*/Z/h + q + \text{one loop}, & g + \bar{q} &\rightarrow \gamma^*/Z/h + \bar{q} + \text{one loop}
\end{aligned} \tag{5.4}$$

and the pure double virtual diagrams are

$$\begin{aligned}
q + \bar{q} &\rightarrow \gamma^*/Z/h + \text{two loop}, \\
g + g &\rightarrow h + \text{two loop}.
\end{aligned} \tag{5.5}$$

In this work, we have computed the double real and real virtual contributions, while the purely virtual form factor contributions were computed in [102]. We describe the methodology of our computation by taking the $g g$ initiated process as an example.

- **double-virtual:** the interference of the two loop and the tree level amplitudes, listed in eq. (5.5)

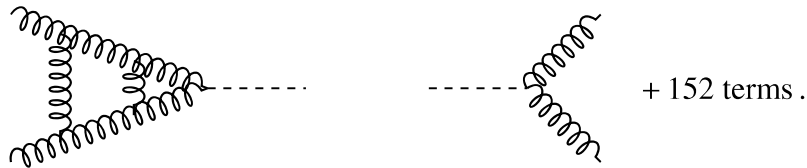


Figure 5.2: Interference of two loop with Born

The Feynman diagrams in above were generated by using the package QGRAF [105]. Using in-house code written in FORM [106, 107], the output from QGRAF was converted to a suitable format. Using our codes in FORM, the born square of the above diagram was evaluated by summing over colors and spins. The matrix elements contain hundreds of different loop integrals, which were reduced to only a few number of master integrals (MIs) by making use of the integration-by-parts (IBP) [108, 109] and Lorentz invariance (LI) [110] identities. The reduction to MIs was achieved using the mathematica based package LiteRed [111]. The above form factor results can be found in [102].

- **double-real:** the self-interference of the tree level amplitudes for the processes contributing to pure double-real emissions. For example, for the process $g+g \rightarrow h+g+g$

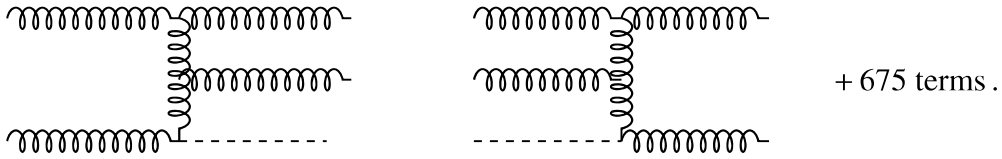


Figure 5.3: self interference of double real emission

To evaluate the above diagrams we have to perform a phase space integration over the final state gluons, which can be quite non-trivial to calculate. To compute the NNLO QCD correction to the DY pair production in [54], the phase space integrals were performed through evaluation of the two parametric and two angular integrations in three different frames. The phase space integration in inclusive production cross section of the Higgs boson were done by three different techniques. In [112], the partonic cross section was obtained by performing an expansion around the soft limit. In the meantime a completely new and elegant formalism was developed in [2] by Anastasiou and Melnikov to get the same result. The phase space integrals were converted to loop integrals by using the idea of reverse unitarity. Thus evaluation of real emission diagrams boils down to computing virtual diagrams. We describe it in details below.

The contribution coming from fig. 5.3 when the two parts are multiplied is proportional to

$$\int \frac{d^n q_1}{(2\pi)^{n-1}} \frac{d^n q_2}{(2\pi)^{n-1}} \delta_+(q_1^2) \delta_+(q_2^2) \delta_+(q^2 - m_h^2) [\dots] \quad (5.6)$$

where, p_1, p_2, q_1, q_2 are the momentas of incoming and outgoing gluons respectively, q is the momenta of spin-2 particle. In above $\delta_+(q^2 - m^2) \equiv \delta(q^2 - m^2)\theta(q^0)$. The δ_+ functions can be replaced by the difference between two propagators with opposite prescriptions for their imaginary parts, which follows from Cutkosky rules [113]:

$$\delta_+(q^2 - m^2) \sim \frac{1}{q^2 - m^2 + i\varepsilon} - \frac{1}{q^2 - m^2 - i\varepsilon} \quad (5.7)$$

with $\varepsilon \rightarrow 0$. Upon this substitution, the square of the diagram becomes equivalent to the forward scattering amplitude, presented in fig. 5.4, where, the blue dotted line denotes the cut propagators which should be replaced by the RHS of eq. 5.7.

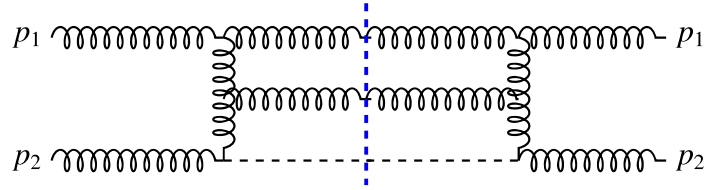


Figure 5.4: Effective two loop diagram with three cut propagators

We begin our computation by evaluating the normal Born square of the above diagram (5-external on-shell legs) where the sum over colors and spins are performed. The color simplification is done in general $SU(N)$ gauge theory. The Dirac and Lorentz algebra are carried out in n -dimensions ($n = 4 + \epsilon$). We multiply the phase space factor with the final answer, which contains the three δ_+ functions corresponding to the final state particles. We convert it into a cut two-loop Feynman diagram through the application of reverse unitarity as discussed above. As a result the phase space integral can now be handled in the same way as the multiloop integrals. We make use of the IBP and LI identities to reduce this two loop diagram into a set of MIs. The sign of the imaginary parts of the

cut propagators are irrelevant for the above identities; the two terms of those propagators which are differed by the different prescriptions of the imaginary parts give rise to same IBP relations. Each of these two terms have the same form of the IBP relations as the original two-loop integral without the cut. Therefore instead of considering the two terms, we can take only one term, which is equivalent to substituting the δ_+ functions by its first propagator from the RHS of eq. 5.7. During reduction to MIs, in order to keep intact the cut propagators in its original form even in the MIs, we make sure not to apply any transformation on the momenta of the cut propagators. After the reduction, we must put those MIs to zero which do not contain any of the three cut propagators. Putting the δ_+ functions in place of all the cut propagators, we get the final set of phase space MIs. These integrals are identified with the ones appearing as phase space MIs for the evaluation of the NNLO QCD correction to the inclusive production cross section of the Higgs boson which are obtained in the article [114]. Same set of MIs were also evaluated in [115].

- **real-virtual:** the interference of the one-loop and the tree level amplitudes.

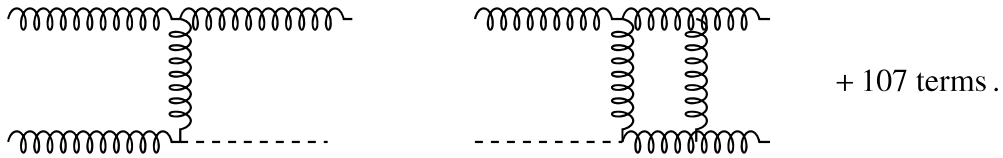


Figure 5.5: Interference of real-virtual with single real emission

The evaluation of the above kind of processes follow exactly the similar method as double real emission process. The polarization sum of the external gluons is carried out in axial gauge to ensure the exclusion of the unphysical degrees of freedom. We include the ghost loops to cancel the unphysical degrees of freedom of the internal gluons present in the virtual loops.

Up to NNLO we have 2979 number of double real, 948 real-virtual and 207 double virtual Feynman diagrams. The partonic cross sections obtained from all the subprocesses

contain UV and IR divergences. We eliminate the UV divergences by renormalizing the strong coupling constant. The IR divergences appearing are of two types: soft and collinear divergences. By adding all the real emission processes and the virtual diagrams, the soft divergences and the final state collinear singularities cancel, by KLN theorem. The initial state collinear singularities are removed by mass factorization. Thus we get completely finite partonic cross sections or partonic coefficient function at NNLO QCD. The final results of the partonic coefficient functions involving spin-2 particle for different channels are presented in the Appendix [11.4](#).

In the next section we present the numerical impact of the NNLO corrections on the dilepton production in the ADD model at the LHC.

5.3 Phenomenology

The two loop QCD corrections that we computed above was done in a model independent framework. To observe its numerical impact at the LHC, we consider lepton pair production in the ADD model. By convoluting the partonic coefficient functions order-by-order with the corresponding PDFs (taken from `lhpdf` [116]), we obtain the LO, NLO and NNLO corrected hadronic cross sections. We have set the number of flavors $n_f = 5$, fine structure constant $\alpha_{em} = 1/128$ and the weak mixing angle $\sin^2\theta_W = 0.227$ and use `MSTW2008lo/nlo/nnlo` with the corresponding values of a_s for LO, NLO and NNLO. Except for studying the scale variations, the factorization and the renormalization scales are set equal to the invariant mass of the di-lepton, i.e., $\mu_F = \mu_R = Q$. We note that in the past there have been a series of experimental searches for large extra dimensions using di-lepton events at both Tevatron and the LHC. Consequently, stringent bounds have been obtained on the scale M_s of the ADD model as a function of the number of extra dimensions d . For instance, the lower limits on the scale M_s obtained from both ATLAS and CMS collaborations using 7 TeV data are $M_s = 2.4(3.9)$ TeV corresponding to $d = 7(3)$ [117, 118]. With the availability of 8 TeV data [119, 120], the lower limits on these parameters are further pushed to about $M_s = 3.3(4.9)$ TeV corresponding to $d = 7(3)$. There have already been some preliminary results on search for narrow resonances in di-lepton final state using 13 TeV data [121]. In addition, the ATLAS and CMS collaborations have observed di-lepton events with invariant mass as large as 1800 GeV using 8TeV LHC data corresponding to a luminosity of about $20fb^{-1}$ [119, 120]. For the illustration of the impact of QCD corrections, we choose the model parameters to be $M_s = 4$ TeV and $d = 3$.

At NNLO there are different partonic channels that contribute to the hadronic cross section. Although all these channels add up their contribution to give the final physical hadronic cross section yet the individual contributions are unphysical. These bare par-

tonic cross sections contain initial state IR divergences which are removed by mass factorization, where the latter is performed in some scheme which for our case is the $\overline{\text{MS}}$. In the fig. 5.6, we present the Q distributions for various subprocesses at NNLO in the ADD model along with the contribution from SM at NNLO [54, 78, 79]. Both in the SM and

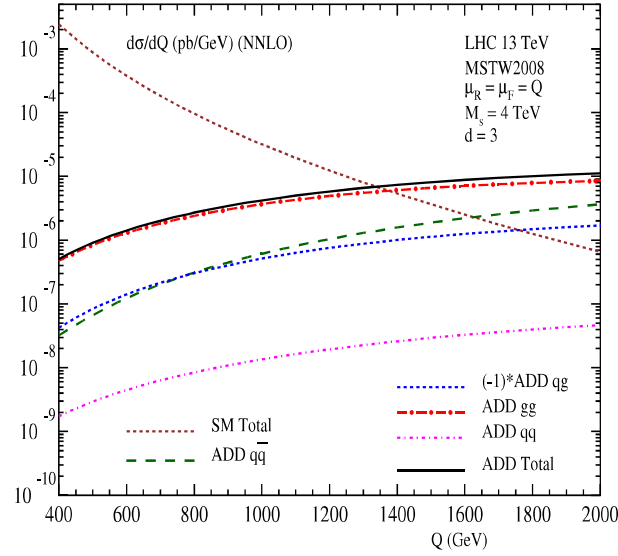


Figure 5.6: Various sub-process contributions to the di-lepton production computed at $O(a_s^2)$ QCD in ADD model. The SM background contains the full a_s^2 correction.

ADD model, the quark anti-quark initiated sub-process ($q\bar{q}$) contributes at LO. However, the gluon fusion sub-process (gg) starts contributing at the LO in the ADD model unlike in the SM where its contribution begins at NNLO. Because of the large gluon flux at the LHC, the contributions arising from the gg sub-process in the ADD model dominates over the rest, which is same as for the Higgs boson at the LHC. The crucial difference between these two production channels is the presence of strong coupling constant $a_s(\mu_R)$ at the leading order for the Higgs boson production cross section. It is worthwhile to notice the numerical impact of the contributions coming from quark-gluon (qg) sub-process beyond LO. The qg sub-process contribution both in the SM and in the ADD model is found to be negative but significantly large in magnitude. The same trend continues even at NNLO. Particularly, we notice that the NNLO QCD corrections from qg sub-process are considerably larger in magnitude than the sum of all the quark initiated sub-processes

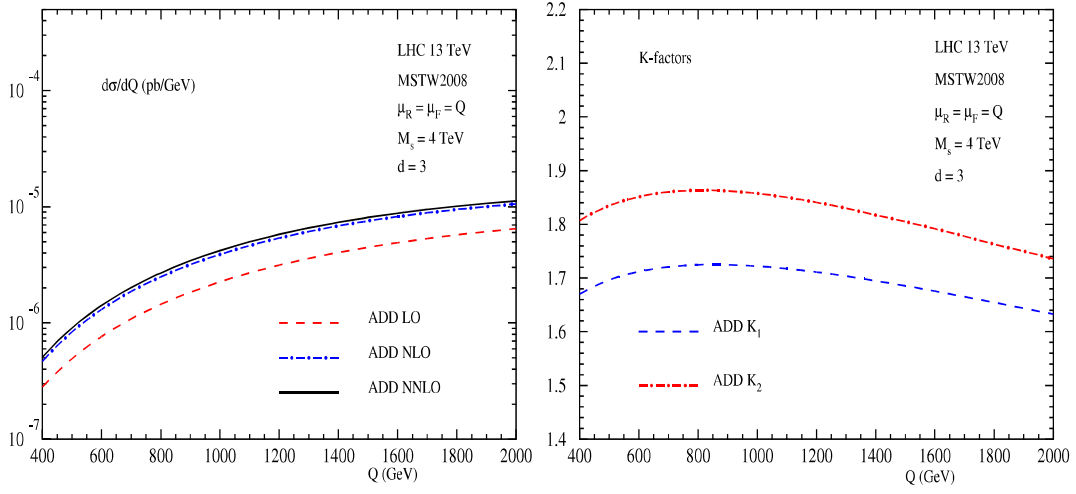


Figure 5.7: Pure graviton contribution to the Drell-Yan production cross section (left panel) up to NNLO QCD in the ADD model for LHC13 and the corresponding K-factors (right panel).

$(q\bar{q}, qq, q_1q_2, q_1\bar{q}_2)$. Although their contribution is less, yet they are important to stabilize the cross section under renormalization and factorization scale variations through renormalization group equations. A generic pattern in all of these sub-processes is that their contributions increase with Q , simply because of the increase in the number of accessible KK-modes with Q .

In fig 5.7 we present in the left panel $d\sigma/dQ$ as a function of invariant mass Q at LO, NLO and NNLO for ADD model(i.e. setting the SM contributions to zero). It is found that the contributions from the interference terms between the SM and spin-2 is zero. There is also a moderate increase in NNLO cross section over the NLO counterpart. In order to have an estimate of the corrections coming from different orders, we have plotted the K factors which is defined as

$$K_i = \frac{d\sigma^i}{d\sigma^{\text{LO}}}, \quad i = 1(\text{NLO}), 2(\text{NNLO}). \quad (5.8)$$

The NLO QCD corrections here increase the LO cross sections by about 68% for $Q = 1.5$ TeV, while the NNLO corrections that are still reasonably large contribute an additional 12% ($K_1 = 1.68$ and $K_2 = 1.80$). The K-factors depend on the invariant mass through

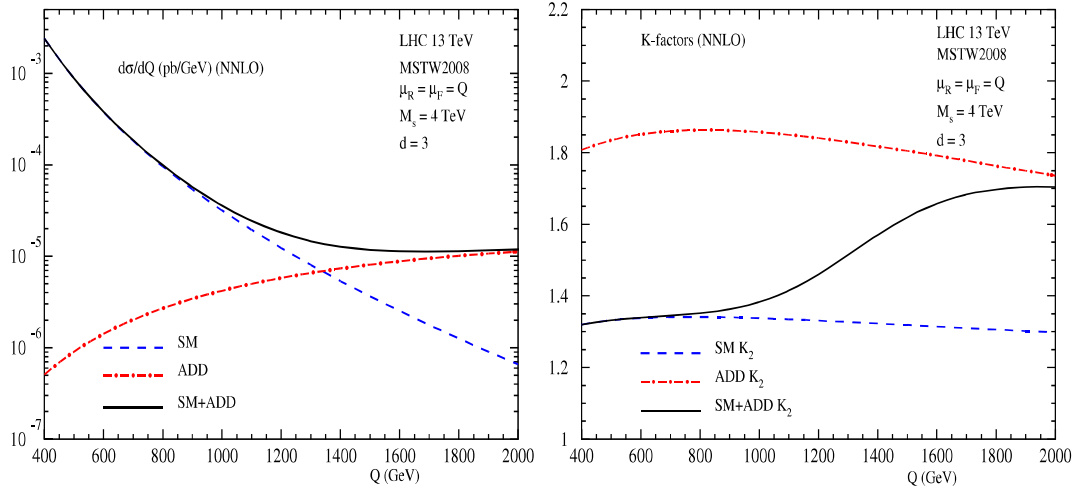


Figure 5.8: Drell-Yan production cross section (left panel) for SM, GR and the signal in the ADD model for LHC13 along with the corresponding K-factors (right panel). Here, $M_s = 4$ TeV and $d = 3$.

the logarithm corrections both in partonic cross sections as well as in the evolution of PDFs. Hence it is not good choice to use the constant K-factor for constraining the model parameters. We also find that the conservative estimate of the K-factor for the Drell-Yan production in ADD model resembles closely to that of the Higgs boson production. However, because of the large negative contribution from the qg sub-process, the exact values of the K -factors differ in these two cases. It is to be noted that K_2 in ADD model alone is bigger than the corresponding one for the SM simply because of the dominance of gg sub-process over others.

Being an effective theory, the ADD model is valid below the cut-off scale M_s and above M_s , the formalism ceases to be valid. As the number of accessible KK modes increases with Q as can be seen from eq. 4.18, the cross sections in the pure ADD model will increase with Q . This implies that in the kinematic regime $Q < M_s$, the spin-2 should give reliable predictions for the LHC. Due to the increase in the spin-2 contributions with Q in the ADD model, they can dominate the SM contribution at some invariant mass $Q_0 (< M_s)$, the precise value of which depends on the choice of model parameters. This is demonstrated in fig. 5.8. In the left panel of the figure, we present the NNLO cross

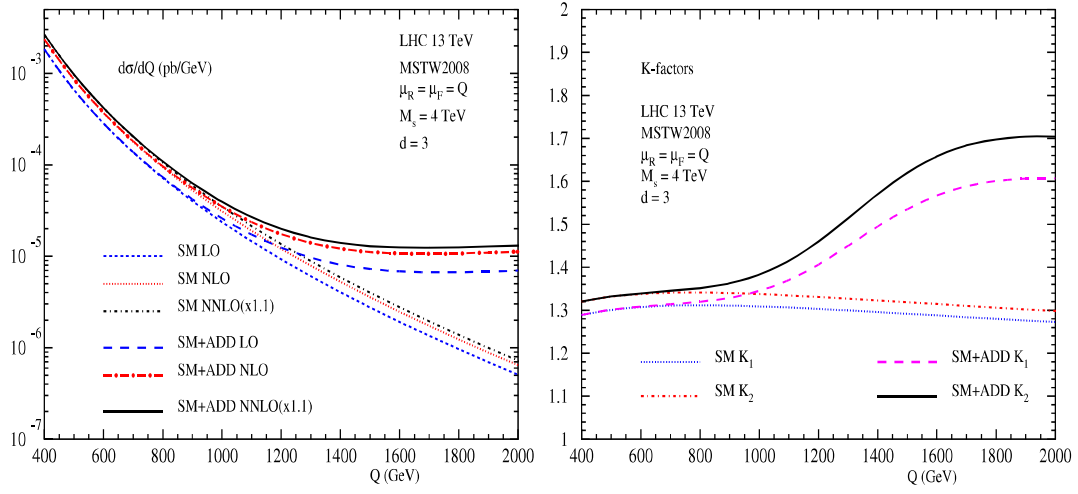


Figure 5.9: Drell-Yan production cross section (left panel) for SM as well as the signal in the ADD model for LHC13 along with the corresponding K-factors (right panel).

sections for the SM, spin-2 (GR) and the signal (SM+GR) together with the corresponding NNLO K-factor i.e. K_2 in the right panel. From the above discussion we see that the phenomenologically interesting kinematic regime is $Q_0 < Q < M_s$ where the spin-2 signals can give significant deviations from the SM predictions. For our default choice of model parameters, Q_0 is about 1.4 TeV. Thus the signal is dominated by SM contributions well below 1.4 TeV and by ADD model contributions well above 1.4 TeV.

Owing to the importance in the experimental searches for extra dimensions, it is important to give the signal contributions along with the corresponding SM background. The differential distributions in SM and ADD model at LO, NLO and NNLO are presented in the left panel of fig. 5.9 along with the corresponding K factors on the right panel.

Till now we have studied the variation of differential cross section with Q by keeping the scale of extra dimensions (M_s) and the number of extra dimensions (d) fixed at some values that are consistent with the experimental bounds. It is also of interest to investigate the case when the Q -distribution is a function of M_s . This is shown in the left panel of fig. 5.11 where as we decrease M_s , the value of Q_0 also goes down. When $Q \gg Q_0$ the SM contribution can be neglected and the SM+ADD K-factor becomes equal to the pure ADD K-factor which is independent of choice of model parameters. This effect

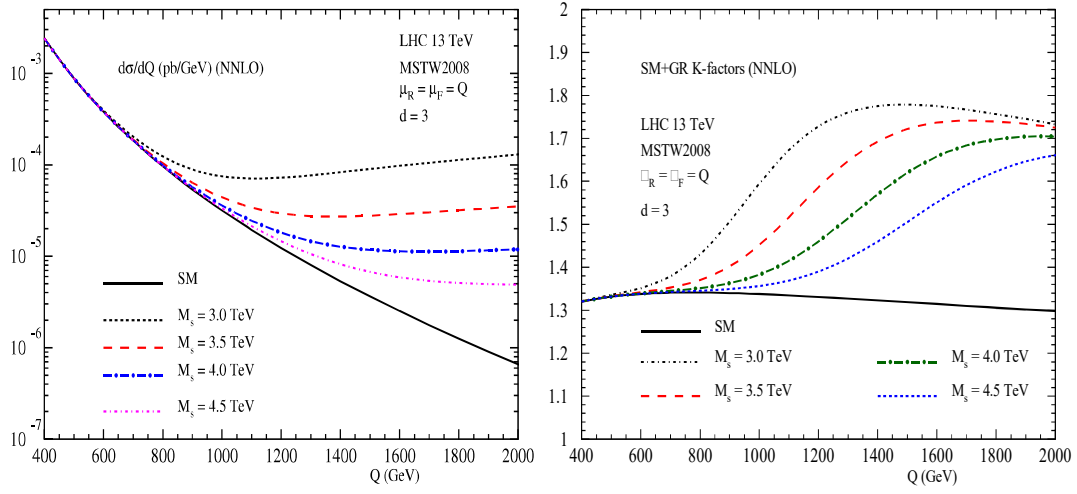


Figure 5.10: Dependence of the signal production cross sections at NNLO on the the scale of the ADD model M_s (left panel) and the corresponding signal K-factors(right panel) for $d=3$.

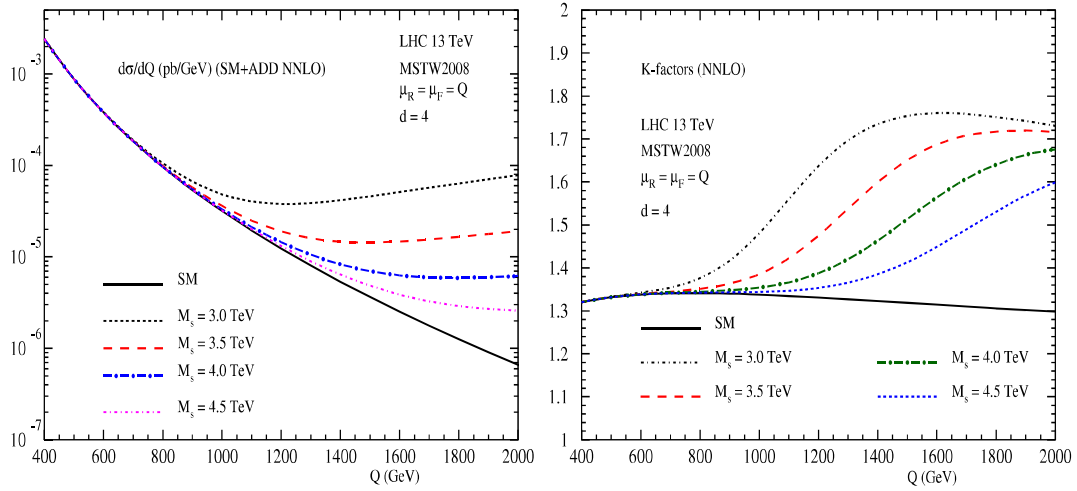


Figure 5.11: Dependence of the signal production cross sections at NNLO on the the scale of the ADD model M_s (left panel) and the corresponding signal K-factors(right panel).

is reflected in the right panel, where far beyond Q_0 , the SM+ADD K-factors tend to converge to each other. The dependence on the number of extra dimension is shown in fig. 5.12.

We shall now study the variation of signal production cross section with the renormalization scale μ_R and the factorization scale μ_F . The LO cross section depends strongly on

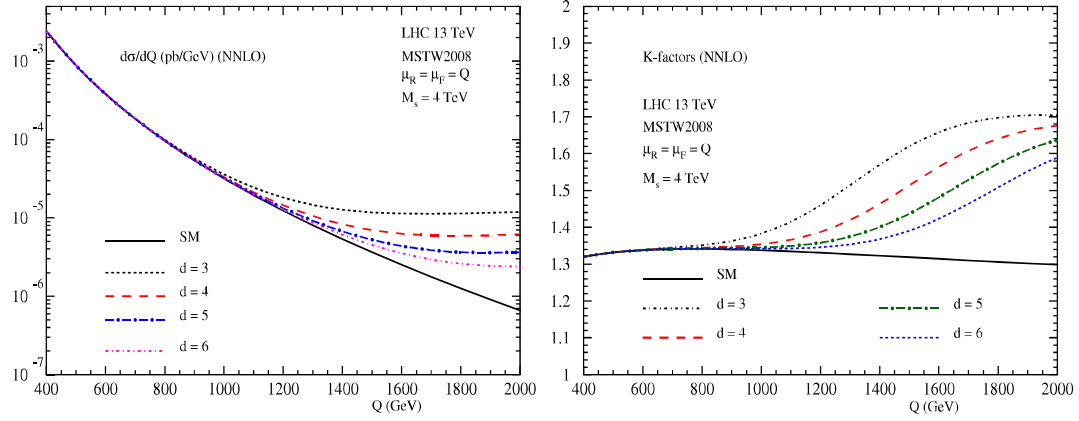


Figure 5.12: Dependence of the signal production cross sections at NNLO on the number of extra dimensions d (left panel) and the corresponding K-factors (right panel).

the factorization scale μ_F through the PDFs. This dependence on μ_F starts reducing at higher orders leaving a residual scale dependence that is proportional to $\alpha_s^n, n > 1$. For spin-2 production, dependence on μ_R starts at NLO and the result up to NLO will now become sensitive to the choice of μ_R . Hence at NLO the factorization scale dependence gets reduced, the renormalisation scale dependence crops up. The cross section becomes less sensitive to the scales μ_R and μ_F as we include more and more higher order terms. This is a consequence of the renormalization group equation. In order to demonstrate the

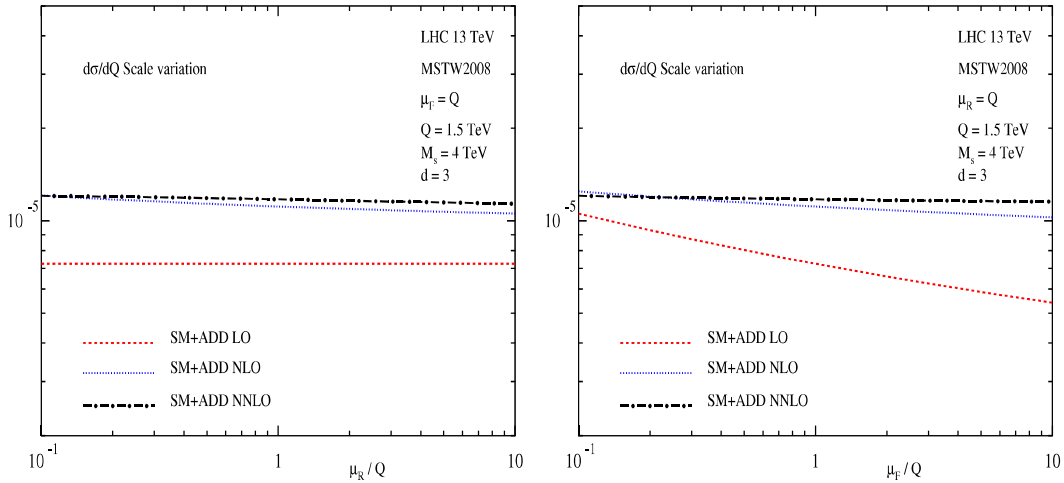


Figure 5.13: Uncertainties in the signal production cross section due to the choice of renormalisation scale μ_R (left panel) and factorization scale μ_F (right panel).

reduction in the scale dependence, we have plotted the $d\sigma/dQ$ in the fig. 5.13 at a fixed

value of $Q = 1.5$ TeV, the choice where the new physics dominates, as function of μ_R (left panel), μ_F (right panel) and then $\mu = \mu_F = \mu_R$ (see fig. 5.14.) in the range between $Q/10$ to $10Q$, for wider scale variations. We find according to our expectation that the inclusion of higher terms in the perturbation theory indeed reduce the dependence on these unphysical scales.

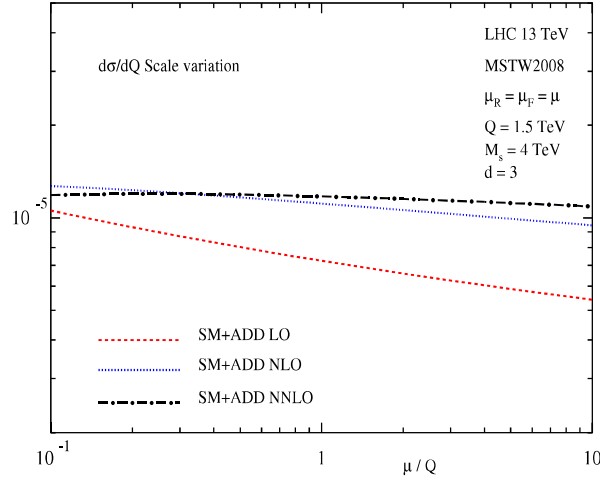


Figure 5.14: Uncertainties in the signal production cross section due to the choice of the scale $\mu = \mu_R = \mu_F$.

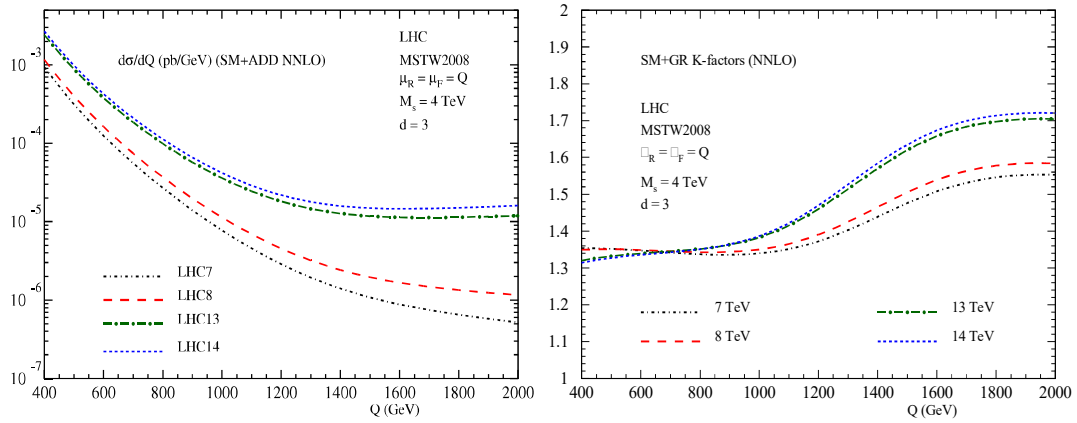


Figure 5.15: Dependence of the signal production cross sections at NNLO on the center of mass energy at LHC (left panel) and the corresponding K-factors (right panel).

We will now present in fig. 5.15 the predictions for the differential cross section for various center of mass energies, namely 7, 8, 13 and 14 TeV at the LHC. With the increase in

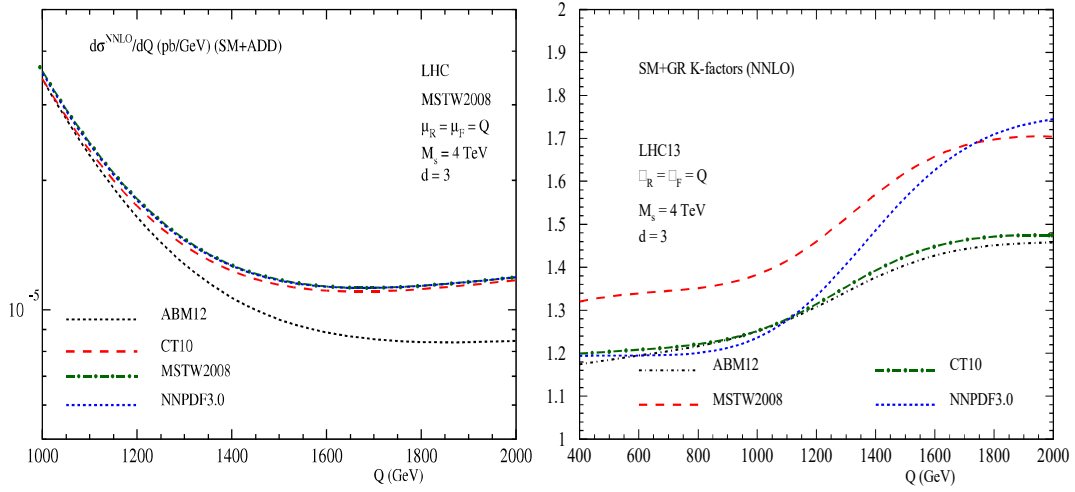


Figure 5.16: Dependence of the signal production cross sections at NNLO on the choice of PDFs (left panel). Signal K-factors at NNLO for different PDFs (right panel).

the centre of mass energy, both the NNLO SM+ADD cross sections (left panel) and the corresponding signal K-factors (right panel) increases. This is because the parton fluxes particularly the gluon flux will increase with energy and hence the sensitivity to the ADD model also goes up.

In fig. 5.16 we present the differential cross sections at NNLO for different choice of PDFs. The precise value of the strong coupling constant consistent with a given PDF set influences the prediction. We have used PDF sets such as MSTW2008, ABM12, CT10, NNPDF3.0 to demonstrate our result. The perturbatively computed partonic cross sections at an order α_s is convoluted with the PDFs extracted to the same order in α_s for all the PDF sets except ABMP12 for which we have used only the available NNLO PDFs for computing all the LO, NLO and NNLO hadron level cross sections. From the left panel of fig. 5.16 we see that the cross sections for different PDF sets differ from one another. But the the K factor may not show the similar pattern as cross sections because PDFs of different orders enter in the ratio of K- factors, as can be seen in the right panel of fig. 5.16.

Finally, we address the impact of soft-plus corrections on our fixed order predictions. Note that for ADD, the numerical impact of soft-plus-virtual (SV) were already reported

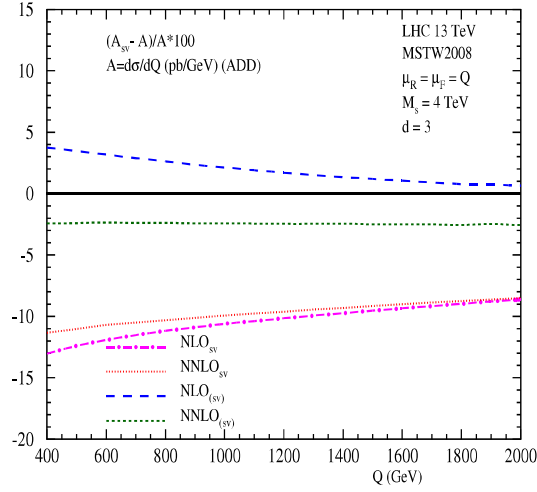


Figure 5.17: NLO and NNLO predictions obtained from modified SV approximation for the signal only with the gg subprocess contribution.

in [101]. Now that we have a complete result at NNLO level, it is important to study the validity of SV approximation. As mentioned before that the gg initiated sub-process in the pure spin-2 case is similar to the SM Higgs production in gluon fusion channel. For the latter case, the SV corrections (or rather with the modified parton fluxes) are found to be a very good approximate for the fixed order results. This indeed is the case even for our ADD model predictions provided we just take only the gg initiated subprocesses. In addition, if we use the modified SV approximation as described in [122], we find that it is closer to the exact result, resulting from gg subprocesses alone see fig. 5.17. Inclusion of qg initiated sub processes spoil this approximation as their contribution is negative and significantly large. Hence, the SV approximation at a_s^2 does not seem to be working very well unlike in the Higgs production in gluon fusion.

5.4 Conclusion

For the first time we have performed the NNLO QCD correction for the production of a lepton pair in the DY type of processes with a massive spin-2 particle appearing in the intermediate stages. Unlike SM, both gg and $q\bar{q}$ appear at the LO; there are 14 partonic subprocesses that contribute at NNLO. We have systematically employed the methodology of reverse unitarity to achieve the two loop computation. At the energies of LHC, the spin-2 mediated process is dominated by the gluon initiated processes due to the large gluon flux at the collider. We also find that the qg initiated process gives large negative contribution at NNLO. In order to estimate the corrections coming from each order, we have reported the K factors in ADD model which is 1.68 at NLO and 1.80 at NNLO. The K factor in ADD model is larger than the corresponding one in the SM due to the dominance of gg subprocess over the others. The QCD corrections play an important role to stabilise the differential cross section with respect to the unphysical renormalization and factorization scale. We find that the higher order corrections decrease the scale uncertainties: from 71% at LO to 29% at NLO which goes down to 8% at NNLO.

6 Form factors with nonuniversal coupling

In the previous chapter we have computed the NNLO QCD corrections in DY type of processes where a massive spin-2 particle appearing in the intermediate stage couple universally to all the SM fields. In this chapter we extend our study of higher order QCD corrections for a more general case, namely when the spin-2 field couples differently to gauge and fermionic sector of the SM.

6.1 Introduction

In chapter 4 we discussed about the theoretical aspects of a scenario where a generic spin-2 particle couples to all the SM fields through the conserved energy momentum tensor of QCD, with a universal coupling strength κ . Most of the popular extra dimensional models have this universal nature of coupling of spin-2 particle and their phenomenology have been studied rigorously. These extra dimensional models are described by effective theories and hence non-renormalizable in the conventional sense. In the ADD and the RS, thanks to conservation of the energy momentum tensor of the SM, the leading interaction term that describes the coupling of spin-2 with those of the SM does not require any additional renormalization. For most of the phenomenological studies this order in coupling

is sufficient, thus the IR structure of the SM is also not affected and hence factorization properties continue to hold. One of the consequences of the above is that we can compute successfully various observables beyond leading order in the SM coupling using the perturbative methods. Thus we computed the NNLO QCD corrections in DY process where a generic spin-2 particle appeared in the intermediate stages and then decayed to a lepton pair. All the infrared singularities cancelled and we got finite perturbative results that could be used to constrain the model parameters unambiguously. We then studied the phenomenological impact of such higher order corrections in the context of the ADD model, where we saw that the scale uncertainties reduce on inclusion of the NNLO corrections.

However this universal nature of coupling may not be the most general way in which the spin-2 interacts with the SM fields. There may be a scenario where the spin-2 field interacts differently with the fermion and gauge fields of the SM. In other words instead of one coupling strength κ we can have two different coupling strengths k_q, k_g . While this type of scenarios are not a part of most of the extra dimensional models, they can provide an opportunity to study the distinct signatures at the colliders which is not possible with theories containing universal coupling strength. For example in the work [6] the p_T^x distributions of the spin-2 particle for various values of the quark and gluon couplings were analyzed and the signatures of the unitarity violating behavior associated with nonuniversal coupling strengths were also pointed out.

The discovery of the 125 GeV Higgs boson has been one of the spectacular achievements in the history of particle physics. To ascertain its nature, it was important to analyze the models with spin-2 nonuniversal coupling which could act as an imposter to the Higgs boson [123–125]. In addition for extra dimensional models like the RS, experimental bounds on RS resonance (for universal coupling) was much higher [126–133]. From the above discussion we can see the necessity of studying the scenario where a massive spin-2 particle interacts with the SM fields with nonuniversal coupling strengths. To NLO in QCD the UV and IR behavior for the nonuniversal couplings for a spin-2 had been

studied in the context of Higgs Characterization [6]. Due to the nonuniversal nature of the coupling, UV renormalisation was needed and the one loop anomalous dimensions were also computed. The IR structure was studied and the cancellation which results from adding the virtual and real processes, followed by mass factorization was demonstrated. Thus the IR factorization to NLO order in QCD for the nonuniversal coupling scenario was shown in [6].

With the unprecedented level of precision at which the SM is being scrutinized at the LHC, it is only natural to have the competing BSM scenarios match the same order of accuracy in QCD as the SM observables. The first step to such a phenomenological study would be to compute form factors to the production of a singlet on shell state X via the quark $q\bar{q} \rightarrow X$ or gluon $gg \rightarrow X$ production channels. Presently, form factors are available to up to three-loop level in the SM [134–138], for some BSM spin-2 that couples to the energy momentum tensor [102, 103] and for the pseudo-scalar Higgs boson [139]. For extra dimensional models *viz.* ADD and RS for most of the di-final state process, NLO QCD corrections have been computed in [68, 89–93, 95, 96] and extended to NLO+PS accuracy in [97–99].

In this chapter we describe the computation of form factors for a nonuniversal interaction term up to three loop level in QCD. We restrict ourself to the QCD sector of the SM because the phenomenology with such operators have immediate application at the LHC where such interactions are probed. In the previous chapter we saw how spin-2 couples to the conserved and gauge invariant EM tensor of the QCD [140]. Now we divide the EM tensor of QCD into two rank 2 operators such that each of them are not conserved but they are invariant under the gauge group of QCD. Note that spin-2 is gauge singlet. As a consequence of this, both the operators as well as the couplings get additional UV renormalization order by order in the perturbation theory. These additional UV divergences can be removed by multiplying overall operator renormalization constants. We will find out these constants by computing the on-shell form factors of the operators between quark

and gluon states. These form factors are important ingredients of any observable at the LHC to study such interactions. In the next section we discuss about the theory and then describe the methodology adopted to compute the anomalous dimensions up to three loop order in QCD.

6.2 Theoretical Framework

6.2.1 The Effective Action

We consider the minimal effective action that describes the coupling of spin-2 fields denoted by $h_{\mu\nu}$ with those of QCD which consists of two gauge invariant operators $\hat{\mathcal{O}}^{G,\mu\nu}$ and $\hat{\mathcal{O}}^{Q,\mu\nu}$ ¹:

$$S = \int d^4x \mathcal{L}_{QCD} - \frac{1}{2} \int d^4x h_{\mu\nu}(x) \left(\hat{\kappa}_G \hat{\mathcal{O}}^{G,\mu\nu}(x) + \hat{\kappa}_Q \hat{\mathcal{O}}^{Q,\mu\nu}(x) \right) \quad (6.1)$$

where $\hat{\kappa}_I, I = G, Q$ are dimensionful couplings. The pure gauge sector is denoted by G while Q represents the fermionic sector and its gauge interaction. The gauge invariant operators $\hat{\mathcal{O}}^{G,\mu\nu}$ and $\hat{\mathcal{O}}^{Q,\mu\nu}$ reads as

$$\begin{aligned} \hat{\mathcal{O}}_{\mu\nu}^G &= \frac{1}{4} g_{\mu\nu} \hat{F}_{\alpha\beta}^a \hat{F}^{a\alpha\beta} - \hat{F}_{\mu\rho}^a \hat{F}_\nu^{a\rho} - \frac{1}{\hat{\xi}} g_{\mu\nu} \partial^\rho (\hat{A}_\rho^a \partial^\sigma \hat{A}_\sigma^a) - \frac{1}{2\hat{\xi}} g_{\mu\nu} \partial_\alpha \hat{A}^{a\alpha} \partial_\beta \hat{A}^{a\beta} \\ &\quad + \frac{1}{\hat{\xi}} (\hat{A}_\nu^a \partial_\mu (\partial^\sigma \hat{A}_\sigma^a) + \hat{A}_\mu^a \partial_\nu (\partial^\sigma \hat{A}_\sigma^a)) + \partial_\mu \bar{\hat{\omega}}^a (\partial_\nu \hat{\omega}^a - \hat{g}_s f^{abc} \hat{A}_\nu^c \hat{\omega}^b) \\ &\quad + \partial_\nu \bar{\hat{\omega}}^a (\partial_\mu \hat{\omega}^a - \hat{g}_s f^{abc} \hat{A}_\mu^c \hat{\omega}^b) - g_{\mu\nu} \partial_\alpha \bar{\hat{\omega}}^a (\partial^\alpha \hat{\omega}^a - \hat{g}_s f^{abc} \hat{A}^{c\alpha} \hat{\omega}^b), \\ \hat{\mathcal{O}}_{\mu\nu}^Q &= \frac{i}{4} \left[\bar{\hat{\psi}} \gamma_\mu (\vec{\partial}_\nu - i\hat{g}_s T^a \hat{A}_\nu^a) \hat{\psi} - \bar{\hat{\psi}} (\overleftarrow{\partial}_\nu + i\hat{g}_s T^a \hat{A}_\nu^a) \gamma_\mu \hat{\psi} + \bar{\hat{\psi}} \gamma_\nu (\vec{\partial}_\mu - i\hat{g}_s T^a \hat{A}_\mu^a) \hat{\psi} \right. \\ &\quad \left. - \bar{\hat{\psi}} (\overleftarrow{\partial}_\mu + i\hat{g}_s T^a \hat{A}_\mu^a) \gamma_\nu \hat{\psi} \right] - i g_{\mu\nu} \bar{\hat{\psi}} \gamma^\alpha (\vec{\partial}_\alpha - i\hat{g}_s T^a \hat{A}_\alpha^a) \hat{\psi} \end{aligned} \quad (6.2)$$

¹This is not the unique decomposition of original EM tensor. One can adjust gauge invariant terms between these two.

where \hat{A}_μ^a , $\hat{\psi}$, $\hat{\omega}^a$ and $h_{\mu\nu}$ are gauge, quark, ghost and spin-2 fields, respectively. \hat{g}_s is the strong coupling constant and $\hat{\xi}$ is the gauge fixing parameter. The bare/unrenormalized quantities are indicated by a hat. T^a and f^{abc} are the Gell-Mann matrices and structure constants of SU(N) gauge theory, respectively. For the purpose of our analysis we retain terms only up to order \hat{k} and in the rest of the thesis, we restrict ourselves to this approximation.

6.2.2 Ultraviolet renormalization

The sum $\hat{\mathcal{O}}^{G,\mu\nu} + \hat{\mathcal{O}}^{Q,\mu\nu}$ is nothing but the energy momentum tensor of QCD. As can be seen from eq. 6.2 the operator $\hat{\mathcal{O}}^{G,\mu\nu}$ is free from quark fields which means that in the theory where spin-2 field couples exclusively to the pure Yang-Mills, the operator $\hat{\mathcal{O}}^{G,\mu\nu}$ is conserved. However, in the presence of the quark fields in QCD, this property ceases to hold true beyond the tree level. These two operators being non conserved, develop additional UV divergences which need to be factored out in terms of UV renormalization constants. These constants then renormalize the bare couplings $\hat{k}_I, I = G, Q$. The resulting interaction terms expressed in terms of renormalized operators with appropriate renormalized couplings are guaranteed to predict UV finite correlation functions to all orders in the strong coupling constant. The most commonly used method of obtaining the renormalization constants in quantum field theory is to compute off-shell amplitudes and extract the UV divergent contributions order by order in the perturbation theory. For composite operators there exists the method of operator product expansion. We will not follow any of these approaches in this thesis. Instead, we apply the method discussed in [139] to obtain both UV renormalisation constants as well as on-shell form factors of these operators. In the work [139] it was demonstrated that UV renormalisation constants of composite operators can be extracted order by order in perturbation theory from their on-shell form factors by exploiting their universal IR structure. The form factors consist of UV divergences coming from two sources : the coupling constant and the two compos-

ite operators. The renormalization of the coupling constant has already been discussed before (see eq. 2.5, 2.6). In the following we describe the methodology to handle the UV singularities coming from the two operators.

According to the Joglekar and Lee theorem [141], the two operators O^I are closed under renormalization which can be accomplished through the renormalization mixing matrix Z , as follows

$$\begin{bmatrix} O^G \\ O^Q \end{bmatrix} = \begin{bmatrix} Z_{GG} & Z_{GQ} \\ Z_{QG} & Z_{QQ} \end{bmatrix} \begin{bmatrix} \hat{O}^G \\ \hat{O}^Q \end{bmatrix}. \quad (6.3)$$

The renormalization constants Z_{IJ} satisfy following renormalization group equation (RGE)

$$\mu_R^2 \frac{d}{d\mu_R^2} Z_{IJ} \equiv \gamma_{IK} Z_{KJ} \quad \text{with} \quad I, J, K = G, Q \quad (6.4)$$

where γ_{IK} 's are the corresponding anomalous dimensions and the summation over repeated index is understood. The general solution to the RGE up to a_s^3 is as follows

$$\begin{aligned} Z_{IJ} = & \delta_{IJ} + a_s \left[\frac{2}{\epsilon} \gamma_{IJ}^{(1)} \right] + a_s^2 \left[\frac{1}{\epsilon^2} \left\{ 2\beta_0 \gamma_{IJ}^{(1)} + 2\gamma_{IK}^{(1)} \gamma_{KJ}^{(1)} \right\} + \frac{1}{\epsilon} \left\{ \gamma_{IJ}^{(2)} \right\} \right] + a_s^3 \left[\frac{1}{\epsilon^3} \left\{ \frac{8}{3} \beta_0^2 \gamma_{IJ}^{(1)} \right. \right. \\ & + 4\beta_0 \gamma_{IK}^{(1)} \gamma_{KJ}^{(1)} + \frac{4}{3} \gamma_{IK}^{(1)} \gamma_{KL}^{(1)} \gamma_{LJ}^{(1)} \left. \right\} + \frac{1}{\epsilon^2} \left\{ \frac{4}{3} \beta_1 \gamma_{IJ}^{(1)} + \frac{4}{3} \beta_0 \gamma_{IJ}^{(2)} + \frac{2}{3} \gamma_{IK}^{(1)} \gamma_{KJ}^{(2)} + \frac{4}{3} \gamma_{IK}^{(2)} \gamma_{KJ}^{(1)} \right\} \\ & \left. + \frac{1}{\epsilon} \left\{ \frac{2}{3} \gamma_{IJ}^{(3)} \right\} \right] \end{aligned} \quad (6.5)$$

where, γ_{IJ} is expanded in powers of a_s as

$$\gamma_{IJ} = \sum_{n=1}^{\infty} a_s^n \gamma_{IJ}^{(n)}. \quad (6.6)$$

The second term of the action in eq. 6.1 can be written in terms of renormalized quantities:

$$-\frac{1}{2} \int d^4x h_{\mu\nu} (\kappa_G O^{G,\mu\nu} + \kappa_Q O^{Q,\mu\nu}) \quad (6.7)$$

where the κ_I are related to the bare ones by

$$\begin{bmatrix} \hat{\kappa}_G & \hat{\kappa}_Q \end{bmatrix} = \begin{bmatrix} \kappa_G & \kappa_Q \end{bmatrix} \begin{bmatrix} Z_{GG} & Z_{GQ} \\ Z_{QG} & Z_{QQ} \end{bmatrix}. \quad (6.8)$$

6.3 Form factors and its infrared structure

We need to compute the on-shell form factors and then employ its universal IR structure to extract the UV renormalization constants order by order in perturbation theory. To calculate the form factors we have to find the matrix elements of unrenormalized composite operators $\hat{\mathcal{O}}^I$, $I = G, Q$ between a pair of on-shell partonic states $i = q, g$ and the vacuum state. In the color space these matrix elements are expanded in the powers of bare coupling constant \hat{a}_s as

$$|\mathcal{M}_i^I\rangle = \sum_{n=0}^{\infty} \hat{a}_s^n \left(\frac{Q^2}{\mu^2} \right)^{n\epsilon/2} S_\epsilon^n |\hat{\mathcal{M}}_i^{I,(n)}\rangle \quad (6.9)$$

where $i = q, \bar{q}, g$. Then we can define the on-shell form factor of $\hat{\mathcal{O}}^I$ by taking the the overlap of $|\mathcal{M}_i^I\rangle$ with its leading order amplitude normalized with respect to the leading order contribution. With these two operators, there exists four independent form factors:

$$\hat{\mathcal{F}}^{I,g,(n)} = \frac{\langle \hat{\mathcal{M}}_g^{G,(0)} | \hat{\mathcal{M}}_g^{I,(n)} \rangle}{\langle \hat{\mathcal{M}}_g^{G,(0)} | \hat{\mathcal{M}}_g^{G,(0)} \rangle}, \quad \hat{\mathcal{F}}^{I,q,(n)} = \frac{\langle \hat{\mathcal{M}}_q^{Q,(0)} | \hat{\mathcal{M}}_q^{I,(n)} \rangle}{\langle \hat{\mathcal{M}}_q^{Q,(0)} | \hat{\mathcal{M}}_q^{Q,(0)} \rangle} \quad I = G, Q. \quad (6.10)$$

While the diagonal elements $|\hat{\mathcal{M}}_g^{G,(n)}\rangle$ and $|\hat{\mathcal{M}}_q^{Q,(n)}\rangle$ have leading order contributions, the non-diagonal amplitudes $|\hat{\mathcal{M}}_g^{Q,(n)}\rangle$ and $|\hat{\mathcal{M}}_q^{G,(n)}\rangle$, start at one-loop level. In other words, the form factors for diagonal ones start at $\mathcal{O}(\hat{a}_s^0)$; the non-diagonal terms starts to contribute at $\mathcal{O}(\hat{a}_s)$.

The form factors are often ill-defined in 4-dimensions even after UV renormalization due the presence of soft and collinear singularities. The massless gluons and light quarks and

anti-quarks bring in these divergences beyond the leading order in perturbation theory, which manifests as poles in the dimensional regularization parameter ϵ . Thanks to factorization properties and universality of the IR divergences, these on-shell form factors satisfy Sudakov differential equation, famously known as K-G equation². Using the universal IR di-pole subtraction operators, Catani [142] proposed a generalization to multiparton amplitudes up to two loop level in QCD, see also [143]. The generalization of IR subtraction operators of Catani beyond two loops were proposed by Becher and Neubert [144] and by Gardi and Magnea [145]. Following closely the notation used in [146], we find that the UV finite form factors $\mathcal{F}^{I,i}(\hat{a}_s, Q^2, \mu^2, \epsilon)$, after performing strong coupling constant and operator renormalizations, satisfy the integro-differential K-G equation, where the later follows from gauge and renormalization group invariances [147–150]. The equation reads as following

$$Q^2 \frac{d}{dQ^2} \ln \mathcal{F}^{I,i}(\hat{a}_s, Q^2, \mu^2, \epsilon) = \frac{1}{2} \left[K^i \left(\hat{a}_s, \frac{\mu_R^2}{\mu^2}, \epsilon \right) + G^{I,i} \left(\hat{a}_s, \frac{Q^2}{\mu_R^2}, \frac{\mu_R^2}{\mu^2}, \epsilon \right) \right] \quad (6.11)$$

where the $Q^2 = -q^2 = -(p_1 + p_2)^2$ with p_i being the momenta of external on-shell states. The function K^i contains all poles in ϵ and is independent of the scale Q^2 . The finite terms in $\epsilon \rightarrow 0$ are encapsulated in $G^{I,i}$.

The solutions present a universal structure of the singularities, except the single pole in ϵ . Single poles are controlled by the finite functions $G^{I,i}$. We find

$$\begin{aligned} G^{I,i} \left(\hat{a}_s, \frac{Q^2}{\mu_R^2}, \frac{\mu_R^2}{\mu^2}, \epsilon \right) &= G^{I,i} \left(a_s(\mu_R^2), \frac{Q^2}{\mu_R^2}, \epsilon \right) \\ &= G^{I,i} \left(a_s(Q^2), 1, \epsilon \right) + \int_{\frac{Q^2}{\mu_R^2}}^1 \frac{d\lambda^2}{\lambda^2} A^i(\lambda^2 \mu_R^2) \end{aligned} \quad (6.12)$$

where A^i are cusp anomalous dimension and is operator independent.

It was first observed in [28, 134] that the coefficient $G^{I,i}$ of the single pole in ϵ manifests a

²The name is due to the presence of two functions in Sudakov differential equation which are popularly denoted by letters K and G .

universal structure, in terms of the anomalous dimensions. The factorization of the single pole in quark and gluon form factors in terms of soft and collinear anomalous dimensions was first revealed up to two loop level in [28], whose validity at three loop was later established in the article [134]. Expanding $G^{I,i}$ as

$$G^{I,i}(a_s(Q^2), 1, \epsilon) = \sum_{n=1}^{\infty} a_s^n(Q^2) G_n^{I,i}(\epsilon) \quad (6.13)$$

we find

$$G_n^{I,i}(\epsilon) = 2B_n^i + f_n^i + C_n^{I,i} + \sum_{k=1}^{\infty} \epsilon^k g_n^{I,i,k}, \quad (6.14)$$

where, the constants $C_n^{I,i}$ up to three-loop are [151]

$$\begin{aligned} C_1^{I,i} &= 0, \\ C_2^{I,i} &= -2\beta_0 g_1^{I,i,1}, \\ C_3^{I,i} &= -2\beta_1 g_1^{I,i,1} - 2\beta_0 (g_2^{I,i,1} + 2\beta_0 g_1^{I,i,2}). \end{aligned} \quad (6.15)$$

In the above expressions, $X_n^{I,i}$ with $X = A, B, f$ are defined through

$$X^{I,i} \equiv \sum_{n=1}^{\infty} a_s^n X_n^{I,i}. \quad (6.16)$$

The constant $G_n^{I,i}(\epsilon)$ in eq. 6.14 depends not only on the universal collinear (B_n^i) and soft (f_n^i) anomalous dimensions, but also the operator as well as process dependent constants $g_n^{I,i,k}$. Since A^i [56, 152–156], B^i [153] and f^i [28, 134] are known up to three loop level, we can use the solution to K-G equation to determine the renormalisation constants Z_{IJ} . Hence our next task is to compute the on-shell form factors order by order in perturbation theory and compare them against the predictions of K-G equation to determine the unknown renormalisation constants γ_{IJ} in Z_{IJ} . Using these renormalisation constants, we obtain UV finite on-shell form factors of O^I up to three loop level.

6.4 Computation and results

We briefly describe the methodology used in computing the unrenormalized form factors $\hat{\mathcal{F}}^{I,i,(n)}$ and subsequently the anomalous dimension γ_{IJ} up to three loop level in perturbation theory. We closely follow the steps used in the derivation of three loop unrenormalized form factors of scalar and vector form factors [137, 138], see also [103, 139, 157]. We have generated the Feynman diagrams using QGRAF [105]. At three loop the number of diagrams for the amplitude $|\hat{\mathcal{M}}_g^{G,(3)}\rangle$ were 1586, 447 for $|\hat{\mathcal{M}}_g^{Q,(3)}\rangle$, 400 for $|\hat{\mathcal{M}}_q^{G,(3)}\rangle$ and 244 for $|\hat{\mathcal{M}}_q^{Q,(3)}\rangle$. Using an in-house routine in FORM [106], we convert the QGRAF output to a suitable format to perform substitution of Feynman rules, contraction of Lorentz and color indices and simplification of Dirac and Gell-Mann matrices. We have included ghost loops in the Feynman gauge. For the external on-shell gluons, we have kept only transversely polarization states of gluons in n-dimensions. The resulting matrix elements consist of huge number of scalar Feynman integrals which are reduced to few scalar integrals, called master integrals (MIs) by employing integration-by-parts (IBP) [108, 109] and Lorentz invariance (LI) [110] identities. The reduction to MIs is achieved using Laporta algorithm, [158] implemented in various symbolic manipulation packages such as AIR [159], FIRE [160], Reduze2 [161, 162] and LiteRed [111, 163]. For our computational purposes we have used Reduze2 [161, 162] to shift the loop momenta in Feynman diagrams in order to belong them to suitable integral classes. Then we make extensive use of LiteRed [111, 163] to reduce the integrals to MIs. We find that at three loop level, there are 22 topologically different master integrals (MIs) involving genuine three-loop integrals with vertex functions ($A_{t,i}$), three-loop propagator integrals ($B_{t,i}$) and products of one- and two-loop integrals ($C_{t,i}$). The integrals, computed analytically as a Laurent series in ϵ can be found in [164–168]. On substituting these MIs we compute the unrenormalized form factors.

Next we shall determine the operator renormalisation constants Z_{IJ} . We compute them by

exploiting the universal IR structure of the form factors *i.e.* by comparing order by order the results of renormalized form factors expressed in terms of unknown γ_{IJ} against the predictions of the K-G equation expressed in terms of A^i , B^i and f^i anomalous dimensions that are known up to three loop level. The $\gamma_{IJ}^{(n)}$ are given below:

$$\gamma_{GG}^{(1)} = -\frac{2}{3}n_f \quad (6.17)$$

$$\gamma_{GG}^{(2)} = -\frac{35}{27}C_A n_f - \frac{74}{27}C_F n_f \quad (6.18)$$

$$\begin{aligned} \gamma_{GG}^{(3)} = & C_A^2 n_f \left(-\frac{3589}{162} + 24\zeta_3 \right) + C_A C_F n_f \left(\frac{139}{9} - \frac{104}{3}\zeta_3 \right) + C_F^2 n_f \left(-\frac{2155}{243} + \frac{32}{3}\zeta_3 \right) \\ & + C_A n_f^2 \left(\frac{1058}{243} \right) - C_F n_f^2 \left(\frac{173}{243} \right) \end{aligned} \quad (6.19)$$

$$\gamma_{GQ}^{(1)} = C_F \left(\frac{8}{3} \right) \quad (6.20)$$

$$\gamma_{GQ}^{(2)} = C_A C_F \left(\frac{376}{27} \right) - C_F^2 \left(\frac{112}{27} \right) - C_F n_f \left(\frac{104}{27} \right) \quad (6.21)$$

$$\begin{aligned} \gamma_{GQ}^{(3)} = & C_A^2 C_F \left(\frac{20920}{243} + \frac{64}{3}\zeta_3 \right) + C_A C_F^2 \left(-\frac{8528}{243} - 64\zeta_3 \right) + C_F^3 \left(-\frac{560}{243} + \frac{128}{3}\zeta_3 \right) \\ & + C_A C_F n_f \left(-\frac{22}{9} - \frac{128}{3}\zeta_3 \right) + C_F^2 n_f \left(-\frac{7094}{243} + \frac{128}{3}\zeta_3 \right) - C_F n_f^2 \left(\frac{284}{81} \right) \end{aligned} \quad (6.22)$$

where $C_A = N$ and $C_F = (N^2 - 1)/2N$ are the quadratic Casimir of the $SU(N)$ group. $T_F = 1/2$ and n_f is the number of light active quark flavors. ζ_i is the Riemann Zeta function. The remaining entries are $\gamma_{QG}^{(n)} = -\gamma_{GG}^{(n)}$ and $\gamma_{QQ}^{(n)} = -\gamma_{GQ}^{(n)}$ where $n = 1, 2, 3$. These relations are due to the fact that the sum of these operators is conserved. This serves as a crucial check on the correctness of our computation. Interestingly, all the $\gamma_{GG}^{(n)}$ are proportional to n_f which is consistent with the expectation that the conservation property of the operator $\hat{O}^{G,\mu\nu}$ breaks down beyond tree level due to the presence of quark loops.

The renormalized form factors can be obtained using eq. 4.34, 4.35, 6.3, 6.5. Setting

$\mu_R^2 = Q^2$, expanding in terms of $a_s(Q^2)$ as

$$\mathcal{F}^{I,i}(Q^2) = \sum_{n=0}^{\infty} a_s^n(Q^2) \mathcal{F}^{I,i,(n)}, \quad I = G, Q \quad i = g, q. \quad (6.23)$$

where $\mathcal{F}^{I,i,(n)}$ up to three loop level are given by

$$\begin{aligned} \mathcal{F}^{G,g,(1)} &= \frac{2}{\epsilon} \gamma_{GG}^{(1)} + \hat{\mathcal{F}}^{G,g,(1)} \\ \mathcal{F}^{G,g,(2)} &= \frac{2}{\epsilon^2} \left\{ \beta_0 \gamma_{GG}^{(1)} + (\gamma_{GG}^{(1)})^2 + \gamma_{GQ}^{(1)} \gamma_{QG}^{(1)} \right\} + \frac{1}{\epsilon} \left\{ 2 \hat{\mathcal{F}}^{G,g,(1)} (\beta_0 + \gamma_{GG}^{(1)}) \right. \\ &\quad \left. 2 \hat{\mathcal{F}}^{Q,g,(1)} \gamma_{GQ}^{(1)} + \gamma_{GG}^{(2)} \right\} + \hat{\mathcal{F}}^{G,g,(2)} \\ \mathcal{F}^{G,g,(3)} &= \frac{1}{\epsilon^3} \left\{ \frac{8}{3} \beta_0^2 \gamma_{GG}^{(1)} + 4 \beta_0 (\gamma_{GG}^{(1)})^2 + \frac{4}{3} (\gamma_{GG}^{(1)})^3 + 4 \beta_0 \gamma_{GQ}^{(1)} \gamma_{QG}^{(1)} + \frac{8}{3} \gamma_{GG}^{(1)} \gamma_{GQ}^{(1)} \gamma_{QG}^{(1)} \right. \\ &\quad \left. + \frac{4}{3} \gamma_{GQ}^{(1)} \gamma_{QG}^{(1)} \gamma_{QG}^{(1)} \right\} + \frac{1}{\epsilon^2} \left\{ 4 \beta_0^2 \hat{\mathcal{F}}^{G,g,(1)} + \frac{4}{3} \beta_1 \gamma_{GG}^{(1)} + 6 \beta_0 \hat{\mathcal{F}}^{G,g,(1)} \gamma_{GG}^{(1)} \right. \\ &\quad \left. + 2 \hat{\mathcal{F}}^{G,g,(1)} (\gamma_{GG}^{(1)})^2 + 6 \beta_0 \hat{\mathcal{F}}^{Q,g,(1)} \gamma_{GQ}^{(1)} + 2 \hat{\mathcal{F}}^{Q,g,(1)} \gamma_{GG}^{(1)} \gamma_{GQ}^{(1)} + \hat{\mathcal{F}}^{G,g,(1)} \gamma_{GQ}^{(1)} \gamma_{QG}^{(1)} \right. \\ &\quad \left. + \hat{\mathcal{F}}^{Q,g,(1)} \gamma_{GQ}^{(1)} \gamma_{QG}^{(1)} + \frac{4}{3} \beta_0 \gamma_{GG}^{(2)} + 2 \gamma_{GG}^{(1)} \gamma_{GG}^{(2)} + \frac{4}{3} \gamma_{GQ}^{(2)} \gamma_{QG}^{(1)} + \frac{2}{3} \gamma_{GQ}^{(1)} \gamma_{QG}^{(2)} \right\} \\ &\quad + \frac{1}{\epsilon} \left\{ \beta_1 \hat{\mathcal{F}}^{G,g,(1)} + 4 \beta_0 \hat{\mathcal{F}}^{G,g,(2)} + 2 \hat{\mathcal{F}}^{G,g,(2)} \gamma_{GG}^{(1)} + 2 \hat{\mathcal{F}}^{Q,g,(2)} \gamma_{GQ}^{(1)} + \hat{\mathcal{F}}^{G,g,(1)} \gamma_{GG}^{(2)} \right. \\ &\quad \left. + \hat{\mathcal{F}}^{Q,g,(1)} \gamma_{GQ}^{(2)} + \frac{2}{3} \gamma_{GG}^{(3)} \right\} + \hat{\mathcal{F}}^{G,g,(3)} \\ \mathcal{F}^{G,q,(1)} &= \frac{2}{\epsilon} \gamma_{GQ}^{(1)} + \hat{\mathcal{F}}^{G,q,(1)} \\ \mathcal{F}^{G,q,(2)} &= \frac{2}{\epsilon^2} \left\{ \beta_0 \gamma_{GQ}^{(1)} + \gamma_{GG}^{(1)} \gamma_{GQ}^{(1)} + \gamma_{GQ}^{(1)} \gamma_{QG}^{(1)} \right\} + \frac{1}{\epsilon} \left\{ 2 \beta_0 \hat{\mathcal{F}}^{G,q,(1)} + 2 \hat{\mathcal{F}}^{G,q,(1)} \gamma_{GG}^{(1)} \right. \\ &\quad \left. + 2 \hat{\mathcal{F}}^{Q,q,(1)} \gamma_{GQ}^{(1)} + \gamma_{GQ}^{(2)} \right\} + \hat{\mathcal{F}}^{G,q,(2)} \\ \mathcal{F}^{G,q,(3)} &= \frac{1}{\epsilon^3} \left\{ \frac{8}{3} \beta_0^2 \gamma_{GQ}^{(1)} + 4 \beta_0 \gamma_{GG}^{(1)} \gamma_{GQ}^{(1)} + \frac{4}{3} (\gamma_{GG}^{(1)})^2 \gamma_{GQ}^{(1)} + \frac{4}{3} (\gamma_{GQ}^{(1)})^2 \gamma_{QG}^{(1)} + 4 \beta_0 \gamma_{GQ}^{(1)} \gamma_{QG}^{(1)} \right. \\ &\quad \left. + \frac{4}{3} \gamma_{GG}^{(1)} \gamma_{GQ}^{(1)} \gamma_{QG}^{(1)} + \frac{4}{3} \gamma_{GQ}^{(1)} (\gamma_{QG}^{(1)})^2 \right\} + \frac{1}{\epsilon^2} \left\{ 4 \beta_0^2 \hat{\mathcal{F}}^{G,q,(1)} + 6 \beta_0 \hat{\mathcal{F}}^{G,q,(1)} \gamma_{GG}^{(1)} \right. \\ &\quad \left. + 2 \hat{\mathcal{F}}^{G,q,(1)} (\gamma_{GG}^{(1)})^2 + \frac{4}{3} \beta_1 \gamma_{GQ}^{(1)} + 6 \beta_0 \hat{\mathcal{F}}^{Q,q,(1)} \gamma_{GQ}^{(1)} + 2 \hat{\mathcal{F}}^{Q,q,(1)} \gamma_{GG}^{(1)} \gamma_{GQ}^{(1)} \right. \\ &\quad \left. + 2 \hat{\mathcal{F}}^{G,q,(1)} \gamma_{GQ}^{(1)} \gamma_{QG}^{(1)} + 2 \hat{\mathcal{F}}^{Q,q,(1)} \gamma_{GQ}^{(1)} \gamma_{QG}^{(1)} + \frac{4}{3} \gamma_{GQ}^{(1)} \gamma_{GG}^{(2)} + \frac{4}{3} \beta_0 \gamma_{GQ}^{(2)} + \frac{2}{3} \gamma_{GG}^{(1)} \gamma_{GQ}^{(2)} \right. \\ &\quad \left. + \frac{4}{3} \gamma_{QG}^{(1)} \gamma_{GQ}^{(2)} + \frac{2}{3} \gamma_{GQ}^{(1)} \gamma_{QG}^{(2)} \right\} + \frac{1}{\epsilon} \left\{ \beta_1 \hat{\mathcal{F}}^{G,q,(1)} + 4 \beta_0 \hat{\mathcal{F}}^{G,q,(2)} + 2 \hat{\mathcal{F}}^{G,q,(2)} \gamma_{GG}^{(1)} \right. \\ &\quad \left. + 2 \hat{\mathcal{F}}^{Q,q,(2)} \gamma_{GQ}^{(1)} + \hat{\mathcal{F}}^{G,q,(1)} \gamma_{GG}^{(2)} + \hat{\mathcal{F}}^{Q,q,(1)} \gamma_{GQ}^{(2)} + \frac{2}{3} \gamma_{GQ}^{(3)} \right\} + \hat{\mathcal{F}}^{G,q,(3)} \end{aligned}$$

$$\begin{aligned}
\mathcal{F}^{\mathcal{Q},g,(1)} &= \frac{2}{\epsilon} \gamma_{QG}^{(1)} + \hat{\mathcal{F}}^{\mathcal{Q},g,(1)} \\
\mathcal{F}^{\mathcal{Q},g,(2)} &= \frac{2}{\epsilon^2} \left\{ \beta_0 \gamma_{QG}^{(1)} + \gamma_{GG}^{(1)} \gamma_{QG}^{(1)} + \gamma_{QG}^{(1)} \gamma_{QQ}^{(1)} \right\} + \frac{1}{\epsilon} \left\{ 2\beta_0 \hat{\mathcal{F}}^{\mathcal{Q},g,(1)} + 2\hat{\mathcal{F}}^{G,g,(1)} \gamma_{QG}^{(1)} \right. \\
&\quad \left. + 2\hat{\mathcal{F}}^{\mathcal{Q},g,(1)} \gamma_{QQ}^{(1)} + \gamma_{QG}^{(2)} \right\} + \hat{\mathcal{F}}^{\mathcal{Q},g,(2)} \\
\mathcal{F}^{\mathcal{Q},g,(3)} &= \frac{1}{\epsilon^3} \left\{ \frac{8}{3} \beta_0^2 \gamma_{QG}^{(1)} + 4\beta_0 \gamma_{GG}^{(1)} \gamma_{QG}^{(1)} + \frac{4}{3} (\gamma_{GG}^{(1)})^2 \gamma_{QG}^{(1)} + \frac{4}{3} \gamma_{GQ}^{(1)} (\gamma_{QG}^{(1)})^2 + 4\beta_0 \gamma_{QG}^{(1)} \gamma_{QQ}^{(1)} \right. \\
&\quad \left. + \frac{4}{3} \gamma_{GG}^{(1)} \gamma_{QG}^{(1)} \gamma_{QQ}^{(1)} + \frac{4}{3} \gamma_{QG}^{(1)} (\gamma_{QQ}^{(1)})^2 \right\} + \frac{1}{\epsilon^2} \left\{ 4\beta_0^2 \hat{\mathcal{F}}^{\mathcal{Q},g,(1)} + \frac{4}{3} \beta_1 \gamma_{QG}^{(1)} \right. \\
&\quad \left. + 6\beta_0 \hat{\mathcal{F}}^{G,g,(1)} \gamma_{QG}^{(1)} + 2\hat{\mathcal{F}}^{G,g,(1)} \gamma_{GG}^{(1)} \gamma_{QG}^{(1)} + 2\hat{\mathcal{F}}^{\mathcal{Q},g,(1)} \gamma_{GQ}^{(1)} \gamma_{QG}^{(1)} + 6\beta_0 \hat{\mathcal{F}}^{\mathcal{Q},g,(1)} \gamma_{QQ}^{(1)} \right. \\
&\quad \left. + 2\hat{\mathcal{F}}^{G,g,(1)} \gamma_{QG}^{(1)} \gamma_{QQ}^{(1)} + 2\hat{\mathcal{F}}^{\mathcal{Q},g,(1)} (\gamma_{QQ}^{(1)})^2 + \frac{2}{3} \gamma_{QG}^{(1)} \gamma_{GG}^{(2)} + \frac{4}{3} \beta_0 \gamma_{QG}^{(2)} + \frac{4}{3} \gamma_{GG}^{(1)} \gamma_{QG}^{(2)} \right. \\
&\quad \left. + \frac{2}{3} \gamma_{QQ}^{(1)} \gamma_{QG}^{(2)} + \frac{4}{3} \gamma_{QG}^{(1)} \gamma_{QQ}^{(2)} \right\} + \frac{1}{\epsilon} \left\{ \beta_1 \hat{\mathcal{F}}^{\mathcal{Q},g,(1)} + 4\beta_0 \hat{\mathcal{F}}^{\mathcal{Q},g,(2)} + 2\hat{\mathcal{F}}^{G,g,(2)} \gamma_{QG}^{(1)} \right. \\
&\quad \left. + 2\hat{\mathcal{F}}^{\mathcal{Q},g,(2)} \gamma_{QQ}^{(1)} + \hat{\mathcal{F}}^{G,g,(1)} \gamma_{QG}^{(2)} + \hat{\mathcal{F}}^{\mathcal{Q},g,(1)} \gamma_{QQ}^{(2)} + \frac{2}{3} \gamma_{QG}^{(3)} \right\} + \hat{\mathcal{F}}^{\mathcal{Q},g,(3)} \\
\mathcal{F}^{\mathcal{Q},q,(1)} &= \frac{2}{\epsilon} \gamma_{QQ}^{(1)} + \hat{\mathcal{F}}^{\mathcal{Q},q,(1)} \\
\mathcal{F}^{\mathcal{Q},q,(2)} &= \frac{2}{\epsilon^2} \left\{ \gamma_{GQ}^{(1)} \gamma_{QG}^{(1)} + \beta_0 \gamma_{QQ}^{(1)} + (\gamma_{QQ}^{(1)})^2 \right\} + \frac{1}{\epsilon} \left\{ 2\beta_0 \hat{\mathcal{F}}^{\mathcal{Q},q,(1)} + 2\hat{\mathcal{F}}_q^{G,(1)} \gamma_{QG}^{(1)} \right. \\
&\quad \left. + 2\hat{\mathcal{F}}^{\mathcal{Q},q,(1)} \gamma_{QQ}^{(1)} + \gamma_{QQ}^{(2)} \right\} + \hat{\mathcal{F}}^{\mathcal{Q},q,(2)} \\
\mathcal{F}^{\mathcal{Q},q,(3)} &= \frac{1}{\epsilon^3} \left\{ 4\beta_0 \gamma_{GQ}^{(1)} \gamma_{QG}^{(1)} + \frac{4}{3} \gamma_{GG}^{(1)} \gamma_{GQ}^{(1)} \gamma_{QG}^{(1)} + \frac{8}{3} \left\{ \beta_0^2 \gamma_{QQ}^{(1)} + \gamma_{GQ}^{(1)} \gamma_{QG}^{(1)} \gamma_{QQ}^{(1)} \right\} \right. \\
&\quad \left. + 4\beta_0 (\gamma_{QQ}^{(1)})^2 + \frac{4}{3} (\gamma_{QQ}^{(1)})^3 \right\} + \frac{1}{\epsilon^2} \left\{ 4\beta_0^2 \hat{\mathcal{F}}^{\mathcal{Q},q,(1)} + 6\beta_0 \hat{\mathcal{F}}^{G,q,(1)} \gamma_{QG}^{(1)} \right. \\
&\quad \left. + 2\hat{\mathcal{F}}^{G,q,(1)} \gamma_{GG}^{(1)} \gamma_{QG}^{(1)} + 2\hat{\mathcal{F}}^{\mathcal{Q},q,(1)} \gamma_{GQ}^{(1)} \gamma_{QG}^{(1)} + \frac{4}{3} \beta_1 \gamma_{QG}^{(1)} + 6\beta_0 \hat{\mathcal{F}}^{\mathcal{Q},q,(1)} \gamma_{QQ}^{(1)} \right. \\
&\quad \left. + 2\hat{\mathcal{F}}^{G,q,(1)} \gamma_{QG}^{(1)} \gamma_{QQ}^{(1)} + 2\hat{\mathcal{F}}^{\mathcal{Q},q,(1)} (\gamma_{QQ}^{(1)})^2 + \frac{2}{3} \gamma_{QG}^{(1)} \gamma_{GQ}^{(2)} + \frac{4}{3} \gamma_{GQ}^{(1)} \gamma_{QG}^{(2)} + \frac{4}{3} \beta_0 \gamma_{QQ}^{(2)} \right. \\
&\quad \left. + 2\gamma_{QQ}^{(1)} \gamma_{QQ}^{(2)} \right\} + \frac{1}{\epsilon} \left\{ \beta_1 \hat{\mathcal{F}}^{\mathcal{Q},q,(1)} + 4\beta_0 \hat{\mathcal{F}}^{\mathcal{Q},q,(2)} + 2\hat{\mathcal{F}}^{G,q,(2)} \gamma_{QG}^{(1)} + 2\hat{\mathcal{F}}^{\mathcal{Q},q,(2)} \gamma_{QQ}^{(1)} \right. \\
&\quad \left. + \hat{\mathcal{F}}^{G,q,(1)} \gamma_{QG}^{(2)} + \hat{\mathcal{F}}^{\mathcal{Q},q,(1)} \gamma_{QQ}^{(2)} + \frac{2}{3} \gamma_{QQ}^{(3)} \right\} + \hat{\mathcal{F}}^{\mathcal{Q},q,(3)} \tag{6.24}
\end{aligned}$$

where the terms $\hat{\mathcal{F}}^{I,i,(n)}$ are the unrenormalized form factors, presented in Appendix 11.3.

In the next section we shall discuss about some interesting connections between the form factor results in QCD with that of $\mathcal{N} = 4$ supersymmetric Yang-Mills theory (SYM).

6.5 Leading Transcendentality principle

The on-shell form factors in the supersymmetric Yang-Mills theory has helped to understand the intricacies of quantum field theory. $\mathcal{N} = 4$ SYM is UV finite in $n = 4$ dimensions and also dual to type IIB string theory on $AdS_5 \times S^5$ with self dual RR field strength. This makes it possible to relate quantities computed in $\mathcal{N} = 4$ SYM in the strong coupling limit with those obtained in the weak coupling limit of the gravity theory. By expanding in a perturbative series of the strong coupling constant, on-shell amplitudes and form factors have been computed to very good accuracy in order to make non-perturbative predictions through systematic resummation procedures. There are works on resummation of perturbative contributions [169, 170] for MHV amplitudes to all orders in 't Hooft coupling. $\mathcal{N} = 4$ SYM being maximally supersymmetric, large cancellations take place between various contributions which results in elegant and simple looking predictions that have a lot of resemblance with those in QCD. In this regard it is important to mention about the principle of the leading transcendentality (LT) [171–173].

By extending the BFKL and DGLAP evolution equations for the supersymmetric case, Kotikov and Lipatov [171, 174, 175] conjectured maximum transcendentality principle which implies that the anomalous dimensions of leading twist two operators in $\mathcal{N} = 4$ SYM contain uniform transcendental terms which are related to those in the corresponding QCD results [152, 153]. This property is seen in scattering amplitudes of certain type [176, 177], FFs of the BPS type operators [178–180], light-like Wilson loops [181, 182] and correlation functions [180, 182] in $\mathcal{N} = 4$ SYM. In any perturbative computation of amplitudes and form factors we get terms such as $\zeta(n)$, ϵ^{-n} and Harmonic polylogarithms, that can be assigned certain transcendental weights. The maximum degree of transcendentality depends on the order (l) of perturbation theory eg. at two loops it is 4. Thus the terms $\zeta(n)$, ϵ^{-n} carry weight n ; ϵ^n is of weight $-n$. The form factors of half-BPS operators in $\mathcal{N} = 4$ SYM theory have uniform transcendental weight, owing to its protected nature.

However QCD results contain terms of all transcendental weights (up to $2l$) in addition to rational terms (zero transcendentality). It was observed that the the QCD quark and gluon form factors [137] and scalar form factor in $\mathcal{N} = 4$ SYM share an interesting relation. On putting the color substitution [172] $C_A = C_F = N$ and $n_f = N$ in the quark and gluon form factors, their LT parts not only coincide with each other but also become identical, to the form factors of half-BPS operator in $\mathcal{N} = 4$ SYM [183]. In the work [139] the diagonal terms for the pseudo-scalar form factors $\mathcal{F}^{G,g}$ and $\mathcal{F}^{J,q}$ were found to exhibit similar type of behavior. The LT terms for the three point form factors, $H \rightarrow ggg$ in QCD [184] at two loop level were found to be same as those of half-BPS operator in $\mathcal{N} = 4$ SYM [179].

Our computation of form factors also show some interesting behaviors in terms of their LT parts. We have found that the LT terms of the diagonal form factors, $\hat{\mathcal{F}}^{G,g}, \hat{\mathcal{F}}^{Q,q}$ with the above prescribed color replacement, are not only identical to each other but also coincide with the LT terms of the scalar form factors in $\mathcal{N} = 4$ SYM [183]. This is found to be true for terms containing positive powers in ϵ available up to transcendentality 8 [185]. In addition, for the off diagonal terms namely $\hat{\mathcal{F}}^{G,q}, \hat{\mathcal{F}}^{Q,g}$, the LT parts are identical to one another; however they do not coincide with the diagonal ones.

6.6 Conclusion

Most of the extra dimensional models assume the coupling of the SM fields to that of a massive spin-2 field to be same. In our current study we have investigated in details the theoretical issues that arise when the gauge and fermion fields of the SM interact with unequal coupling strengths with a massive spin-2 field. We have divided the energy momentum tensor of QCD into two parts in such a way that purely gauge interactions form one tensor operator, $\hat{\mathcal{O}}^{G,\mu\nu}$, while the fermions and their interaction with the gauge fields are encapsulated in another operator, $\hat{\mathcal{O}}^{Q,\mu\nu}$. These composite operators are gauge invariant but are not conserved like the usual energy momentum tensor. Hence they require

additional UV renormalisation. We have exploited the universal IR structure of on-shell amplitudes for the composite operators to compute these UV renormalization constants. The form factors are computed up to three loop order in perturbation theory; then using the K-G equation we obtain the UV anomalous dimensions and thus the renormalisation constants up to three loop level. We find that all the anomalous dimension $\gamma_{GG}^{(n)}$ are proportional to n_f which implies that the conservation property of the operator $\hat{\mathcal{O}}^{G,\mu\nu}$ breaks down beyond the tree level due to the presence of fermion loops. The renormalization constants and the on-shell FFs are important components of observables that can probe the physics of spin-2 fields. In the next chapter we shall discuss in details, the phenomenological study of the NNLO QCD corrections involving these two operators.

7

Second order QCD corrections in models of gravity with nonuniversal coupling

In the previous chapter we discussed about a scenario where a massive spin-2 field interacts with the SM ones through different coupling strengths. This introduced additional UV divergences which were regulated by multiplying overall UV renormalization constants. We computed the form factors and used the universal IR structure of QCD amplitudes to extract these anomalous dimensions up to three loop order in perturbative QCD. In this chapter we shall extend our study with the two operators to compute the NNLO QCD corrections for production of a lepton pair and present its numerical impact at the energies of LHC.

7.1 Introduction

Currently with the energies at which the LHC is operating, there are no signals of new physics; thus searches of beyond the SM (BSM) physics depend on the ability to make very precise theoretical predictions within the SM. This will help to look for possible deviations between experimental observations and theoretical predictions which can give

hints of the physics beyond the SM. In order to constrain the new physics model parameters, one needs to also compute the BSM signals to the same level of theoretical precision as the SM and compare with the observations made at the LHC. For many observables, QCD corrections are large at the LHC and inclusion of higher order terms reduces the theoretical uncertainties substantially. Many SM processes have been measured at the LHC and the cross sections are in excellent agreement with higher order QCD predictions. This has helped in the discovery of the Higgs boson by ATLAS [17] and CMS [18] collaborations at the LHC which has resulted in the measurement of the important fundamental parameter of the SM, the Higgs mass m_H (see [2, 24, 112]). In addition to understand the stability of electroweak vacuum [186], it is essential to precisely measure the Higgs mass.

Despite the fact that the SM is in excellent agreement with experimental observations, there also are compelling reasons to go beyond the SM. For example models with spin-2 were necessary to ascertain the spin and parity of the 125 GeV boson discovered in the di-photon channel. Most of the popular extra-dimensional models consist of a massive spin-2 particle coupling universally to the SM fields. For universal coupling, depending on the geometry of extra dimensions, viz. large extra dimensions or warped extra dimension models, studies have been extensively carried out up to higher orders in QCD in various channels that are relevant for the LHC. The NLO QCD corrections in this model has been studied in [68, 89, 90] for various observables. Di-vector boson final state have been studied to NLO level in [91–96]. In the framework of aMC@NLO, all the non-color, di-final states have been studied to NLO+PS accuracy [97–99]. Production of a generic spin-2 particle in association with colored particles, vector bosons and the Higgs boson have been studied in [100] to NLO+PS accuracy. The form factor of a spin-2 universally coupled to quarks and gluons up to two loops was computed in [102]. Subsequently the NNLO computation in the threshold limit was done in [101] and finally the full NNLO computation was achieved, as described in the chapter 5. Production of a spin-2 in association with a jet to full two-loop QCD corrections has also been completed with the

evaluation of generic spin-2 decaying to $g g$ [104] and $q \bar{q} g$ [187].

Although there are many works on models of spin-2 with universal coupling, there are stringent bounds on the parameters of these types of models. For example heavy constraints have been put on models with universally-coupled spin-2 particle [188, 189]. Hence models with nonuniversal coupling of a spin-2 to SM are a suitable alternative. Such models consist of a massive spin-2 particle interacting with two gauge invariant SM tensorial operators with different coupling strengths, although each operator is not individually conserved. Models with nonuniversal coupling were incorporated in tools like Higgs characterization [6] to NLO in QCD. There were additional challenges that accompanied such models namely: (a) additional UV renormalization were needed, (b) in the IR sector, additional double and single pole terms had to be cancelled with the counter parts from real emission processes and mass factorization counter terms, thus demonstrating the IR factorization to NLO for nonuniversal coupling [6]. The nonuniversal coupling of spin-2 to SM has been actively considered by the ATLAS Collaboration [190, 191] to provide exclusion of several non-SM spin hypotheses. It is thus necessary to compute NNLO corrections which will help to provide bounds on the parameters for such models. The three loop form factors have been computed, as described in chapter 6. In this chapter we compute the real-real and real-virtual processes up to two loop order in perturbative expansion. The theoretical background necessary to perform the aforementioned computation has already been described in chapter 6; the formula to compute the lepton pair invariant mass distribution is given in eq. 4.43; the necessary steps to arrive at the formula has been elaborated in section 4.2.1. In the next section we present the phenomenological implications of NNLO computation for such a nonuniversal model.

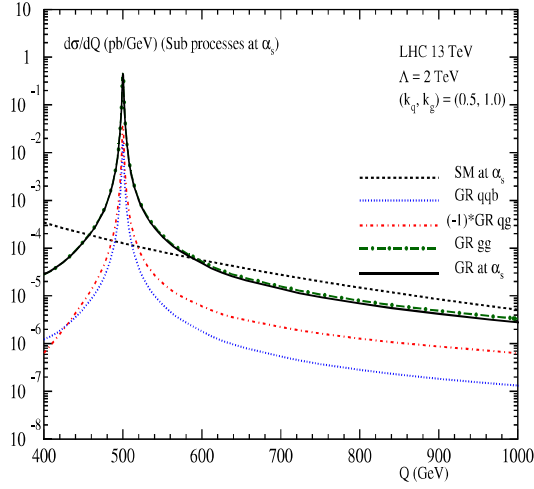


Figure 7.1: First order QCD corrections from different subprocesses to di-lepton production. The choice of the model parameters is as mentioned in the text.

7.2 Phenomenology

The results for the mass factorized partonic cross section are presented in Appendix 11.5. We present in this section, the detailed phenomenology with our NNLO result on the production of di-leptons, applicable for the energies at the LHC. We have considered a minimal scenario of nonuniversal couplings of spin-2 particle with the SM fields, where the spin-2 particle couples to all the SM fermions with coupling $\kappa_Q = \sqrt{2}k_q/\Lambda$ and to all the SM gauge bosons with a coupling strength of $\kappa_G = \sqrt{2}k_g/\Lambda$. Our numerical results are presented for the default choice of model parameters, namely spin-2 particle of mass $m_G = 500$ GeV, the scale $\Lambda = 2$ TeV and the couplings $(k_q, k_g) = (0.5, 1.0)$. We have set the renormalization and factorization scales equal to the invariant mass of the di-lepton, i.e., $\mu_R = \mu_F = Q$. Unless otherwise stated we use MSTW2008nnlo parton distribution functions (PDFs) with the corresponding a_s provided from LHAPDF. We choose $\sqrt{S} = 13$ TeV, the center of mass energy of the incoming hadrons at the LHC.

Throughout our analysis we have restricted ourselves to scenarios where spin-2 particle decays only to SM fields. The spin-2 particle decay widths for nonuniversal couplings are

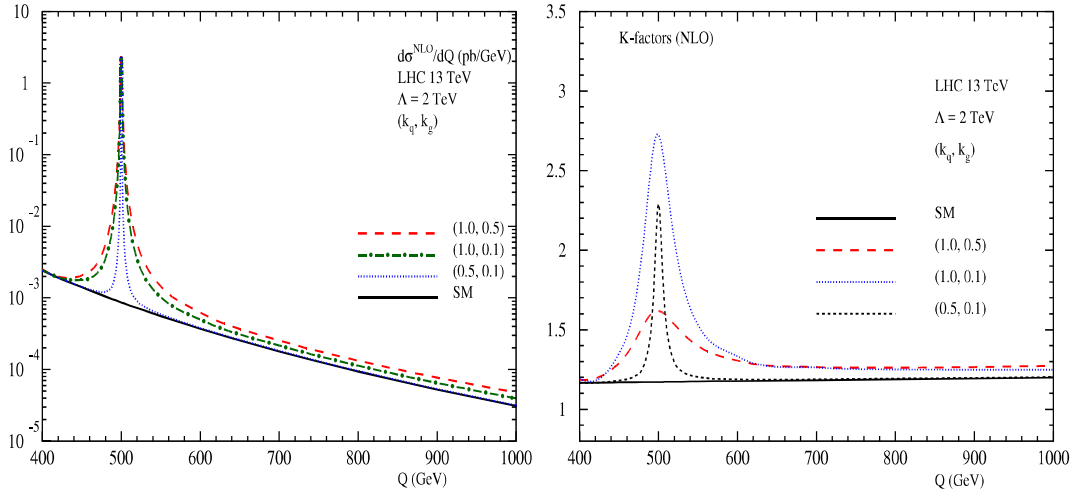


Figure 7.2: Di-lepton invariant mass distributions are presented to NLO QCD for different choice of couplings (k_q, k_g) in the left panel. The corresponding K-factors are presented in the right panel.

same as those given in [67]. In our analysis, the coupling of spin-2 to all bosons are taken to be identical; thus spin-2 decaying to $Z\gamma$ vanishes identically $\Gamma(h \rightarrow Z\gamma) = 0$ [192]. In fig. 7.1, we present the NLO corrections (only at order a_s) from various subprocess contributions to the di-lepton production. As per our choice of model parameters, we find that gg subprocess contribution dominates over the rest. In addition, the total NLO correction is smaller than the gg contribution because of negative contribution from qg subprocess.

The impact of higher order QCD corrections can be captured through the K-factors which are defined as

$$K_1 = \frac{d\sigma^{\text{NLO}}/dQ}{d\sigma^{\text{LO}}/dQ} \quad \text{and} \quad K_2 = \frac{d\sigma^{\text{NNLO}}/dQ}{d\sigma^{\text{LO}}/dQ}. \quad (7.1)$$

In the left panel of fig. 7.2, we present di-lepton invariant mass distributions to NLO for different choices of nonuniversal couplings $(k_q, k_g) = (1.0, 0.5), (1.0, 0.1)$ and $(0.5, 0.1)$. As per expectation for universal couplings, at the resonance region the cross sections i.e. the height of the peak will be same simply because the couplings at the matrix element

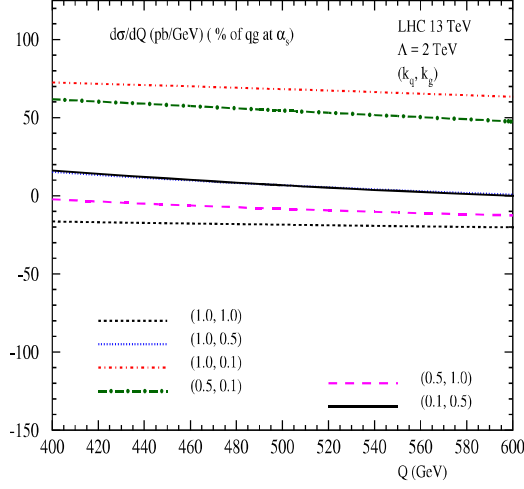


Figure 7.3: Percentage of qg subprocess contribution $R_{qg}^{(1)}$ as defined in the text for different choice of nonuniversal couplings.

level will cancel with those from the decay width of the spin-2 particle. However, for nonuniversal couplings this is not the case thus cross sections at the resonance region for different choices of nonuniversal couplings will be different. Thus, compared to the warped extra dimensional models, the precision as well as the phenomenological studies of the spin-2 particle production in this model will be different. To highlight the impact of different couplings on higher order corrections, we present the NLO K-factor (K_1) in the right panel of fig. 7.2 for various choices of (k_q, k_g) . We observe that the K-factor crucially depends on the choice of nonuniversal couplings. In particular we notice that the K-factors are larger for the choice of couplings (1.0,0.1). To understand this behavior better, we study the percentage contribution of various subprocesses to the total correction at NLO level, particularly from qg subprocess due to its large flux at LHC energies. To quantify we define the percentage of contribution of a given subprocess ab as $R_{ab}^{(i)} = (d\sigma_{ab}^{H_1 H_2, (i)} / dQ^2) / (d\sigma^{H_1 H_2, (i)} / dQ^2) \times 100$, where in the numerator we have contribution from $\Delta_{ab}^{h, (i)}$ and for the denominator, we include all the partonic channels.

We present in fig. 7.3, $R_{qg}^{(1)}$ for different choices of nonuniversal couplings and we observe that the sign of the qg subprocess crucially depends on the choice of couplings. The reason for the large K-factor at the resonance region is because of large positive values of

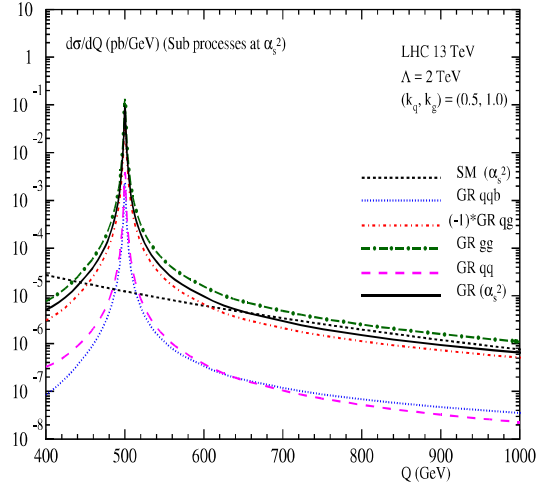


Figure 7.4: Second order QCD corrections from various subprocess to the di-lepton invariant mass distribution.

$R_{qg}^{(1)}$ for some values of coupling. For example $R_{qg}^{(1)}$ is about 70% for the coupling (1.0, 0.1). However, the sign of the contribution from other subprocesses $q\bar{q}$ and gg is found to be positive for various couplings.

The second order QCD corrections (at (α_s^2)) from various subprocesses to the di-lepton production is presented in fig. 7.4, for the default choice of couplings $(k_q, k_g) = (0.5, 1.0)$. We observe that the gg subprocess has the dominant contribution over the rest while qg has a negative contribution which is comparable in magnitude to the dominant channel. In addition we also study the percentage of the relative contribution, $R_{qg}^{(2)}$ to the total second order correction. In fig. 7.5, we present $R_{qg}^{(2)}$ for different choice of couplings. We observe that for the choice of couplings as considered here, the qg contribution varies from about -70% to about 35%. For the couplings (1.0, 0.1) and (0.5, 0.1) the qg contribution is positive while it is negative for the rest of the choices, as well as in the SM. We can conclude that the K-factors for the choice of (1.0, 0.1) coupling is large for a wide range of invariant mass distribution. It is worth mentioning here that in general qg subprocess has a negative contribution both in the SM as well as in the case of universal couplings, irrespective of the value of the latter.

Now we shall study the di-lepton invariant mass distribution to various orders in QCD for

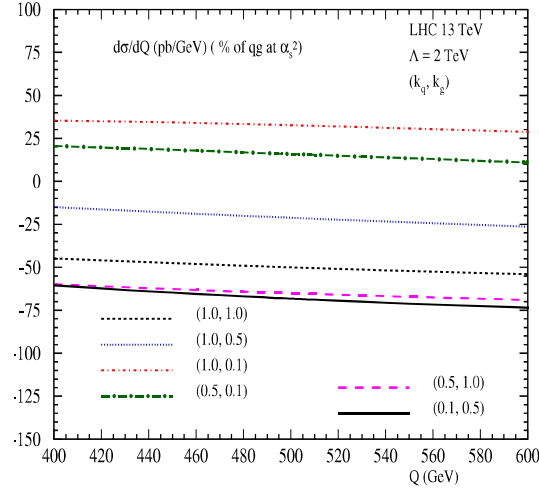


Figure 7.5: Percentage of qg contribution $R_{qg}^{(2)}$ as defined in the text.

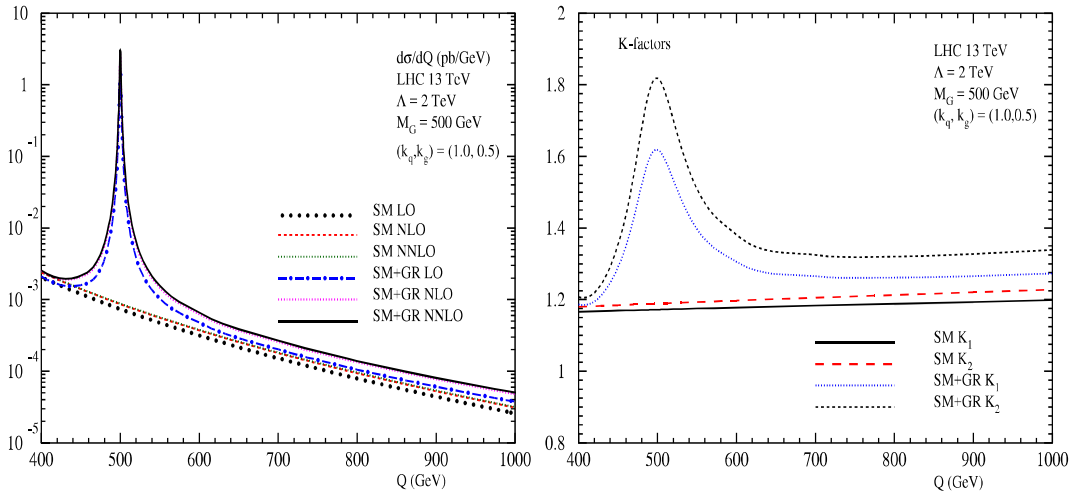


Figure 7.6: Cross sections at different orders (left panel) and the corresponding K-factors K_1 and K_2 (right panel) are presented for different couplings.

a particular choice of couplings (1.0, 0.5), as shown in fig. 7.6. At the resonance we find that the NLO QCD corrections for the signal (SM+spin-2) are about 60% while those at NNLO are about 80%. Similar result for the default choice of model parameters is presented in fig. 7.7. In this case the corresponding NLO corrections to the signal are about 45% while those of NNLO are about 55%.

We now present the invariant mass distributions of the di-leptons at NNLO for 9 different choice of couplings through fig. 7.8, 7.9, 7.10. In the left panel the distributions are shown

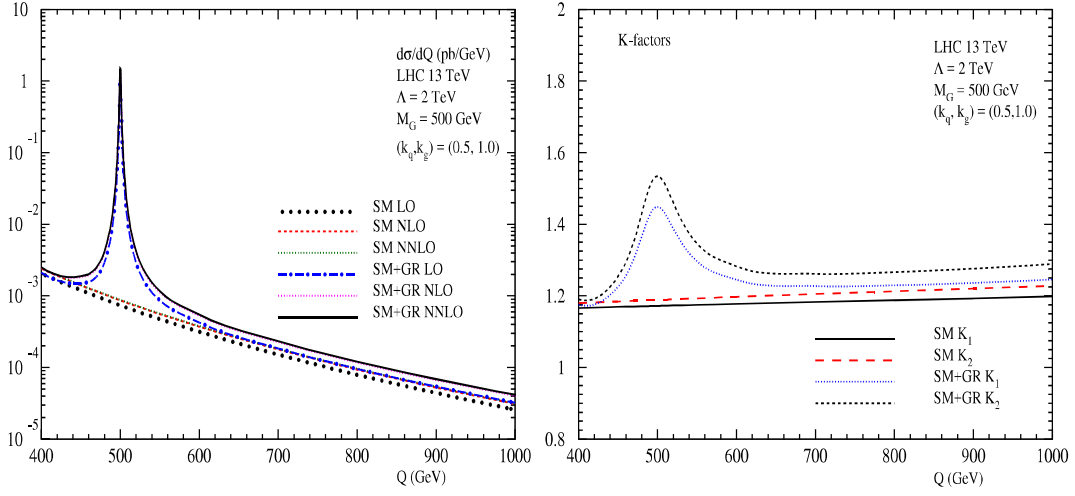


Figure 7.7: Same as fig. 7.6 but for a different set of couplings.

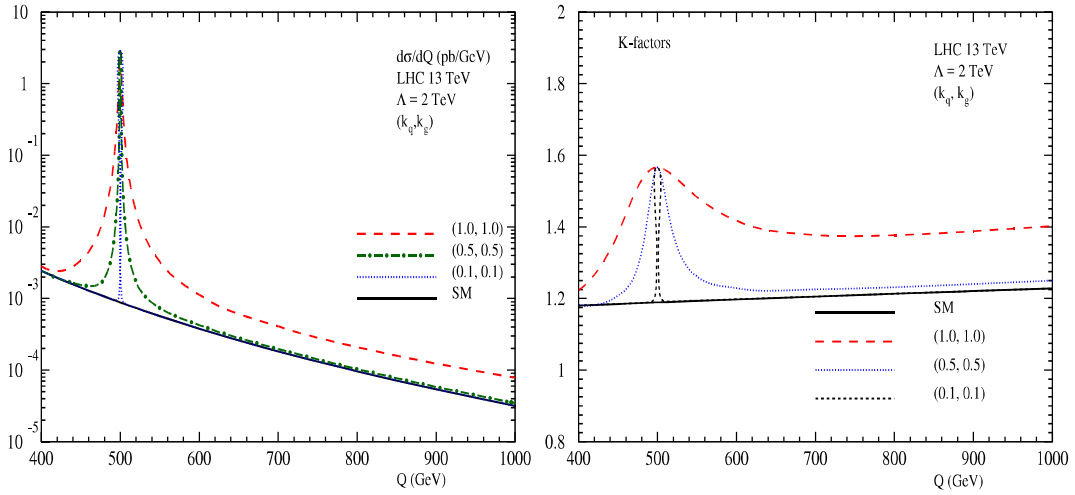


Figure 7.8: Di-lepton invariant mass distributions to NNLO for different choice of couplings (left panel) and the corresponding K-factors (right panel) are presented.

and the corresponding NNLO K-factors (K_2) are given in the right panel. The respective K-factors for the signal at the resonance region are found to vary from about 1.5 to as large as 3.0, due to different contributions from qg subprocess to the signal as explained before.

The dependence of the invariant mass distributions on the center of mass energy E_{cm} of the protons at the LHC will now be presented. We show our results for $E_{\text{cm}} = 7, 8, 13$ and 14 TeV energies for two different sets of couplings. In fig. 7.11, we present the invariant mass

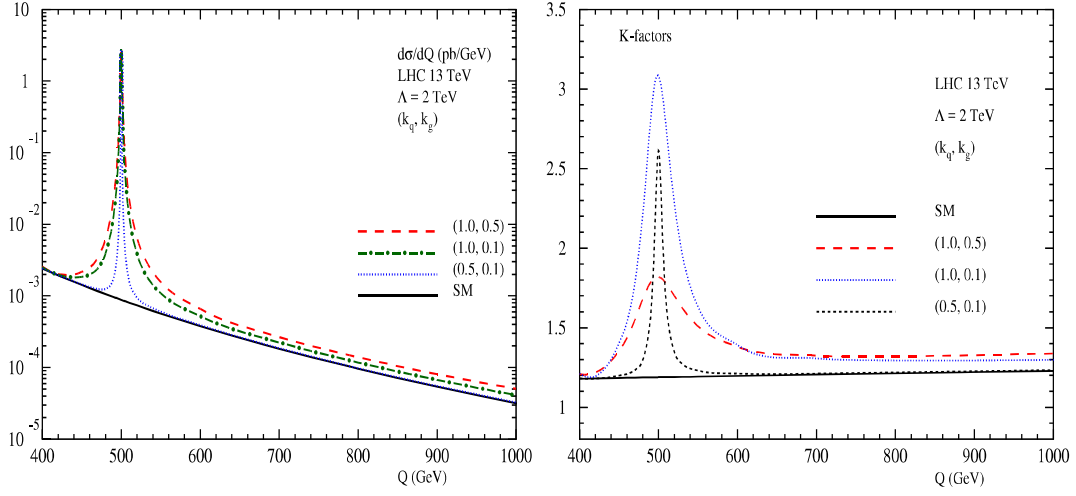


Figure 7.9: Same as fig. 7.8 but for a different set of couplings.

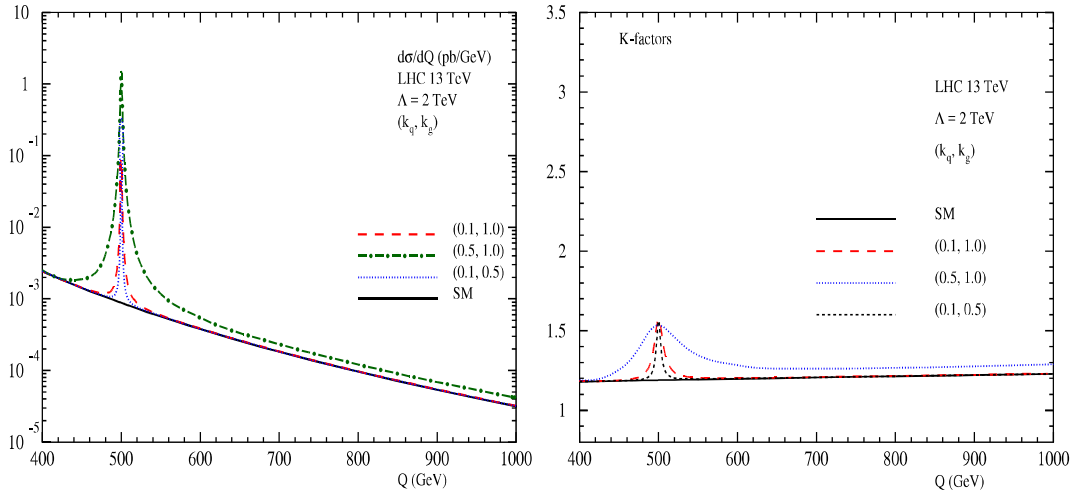


Figure 7.10: Same as fig. 7.8 but for a different set of couplings.

distributions and the corresponding K-factors for the universal couplings of $(1.0, 1.0)$. For the nonuniversal coupling $(0.5, 1.0)$, similar results are presented in fig. 7.12. In both the cases, the K-factors at the resonance region are found to be larger for 7 TeV case and are about 1.6.

The partonic cross section obtained after UV renormalization and mass factorization contains two unphysical scales μ_R, μ_F . This scale dependence arises due to truncation of the perturbative expansion up to a finite order. The LO cross section is μ_R independent but contains μ_F dependence through mass factorization. At NLO the partonic cross section

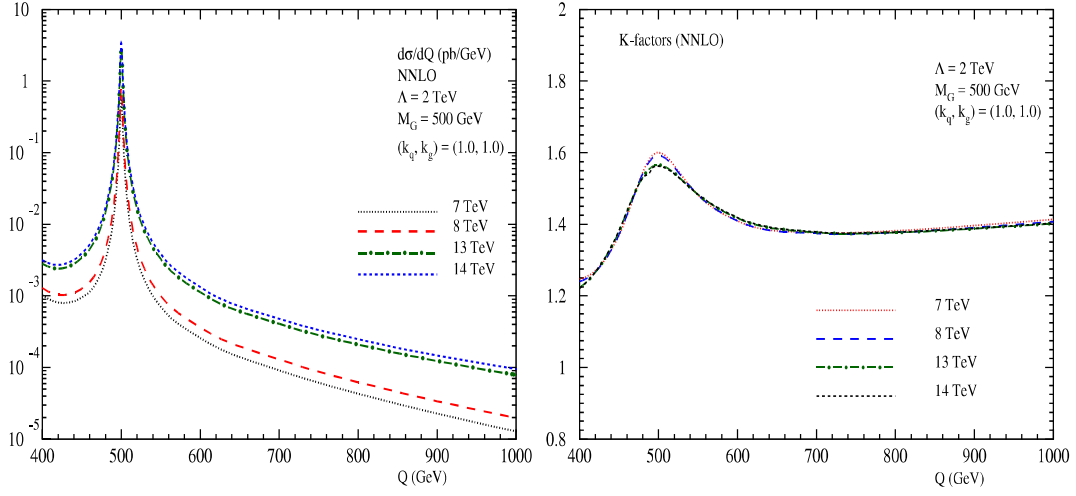


Figure 7.11: Dependence of cross sections on the di-lepton invariant mass distribution for universal couplings (1.0, 1.0).

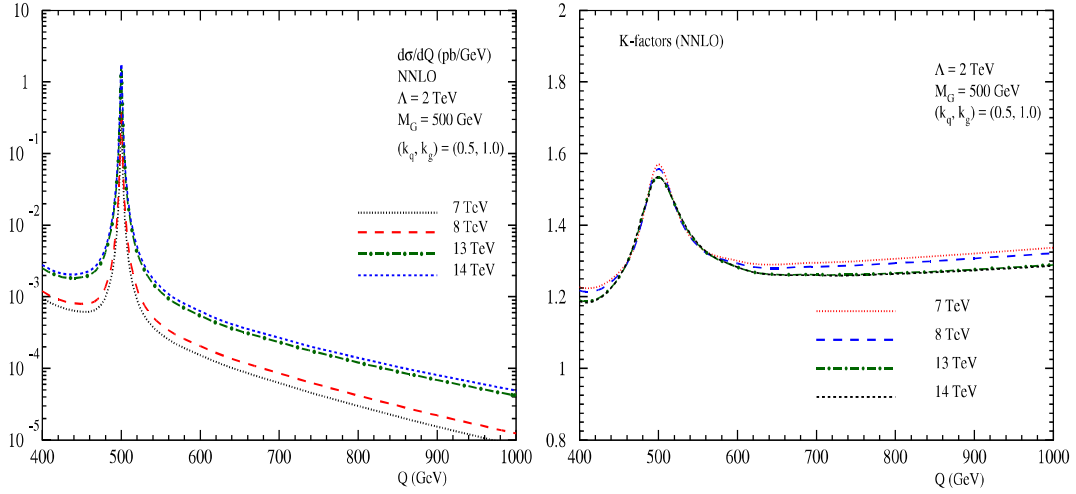


Figure 7.12: Same as fig. 7.11 but for the default choice of nonuniversal couplings (0.5, 1.0).

starts depending on μ_R ; the sensitivity to factorization scale gets reduced at this level. The cross section becomes less sensitive to the scales μ_R and μ_F as we include more and more higher order terms. We study the uncertainties in our predictions due to μ_R and μ_F through fig. 7.13, 7.14. For this, we define the ratios $R(\mu_R, \mu_F)$ of the invariant mass distributions computed at arbitrary scale to those computed at the fixed scale. These are defined as

$$R(\mu_R, \mu_F) = \frac{d\sigma(\mu_R, \mu_F)/dQ}{d\sigma(Q_0, Q_0)/dQ}.$$

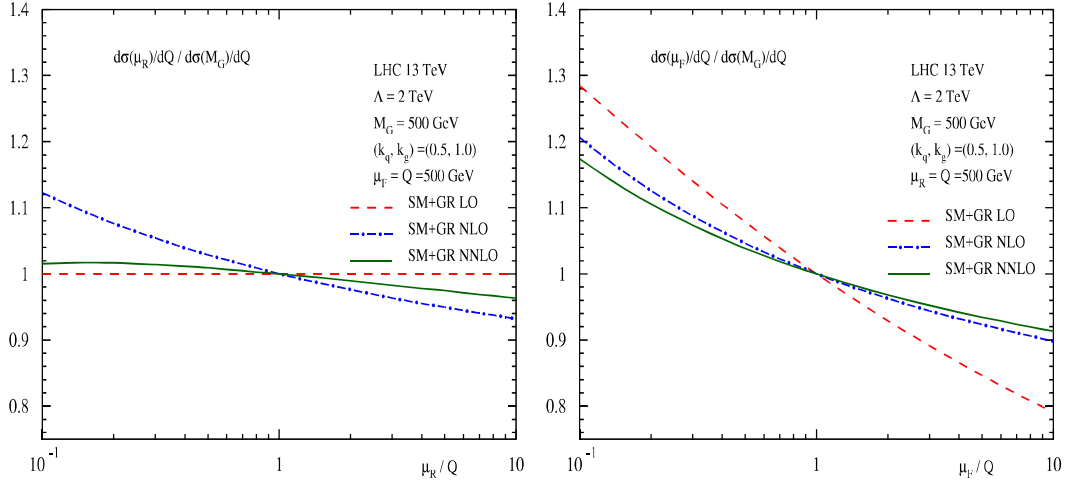


Figure 7.13: Renormalization (left) and factorization (right) scale dependence of the di-lepton invariant mass distribution at LO, NLO and NNLO.

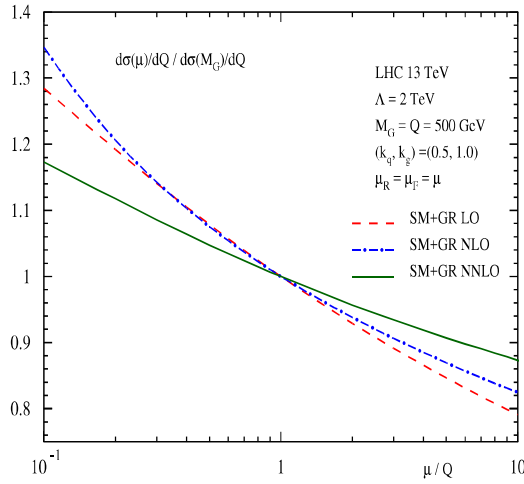


Figure 7.14: Same as fig. 7.13 but with $\mu_R = \mu_F = \mu$.

For a systematic study of these scale uncertainties, we use LO (NLO and NNLO) PDFs for LO (NLO and NNLO) cross sections respectively. We shall focus at the resonance region i.e. $Q = M = 500$ GeV. The fixed scale is set equal to $Q_0 = M$. In the left panel of fig. 7.13, we present $R(\mu_R, Q_0)$ by varying μ_R from $0.1Q$ to $10Q$ and keeping $\mu_F = Q_0$ fixed. At LO, there is no scale μ_R entering the cross section. The corresponding scale uncertainties at NLO and NNLO are 19% and 5% respectively. In the right panel of fig. 7.13, we present $R(Q_0, \mu_F)$ by varying μ_F from $0.1Q$ to $10Q$ and keeping $\mu_R = Q_0$ fixed. In this range of factorization scale variation, the uncertainties in the distributions at

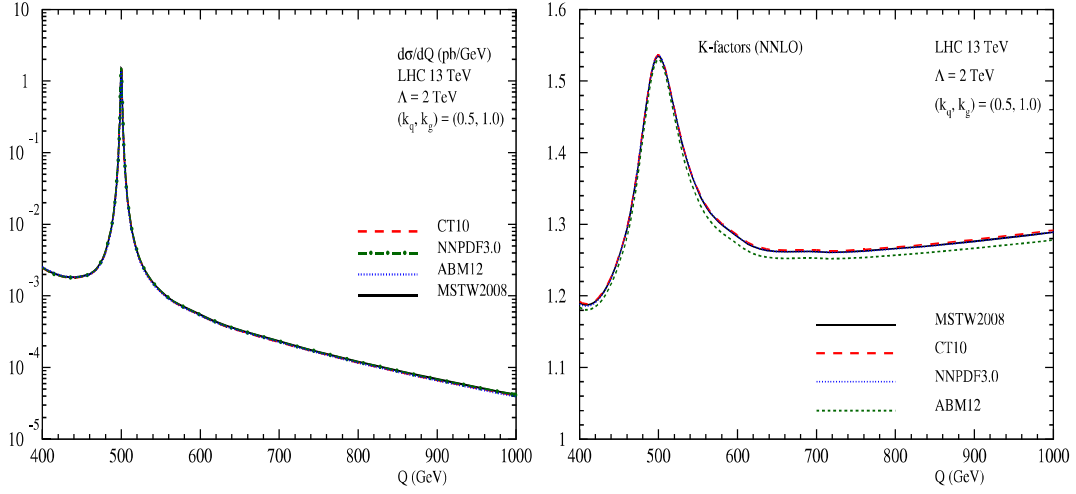


Figure 7.15: Di-lepton invariant mass distributions for different choice parton distribution functions (PDFs).

LO, NLO and NNLO are respectively about 49%, 31% and 26%.

Finally in fig. 7.14, we present $R(\mu, \mu)$ (where $\mu_R = \mu_F = \mu$) by varying μ from $0.1Q$ to $10Q$. The corresponding scale uncertainties at LO, NLO and NNLO are respectively about 49%, 52% and 30%.

We have also studied the uncertainties in our predictions that comes due to different choices of PDFs. For this we use the PDF groups MSTW2008, CT10, NNPDF3.0 and ABM12. The results for the invariant mass distributions for the signal at NNLO are presented in the left panel of fig. 7.15 and the corresponding K-factors are presented in the right panel of fig. 7.15. The K-factors here are found to vary from 1.18 at $Q = 400$ GeV to about 1.28 at $Q = 1000$ GeV, while at the resonance they are about 1.54.

7.3 Conclusion

In this chapter we have computed the NNLO QCD corrections in the DY type of process with a massive spin-2 particle appearing in the intermediate stages. We consider a minimal scenario where a spin-2 couples differently to the gauge and fermionic sector of the SM. In the previous chapter we studied a similar scenario for the form factors and saw how the universal IR structure of the QCD amplitudes remained unaffected in the presence of nonuniversal couplings. In this chapter we have seen that the IR universality remains true even for purely real and real-virtual type of processes. By multiplying the additional UV renormalization constants for the two composite operators, adding all the virtual and real emission diagrams and then performing mass factorization, we obtained the partonic cross section free of UV and IR singularities. We then multiply the appropriate PDFs with these partonic cross sections and obtain the final hadronic cross section that we use for further phenomenological investigations.

In contrast to the models with universal coupling, the phenomenological study that we have performed in this chapter is both interesting as well as different. We present the invariant mass distribution for production of di-leptons at the energies of the LHC. Even at LO, we can notice that the signal has different cross sections at the resonance region in contrast to the gravity mediated models where the signal has the same cross section for different universal couplings. From NLO onwards the spin-2 exploits its freedom of being produced with different coupling strengths even for a given subprocess, which makes the QCD radiative corrections crucially dependent on the choice of the spin-2 coupling strength. Therefore the impact of the QCD corrections here is very much different from those of di-lepton or Higgs production in the SM.

Our numerical results show that the QCD corrections for $(k_q, k_g) = (1.0, 0.1)$ are dominant over the rest of the choice of couplings, making the K-factors as large as 2.5 or more. For

this choice of couplings, the LO gluon fusion contribution is very small although gluon fluxes are high for the kinematic region of producing a 500 GeV particle. But at higher orders where the spin-2 can be emitted off from a quark line with large coupling strength, the large quark-gluon fluxes at LHC energies can potentially enhance the spin-2 production rate, as is evident from the numerical results. For di-lepton production the ‘sign’ of qg subprocess is usually negative both in the SM as well as in the models of universal couplings. But here we note that the ‘sign’ of qg subprocess contribution changes with the nonuniversal couplings and for the above choice it is positive.

We have also presented our predictions for different center of mass energies of the incoming protons at the LHC and found that the K-factors are larger for 7 TeV case. In addition, the K factors that we have presented for different scenarios of nonuniversal couplings can help different experimental collaborations by providing an accurate theoretical input for an in depth analysis of a more general model in order to constrain it more precisely. Such higher order corrections are used mainly to constrain the model parameters with least theoretical uncertainty.

The variation of the differential distribution with the renormalization and factorization scales have been quantified and presented in this thesis. For the variation of the scales μ_R and μ_F between $0.1Q$ and $10Q$, the uncertainties are found to get reduced from about 50% at LO to about 30% at NNLO. For completeness, we also present the uncertainty in our predictions due to different choice of the PDFs.

These NNLO QCD predictions for the hadroproduction of a massive spin-2 with nonuniversal couplings will augment the similar results previously computed at NLO level and compliment the earlier results for NNLO QCD corrections in models with spin-2 universal couplings.

8 Soft gluon resummation in two dimensional Mellin space

8.1 Introduction

In the previous chapters we have seen the importance of the DY process in probing physics beyond the SM. This helped us to obtain the NNLO QCD corrections for a spin-2 particle decaying to a lepton pair. The UV and IR finite fixed order partonic cross sections that we obtained (presented in Appendix 11.4) contain polynomials, plus distributions and other logarithms, all expressed in terms of some dimensionless variable z , where the latter is the ratio of the invariant mass of the final state and the partonic centre of mass energy. The plus distributions are the result of soft and/or collinear gluon emissions from the final state. In spite of the existing state-of-art calculation for cross section of the DY process, the threshold region of the phase space often lacks a concrete physical description. The threshold region is defined in the soft limit $z \rightarrow 1$. The perturbative evaluation of the partonic cross section near the boundary of the phase space for a hard scattering process, exhibits large logarithmic corrections arising from the emission of soft gluons. These threshold logarithms originate when a generic scale q^2 in a scattering process becomes equal to the square of the partonic centre-of-mass energy. In such cases the phase space of the real emission processes become highly constrained. In the threshold limit the UV

and IR finite cross section can be divided into two parts : Soft virtual (SV) or threshold and hard part. At any order α_s^k , the SV category consist of plus distributions like $\left[\frac{\ln^{m-1}(1-z)}{1-z}\right]_+$ ($m \leq 2k$) and delta functions; the polynomials and other logarithms like $\ln(1-z)$ can be listed under the hard contributions. In the threshold limit $z \rightarrow 1$, the distributions become singular. However it is to be noted that these functions are integrable. At the level of hadronic cross sections, they often dominate over the hard part when folded with the appropriate PDFs, in the above mentioned kinematic regions at every order in perturbation theory. Hence, they can potentially disturb the reliability of the perturbative predictions. The resolution is to resum these large terms, often the logarithms, to all orders to obtain any sensible prediction. This is called threshold resummation. We describe in details the necessary theoretical framework in the next section.

8.2 Theoretical framework

In this thesis we shall discuss about the threshold resummation of rapidity distribution for the SM DY process, where the partonic scaling variables z_1, z_2 approach unity *i.e.* $z_1 \rightarrow 1$ and $z_2 \rightarrow 1$. We discuss about the SV cross section which can be expressed in terms of these two variables and then layout the derivation of the soft distribution function.

8.2.1 The Soft-virtual cross section

In this section we define our notations and outline the derivation of the soft distribution function, which is closely related to the standard threshold resummation formula. In the regime of QCD improved parton model, we consider the interaction of two partons $a(k_1)$ and $b(k_2)$ to produce $c(q)$ *i.e.*

$$a(k_1) + b(k_2) \rightarrow c(q), \quad (8.1)$$

where k_i 's are the momenta of the incoming partons and $q = k_1 + k_2$. For the DY process c can be an intermediate vector boson decaying to a di-lepton pair; it is the scalar Higgs boson for Higgs produced through gluon fusion as well as annihilation of bottom quarks. The square of the hadronic centre of mass energy is defined by $S \equiv (p_1 + p_2)^2$, where p_i 's denote the initial momenta of the hadrons P_1 and P_2 . The incoming partons carry a fraction x_i of the initial state hadron momentum *i.e.* $k_i = x_i p_i$. The square of the partonic centre of mass energy is defined through $(k_1 + k_2)^2 = \hat{s}$.

The differential cross section can be written as

$$\frac{d}{dx} \sigma^I(q^2, x, \tau) = \sigma_{\text{Born}}^I(\mu_R^2, q^2, \tau) W^I(\mu_R^2, x, q^2, \tau), \quad (8.2)$$

where $\tau = q^2/S$. For DY production, $I = q$ and $\sigma^I = d\sigma^q(\tau, q^2, x)/dq^2$. The invariant mass of the di-lepton pair is $q^2 = M_{l^+l^-}^2$. For Higgs production through bottom quark annihilation $I = b$ and $\sigma^I = \sigma^b(\tau, q^2, x)$ while for Higgs production through gluon fusion $I = g$ and $\sigma^I = \sigma^g(\tau, q^2, x)$ with $q^2 = M_H^2$, where M_H is the mass of the Higgs boson. x can be the Feynman variable (x_F) or rapidity(y), both defined in the centre-of-mass frame in following way:

$$x_F = \frac{2(p_1 - p_2) \cdot q}{S}, \quad \text{and} \quad y = \frac{1}{2} \ln \left(\frac{p_2 \cdot q}{p_1 \cdot q} \right). \quad (8.3)$$

σ_{Born}^I is the lowest order contribution in the perturbative expansion. $\sigma^I(q^2, x, \tau)$ is the hadronic cross section, which is related to the partonic cross section through $W^I(\mu_R^2, x, q^2, \tau)$. In the parton model the function $W^I(\mu_R^2, x, q^2, \tau)$ can be expressed as convolution of two functions \mathcal{H}^I and \mathcal{A}^I in the following way:

$$\begin{aligned} W^I(\mu_R^2, x, q^2, \tau) = & \sum_{ac=q,\bar{q},g} \int_0^1 dx_1 \int_0^1 dx_2 \mathcal{H}_{ac}^I(x_1, x_2, \mu_F^2) \\ & \times \int_0^1 dz \delta(\tau - zx_1x_2) \mathcal{A}_{d,ac}^I(x, z, a_s, q^2, \mu_F^2, \mu_R^2). \end{aligned} \quad (8.4)$$

In above $\mathcal{A}_{d,ac}^I(x, z, a_s, q^2, \mu_F^2, \mu_R^2) = \frac{1}{\sigma_{\text{Born}}^I} \int dPS_{1+X} |\mathcal{M}_{ac \rightarrow H+X}|^2 \delta(x - \Omega)$, where for $x = x_F$, $\Omega = \frac{2(p_1 - p_2) \cdot q}{s}$ and for $x = y$, $\Omega = \frac{1}{2} \ln\left(\frac{p_2 \cdot q}{p_1 \cdot q}\right)$. The phase space element for the $H + X$ system is dPS_{1+X} and $\mathcal{M}_{ac \rightarrow H+X}$ denotes the scattering amplitude at partonic level where the latter can be computed order by order in perturbation series. The subscript d denotes differential part of the cross section. μ_R and μ_F are the renormalization and factorization scale respectively. The renormalized strong coupling constant is $a_s = g_s^2(\mu_R^2)/16\pi^2$; its relation to the bare one $\hat{a}_s = \hat{g}_s^2/16\pi^2$ has been described in eq. 2.5 and 2.6. The function $\mathcal{H}_{ac}^I(x_1, x_2, \mu_F^2)$ is the product of PDFs $f_a(x_1, \mu_F^2)$ and $f_c(x_2, \mu_F^2)$ mass factorized at the scale μ_F^2 as expressed in eq. 4.46.

The renormalized PDFs are related to unrenormalized ones through the Altarelli-Parisi kernel Γ_{cd} as follows:

$$f_c(x_i, \mu_F^2) = \sum_{d=q, \bar{q}, g} \int_{x_i}^1 \frac{dz}{z} \Gamma_{cd}(\hat{a}_s, \mu^2, \mu_F^2, z, \epsilon) \hat{f}_d\left(\frac{x_i}{z}\right) \quad c = q, \bar{q}, g. \quad (8.5)$$

The factorization kernel $\Gamma_{cd}(\hat{a}_s, \mu^2, \mu_F^2, z, \epsilon)$ cancels the initial state collinear singularity due to massless partons. It can be expanded in power series in \hat{a}_s ,

$$\Gamma_{cd}(\hat{a}_s, \mu^2, \mu_F^2, z, \epsilon) = \delta_{cd} \delta(1 - z) + \hat{a}_s S_\epsilon \left(\frac{\mu_F^2}{\mu^2}\right)^{\frac{\epsilon}{2}} \frac{1}{\epsilon} P_{cd}^{(0)}(z) + \mathcal{O}(\hat{a}_s^2) \quad (8.6)$$

where $P_{cd}^{(0)}(z)$ is the leading order DGLAP splitting function. The splitting functions are known fully up to three loop level [152, 153] and in the large n_f limit at four loop level [193] in perturbative expansion:

$$P(z_j, \mu_F^2) = \sum_{i=1}^{\infty} a_s^i(\mu_F^2) P^{(i-1)}(z_j). \quad (8.7)$$

The diagonal term of the splitting function is as follows,

$$P_{II}^{(i)}(z_j) = 2 \left[B_{i+1}^I \delta(1 - z_j) + A_{i+1}^I \mathcal{D}_0(z_j) \right] + P_{\text{reg}, II}^{(i)}(z_j). \quad (8.8)$$

The last term in the above equation ($P_{\text{reg},II}^{(i)}(z_j)$) is regular in the kinematical limit $z_j \rightarrow 1$. $\mathcal{D}_i(z_1)$, $\bar{\mathcal{D}}_i(z_2)$ are the plus distributions defined in the following way:

$$\mathcal{D}_i = \left[\frac{\ln^i(1 - z_1)}{(1 - z_1)} \right]_+, \quad \bar{\mathcal{D}}_i = \left[\frac{\ln^i(1 - z_2)}{(1 - z_2)} \right]_+ \quad i = 0, 1, \dots \quad (8.9)$$

The subscript ‘+’ denotes the customary ‘plus-distribution’ $f_+(z)$ which acts on functions regular in $z \rightarrow 1$ limit as

$$\int_0^1 dz f_+(z) g(z) = \int_0^1 dz f(z) (g(z) - g(1)) \quad (8.10)$$

The renormalized \mathcal{H} is related to the corresponding unrenormalized ones through the kernels Γ_{cd} as follows :

$$\mathcal{H}_{ac}(x_1, x_2, \mu_F^2) = \int_{x_1}^1 \frac{dy_1}{y_1} \int_{x_2}^1 \frac{dy_2}{y_2} \Gamma_{aa'}(\hat{a}_s, \mu^2, \mu_F^2, y_1, \epsilon) \hat{\mathcal{H}}_{a'c'}\left(\frac{x_1}{y_1}, \frac{x_2}{y_2}\right) \Gamma_{cc'}(\hat{a}_s, \mu^2, \mu_F^2, y_2, \epsilon). \quad (8.11)$$

It is often convenient to work with two scaling variables x_1^0 and x_2^0 instead of x and τ . For the rapidity distribution, the variables x_1^0 and x_2^0 are related to x and τ as follows,

$$x = y = \frac{1}{2} \ln \left(\frac{x_1^0}{x_2^0} \right), \quad \tau = x_1^0 x_2^0. \quad (8.12)$$

For x_F distribution the relations are,

$$x = x_F = x_1^0 - x_2^0, \quad \tau = x_1^0 x_2^0. \quad (8.13)$$

We can now express the hadronic as well as the partonic cross section in terms of the new variables x_1^0 and x_2^0 . It can be shown that the partonic cross sections can be expressed in terms of z_i , which acts as scaling variable at the partonic level, where $z_i = \frac{x_i^0}{x_i}$. Therefore

in terms of these variables, eq. 8.4 can be rewritten in the following way:

$$W^I(x_1^0, x_2^0, q^2, \mu_R^2) = \sum_{ac=b, \bar{b}, g} \int_{x_1^0}^1 \frac{dz_1}{z_1} \int_{x_2^0}^1 \frac{dz_2}{z_2} \mathcal{H}_{ac}\left(\frac{x_1^0}{z_1}, \frac{x_2^0}{z_2}, \mu_F^2\right) \times \Delta_{d,ac}^I(z_1, z_2, a_s(\mu_R^2), q^2, \mu_F^2, \mu_R^2), \quad (8.14)$$

where $\frac{1}{x_1 x_2} \Delta_{d,ac}^I(z_1, z_2, a_s(\mu_R^2), q^2, \mu_F^2, \mu_R^2) = \frac{1}{\sigma_{\text{Born}}^I} \int dPS_{1+X} \int dz \delta(\tau - z x_1 x_2) |\mathcal{M}_{ac \rightarrow H+X}|^2 \delta(x - \Omega)$. Thus our task boils down to computing $\Delta_{d,ac}^I(z_1, z_2, a_s(\mu_R^2), q^2, \mu_F^2, \mu_R^2)$. The infrared safe coefficient functions $\Delta_{d,ac}^I$ get contributions from both soft gluons as well as from hard partons. Contributions from soft gluons consist of terms proportional to the distributions $\mathcal{D}_i(z_j)$ in eq. 8.9 and $\delta(1 - z_j)$. The remaining part of the differential cross section is called hard contribution, which can be obtained by the standard procedure given in [194, 195]. Thus we rewrite the differential partonic cross section as

$$\Delta_{d,ab}^I(a_s, z_1, z_2, q^2, \mu_F^2, \mu_R^2) = \Delta_{d,ab}^{I,\text{hard}}(a_s, z_1, z_2, q^2, \mu_F^2, \mu_R^2) + \delta_{ab} \Delta_d^{I,\text{SV}}(a_s, z_1, z_2, q^2, \mu_F^2, \mu_R^2). \quad (8.15)$$

We are interested in the SV part of the above cross section. It is to be remembered that only diagonal terms of Γ_{cd} contribute to SV part of the cross section. In the threshold limit ($z_i \rightarrow 1$) the SV part of the cross section contributes dominantly as compared to the hard part. To evaluate this, we will follow the approach prescribed in [8, 146]. The SV part of the finite partonic cross section can be written in a factorized way as follows

$$\begin{aligned} \Delta_d^{I,\text{SV}}(a_s, z_1, z_2, q^2, \mu_F^2, \mu_R^2) &= (Z^I(\hat{a}_s, \mu_R^2, \mu^2, \epsilon))^2 \left| \hat{\mathcal{F}}^I(\hat{a}_s, Q^2, \mu^2, \epsilon) \right|^2 \delta(1 - z_1) \delta(1 - z_2) \\ &\otimes C e^{2\phi_d^I(\hat{a}_s, q^2, \mu^2, z_1, z_2, \epsilon)} \otimes \Gamma_H^{-1}(\hat{a}_s, \mu^2, \mu_F^2, z_1, \epsilon) \delta(1 - z_2) \\ &\otimes \Gamma_H^{-1}(\hat{a}_s, \mu^2, \mu_F^2, z_2, \epsilon) \delta(1 - z_1). \end{aligned} \quad (8.16)$$

The term $\hat{\mathcal{F}}^I(\hat{a}_s, Q^2 = -q^2, \mu^2, \epsilon)$ is the bare form factor which we describe in details in the next section. The symbol C denotes convolution and its operation on the exponential

of a function $f(z_1, z_2)$ indicates

$$\begin{aligned} C_e f(z_1, z_2) &= \delta(1 - z_1)\delta(1 - z_2) + \frac{1}{1!}f(z_1, z_2) + \frac{1}{2!}f(z_1, z_2) \otimes f(z_1, z_2) \\ &\quad + \frac{1}{3!}f(z_1, z_2) \otimes f(z_1, z_2) \otimes f(z_1, z_2) + \cdots \end{aligned} \quad (8.17)$$

The functions $f(z_1, z_2)$ are distributions of type $\delta(1 - z_i)$ or $\mathcal{D}_j(z_i)$. The symbol \otimes indicates the “double” Mellin convolution, which convolutes with respect to the variables z_1 and z_2 separately. As we are interested in evaluating the SV part of the cross sections, we neglect all the regular functions that come from different convolutions. The term $\phi_d^I(\hat{a}_s, q^2, \mu^2, z_1, z_2, \epsilon)$ is the soft distribution function which we shall discuss later. In eq. 8.16, $Z^I(\hat{a}_s, \mu_R^2, \mu^2, \epsilon)$ is the overall operator renormalization constant. For gluon operator [147] and bottom quark coupling to Higgs, [148] $Z^I(\hat{a}_s, \mu_R^2, \mu^2, \epsilon)$ satisfy the following renormalization group equations:

$$\begin{aligned} \mu_R^2 \frac{d}{d\mu_R^2} \ln Z^g(\hat{a}_s, \mu_R^2, \mu^2, \epsilon) &= \sum_{i=1}^{\infty} a_s^i(\mu_R^2) (i \beta_{i-1}), \\ \mu_R^2 \frac{d}{d\mu_R^2} \ln Z^b(\hat{a}_s, \mu_R^2, \mu^2, \epsilon) &= \sum_{i=1}^{\infty} a_s^i(\mu_R^2) \gamma_{i-1}^b, \end{aligned} \quad (8.18)$$

where the anomalous dimension γ_i^b are given in [195–197]. For the DY process we have $Z^q(\hat{a}_s, \mu_R^2, \mu^2, \epsilon) = 1$.

8.2.2 Solution of the form factor

The function $\hat{\mathcal{F}}^I(\hat{a}_s, Q^2, \mu^2, \epsilon)$ in eq. 8.16 is the bare form factor. In section 6.3 we discussed about the renormalized FF’s in the context of the two composite operators and briefly mentioned about the differential equation that they satisfied. In this section we shall again revisit the solution of the FFs in great details, as their general solution will be required in the next section to find the solution of the soft distribution function. The bare

form factors satisfy the KG equation, which is a consequence of factorization, gauge and renormalization group (RG) invariances [147–150]

$$Q^2 \frac{d}{dQ^2} \ln \hat{\mathcal{F}}^I(\hat{a}_s, Q^2, \mu^2, \epsilon) = \frac{1}{2} \left[K^I\left(\hat{a}_s, \frac{\mu_R^2}{\mu^2}, \epsilon\right) + G^I\left(\hat{a}_s, \frac{Q^2}{\mu_R^2}, \frac{\mu_R^2}{\mu^2}, \epsilon\right) \right], \quad (8.19)$$

where the K^I contains all the singularities in ϵ , G^I involves finite terms in the limit $\epsilon \rightarrow 0$. Using the property of RG invariance of $\hat{\mathcal{F}}^I(\hat{a}_s, Q^2, \mu^2, \epsilon)$ and the finiteness of G^I we can obtain the solution of the above equation. The formal solution, which is a series expansion in the bare coupling constant is presented in [135, 146] up to four loop level. The solution for K^I reads as

$$K^I(\hat{a}_s, \mu^2, \mu_R^2, \epsilon) = \sum_{i=1}^{\infty} \hat{a}_s^i \left(\frac{\mu_R^2}{\mu^2} \right)^{i \frac{\epsilon}{2}} S_\epsilon^i K^{I,(i)}(\epsilon), \quad (8.20)$$

with

$$\begin{aligned} K^{I,(1)}(\epsilon) &= \frac{1}{\epsilon} \left\{ -2A_1^I \right\}, \quad K^{I,(2)}(\epsilon) = \frac{1}{\epsilon^2} \left\{ 2\beta_0 A_1^I \right\} + \frac{1}{\epsilon} \left\{ -A_2^I \right\}, \\ K^{I,(3)}(\epsilon) &= \frac{1}{\epsilon^3} \left\{ -\frac{8}{3}\beta_0^2 A_1^I \right\} + \frac{1}{\epsilon^2} \left\{ \frac{2}{3}\beta_1 A_1^I + \frac{8}{3}\beta_0 A_2^I \right\} + \frac{1}{\epsilon} \left\{ -\frac{2}{3}A_3^I \right\}. \end{aligned} \quad (8.21)$$

where A_i^I are the cusp anomalous dimensions [56, 152–155]. For $I = q$ they are given by,

$$\begin{aligned} A_1^q &= 4C_F, \\ A_2^q &= 8C_F C_A \left\{ \frac{67}{18} - \zeta_2 \right\} + 8C_F n_f \left\{ -\frac{5}{9} \right\}, \\ A_3^q &= 16C_F C_A^2 \left\{ \frac{245}{24} - \frac{67}{9}\zeta_2 + \frac{11}{6}\zeta_3 + \frac{11}{5}\zeta_2^2 \right\} + 16C_F^2 n_f \left\{ -\frac{55}{24} + 2\zeta_3 \right\} \\ &\quad + 16C_F C_A n_f \left\{ -\frac{209}{108} + \frac{10}{9}\zeta_2 - \frac{7}{3}\zeta_3 \right\} + 16C_F n_f^2 \left\{ -\frac{1}{27} \right\}. \end{aligned} \quad (8.22)$$

A_i^b are same as A_i^q , as they are flavor independent. We can extract A^g from A^q by making use of its maximally non-Abelian property,

$$A^g = \frac{C_A}{C_F} A^q. \quad (8.23)$$

The renormalization group equation for the function G^I has the following solution

$$\begin{aligned} G^I\left(\hat{a}_s, \frac{Q^2}{\mu_R^2}, \frac{\mu_R^2}{\mu^2}, \epsilon\right) &= G^I\left(a_s(\mu_R^2), \frac{Q^2}{\mu_R^2}, \epsilon\right) \\ &= G^I\left(a_s(Q^2), 1, \epsilon\right) + \int_{Q^2/\mu_R^2}^1 \frac{d\lambda^2}{\lambda^2} A^I\left(a_s(\lambda^2 \mu_R^2)\right) \\ &= G^I\left(a_s(Q^2), 1, \epsilon\right) + \sum_{i=1}^{\infty} S_{\epsilon}^i \hat{a}_s^i \left(\frac{\mu_R^2}{\mu^2}\right)^{i\frac{\epsilon}{2}} \left[\left(\frac{Q^2}{\mu_R^2}\right)^{i\frac{\epsilon}{2}} - 1\right] K^{I,(i)}(\epsilon). \end{aligned} \quad (8.24)$$

$G^I\left(a_s(Q^2), 1, \epsilon\right)$ can be expanded in power series of $a_s(Q^2)$ as

$$G^I\left(a_s(Q^2), 1, \epsilon\right) = \sum_{i=1}^{\infty} a_s^i(Q^2) G_i^I(\epsilon), \quad (8.25)$$

where $G_i^I(\epsilon)$ consists of process independent terms – collinear (B_i^I) and soft (f_i^I) anomalous dimensions as well as some vertex dependent terms ($g_{i,F}^I$). They are expressed as

$$G_i^I(\epsilon) = 2(B_i^I - \gamma_i^I) + f_i^I + C_i^I + \sum_{k=1}^{\infty} \epsilon^k g_{i,F}^{I,k}. \quad (8.26)$$

B_i^I [152, 153] are obtained by demanding that physical observables like cross sections should be finite. They are the coefficients of the $\delta(1-z)$ part of the splitting functions in eq. 8.8. Since B_i^q are flavour independent they satisfy $B_i^q \equiv B_i^b$. The soft anomalous dimension, f_i^I for $i = 1, 2$ can be found in [28] and in [153] for $i = 3$. We list them below:

$$\begin{aligned} f_1^q &= 0, \\ f_2^q &= C_A C_F \left\{ -\frac{22}{3} \zeta_2 - 28 \zeta_3 + \frac{808}{27} \right\} + C_F n_f T_F \left\{ \frac{8}{3} \zeta_2 - \frac{224}{27} \right\}, \end{aligned}$$

$$\begin{aligned}
f_3^q = & C_A^2 C_F \left\{ \frac{352}{5} \zeta_2^2 + \frac{176}{3} \zeta_2 \zeta_3 - \frac{12650}{81} \zeta_2 - \frac{1316}{3} \zeta_3 + 192 \zeta_5 + \frac{136781}{729} \right\} \\
& + C_A C_F n_f \left\{ -\frac{96}{5} \zeta_2^2 + \frac{2828}{81} \zeta_2 + \frac{728}{27} \zeta_3 - \frac{11842}{729} \right\} \\
& + C_F^2 n_f \left\{ \frac{32}{5} \zeta_2^2 + 4 \zeta_2 + \frac{304}{9} \zeta_3 - \frac{1711}{27} \right\} + C_F n_f^2 \left\{ -\frac{40}{27} \zeta_2 + \frac{112}{27} \zeta_3 - \frac{2080}{729} \right\}.
\end{aligned} \tag{8.27}$$

Like B_i^I , f_i^I are also flavor independent *i.e.* $f_i^b \equiv f_i^q$. The authors in [28] first noticed that the constants f_i^I are maximally non-Abelian obeying the relation

$$f_i^g = \frac{C_A}{C_F} f_i^q. \tag{8.28}$$

Using the above relation we can predict the single pole in the logarithm of form factor up to two loop level [28]. In [134] it was validated to hold up to three loop level in perturbative expansion. From the above solutions of K and G we can now obtain $\ln \hat{\mathcal{F}}^I$:

$$\ln \hat{\mathcal{F}}^I(\hat{a}_s, Q^2, \mu^2, \epsilon) = \sum_{i=1}^{\infty} \hat{a}_s^i \left(\frac{Q^2}{\mu^2} \right)^{i \frac{\epsilon}{2}} S_{\epsilon}^i \hat{\mathcal{L}}_{\mathcal{F}}^{I,(i)}(\epsilon) \tag{8.29}$$

where

$$\begin{aligned}
\hat{\mathcal{L}}_{\mathcal{F}}^{I,(1)} &= \frac{1}{\epsilon^2} \left(-2A_1^I \right) + \frac{1}{\epsilon} \left(G_1^I(\epsilon) \right), \\
\hat{\mathcal{L}}_{\mathcal{F}}^{I,(2)} &= \frac{1}{\epsilon^3} \left(\beta_0 A_1^I \right) + \frac{1}{\epsilon^2} \left(-\frac{1}{2} A_2^I - \beta_0 G_1^I(\epsilon) \right) + \frac{1}{2\epsilon} G_2^I(\epsilon), \\
\hat{\mathcal{L}}_{\mathcal{F}}^{I,(3)} &= \frac{1}{\epsilon^4} \left(-\frac{8}{9} \beta_0^2 A_1^I \right) + \frac{1}{\epsilon^3} \left(\frac{2}{9} \beta_1 A_1^I + \frac{8}{9} \beta_0 A_2^I + \frac{4}{3} \beta_0^2 G_1^I(\epsilon) \right) \\
&\quad + \frac{1}{\epsilon^2} \left(-\frac{2}{9} A_3^I - \frac{1}{3} \beta_1 G_1^I(\epsilon) - \frac{4}{3} \beta_0 G_2^I(\epsilon) \right) + \frac{1}{\epsilon} \left(\frac{1}{3} G_3^I(\epsilon) \right), \\
\hat{\mathcal{L}}_{\mathcal{F}}^{I,(4)} &= \frac{1}{\epsilon^5} \left(\beta_0^3 A_1^I \right) + \frac{1}{\epsilon^4} \left(-\frac{2}{3} \beta_0 \beta_1 A_1^I - \frac{3}{2} \beta_0^2 A_2^I - 2 \beta_0^3 G_1^I(\epsilon) \right)
\end{aligned}$$

$$\begin{aligned}
& + \frac{1}{\epsilon^3} \left(\frac{1}{12} \beta_2 A_1^I + \frac{1}{4} \beta_1 A_2^I + \frac{3}{4} \beta_0 A_3^I + \frac{4}{3} \beta_0 \beta_1 G_1^I(\epsilon) + 3 \beta_0^2 G_2^I(\epsilon) \right) \\
& + \frac{1}{\epsilon^2} \left(-\frac{1}{8} A_4^I - \frac{1}{6} \beta_2 G_1^I(\epsilon) - \frac{1}{2} \beta_1 G_2^I(\epsilon) - \frac{3}{2} \beta_0 G_3^I(\epsilon) \right) + \frac{1}{\epsilon} \left(\frac{1}{4} G_4^I(\epsilon) \right). \quad (8.30)
\end{aligned}$$

The constants $g_i^{I,k}$ can be extracted from the finite part of the form factors as evident through eq. 8.26 and 8.30. For Higgs production through bottom quark annihilation ($I = b$), the results up to two loop level are available in [146, 151, 198]. The three loop computation is presented in [138], which was later used to compute $g_3^{b,1}$ in [156]. For $I = q, g$ the constants $g_i^{I,k}$ can be found in [134]. The beta function and the constants $g_i^{I,k}$ determine C_i^I . They read as

$$C_1^I = 0, \quad C_2^I = -2\beta_0 g_{1,F}^{I,1}, \quad C_3^I = -2\beta_1 g_{1,F}^{I,1} - 2\beta_0 (g_{2,F}^{I,1} + 2\beta_0 g_{1,F}^{I,2}). \quad (8.31)$$

The solution of the logarithm of the form factor, $\ln \hat{\mathcal{F}}^I(\hat{a}_s, Q^2, \mu^2, \epsilon)$ for DY and Higgs production through gg fusion and bottom quark annihilation can now be obtained from the universal anomalous dimensions $A_i^I, B_i, f_i^I, \gamma_i^I$ and the process dependent constants $g_{i,F}^{I,k}$.

8.2.3 Solution of the soft distribution function

We now need to find the solution of the soft distribution function $\phi_d^I(\hat{a}_s, q^2, \mu^2, z_1, z_2, \epsilon)$. To determine it, we recall that the function $\Delta_d^{I,SV}(a_s, z_1, z_2, q^2, \mu_F^2, \mu_R^2)$ on the left hand side of eq. 8.16 is finite in the limit $\epsilon \rightarrow 0$. This implies that all the pole structure of $\phi_d^I(\hat{a}_s, q^2, \mu^2, z_1, z_2, \epsilon)$ as well as its q^2 dependence should be similar to those of $\ln \hat{\mathcal{F}}^i$. The differential equation that the soft function satisfies was first given in [146]. It is as follows

$$q^2 \frac{d}{dq^2} \phi_d^I = \frac{1}{2} \left[\overline{K}_d^I \left(\hat{a}_s, \frac{\mu_R^2}{\mu^2}, z_1, z_2, \epsilon \right) + \overline{G}_d^I \left(\hat{a}_s, \frac{q^2}{\mu_R^2}, \frac{\mu_R^2}{\mu^2}, z_1, z_2, \epsilon \right) \right]. \quad (8.32)$$

Following the structure of K^I and G^I in the logarithm of the form factor, we include all the singular terms in ϵ of ϕ_d^I in \overline{K}_d^I and keep the finite terms in \overline{G}_d^I . ϕ_d^I also satisfies the RG equation

$$\mu_R^2 \frac{d}{d\mu_R^2} \phi_d^I(\hat{a}_s, q^2, \mu^2, z_1, z_2, \epsilon) = 0 \quad (8.33)$$

which leads to

$$\mu_R^2 \frac{d}{d\mu_R^2} \overline{K}_d^I = -\mu_R^2 \frac{d}{d\mu_R^2} \overline{G}_d^I = -\delta(1-z_1)\delta(1-z_2)\overline{A}^I(a_s(\mu_R^2)). \quad (8.34)$$

The proportionality of the form factor to $\delta(1-z_1)\delta(1-z_2)$ in eq. 8.16 explains the product of deltas in the above equation. The poles from $\phi_d^I(\hat{a}_s, q^2, \mu^2, z_1, z_2, \epsilon)$ have to cancel with those coming from \hat{F}^I and Γ_{II} , to make $\mathcal{A}_d^{I,SV}$ finite. Hence the constants \overline{A}^I should satisfy

$$\overline{A}^I = -A^I. \quad (8.35)$$

Using the above relation the solution for \overline{G}_d^I in eq. 8.34 is

$$\begin{aligned} \overline{G}_d^I\left(\hat{a}_s, \frac{q^2}{\mu_R^2}, \frac{\mu_R^2}{\mu^2}, z_1, z_2, \epsilon\right) &= \overline{G}_d^I\left(a_s(\mu_R^2), \frac{q^2}{\mu_R^2}, z_1, z_2, \epsilon\right) \\ &= \overline{G}_d^I(a_s(q^2), 1, z_1, z_2, \epsilon) - \delta(1-z_1)\delta(1-z_2) \int_{\frac{q^2}{\mu_R^2}}^1 \frac{d\lambda^2}{\lambda^2} A^I(a_s(\lambda^2 \mu_R^2)). \end{aligned} \quad (8.36)$$

The above solutions can be used to solve the Sudakov differential eq. 8.32 for soft function ϕ_d^I ,

$$\begin{aligned} \phi_d^I &= \phi_d^I(\hat{a}_s, q^2(1-z_1)(1-z_2), \mu^2, \epsilon) \\ &= \sum_{i=1}^{\infty} \hat{a}_s^i \left(\frac{q^2(1-z_1)(1-z_2)}{\mu^2} \right)^{i\frac{\epsilon}{2}} S_\epsilon^i \left(\frac{(i\epsilon)^2}{4(1-z_1)(1-z_2)} \right) \hat{\phi}_d^{I,(i)}(\epsilon), \end{aligned} \quad (8.37)$$

where,

$$\hat{\phi}_d^{I,(i)}(\epsilon) = \frac{1}{i\epsilon} \left[\bar{K}_d^{I,(i)}(\epsilon) + \bar{G}_d^{I,(i)}(\epsilon) \right]. \quad (8.38)$$

The form of z_j dependent part in the above solution can be justified through factorization property of QCD amplitudes. The term $[(1 - z_1)(1 - z_2)]^{\epsilon/2}$ is the contribution from the phase space while the $(1 - z_i)$ term in the denominator comes from the matrix elements. Expanding \bar{K}_d^I in powers of \hat{a}_s

$$\bar{K}_d^I \left(\hat{a}_s, \frac{\mu_R^2}{\mu^2}, z_1, z_2, \epsilon \right) = \delta(1 - z_1)\delta(1 - z_2) \sum_{i=1}^{\infty} \hat{a}_s^i \left(\frac{\mu_R^2}{\mu^2} \right)^{i\frac{\epsilon}{2}} S_\epsilon^i \bar{K}_d^{I,(i)}(\epsilon), \quad (8.39)$$

and solving the RG equation in eq. 8.34 we can determine the constants $\bar{K}_d^{I,(i)}(\epsilon)$. They are identical to $K^{I,(i)}(\epsilon)$ given in [146, 151]. $\bar{G}_d^{I,(i)}(\epsilon)$ are related to the finite functions $\bar{G}_d^I(a_s(q^2), 1, z_1, z_2, \epsilon)$. In terms of renormalized coupling constant, we find

$$\begin{aligned} \bar{G}_d^I(a_s(q^2), 1, z_1, z_2, \epsilon) &= \sum_{i=1}^{\infty} \hat{a}_s^i \left(\frac{q^2(1 - z_1)(1 - z_2)}{\mu^2} \right)^{i\frac{\epsilon}{2}} S_\epsilon^i \bar{G}_d^{I,(i)}(\epsilon) \\ &= \sum_{i=1}^{\infty} a_s^i(q^2(1 - z_1)(1 - z_2)) \bar{\mathcal{G}}_{d,i}^I(\epsilon) \end{aligned} \quad (8.40)$$

$\bar{\mathcal{G}}_{d,i}^I(\epsilon)$ are similar to $G_i^I(\epsilon)$ of the form factor and is given by,

$$\bar{\mathcal{G}}_{d,i}^I(\epsilon) = -f_i^I + C_{d,i}^I + \sum_{k=1}^{\infty} \epsilon^k \bar{\mathcal{G}}_{d,i}^{I,k}, \quad (8.41)$$

The coefficients of the single poles in $\hat{\phi}_d^{I,(i)}(\epsilon)$ are controlled by the soft anomalous dimension, f_i^I , which are also maximally non-Abelian and the constants $C_{d,i}^I$. We now need to determine the z independent constants, $\bar{\mathcal{G}}_{d,i}^{I,k}$. We achieve this using the following identity:

$$\begin{aligned} \int_0^1 dx_1^0 \int_0^1 dx_2^0 (x_1^0 x_2^0)^{N-1} (x_1^0 + x_2^0) \frac{d\sigma^I}{dx_F} &= \int_0^1 dx_1^0 \int_0^1 dx_2^0 (x_1^0 x_2^0)^{N-1} \frac{d\sigma^I}{dY} \\ &= \int_0^1 d\tau \tau^{N-1} \sigma^I. \end{aligned} \quad (8.42)$$

σ^I for $I = q, g$ is known to NNLO level [2, 19–24, 51, 52, 54, 77–79, 112] and the N³LO for Higgs production is now known [29]. We can relate $\hat{\phi}_d^{I,(i)}(\epsilon)$ to $\hat{\phi}^{I,(i)}(\epsilon)$ that appears in inclusive threshold corrections to DY process [57, 146, 151, 156], by taking the large N limit of above equation *i.e.* $N \rightarrow \infty$,

$$\hat{\phi}_d^{I,(i)}(\epsilon) = \frac{\Gamma(1+i\epsilon)}{\Gamma^2\left(1+i\frac{\epsilon}{2}\right)} \hat{\phi}^{I,(i)}(\epsilon). \quad (8.43)$$

Using the above two equations we can determine the constants $\overline{\mathcal{G}}_{d,i}^{I,k}$ and hence $\overline{\mathcal{G}}_{d,i}^I(\epsilon)$. Interestingly it is found that $\overline{\mathcal{G}}_{d,i}^I(\epsilon)$ are also maximally non-Abelian *i.e.*

$$\overline{\mathcal{G}}_{d,i}^q = \frac{C_F}{C_A} \overline{\mathcal{G}}_{d,i}^g. \quad (8.44)$$

Finally the constants $C_{d,i}^I$ are given by

$$C_{d,1}^I = 0, \quad C_{d,2}^I = -2\beta_0 \overline{\mathcal{G}}_{d,1}^{I,1}, \quad C_{d,3}^I = -2\beta_1 \overline{\mathcal{G}}_{d,1}^{I,1} - 2\beta_0 (\overline{\mathcal{G}}_{d,2}^{I,1} + 2\beta_0 \overline{\mathcal{G}}_{d,1}^{I,2}). \quad (8.45)$$

From eq. 8.23 and eq. 8.44 we see that the soft distribution functions for the differential cross section satisfy

$$\phi_d^q(\hat{a}_s, q^2, \mu^2, z_1, z_2, \epsilon) = \phi_d^g(\hat{a}_s, q^2, \mu^2, z_1, z_2, \epsilon) = \frac{C_F}{C_A} \phi_d^g(\hat{a}_s, q^2, \mu^2, z_1, z_2, \epsilon), \quad (8.46)$$

up to order a_s^2 , similar to the soft distributions that appear in the total cross sections [146]. The reason for this universality is due to its dependence only on the gauge interactions (SU(N)). In other words the soft part is independent of flavor, color, spin or any other quantum number, once the Born level cross section is factored out.

We now have all the ingredients to write eq. 8.37 in terms of A_I and $\overline{\mathcal{G}}_d^I$. The form of soft

distribution function is as follows [8]

$$\begin{aligned}
\phi_d^I(\hat{a}_s, q^2, \mu^2, z_1, z_2, \epsilon) = & \frac{1}{2} \delta(1 - z_2) \left(\frac{1}{1 - z_1} \left\{ \int_{\mu_F^2}^{q^2(1-z_1)} \frac{d\lambda^2}{\lambda^2} A^I(a_s(\lambda^2)) \right. \right. \\
& \left. \left. + \bar{G}_d^I(a_s(q^2(1 - z_1)), \epsilon) \right\} \right)_+ \\
& + q^2 \frac{d}{dq^2} \left[\left(\frac{1}{4(1 - z_1)(1 - z_2)} \left\{ \int_{\mu_F^2}^{q^2(1-z_1)(1-z_2)} \frac{d\lambda^2}{\lambda^2} A^I(a_s(\lambda^2)) \right. \right. \right. \\
& \left. \left. + \bar{G}_d^I(a_s(q^2(1 - z_1)(1 - z_2)), \epsilon) \right\} \right)_+ \Big] \\
& + \frac{1}{2} \delta(1 - z_1) \delta(1 - z_2) \sum_{i=1}^{\infty} \hat{a}_s^i \left(\frac{q^2}{\mu^2} \right)^{i \frac{\epsilon}{2}} S_{\epsilon}^i \hat{\phi}_d^{I,(i)}(\epsilon) \\
& + \frac{1}{2} \delta(1 - z_2) \left(\frac{1}{1 - z_1} \right)_+ \sum_{i=1}^{\infty} \hat{a}_s^i \left(\frac{\mu_R^2}{\mu^2} \right)^{i \frac{\epsilon}{2}} S_{\epsilon}^i \bar{K}^{I,(i)}(\epsilon) \\
& + (z_1 \leftrightarrow z_2).
\end{aligned} \tag{8.47}$$

Now we can find out the finite soft-virtual function $\Delta_d^{I,SV}(a_s, z_1, z_2, q^2, \mu_F^2, \mu_R^2)$ in eq. 8.16.

Writing it as

$$\Delta_d^{I,SV}(a_s, z_1, z_2, q^2, \mu_R^2, \mu_F^2) = C \exp \left(\Psi_d^I(a_s, z_1, z_2, q^2, \mu_R^2, \mu_F^2, \epsilon) \right) \Big|_{\epsilon=0} \tag{8.48}$$

the finite distribution Ψ_d^I in dimensional regularization can be written as

$$\begin{aligned}
\Psi_d^I = & \delta(\bar{z}_2) \left(\frac{1}{\bar{z}_1} \left\{ \int_{\mu_F^2}^{q^2 \bar{z}_1} \frac{d\lambda^2}{\lambda^2} A^I(a_s(\lambda^2)) \right. \right. \\
& \left. \left. + \bar{G}_d^I(a_s(q^2 \bar{z}_1)) \right\} \right)_+ + \frac{1}{2} \left(\frac{1}{\bar{z}_1 \bar{z}_2} \left\{ A^I(a_s(z_{12})) \right. \right. \\
& \left. \left. + \frac{d\bar{G}_d^I(a_s(z_{12}))}{d \ln z_{12}} \right\} \right)_+ + \frac{1}{2} \delta(\bar{z}_1) \delta(\bar{z}_2) \ln(g_{d,0}^I(a_s(\mu_F^2))) \\
& + \bar{z}_1 \leftrightarrow \bar{z}_2,
\end{aligned} \tag{8.49}$$

where $\bar{z}_1 = 1 - z_1$ and $\bar{z}_2 = 1 - z_2$ and $z_{12} = q^2 \bar{z}_1 \bar{z}_2$.

The finite distribution Ψ_d^I as obtained above contain plus distributions which can give large contributions in the limit $z_1 \rightarrow 1, z_2 \rightarrow 1$. Thus the SV cross section gives large contributions at every order in perturbation theory which can disturb the reliability of the perturbative predictions. The resolution is to resum these large terms, often the logarithms, to all orders to obtain any sensible prediction. In the next section we describe how to obtain an all order resummation formula by computing the integrals in eq. 8.49.

8.3 The resummation formula in double Mellin space

The soft virtual cross section in eq. 8.48 has an all order structure which is depicted through the exponential nature of the solution. It is written in terms of a convoluted exponential where the meaning of the later is given in eq. 8.17. Thus solving the integrals in eq. 8.49 will give us the desired all order resummation formula. However it is easier to work in the conjugate space of z_i , which is the Mellin N_i space, to get a compact form of such an all order formula. Thanks to the convolution structure of the hadronic cross section in terms of the PDFs $f_{a,b}$ and the SV cross section $\Delta_d^{I,SV}$, the two-dimensional Mellin transformation of the Born normalized hadronic cross section becomes a simple product of $\tilde{f}_a(N_1)$, $\tilde{f}_b(N_2)$ and $\tilde{\Delta}_d^{I,SV}(N_1, N_2)$. The double Mellin transformation is defined by

$$\tilde{\Delta}_d^{I,SV}(a_s, N_1, N_2, q^2, \mu_R^2, \mu_F^2) = \int_0^1 dz_1 z_1^{N_1-1} \int_0^1 dz_2 z_2^{N_2-1} \Delta_d^{I,SV}(a_s, z_1, z_2, q^2, \mu_R^2, \mu_F^2). \quad (8.50)$$

The delta functions, plus distributions transform as follows [26] (we show for one variable z_1)

$$\int_0^1 dz_1 z_1^{N_1-1} \delta(1 - z_1) = 1 \quad ,$$

$$\begin{aligned} \int_0^1 dz_1 z_1^{N_1-1} \mathcal{D}_i(z_1) &= \frac{(-1)^{i+1}}{i+1} \ln^{i+1} N_1 + \mathcal{O}(\ln^i N_1) , \\ \int_0^1 dz_1 z_1^{N_1-1} \ln^i(1-z_1) &= \frac{(-1)^i}{N_1} \ln^i N_1 + \mathcal{O}\left(\frac{1}{N_1} \ln^{i-1} N_1\right) . \end{aligned} \quad (8.51)$$

The threshold limit in Mellin space correspond to $N_1 \rightarrow \infty$. In this limit we see that the $\ln^i(N_1)$ terms give dominant contributions compared to the $\mathcal{O}(1/N_1)$ terms. From now we shall write $\tilde{Z}_{d,I}^{\text{SV}}$ as function of N_1, N_2 and suppress the arguments $a_s, q^2, \mu_R^2, \mu_F^2$ for brevity.

In order to derive a compact form of the resummed cross section we follow the methodology adopted in the work [26] where the soft virtual cross section in one dimensional Mellin space was expressed in terms of two quantities: an exponential containing all $\ln(N)$ terms and a prefactor multiplying the exponential, independent of $\ln(N)$ terms. For N_1, N_2 space the large logarithms are of the form $\ln^n(N_i)$, where $n = 1, \dots$ and $i = 1, 2$ and the resummation in double Mellin space resums terms of the form $\omega = a_s \beta_0 \ln(\bar{N}_1 \bar{N}_2)$ through a process independent function $g(\omega)$ and a process dependent but N_i independent function g_0 . Here β_0 is the leading coefficient of the beta function of the strong coupling constant g_s . Thus we can write

$$\begin{aligned} \tilde{Z}_d^{I,\text{SV}}(\omega) &= \int_0^1 dz_1 z_1^{N_1-1} \int_0^1 dz_2 z_2^{N_2-1} \mathcal{A}_d^{I,\text{SV}} \\ &= g_{d,0}^I(a_s) \exp\left(g_d^I(a_s, \omega)\right), \end{aligned} \quad (8.52)$$

where $\bar{N}_i = e^{\gamma_E} N_i, i = 1, 2$ and γ_E is the Euler-Mascheroni constant. The exponent $g_d^I(a_s, \omega)$ takes the canonical form:

$$g_d^I(a_s, \omega) = g_{d,1}^I(\omega) \ln(\bar{N}_1 \bar{N}_2) + \sum_{i=0}^{\infty} a_s^i g_{d,i+2}^I(\omega). \quad (8.53)$$

Hence to obtain an all order resummation formula for the soft-virtual cross section we have to compute the integrals in eq. 8.49 after taking a double Mellin transformation. The result of the integrals are presented in Appendix 11.2. Computing the integrals we

get the left side of eq. 8.52 and then comparing the exponential terms *i.e.* $\exp \Psi_d^I$ and $\exp(g_d^I(a_s, \omega))$ we find $g_d^I(a_s, \omega)$. Identifying $\bar{G}_d^I = D_d^I$ and rescaling the constants by β_0 as $\bar{g}_{d,1}^I = g_{d,1}^I$, $\bar{g}_{d,i+2}^I = g_{d,i+2}^I/\beta_0^i$, $\bar{A}_i^I = A_i^I/\beta_0^i$, $\bar{D}_{d,i}^I = D_{d,i}^I/\beta_0^i$ and $\bar{\beta}_i = \beta_i/\beta_0^{i+1}$, we find

$$\begin{aligned}
\bar{g}_{d,1}^I &= \bar{A}_1^I \frac{1}{\omega} (\omega + (1-\omega) \ln(1-\omega)), \\
\bar{g}_{d,2}^I &= \omega (\bar{A}_1^I \bar{\beta}_1 - \bar{A}_2^I) + \ln(1-\omega) (\bar{A}_1^I \bar{\beta}_1 + \bar{D}_{d,1}^I - \bar{A}_2^I) + \frac{1}{2} \ln^2(1-\omega) \bar{A}_1^I \bar{\beta}_1 \\
&\quad + L_{qr} \ln(1-\omega) \bar{A}_1^I + L_{fr} \omega \bar{A}_1^I, \\
\bar{g}_{d,3}^I &= -\frac{\omega \bar{A}_3^I}{2} - \frac{\omega}{2(1-\omega)} \left(-\bar{A}_3^I + (2+\omega) \bar{\beta}_1 \bar{A}_2^I + ((\omega-2) \bar{\beta}_2 - \omega \bar{\beta}_1^2 - 2\zeta_2) \bar{A}_1^I + 2\bar{D}_{d,2}^I \right. \\
&\quad \left. - 2\bar{\beta}_1 \bar{D}_{d,1}^I \right) - \ln(1-\omega) \left(\frac{\bar{\beta}_1}{(1-\omega)} (\bar{A}_2^I - \bar{D}_{d,1}^I - \bar{A}_1^I \bar{\beta}_1 \omega) - \bar{A}_1^I \bar{\beta}_2 \right) + \frac{\ln^2(1-\omega)}{2(1-\omega)} \bar{A}_1^I \bar{\beta}_1^2 \\
&\quad + L_{fr} \bar{A}_2^I \omega - \frac{1}{2} L_{fr}^2 \bar{A}_1^I \omega - L_{qr} \frac{1}{(1-\omega)} \left((\bar{A}_2^I - \bar{D}_{d,1}^I) \omega - \bar{A}_1^I \bar{\beta}_1 (\omega + \ln(1-\omega)) \right) \\
&\quad + \frac{1}{2} L_{qr}^2 \frac{\omega}{(1-\omega)} \bar{A}_1^I. \tag{8.54}
\end{aligned}$$

where $L_{fr} = \ln(\mu_F^2/\mu_R^2)$, $L_{qr} = \ln(q^2/\mu_R^2)$. The term $g_{d,0}^I(a_s)$ contains fixed order contributions and $\ln(N_i)$ independent terms. In eq. 8.47, the finite parts of the last two terms that remain after the cancellation of singularities, constitutes $g_{d,0}^I(a_s)$. We also include in $g_{d,0}^I(a_s)$, the contributions coming from the Mellin transformation of delta functions. Expanding $\ln(g_{d,0}^I)$ as $\ln(g_{d,0}^I) = \sum_{i=1}^{\infty} a_s^i l_{g_0}^{I,(i)}$, we find

$$\begin{aligned}
l_{g_0}^{I,(1)} &= 2g_{1,F}^{I,1} + 2\bar{\mathcal{G}}_{d,1}^{I,1} + 4A_1^I \zeta_2 - 2L_{fr} B_1^I + 2L_{qr} (B_1^I - \gamma_0^I), \\
l_{g_0}^{I,(2)} &= g_{2,F}^{I,1} + \bar{\mathcal{G}}_{d,2}^{I,1} + 2\beta_0 (g_{1,F}^{I,2} + \bar{\mathcal{G}}_{d,1}^{I,2}) + 2\zeta_2 (2A_2^I + \beta_0 (3B_1^I + 2f_1^I - 3\gamma_0^I)) + \frac{2}{3} A_1^I \beta_0 \zeta_3 \\
&\quad - 2L_{fr} B_2^I + L_{fr}^2 B_1^I \beta_0 + L_{qr} (2B_2^I - 2\gamma_1^I - \beta_0 (2g_{1,F}^{I,1} + 2\bar{\mathcal{G}}_{d,1}^{I,1} + 4A_1^I \zeta_2)) \\
&\quad + L_{qr}^2 \beta_0 (-B_1^I + \gamma_0^I). \tag{8.55}
\end{aligned}$$

Thus we have all the ingredients to perform threshold resummation of rapidity distribution for the production of any colorless particle in the final state. To find $g_d^I(a_s, \omega)$ and $g_{d,0}^I$ we need to know: cusp (A_i^I), collinear (B_i^I), soft (f_i^I), UV (γ_i^I) anomalous dimensions and

universal soft terms $\overline{\mathcal{G}}_{d,j}^{L,i}$ and process dependent constants $g_{j,F}^{L,i}$ of virtual corrections where $I = g, q$. In the next chapter we shall apply the above formalism for the production of lepton pair in the DY process ($I = q$) and analyze its numerical impact at the energies of the LHC up to NNLO+NNLL accuracy.

9 Threshold resummation of the rapidity distribution in the DY process

9.1 Introduction

The DY process has been studied theoretically to a great extent over many decades [49, 77]. The full inclusive production cross section is known up to NNLO [54, 112] for a very long time. The dominant soft-virtual (SV) contributions are now known at next-to-next-to-next-to-leading order (N³LO) level [57, 199]; electroweak corrections beyond leading order are also known and at NLO level [200, 201]. Although inclusive production is important for precise prediction of cross section, differential distributions allow a wider comparison with experiments. Rapidity and transverse momentum distributions for the Drell-Yan are known to up to NNLO level in QCD [80, 81, 83, 84, 202]; at N³LO level [8, 30, 203] soft plus virtual contributions for the rapidity distribution are now known. Studies where both QCD and electroweak corrections are combined can be found in [204]. Parton showers matched with NLO QCD results for the DY are also available in MC@NLO [205], POWHEG [205, 206] and aMC@NLO [207] frameworks. The differential distributions that has been studied extensively is the transverse momentum (p_T) distribution of pair of leptons or the vector bosons such as Z/W^\pm , see [208–212], often in their large p_T region. On the other hand, the rapidity distribution in DY was computed in [208] at NLO level

in QCD and it was later extended to NNLO level in [80, 83]. This stabilized the predictions [81], giving only a few percentage sensitivity to renormalization and factorization scales, for example at the Z mass region. However it has to be noted that the result does vary significantly *w.r.t.* the choices of different parton distribution functions (PDFs). In particular, at large invariant mass or at large rapidity of the final state, the cross sections are sensitive to large Björken x regions of PDFs, where different PDFs show not only differences between them but also exhibit large uncertainties. For a recent review see [213]. This sensitivity of PDFs will in turn help to constraint the PDF sets much better. Hence, it is important to study these distributions.

In certain regions of phase space, the fixed order predictions are often not reliable due to presence of large logarithms arising from some kinematic variables. At the partonic threshold *i.e.* where the initial partons have just enough energy to produce the final state such as a pair of leptons or Z/W^\pm and soft gluons, the phase space available for the gluons become severely constrained which results in large logarithms. To reliably predict different observables, we have to systematically resum these large logarithms to all orders in perturbation theory. Over the years resummation has become an important topic of investigation. For the inclusive production, the resummation of soft gluons in the threshold region was established [154, 155, 214] in the Mellin space and for the transverse momentum distribution, at small p_T , the resulting large logarithms were shown to exponentiate in the impact parameter space [215, 216]. Resummation in momentum space based on soft-collinear effective theory (SCET) have also been studied: for inclusive production see [217] and for transverse momentum distribution see [218]. For the differential distribution with respect to the Feynman variable x_F , resummation was studied in [154] and it was found that there were two thresholds and both could be resummed to all orders. It is to be noted that x_F describes the longitudinal momentum of the final state. The authors established that these logarithms could be exponentiated and also obtained the resummed result at the next-to-leading-logarithmic (NLL) accuracy. For resummation up to NLL accuracy in $\overline{\text{MS}}$ scheme see [219]. Resummation of rapidity distribution similar to the

inclusive one with a single scaling variable can be obtained in certain kinematic region, see [220–224] and an equivalent approach based on SCET can be found in [225, 226]. In the former one, called the standard direct QCD (dQCD) approach [154, 155, 214], since the resummation is performed in Mellin space where the phase space of the soft gluons factorizes under appropriate Mellin transformation, the threshold limit of the partonic scaling variable $z \rightarrow 1$ corresponds to Mellin variable $N \rightarrow \infty$, where $z = Q^2/\hat{s}$, $Q^2 = M_V^2$, $V = Z, W^\pm$ and \hat{s} is the partonic center of mass energy. However in SCET approach [217, 225, 226], resummation can be performed both in Mellin space as well as in z -space using the evolution operators of soft and the hard functions of the coefficient function.

For rapidity distribution resummation of large logarithms has been performed and several results are already available to very good accuracy. In [222] the authors have studied rapidity resummation for W^\pm in Mellin-Fourier (M-F) space based on a conjecture (see [220]) and later on same approach was used for Drell-Yan production in [223]. A more detailed study in the context of W^\pm productions as well as production of a pair of leptons was undertaken in [227], where the role of prescriptions were emphasized that take care of diverging series at a given logarithm accuracy.

Our approach to resum the soft gluon contributions for the rapidity distribution of a pair of leptons will be same as the dQCD approach [154]. The soft gluon effects show up through delta functions and plus distributions in the partonic cross section, when the partonic scaling variables reach the threshold limits, *i.e.*, $z_1 \rightarrow 1$ and $z_2 \rightarrow 1$. These contributions can be resummed to all orders both in z_1, z_2 space and in N_1, N_2 space. By expanding the resummed results up to desired accuracy the fixed order predictions in the soft plus virtual approximation in z_1, z_2 space were obtained in [30, 203, 228]. Using the formalism developed in [8, 203], we [229] have derived a general result that resums the soft gluons to all orders in perturbation theory in two dimensional Mellin (M-M) space spanned by N_1, N_2 . Our result is applicable for production of any colorless final state at the hadron

colliders; in the work [229] we have investigated the numerical impact of the rapidity distribution for Higgs boson production at the LHC. This double threshold limit, denoted by a pair of limits, namely $(z_1 \rightarrow 1, z_2 \rightarrow 1)$ corresponds to $(N_1 \rightarrow \infty, N_2 \rightarrow \infty)$ in M-M space. The corresponding large logarithms are of the form $\ln^n(N_i)$, where $n = 1, \dots$ and $i = 1, 2$ and the resummation in M-M space resums terms of the form $w = a_s \beta_0 \ln(N_1 N_2)$ through a process independent function $g(w)$ and a process dependent but N_i independent function g_0 . Here β_0 is the leading coefficient of the beta function of strong coupling constant g_s and $a_s = g_s^2(\mu_R^2)/16\pi^2$ with μ_R being renormalisation scale.

In this thesis we have studied the numerical impact of resummed contributions in the M-M approach on the fixed order predictions for the rapidity distribution of pair of leptons in the DY process at the LHC. The fixed order results at NNLO show remarkable stability against the factorization and renormalization scales. This is a good news for any phenomenological study with DY process but the question remains whether at every order in perturbative expansion, the fixed order predictions will be plagued by presence of large kinematic logarithms resulting from soft gluons in the threshold regions. In this thesis we have made a detailed study by taking into account these threshold effects from all orders in the perturbative expansion. In addition, owing to various ways by which these logarithms can be resummed, a detailed comparison of different approaches is desirable. This thesis attempts to address all these issues. We shall present our resummed result up to NNLO+NNLL accuracy. The resummation formalism based on the M-M approach has been discussed in the previous chapter. In sec. 9.3 we proceed with a detailed numerical study which is applicable for the energies at the LHC.

9.2 Theoretical framework

The theoretical framework necessary to perform threshold resummation has been described in chapter 8. We shall however write down the main formula that will be needed

in the next section. In the QCD improved parton model, for the production of a pair of leptons with invariant mass q^2 and rapidity y , the double differential cross section can be written as

$$\begin{aligned} \frac{d^2\sigma^q(\tau, q^2, y)}{dq^2 dy} &= \sigma_B^q(x_1^0, x_2^0, q^2) \sum_{ab=q, \bar{q}} \int_{x_1^0}^1 \frac{dz_1}{z_1} \int_{x_2^0}^1 \frac{dz_2}{z_2} \\ &\times f_a\left(\frac{x_1^0}{z_1}, \mu_F^2\right) f_b\left(\frac{x_2^0}{z_2}, \mu_F^2\right) \mathcal{A}_{d,ab}^q(z_1, z_2, q^2, \mu_F^2, \mu_R^2), \end{aligned} \quad (9.1)$$

where $\sigma_B^q(x_1^0, x_2^0, q^2)$ is the Born prefactor, $\tau = q^2/S = x_1^0 x_2^0$ with q being the momentum of the final state lepton pairs and $S = (p_1 + p_2)^2$ where p_i are the momenta of the incoming hadrons. The hadronic rapidity is defined as $y = \frac{1}{2} \ln(p_2 \cdot q / p_1 \cdot q) = \frac{1}{2} \ln(x_1^0 / x_2^0)$; $f_a\left(\frac{x_1^0}{z_1}, \mu_F^2\right)$ and $f_b\left(\frac{x_2^0}{z_2}, \mu_F^2\right)$ are the PDFs having momentum fractions $x_1 = x_1^0/z_1$, $x_2 = x_2^0/z_2$ respectively, renormalized at the factorization scale μ_F . $\mathcal{A}_{d,ab}^q(a_s, z_1, z_2, q^2, \mu_F^2)$ on the other hand is the DY coefficient function for rapidity distribution mass factorized at μ_F . This coefficient function consists of two parts: the hard part and the SV part. We have already discussed about it in eq. 8.15; the necessary steps to arrive at the differential SV cross section in M-M space has been described in the previous chapter

It is to be noted that the approach followed here [229] differs from earlier ones (see [220, 221, 223, 225–227] in the way the threshold limit(s) is(are) taken). In the later approach, the threshold contributions from soft gluons in the partonic cross section are defined by considering only those distributions with respect to the scaling variable $z = z_1 z_2$ which appear in the region when $z \rightarrow 1$. The remaining contributions contain not only regular terms in z but also distributions and regular functions of partonic rapidity variable (y_p). Here, only those distributions in z are resummed to all orders treating the remaining terms as hard part. Interestingly, if one works in M-F space, it can be easily shown that in the limit $z \rightarrow 1$, the threshold logs resulting from $N \rightarrow \infty$ are identical to those of the inclusive cross section. Thus the resummation for the rapidity distributions for the DY has been done using single Mellin variable N corresponding to z keeping the y_p dependent

coefficients as it is.

We employ the technique developed in [229] namely the M-M space approach to perform the soft gluon resummation for the DY rapidity distribution. In the next section we shall investigate the phenomenological impact of our resummation formalism.

9.3 Phenomenology

We consider the production of both leptons, *i.e.* $\ell^+\ell^-$, where $\ell = e, \mu$ through Z and γ^* in the collision of two hadrons at the centre of mass energy 14 TeV. Unless otherwise stated, we will mostly focus on the region containing the Z -pole. We take $n_f = 5$ flavors, MMHT2014(68cl) PDF sets [230] and the corresponding $a_s(M_Z)$ through LHAPDF-6 [231] interface at each order in the perturbation theory. We obtain the fixed order results from the publicly available code Vrap-0.9 [80, 232]. The resummed contribution is obtained from $\tilde{J}_d^{q,SV}(N_1, N_2)$ in eq. 8.52 after performing Mellin inversions which are done using an in house Fortran based code. The $\ln(N_i)$ terms in the resummed exponential g_d^q and the N_i independent terms $\tilde{g}_{d,0}^q$ are already present in the fixed order results; hence care is needed to avoid double counting. This can be achieved simply by employing a matching procedure at every order. The matched result is given below :

$$\frac{d^2\sigma^{q,\text{res}}}{dq^2 dy} = \frac{d^2\sigma^{q,\text{f.o}}}{dq^2 dy} + \sigma_B^q \int_{c_1-i\infty}^{c_1+i\infty} \frac{dN_1}{2\pi i} \int_{c_2-i\infty}^{c_2+i\infty} \frac{dN_2}{2\pi i} e^{y(N_2-N_1)} \left(\sqrt{\tau}\right)^{2-N_1-N_2} \tilde{f}_q(N_1) \tilde{f}_q(N_2) \left[\tilde{J}_d^{q,SV}(N_1, N_2) - \tilde{J}_d^{q,SV}(N_1, N_2) \Big|_{\text{trunc}} \right], \quad (9.2)$$

where σ_B^q is given by

$$\sigma_B^q = \frac{4\pi\alpha^2}{3q^4 N} \left[e_q^2 - \frac{2q^2(q^2 - M_Z^2)e_q g_e^V g_q^V}{((q^2 - M_Z^2)^2 + M_Z^2 \Gamma_Z^2) c_w^2 s_w^2} + \frac{3q^4 \Gamma_Z B_l^Z}{16\alpha M_Z ((q^2 - M_Z^2)^2 + M_Z^2 \Gamma_Z^2) c_w^2 s_w^2} \left(1 + \left(1 - \frac{8}{3} s_w^2 \right)^2 \right) \right]. \quad (9.3)$$

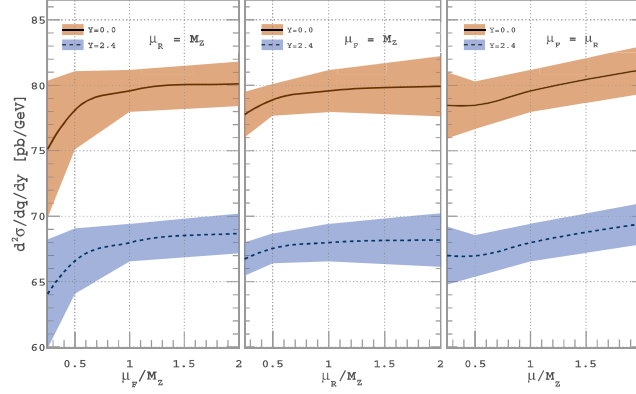


Figure 9.1: Cross sections against μ_F (left), μ_R (middle) and μ (right) variations at NNLO+NNLL for 14 TeV LHC. The bands are obtained by using 7 point scale variation (see text for more details).

with $\alpha = \alpha(M_Z) = 1/127.925$, e_q is the quark charge, $M_Z = 91.1876$ GeV, $\Gamma_Z = 2.4952$ GeV, $s_w^2 = 0.227$, $c_w^2 = 1 - s_w^2$, $g_e^V = -1/4 + s_w^2$, $g_u^V = 1/4 - 2/3 s_w^2$, $g_d^V = -1/4 + 1/3 s_w^2$, $B_e^Z = 0.03363$ and $B_\mu^Z = 0.03366$. The first term in eq. 9.2, $d^2\sigma^{q,\text{f.o.}}/dq^2 dy$, correspond to contributions from a fixed order perturbative computation. On the other hand the second term contains only threshold logarithms $\ln(N_i)$ to all orders in perturbation theory. The subscript “trunc” in the $\tilde{Z}_{d,q}^{\text{SV}}$ indicates that it is truncated at the same order as the fixed order one after expanding in powers of a_s . Thus at $O(a_s^n)$, the non-zero contribution from the second term starts at $O(a_s^{n+1})$ and includes terms from all orders. For the fixed n -th order contribution, namely $N^n\text{LO}$, the contribution from the second term is called $N^n\text{LL}$. For the fixed order predictions we use the notations LO, NLO and NNLO and correspondingly LO+LL, NLO+NLL and NNLO+NNLL for the resummed ones. It is well known that the resummed expression diverges due to the missing non-perturbative contributions. The origin of this divergence is $\omega \rightarrow 1$ in the functions $\bar{g}_{d,i}^q$; they are due to the coupling constant $a_s(\mu_R^2)$ that diverges near the Landau pole. We have adopted the Minimal Prescription (MP) [233] to resolve the above mentioned problem. For the two Mellin inversions, the contours are chosen [234] in such a way that all the poles in the complex plane spanned by N_1, N_2 remain to the left of the contours except for the Landau pole.

The leading order contribution to the DY process is due to electroweak interactions; the

dominant theoretical uncertainty comes from the factorization scale μ_F that enters through the parton distribution functions while the dependence on the renormalization scale μ_R starts only from NLO onwards. In contrary to the leading order term, in the resummed case, the LL contributions do depend on μ_R through ω in $\bar{g}_{d,1}^I(w)|_{l=q}$ given in eq. 8.54. Hence, μ_R dependence will show up even at LO+LL level. This will be evident from fig. 9.4 where one finds larger scale uncertainty from LO+LL contributions compared to the fixed order one at LO level. Thus it is important to understand the impact of these

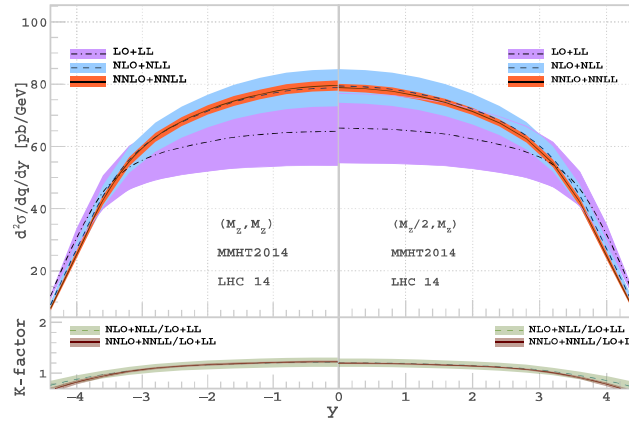


Figure 9.2: Resummed rapidity distribution in Drell-Yan production for the two sets of central scale choices (M_Z, M_Z) and $(M_Z/2, M_Z)$ using MMHT PDFs at 14 TeV LHC. Corresponding bands are obtained using 7-point scale variation around the central scale. The lower panel represents the corresponding K-factors.

two scales at the fixed order as well as at resummed level and also determine the optimal choice for the central scale around which the scale uncertainty remains minimal. In the work [235] the optimal choice has been realized for the fixed order case: it is when both μ_R and μ_F are set to M_Z . In order to find the same for the resummed case, we have plotted in fig. 9.1, dependence of the rapidity distribution on a) $(\mu_R = M_Z, \mu_F)$, b) $(\mu_R, \mu_F = M_Z)$ and finally c) $(\mu = \mu_R = \mu_F)$. The symmetric band is obtained by performing 7-point scale variation [26, 227, 235] around a given central scale with the constraint $(k_1, k_2) \otimes (\mu_R, \mu_F)_{\text{central}}$ where $(k_1, k_2) \in [1/2, 2]$ with $1/2 \leq k_1/k_2 \leq 2$ and by taking maximum absolute deviation from the central scale. From the first and the last panels of fig. 9.1, it is found that the optimal central scale choice is (M_Z, M_Z) whereas

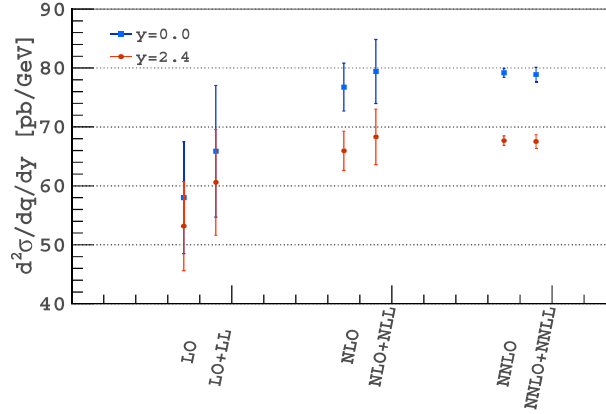


Figure 9.3: Fixed order predictions with the central scale $\mu_R = M_Z, \mu_F = M_Z$ and resummed prediction with the central scale $\mu_R = M_Z/2, \mu_F = M_Z$ for rapidity $y=0$ and $y=2.4$ using MMHT2014 PDF at each order. The uncertainties are obtained by using 7 point scale variation around the central scale (see text for more details).

the middle panel favors $(\frac{M_Z}{2}, M_Z)$ for the central scale. Comparing all three panels, we find that the choice $(\frac{M_Z}{2}, M_Z)$ gives minimum uncertainty band. However, to confirm the above analysis also holds true at each order in the perturbation theory, we have considered two different central scale choices (M_Z, M_Z) and $(M_Z/2, M_Z)$ in fig 9.2. We find that while the acceleration of the perturbative convergence are almost same for both cases, uncertainty band at NLO + NLL and at NNLO + NNLL level are smaller for the central scale choice $(M_Z/2, M_Z)$ compared to the case (M_Z, M_Z) . In fig. 9.3 we compare the predictions of our resummed result using the central scale $(\frac{M_Z}{2}, M_Z)$ against those coming from fixed order result with the central scale choice (M_Z, M_Z) , for two rapidities $y = 0$ and $y = 2.4$. We find that the scale uncertainties from the resummed case at NNLO+NNLL are comparable to what one obtains from NNLO. However, the central values at NLO+NLL and NNLO+NNLL are very close to each other compared to those of fixed order results, demonstrating better perturbative convergence.

In the introduction we mentioned about the works [222, 223, 227] where resummation of threshold logarithms for the rapidity distribution was achieved in the M-F space. The formalism that we have described in the previous chapter and also used in the work [229] differs from the other approaches in the way the threshold contributions are resummed.

$\frac{\mu_R}{M_Z}, \frac{\mu_F}{M_Z}$	LO	LL _{M-F}	LL _{M-M}	NLO	NLL _{M-F}	NLL _{M-M}	NNLO	NNLL _{M-F}	NNLL _{M-M}
2, 2	72.63	+0.99	+3.22	73.45	+1.64	+1.80	70.89	+ 0.63	+0.65
2, 1	63.20	+0.77	+2.59	70.62	+0.76	+1.02	70.36	+0.29	+0.32
1, 2	72.63	+1.09	+3.58	73.53	+1.91	+1.76	70.51	+0.51	+0.40
1, 1	63.20	+0.85	+2.89	71.40	+0.86	+0.90	70.54	+0.25	+0.17
1, $\frac{1}{2}$	53.24	+0.62	+2.22	67.58	+ 0.16	+0.14	69.83	- 0.001	- 0.09
$\frac{1}{2}$, 1	63.20	+0.95	+3.28	72.35	+0.94	+0.68	70.27	+0.09	- 0.01
$\frac{1}{2}$, $\frac{1}{2}$	53.24	+0.69	+2.50	69.26	+0.10	- 0.15	70.28	- 0.04	- 0.15

Table 9.1: Comparison of resummed results for Mellin-Fourier space (M-F) and double Mellin space (M-M) approach in the minimal prescription scheme at $y = 0$ for various choices of scales.

We resum large logarithms resulting from the regions where scaling variables z_1 and z_2 approach unity simultaneously while in the case of M-F, only large logarithms from the region where the partonic threshold variable z approaches unity and the partonic rapidity y_p is zero, are resummed. In the following we will make the numerical comparison of our predictions, namely the M-M formalism against those of M-F reported in [227]. The fixed order contributions are obtained by using Vrap-0.9 [80, 232]; the resummed contributions up to NNLL for M-F are obtained by using publicly available code ReDY [236] and for M-M, we use our in house Fortran routine. We have set all the parameters including the PDF set (NLO set of NNPDF-2.0 [237] at every order) the same as those used in [227]. Both our results and those from ReDY are listed in the Table 9.1 for various scale choices at the central rapidity. From the table we observe that at LL level, both M-F and M-M give positive contributions but the contribution from M-M is about three times larger compared to M-F independent of the scale choice. The additional contribution over LL at NLL for M-F is negative for some scale choices and positive for the rest while for M-M, it is always negative. The magnitude of these additional contributions for M-M is larger than M-F. Interestingly, at NNLL level, the additional contributions over NLL

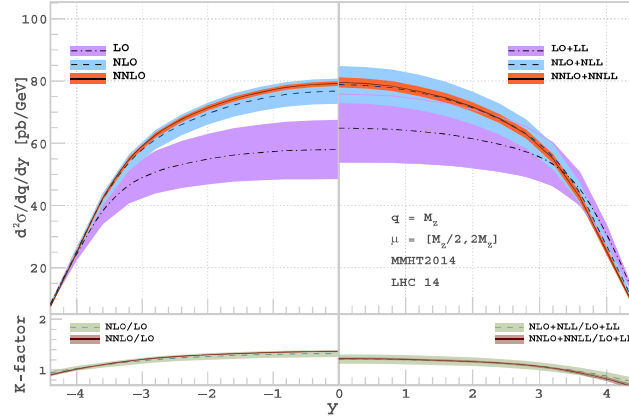


Figure 9.4: Drell-Yan rapidity distribution for 14 TeV LHC at $q = M_Z$ using MMHT PDFs. The fixed order results are plotted in the left panel and the resummed results in the right panel. Central scale is chosen as $\mu_R = \mu_F = M_Z$ for both and the corresponding bands are obtained using 7-point scale variation (see text for more details) around the central scale. The lower panel represents the corresponding K-factors.

for M-F and M-M are both negative in a such a way that the net NNLL contributions from both the approaches become comparable. In the case of M-F, the NLO+NLL is 2% larger compared to LO+LL and NNLO+NNLL is -4.7% larger compared NLO+NLL. For M-M, the corresponding ones are -0.8% and -4.9% respectively at $\mu_R = \mu_F = 2M_Z$.

We now present in fig. 9.4 the differential cross section for production of a lepton pair as a function of the rapidity y for $\sqrt{S} = 14$ TeV at the LHC. In the left panel we plot the fixed order result up to NNLO and in the right panel we present the resum result up to NNLO+NNLL. The respective K factors are also presented below. The K-factor at a given perturbative order, say at $N^n\text{LO}$ ($N^n\text{LO} + N^n\text{LL}$), is defined by the cross section at that order normalized by the same at LO (LO+LL) at the central scale $\mu_R = \mu_F = M_Z$. This choice for the scales has been made because the fixed order perturbative prediction is well behaved around this scale [235]. We obtain the symmetric band at each order by varying μ_R and μ_F between $[M_Z/2, 2M_Z]$ around the central scale $\mu_R = \mu_F = M_Z$ with the constraint $1/2 \leq \mu_R/\mu_F \leq 2$, by adding and subtracting to the central scale the highest possible uncertainties originating from all the scale combinations. We find that magnitude and the sign of the resummed contributions are sensitive to the order of perturbation as

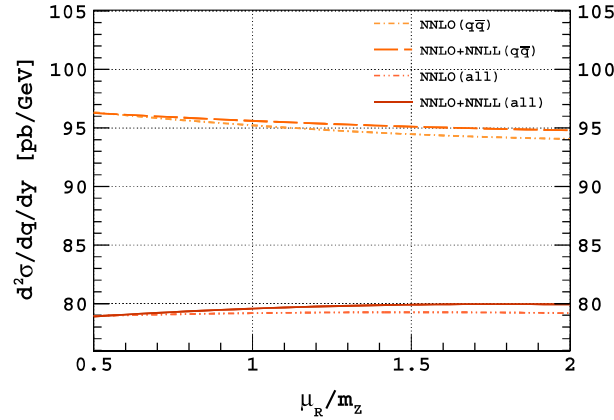


Figure 9.5: Drell-Yan rapidity distribution for 14 TeV LHC at $y = 0$ using MMHT PDFs. The variation of fixed order and resummed results as a function of μ_R are shown separately for $q\bar{q}$ channel and also for all the channels added together.

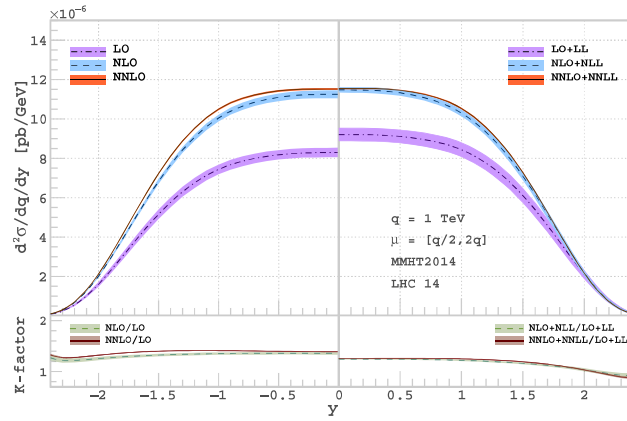


Figure 9.6: Same as fig. 9.4 but for $q = 1$ TeV.

well the exact values of y and the scales μ_R, μ_F . For example, if we choose $\mu_R = M_Z/2$ and $\mu_F = M_Z$ instead of $\mu_R = \mu_F = M_Z$ as the central scale, we obtain a negative contribution from NNLL terms for all values of rapidity.

We observe from fig. 9.4 that the inclusion of N^n LL contributions increase the cross section at every order for wide range of rapidity values. In addition, the overlap among various orders is larger for resummed case compared to the fixed order ones, because the uncertainty band at each order in the resummed case is bigger compared to the fixed order. As far as fixed order results are concerned, in particular at NNLO level, several partonic channels open up, effectively reducing the scale uncertainty considerably. How-

ever, resummed contributions come only from quark anti-quark initiated channels to all orders in the perturbation theory; other channels do not give the threshold logarithms and hence do not contribute. We confirm this through fig. 9.5, where we have studied the effects of resummation over the fixed order contributions, by considering a) only $q\bar{q}$ channel at NNLO and b) all the channels at NNLO. We perform our analysis for $y = 0$ and set $\mu_F = M_Z$ while vary μ_R between $M_Z/2$ to $2M_Z$. For the $q\bar{q}$ channel the resum contributions arising from the two extreme scales are of opposite sign and their individual contributions are such that the NNLO+NNLL ($q\bar{q}$) curve shows a stable behavior as compared to NNLO ($q\bar{q}$). While the fixed order decreases by 2.36% from $M_Z/2$ to $2M_Z$, the corresponding decrease for NNLO+NNLL ($q\bar{q}$) is 1.53%. This confirms the reduction of scale dependence upon adding resummed terms to the fixed order contributions. To estimate the percentage corrections purely coming from the threshold region from this channel at each order of the perturbation theory, we have considered the case where the central scale is chosen to be $\mu_R = \mu_F = M_Z$. As expected, at LO both fixed order and the truncated resummed predictions agree. But, at NLO and at NNLO we find truncated one is 7%-8% and 12%-13% larger compared to respective fixed order at the central rapidity region. The largeness of the truncated results gets compensated by the -ve corrections coming from other channels emerging at respective orders. However the scenario entirely reverses when we consider all the channels at NNLO. We find that the differential cross section at NNLO (all) increases by 0.29% in the entire range of μ_R value; the corresponding increase for NNLO+NNLL (all) is 1.29%. This reduction of the scale dependence at NNLO is due to cancellation among different partonic channels. However the resummation effects come only from $q\bar{q}$ channel which adds to the fixed order in such a way that the resummed uncertainty increases. This explains the increase of scale uncertainty at each resummed order depicted in fig. 9.4. In addition the PDF's do not contain resummed threshold logarithms, hence there is incomplete cancellation of factorization scale against the PDF's, which increases the band. The K-factor at NLO varies between 1.3 and 1.2 and at NNLO between 1.37 and 1.3 over the entire rapidity region. On the other hand, the K-

y	LO	LO+LL	NLO	NLO+NLL	NNLO	NNLO+NNLL	K _{NLO}	K _{NLO+NLL}	K _{NNLO}	K _{NNLO+NNLL}
0.0	58.00± 16.36	64.87± 16.89	76.76± 5.28	78.87± 7.56	79.18± 0.98	79.57± 2.02	1.32	1.216	1.365	1.226
0.8	57.64± 16.07	64.47± 16.61	75.73± 5.26	77.80± 7.53	77.97± 1.04	78.34± 2.03	1.314	1.207	1.352	1.215
1.6	56.23± 15.29	62.93± 15.82	72.30± 5.17	74.27± 7.45	74.24± 1.11	74.59± 2.08	1.286	1.180	1.320	1.185
2.4	53.18± 14.19	59.65± 14.71	65.95± 5.04	67.77± 7.33	67.68± 1.21	67.99± 2.11	1.240	1.136	1.273	1.140

Table 9.2: Fixed order and the resummed cross sections with % scale uncertainties along with the K-factors at the central scale $\mu_R = \mu_F = M_Z$.

factors at both NLO+NLL and NNLO+NNLL significantly overlap with each other over most of the regions of rapidity and stay around 1.2. Thus we find that the perturbative convergence for resummed case is better compared to fixed order. We present the differential cross section for benchmark rapidity values along with the percentage scale uncertainties in Table 9.2. It is to be noted that the differential cross-section at NNLO+NNLL level for the central scale is well approximated by the same at NLO+NLL. In fact, NNLO+NNLL increases approximately by 0.8% with respect to NLO+NLL; the corresponding number for NNLO over NLO is approximately 3%. From the trend that resummed results give, we anticipate $N^3\text{LO}+N^3\text{LL}$ cross-section will fall completely within the NNLO+NNLL band.

We present in fig. 9.6 both the fixed order and resummed results at various orders for a larger invariant mass $q = 1$ TeV. Interestingly, the uncertainty bands at NLO+NLL and NNLO+NNLL levels are better compared to those from fixed order.

In addition the predictions from the resummed terms at various orders are closer compared to those from fixed order which implies better perturbative convergence for the resummed case. In fact the resummed K-factor for the central rapidity at NNLO+NNLL is 1.25 compared to 1.39 at NNLO.

y	MMHT	ABMP	NNPDF	PDF4LHC
0.0	$79.568^{+1.83\%}_{-1.16\%}$	$79.756^{+0.43\%}_{-0.56\%}$	$81.959^{+2.64\%}_{-3.64\%}$	$78.734^{+1.20\%}_{-0.89\%}$
0.8	$78.340^{+1.55\%}_{-0.99\%}$	$78.202^{+0.43\%}_{-0.56\%}$	$80.256^{+2.07\%}_{-3.66\%}$	$77.390^{+1.17\%}_{-0.83\%}$
1.6	$74.588^{+0.90\%}_{-0.63\%}$	$73.738^{+0.42\%}_{-0.52\%}$	$75.178^{+2.61\%}_{-2.31\%}$	$73.505^{+1.26\%}_{-0.61\%}$
2.4	$67.985^{+0.72\%}_{-0.79\%}$	$66.653^{+0.41\%}_{-0.44\%}$	$67.354^{+2.89\%}_{-3.01\%}$	$67.070^{+1.11\%}_{-0.62\%}$

Table 9.3: Cross sections at NNLO+NNLL using different PDF sets along with percentage uncertainties for $y = 0, 0.8, 1.6, 2.4$.

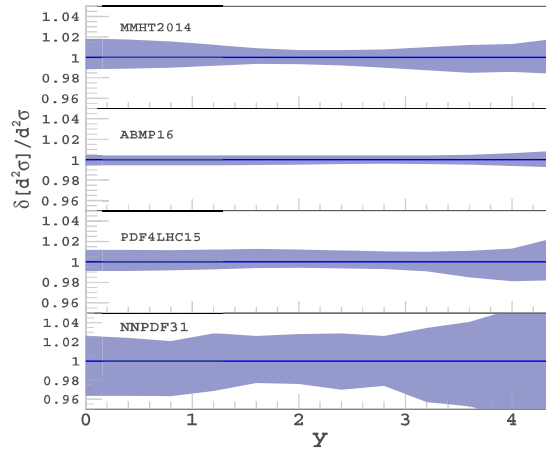


Figure 9.7: PDF variation at NNLO+NNLL using various sets. The y-axis represents the ratio of extremum variation over the central PDF set.

As there are several PDF groups in the literature, each providing sets of PDFs, it is customary to estimate the uncertainty resulting from the choice of PDFs within each set of a given PDF group. We have obtained the cross sections along with the corresponding PDF uncertainty using PDFs from different groups namely MMHT2014nnlo68cl [230], ABMP [238], NNPDF3.1 [239] and PDF4LHC [240]. This we present in fig. 9.7, where we have plotted the uncertainty bands for various PDF sets as function of rapidity in order to demonstrate the correlation of PDF uncertainty with the rapidity values. This will help to better constrain the PDF fits using measurements on rapidity in the Drell-Yan process. In table 9.3, we have also tabulated the cross sections along with % uncertainties resulting from the choice of different PDFs.

In fig. 9.8 we present the q -integrated rapidity distribution for the LHC with 8 TeV centre

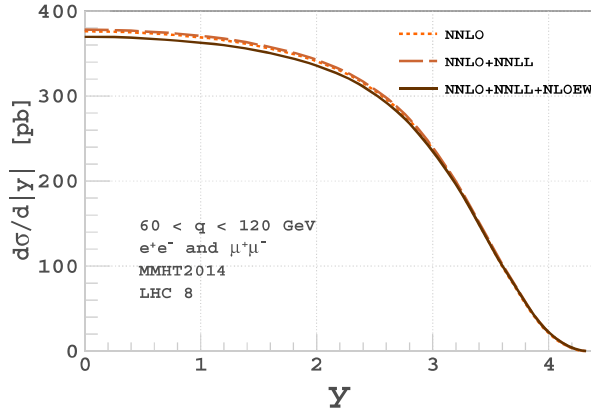


Figure 9.8: Rapidity distribution at NNLO+NNLL for 8 TeV LHC in the invariant mass range $60 < q < 120$ GeV. The dotted line is the fixed order NNLO contribution, the dashed line represents NNLO+NNLL result and the solid line includes electro-weak corrections.

of mass energy at NNLO+NNLL. We choose $\mu_R = \mu_F = M_Z$ and integrate the invariant mass between 60 GeV and 120 GeV. Unlike our earlier analysis, we have included both e^+e^- as well as $\mu^+\mu^-$ final states. The electro-weak (EW) corrections at NLO are comparable to QCD corrections at NNLO+NNLL; we present our result by combining both of them. The EW contributions are obtained by using publicly available code Horace-3.2 [241–244]. We use the G_μ scheme and take $G_F = 1.16639 \times 10^{-5}$, $M_W = 80.395$ GeV, $M_Z = 91.1876$ GeV and use MMHT2014nlo68cl pdf. The electron and muon masses are taken to be $m_e = 0.51099$ MeV and $m_\mu = 0.10566$ GeV respectively. While the NNLL contribution increases the cross-section by roughly around 0.5% with respect to NNLO, however the EW corrections at NLO give negative contribution to the cross-section. We find the corrections are different for e^+e^- and $\mu^+\mu^-$ pairs: for electrons, the EW contributions are twice that of muons. The total contributions from the electron and muon channels gives rise to an overall 2.3% decrease in the cross section w.r.t. the NNLO in the central rapidity region. Since the rapidity distribution in fig. 9.8 is inclusive in the transverse momenta of the final state leptons, hence they can not be directly compared with the results presented in [245] where a minimum transverse momenta cut is applied in the selection of final state leptons. In order to compare, we need distribution exclusive of transverse momenta which at the moment beyond the scope of the current thesis. Both at

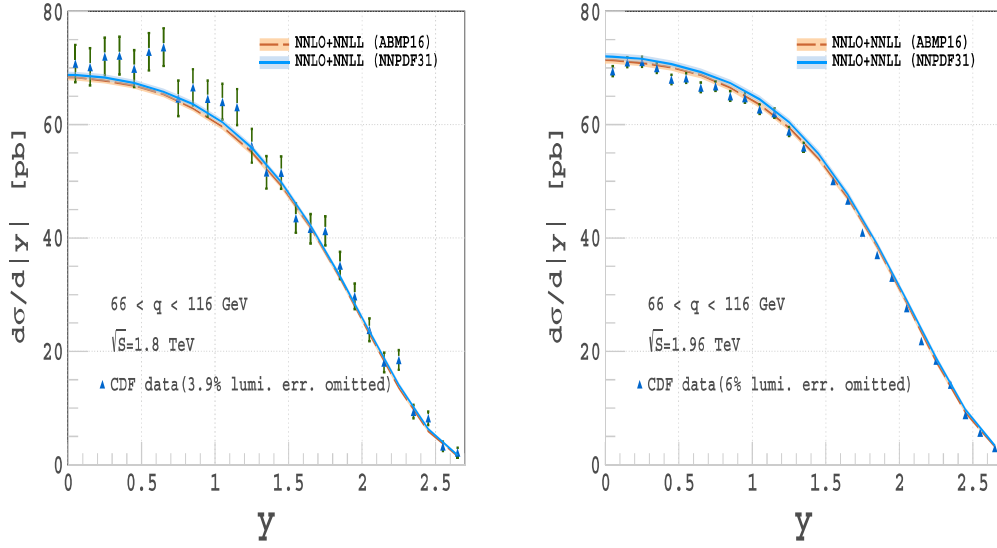


Figure 9.9: Comparison of resummed results with the CDF data [246] at $\sqrt{s} = 1.8$ TeV and [247] at $\sqrt{s} = 1.96$ TeV in the invariant mass range $66 < q < 116$ GeV for two different PDF sets.

Tevatron and at the LHC, there are already precise measurements of rapidity distributions for different ranges of invariant mass q . For one of the earliest set of measurements see NuSea [248, 249]. Since the data from the LHC depends heavily on the kinematic cuts of the final states we cannot directly compare against our predictions. On the other hand CDF [246] has data for the rapidity distributions for wide range of y with invariant mass range $66 < q < 116$ GeV. In fig. 9.9 we have compared our predictions against the data at $\sqrt{s} = 1.8$ TeV and $\sqrt{s} = 1.96$ TeV after integrating q between the above mentioned range for two different choices of PDF sets. The scale uncertainty is obtained as before by using 7-point scale variations around the central value $\mu_R = \mu_F = M_Z$. We note that at NNLO+NNLL level, the resummed contributions over the fixed order is very mild, less than 0.5%. We have also observed that the resummed effects become significant for large invariant mass regions.

9.4 Conclusion

In this chapter we have investigated the role of resummed threshold logarithms for the rapidity distribution of pairs of leptons in the DY process at the LHC. The DY process has been widely studied at different colliders like Tevatron, LHC; the accurate prediction of inclusive as well as differential cross section is known up to NNLO in the context of pQCD. In addition the first order electroweak effects have been computed in the past and they are found to be of same order of magnitude as the NNLO QCD corrections. Owing to the dominant QCD interactions, soft gluons play vital role in most of the observables. They show up in certain kinematic regions through large logarithms in the perturbative computations, thus spoiling the reliability of the fixed order predictions. We have made a detail study on the effect of the soft gluons on rapidity distribution within the resummation framework. There are two approaches that exist in the literature: a) Mellin-Mellin approach and b) Mellin-Fourier approach. Our approach (a) differs from the one in (b) in the way the threshold limits are defined. This is the first time the double Mellin moment approach has been used to derive an all order resummation formula for the DY process. We present the numerical impact of the rapidity distribution of the DY up to NNLO+NNLL accuracy and compare with the already known result, obtained up to the same accuracy in the alternative framework. As these two formalisms resum different type of logarithms to all orders, they are expected to give different numerical predictions. At LL and NLL level they differ very much but surprisingly at the NNLL level both the approaches converge to a few percent correction to the fixed order prediction. This could be accidental, however it is desirable to understand this coincidence at NNLL level. We have performed numerical study on the dependence of renormalization and factorization scales and found out that the optimal central scales for the resummed result are $\mu_R = M_Z/2$ and $\mu_F = M_Z$. In addition we have found that, for wide range of rapidity, the scale uncertainties from NNLL contributions at every order slightly are larger than those from fixed order results. We be-

lieve that this could be due to an incomplete cancellation scale dependent terms between resummed result and the PDFs. It is to be noted that the PDFs that we use are extracted from data using the fixed order perturbative predictions for the observables and also using evolutions equations controlled by splittings functions computed to desired order in strong coupling constant. Hence, we expect that there will be a better cancellation of scale if appropriate resummed PDF sets are available. We have also presented our predictions for various choices of PDFs from various PDF groups. The result on q integrated rapidity distribution is also presented in this thesis. Since our resummation formalism cannot take into the experimental cuts such as the transverse momentum and/or polar angles of the final state leptons, we cannot make any direct comparison with the existing data on the q integrated rapidity distribution measured at the LHC which are extracted after employing cuts on transverse momentum of final state leptons. On the other hand we have compared our predictions against CDF data at Tevatron for the invariant mass range $66 < q < 116$ GeV and found good agreement within both theoretical and experimental uncertainties.

10 Conclusion

To incorporate the gravitational force within the SM of particle physics, extra dimensional models have been constructed which allows the interaction of a generic massive spin-2 field with the gauge and fermionic fields of the SM. We have studied such an interaction term in the most general framework: when the coupling of the spin-2 to the SM fields is universal as well as non-universal. In order to precisely constrain the parameters of the models constructed out of such interactions, it is important to compute the higher order QCD corrections, where the latter plays an important role at the LHC. For the scenario of universal coupling, we have computed second order QCD corrections in models of TeV scale gravity. We employed the method of reverse unitarity to achieve the computation. At NNLO level, we observe reduction of scale uncertainties, where the latter originates due to the unphysical renormalization and factorization scales. To understand how the spin-2 particle interacts with the gauge and fermionic fields through different coupling strengths, we have computed form factors up to three loop orders in perturbation theory. The additional UV divergences that appeared were regulated by multiplying overall renormalization constants. We then computed the QCD corrections for such an interaction term up to second order. Study of the phenomenology of such a nonuniversal model revealed interesting aspects, like the dependence of the partonic cross section on different values of the coupling strengths. Our detailed study on the phenomenological aspects of the massive spin-2 particle will help to constrain the model parameters in a better way.

However in certain regions of phase space, the fixed order predictions are often not reli-

able, for example when the initial partons have just enough energy to produce the final state such as a pair of leptons or Z/W^\pm and soft gluons. In such cases large logarithms of some kinematic variables can appear at the partonic level; when multiplied by the PDF's, these contributions can dominate over the hard part of the hadronic cross section. These large contributions can spoil the reliability of the perturbation theory. The resolution to the problem is to add all these logarithmic contributions at every order in the perturbation theory. This is called threshold resummation of the soft gluon contributions. In this thesis, we have performed threshold resummation of the rapidity distribution for the DY production of a lepton pair in the final state. We have performed the resummation in the most general framework, where we take into account all the plus distributions and delta functions in the partonic variables z_1 and z_2 . We present our results up to NNLO+NNLL accuracy and they show improved perturbative convergence as compared to the fixed order counterparts. In addition we have also studied the q integrated rapidity distribution and compared our predictions with the CDF data at $\sqrt{s} = 1.8$ TeV in the invariant mass range of $66 < q < 116$ GeV for two different PDF sets. We have observed that the resummed effects become significant for large invariant mass regions. We believe that the perturbative results that take into account both the fixed order as well as the resummed contributions will provide a precise determination of PDFs from the ample data that are already available at the LHC.

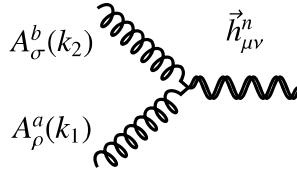
11

Appendix

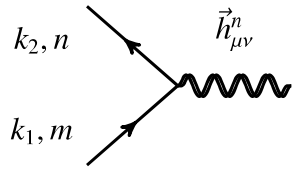
11.1 Feynman rules for spin-2 particle

We present the Feynman rules for massive spin-2 field ($\vec{h}_{\mu\nu}^n$) interacting with the SM fields via the energy momentum tensor of QCD where the latter is given in eq. 4.7.

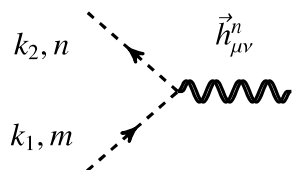
The Feynman rules for the three point vertices are:



$$\vec{h}_{\mu\nu}^n AA : -i \frac{\kappa}{2} \delta^{ab} \left((m_A^2 + k_1 \cdot k_2) C_{\mu\nu, \rho\sigma} + D_{\mu\nu, \rho\sigma}(k_1, k_2) + 1/\xi E_{\mu\nu, \rho\sigma}(k_1, k_2) \right)$$

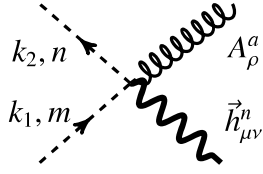


$$\vec{h}_{\mu\nu}^n \psi\psi : -i \frac{\kappa}{8} \delta^{mn} \left(\gamma_\mu (k_{1\nu} + k_{2\nu}) + \gamma_\nu (k_{1\mu} + k_{2\mu}) - 2 \eta_{\mu\nu} (\not{k}_1 + \not{k}_2 - 2 m_\psi) \right)$$

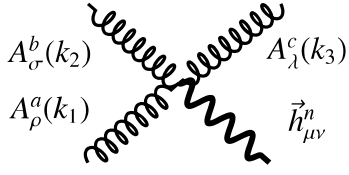


$$\vec{h}_{\mu\nu}^n \phi\phi : -i \frac{\kappa}{2} \delta^{mn} \left(m_\phi^2 \eta_{\mu\nu} + C_{\mu\nu, \rho\sigma} k_1^\rho k_2^\sigma \right)$$

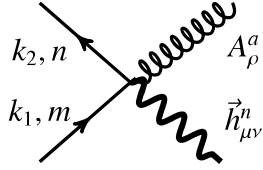
The Feynman rules for the four point vertices are:



$$\vec{h}_{\mu\nu}^n \phi\phi A : i g_s \frac{\kappa}{2} T_{nm}^a C_{\mu\nu,\rho\sigma} (k_1^\sigma + k_2^\sigma)$$

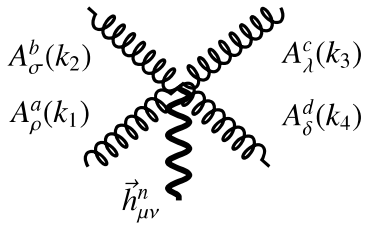


$$\begin{aligned} \vec{h}_{\mu\nu}^n A A A : g_s \frac{\kappa}{2} f^{abc} & \left(C_{\mu\nu,\rho\sigma} (k_{1\lambda} - k_{2\lambda}) + C_{\mu\nu,\rho\lambda} (k_{3\sigma} - k_{1\sigma}) \right. \\ & + C_{\mu\nu,\sigma\lambda} (k_{2\rho} - k_{3\rho}) \\ & \left. + F_{\mu\nu,\rho\sigma\lambda} (k_1, k_2, k_3) \right) \end{aligned}$$

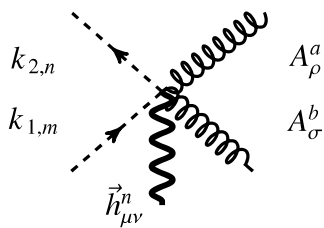


$$\vec{h}_{\mu\nu}^n \psi\psi A : i g_s \frac{\kappa}{4} T_{nm}^a (C_{\mu\nu,\rho\sigma} - \eta_{\mu\nu} \eta_{\rho\sigma}) \gamma^\sigma$$

The Feynman rules for the five point vertices are:

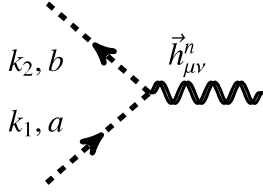


$$\begin{aligned} \vec{h}_{\mu\nu}^n A A A A : i g_s^2 \frac{\kappa}{2} & \left(f^{eac} f^{edb} G_{\mu\nu,\rho\sigma\lambda\delta} + f^{eab} f^{ecd} G_{\mu\nu,\rho\lambda\sigma\delta} \right. \\ & \left. + f^{ead} f^{ebc} G_{\mu\nu,\rho\sigma\delta\lambda} \right) \end{aligned}$$



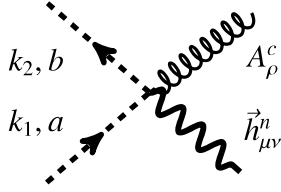
$$\vec{h}_{\mu\nu}^n \phi\phi A A : -i g_s^2 \frac{\kappa}{2} C_{\mu\nu,\rho\sigma} \{T^a, T^b\}_{mn}$$

The graviton-ghost-ghost vertex is as follows:



$$\vec{h}_{\mu\nu}^n \omega\omega : -i \frac{\kappa}{2} \delta^{ab} (C_{\mu\nu,\rho\sigma} k_1^\rho k_2^\sigma)$$

The graviton-ghost-ghost-gluon vertex is as follows:



$$\vec{h}_{\mu\nu}^n \omega\omega A : g_s \frac{\kappa}{2} f^{abc} C_{\mu\nu,\rho\sigma} k_2^\sigma$$

The terms $C_{\mu\nu,\rho\sigma}$, $D_{\mu\nu,\rho\sigma}$, $E_{\mu\nu,\rho\sigma}$, $F_{\mu\nu,\rho\sigma,\lambda}$, $G_{\mu\nu,\rho\sigma,\lambda\delta}$ are given below:

$$\begin{aligned} C_{\mu\nu,\rho\sigma} &= \eta_{\mu\rho}\eta_{\nu\sigma} + \eta_{\mu\sigma}\eta_{\nu\rho} - \eta_{\mu\nu}\eta_{\rho\sigma} , \\ D_{\mu\nu,\rho\sigma}(k_1, k_2) &= \eta_{\mu\nu}k_{1\sigma}k_{2\rho} - \left[\eta_{\mu\sigma}k_{1\nu}k_{2\rho} + \eta_{\mu\rho}k_{1\sigma}k_{2\nu} - \eta_{\rho\sigma}k_{1\mu}k_{2\nu} + (\mu \leftrightarrow \nu) \right] , \\ E_{\mu\nu,\rho\sigma}(k_1, k_2) &= \eta_{\mu\nu}(k_{1\rho}k_{1\sigma} + k_{2\rho}k_{2\sigma} + k_{1\rho}k_{2\sigma}) \\ &\quad - \left[\eta_{\nu\sigma}k_{1\mu}k_{1\rho} + \eta_{\nu\rho}k_{2\mu}k_{2\sigma} + (\mu \leftrightarrow \nu) \right] , \\ F_{\mu\nu,\rho\sigma,\lambda}(k_1, k_2, k_3) &= \eta_{\mu\rho}\eta_{\sigma\lambda}(k_2 - k_3)_\nu + \eta_{\mu\sigma}\eta_{\rho\lambda}(k_3 - k_1)_\nu \\ &\quad + \eta_{\mu\lambda}\eta_{\rho\sigma}(k_1 - k_2)_\nu + (\mu \leftrightarrow \nu) , \\ G_{\mu\nu,\rho\sigma,\lambda\delta} &= \eta_{\mu\nu}(\eta_{\rho\sigma}\eta_{\lambda\delta} - \eta_{\rho\delta}\eta_{\sigma\lambda}) + \left(\eta_{\mu\rho}\eta_{\nu\delta}\eta_{\lambda\sigma} + \eta_{\mu\lambda}\eta_{\nu\sigma}\eta_{\rho\delta} \right. \\ &\quad \left. - \eta_{\mu\rho}\eta_{\nu\sigma}\eta_{\lambda\delta} - \eta_{\mu\lambda}\eta_{\nu\delta}\eta_{\rho\sigma} + (\mu \leftrightarrow \nu) \right) . \end{aligned}$$

11.2 Computation of the integrals in double Mellin space

In this section we shall compute the integrals appearing in the soft function in the eq. 8.47 in Mellin space, which will help to obtain the resummation exponents given in eq. 8.54.

We shall compute the Mellin transform

$$\int_0^1 dz_1 z_1^{N_1-1} \int_0^1 dz_2 z_2^{N_2-1} 2\phi_d(z_1, z_2) = \phi_d(N_1, N_2).$$

The first two terms of eq. 8.47 contain plus distributions and gives $\ln(N_i)$ type of terms after Mellin transformation. In order to calculate $g_d^I(a_s, \omega)$ we need the above mentioned terms. On the other hand the last two terms contain singularities which cancel with each other and leave finite parts. These finite parts will be $\ln(N_i)$ independent and we shall absorb them into $g_{d,0}^I(a_s)$. We also include in $g_{d,0}^I(a_s)$, the contributions coming from the Mellin transformation of delta functions. We take into account the first two terms and compute the required integrals. We write them as

$$\begin{aligned} \phi_d(N_1, N_2) &= \int_0^1 dz_1 \frac{z_1^{N_1-1} - 1}{1 - z_1} \left[\int_{\mu_F^2}^{q^2} \frac{d\lambda^2}{\lambda^2} A(a_s(\lambda^2)) + \int_{q^2}^{q^2(1-z_1)} \frac{d\lambda^2}{\lambda^2} A(a_s(\lambda^2)) \right. \\ &\quad \left. + \bar{G}_d(a_s(q^2(1-z_1))) \right] \\ &\quad + \frac{1}{2} \int_0^1 dz_1 \frac{z_1^{N_1-1} - 1}{1 - z_1} \int_0^1 dz_2 \frac{z_2^{N_2-1} - 1}{1 - z_2} A(a_s(q^2(1-z_1)(1-z_2))) \\ &\quad + \frac{1}{2} \int_0^1 dz_1 \frac{z_1^{N_1-1} - 1}{1 - z_1} \int_0^1 dz_2 \frac{z_2^{N_2-1} - 1}{1 - z_2} \left\{ q^2 \frac{d}{dq^2} \bar{G}_d(a_s(q^2(1-z_1)(1-z_2))) \right\} \\ &\quad + (z_1 \leftrightarrow z_2)(N_1 \leftrightarrow N_2) \\ &= I_A + I_B + I_C + (z_1 \leftrightarrow z_2)(N_1 \leftrightarrow N_2) \end{aligned} \tag{11.1}$$

To solve the integrals we need the following relations [26]

$$z^{N-1} - 1 = -\tilde{r} \left(1 - \frac{\partial}{\partial \ln N} \right) \Theta \left(1 - z - \frac{N_0}{N} \right) + \mathcal{O} \left(\frac{1}{N} \right), \quad (11.2)$$

$$\begin{aligned} -\tilde{r} \left(1 - \frac{\partial}{\partial \ln \bar{N}} \right) &= \Gamma_2 \left(\frac{\partial}{\partial \ln \bar{N}} \right) \left(\frac{\partial}{\partial \ln \bar{N}} \right)^2 - 1, \\ \Gamma_2(x) &= \frac{1}{x^2} \left(1 - \exp \left(\sum_{n=2}^{\infty} \frac{\zeta(n)}{n} x^n \right) \right), \end{aligned} \quad (11.3)$$

with $\bar{N} = \frac{N}{N_0}$. We follow the methodology adopted in [250] where the computation was performed for only one Mellin variable. In this thesis we show how to perform the integrals for two Mellin variables.

11.2.1 I_A

Using the above relations and $\tilde{r}_1 = 1 - \Gamma_2 \left(\frac{\partial}{\partial \ln \bar{N}_1} \right) \left(\frac{\partial}{\partial \ln \bar{N}_1} \right)^2$ we can write

$$\begin{aligned} I_A &= \ln \bar{N}_1 \int_{q^2}^{\mu_F^2} \frac{d\mu^2}{\mu^2} A(a_s(\mu^2)) - \tilde{r}_1 \left[\int_{q^2/\bar{N}_1}^{q^2} \frac{d\mu^2}{\mu^2} \left\{ \ln \left(\frac{q^2}{\mu^2 \bar{N}_1} \right) A(a_s(\mu^2)) + \bar{G}_d(a_s(\mu^2)) \right\} \right] \\ &\equiv \ln \bar{N}_1 \int_{q^2}^{\mu_F^2} \frac{d\mu^2}{\mu^2} A(a_s(\mu^2)) - \int_{q^2/\bar{N}_1}^{q^2} \frac{d\mu^2}{\mu^2} \left\{ \ln \left(\frac{q^2}{\mu^2 \bar{N}_1} \right) A(a_s(\mu^2)) + \tilde{G}_d(a_s(\mu^2)) \right\} - \ln \tilde{C}. \end{aligned} \quad (11.4)$$

Thus we find

$$\begin{aligned} \ln \tilde{C} &= -\Gamma_2 \left[\frac{\partial}{\partial \ln \bar{N}_1} \bar{G}_d(a_s(k^2)) - A(a_s(k^2)) \right] \Big|_{\bar{N}_1=1}, \\ \tilde{G}_d(a_s(k^2)) &= -\frac{\partial}{\partial \ln \bar{N}_1} \Gamma_2 \left[\frac{\partial}{\partial \ln \bar{N}_1} \bar{G}_d(a_s(k^2)) - A(a_s(k^2)) \right] + \bar{G}_d(a_s(k^2)) \end{aligned} \quad (11.5)$$

with $k^2 = \frac{q^2}{\bar{N}_1}$.

11.2.2 I_B

$$\begin{aligned}
I_B &= (-\tilde{T}_{12})^2 \int_{q^2/\bar{N}_{12}}^{q^2} \frac{d\lambda^2}{\lambda^2} \ln \frac{\lambda^2 \bar{N}_{12}}{q^2} A(a_s(\lambda^2)) - \tilde{T}_1 \int_{q^2/\bar{N}_1}^{q^2} \frac{d\lambda^2}{\lambda^2} \ln \frac{\lambda^2 \bar{N}_1}{q^2} A(a_s(\lambda^2)) \\
&\quad - \tilde{T}_2 \int_{q^2/\bar{N}_2}^{q^2} \frac{d\lambda^2}{\lambda^2} \ln \frac{\lambda^2 \bar{N}_2}{q^2} A(a_s(\lambda^2)) \\
&= I_1 + I_2 + I_3
\end{aligned} \tag{11.6}$$

where $(-\tilde{T}_{12})^2 = (-\tilde{T}_1)(-\tilde{T}_2)$ and $\bar{N}_{12} = \bar{N}_1 \bar{N}_2$. The three integrals are as follows:

$$\begin{aligned}
I_1 &= (-\tilde{T}_{12})^2 \int_{q^2/\bar{N}_{12}}^{q^2} \frac{d\lambda^2}{\lambda^2} \ln \frac{\lambda^2 \bar{N}_{12}}{q^2} A(a_s(\lambda^2)) \\
&\equiv - \int_{q^2/\bar{N}_{12}}^{q^2} \frac{d\lambda^2}{\lambda^2} \left[\ln \frac{q^2}{\lambda^2 \bar{N}_{12}} A(a_s(\lambda^2)) + \tilde{B}(a_s(\lambda^2)) \right] - \ln \tilde{C}
\end{aligned} \tag{11.7}$$

where

$$\begin{aligned}
\ln \tilde{C} &= \left\{ \Gamma_2 \frac{\partial^2}{\partial (\ln \bar{N}_{12})^2} - 2 \right\} \Gamma_2 \left(-A(a_s(k^2)) \right) \Big|_{\bar{N}_{12}=1}, \\
\tilde{B}(a_s(k^2)) &= \frac{\partial}{\partial \ln \bar{N}_{12}} \left\{ \Gamma_2 \frac{\partial^2}{\partial (\ln \bar{N}_{12})^2} - 2 \right\} \Gamma_2 \left(-A(a_s(k^2)) \right).
\end{aligned} \tag{11.8}$$

where $k^2 = \frac{q^2}{\bar{N}_{12}}$.

$$\begin{aligned}
I_2 &= -\tilde{T}_1 \int_{q^2/\bar{N}_1}^{q^2} \frac{d\lambda^2}{\lambda^2} \ln \frac{\lambda^2 \bar{N}_1}{q^2} A(a_s(\lambda^2)) \\
&\equiv \int_{q^2/\bar{N}_1}^{q^2} \frac{d\lambda^2}{\lambda^2} \left\{ \ln \frac{q^2}{\lambda^2 \bar{N}_1} A(a_s(\lambda^2)) + \tilde{B}(a_s(\lambda^2)) \right\} + \ln \tilde{C}
\end{aligned} \tag{11.9}$$

where

$$\ln \tilde{C} = \Gamma_2 \left\{ A(a_s(k^2)) \right\} \Big|_{\bar{N}_1=1},$$

$$\tilde{B}(a_s(k^2)) = \frac{\partial}{\partial \ln \bar{N}_1} \Gamma_2 \left(A(a_s(k^2)) \right). \quad (11.10)$$

with $k^2 = \frac{q^2}{\bar{N}_1}$. The last integral I_3 can be obtained from I_2 with $\bar{N}_1 \leftrightarrow \bar{N}_2$.

11.2.3 I_C

We observe that the integrals I_B and I_C are similar to one another except for the derivative of \bar{G}_d present in I_C . To solve this we note that we can write $q^2 \frac{d}{dq^2} \bar{G}_d = \beta(a_s(k^2)) \frac{d}{da_s(k^2)} \bar{G}_d$, where β is the QCD beta function. Both β and \bar{G}_d can be expanded in power series of the strong coupling constant. There will be two values of k^2 depending on the type of integral I_1 or I_2/I_3 , similar to what it appears in I_B . Thus we have

$$\begin{aligned} k^2 &= \frac{q^2}{\bar{N}_{12}} & \text{for } I_1, \\ k^2 &= \frac{q^2}{\bar{N}_1} & \text{for } I_2, \\ k^2 &= \frac{q^2}{\bar{N}_2} & \text{for } I_3. \end{aligned} \quad (11.11)$$

We now have to solve the following : eq. 11.5 for I_A ; eq. 11.8 and eq. 11.10 for I_B and eq. 11.11 for I_C . We solve this by writing an in-house code in Mathematica. The solution of the integrals will give us eq. 8.49 in Mellin space and hence $\tilde{J}_d^{I,SV}(\omega)$.

11.3 Unrenormalized form factors

In this section we present the unrenormalized form factors that appears in eq. 6.24.

$$\hat{\mathcal{F}}^{G,g,(0)} = 1, \quad (11.12)$$

$$\begin{aligned} \hat{\mathcal{F}}^{G,g,(1)} = C_A \bigg\{ & \frac{1}{\epsilon^2} \left(-8 \right) + \frac{1}{\epsilon} \left(\frac{22}{3} \right) + \left(-\frac{203}{18} + \zeta_2 \right) + \epsilon \left(+\frac{2879}{216} - \frac{7}{3} \zeta_3 - \frac{11}{12} \zeta_2 \right) \\ & + \epsilon^2 \left(-\frac{37307}{2592} + \frac{77}{36} \zeta_3 + \frac{203}{144} \zeta_2 + \frac{47}{80} \zeta_2^2 \right) + \epsilon^3 \left(\frac{465143}{31104} - \frac{31}{20} \zeta_5 - \frac{1421}{432} \zeta_3 \right. \\ & - \frac{2879}{1728} \zeta_2 + \frac{7}{24} \zeta_2 \zeta_3 - \frac{517}{960} \zeta_2^2 \bigg) + \epsilon^4 \left(-\frac{5695811}{373248} + \frac{341}{240} \zeta_5 + \frac{20153}{5184} \zeta_3 - \frac{49}{144} \zeta_3^2 \right. \\ & \left. \left. + \frac{37307}{20736} \zeta_2 - \frac{77}{288} \zeta_2 \zeta_3 + \frac{9541}{11520} \zeta_2^2 + \frac{949}{4480} \zeta_2^3 \right) \right\}, \quad (11.13) \end{aligned}$$

$$\begin{aligned} \hat{\mathcal{F}}^{G,g,(2)} = C_F n_f \bigg\{ & \frac{1}{\epsilon^2} \left(\frac{32}{9} \right) + \frac{1}{\epsilon} \left(-\frac{260}{27} \right) + \left(\frac{3037}{162} - \frac{8}{3} \zeta_2 \right) + \epsilon \left(-\frac{61807}{1944} + \frac{62}{27} \zeta_3 \right. \\ & + \frac{65}{9} \zeta_2 \bigg) + \epsilon^2 \left(\frac{1158007}{23328} - \frac{461}{81} \zeta_3 - \frac{3185}{216} \zeta_2 - \frac{31}{45} \zeta_2^2 \right) + \epsilon^3 \left(-\frac{20551495}{279936} - \frac{28}{45} \zeta_5 \right. \\ & \left. + \frac{26131}{1944} \zeta_3 + \frac{22759}{864} \zeta_2 - \frac{17}{6} \zeta_2 \zeta_3 + \frac{1721}{1080} \zeta_2^2 \right) \bigg\} + C_A n_f \bigg\{ \frac{1}{\epsilon^3} \left(-\frac{8}{3} \right) + \frac{1}{\epsilon^2} \left(\frac{64}{9} \right) \\ & + \frac{1}{\epsilon} \left(-\frac{499}{27} + 2\zeta_2 \right) + \left(\frac{6863}{162} - \frac{38}{9} \zeta_3 - \frac{16}{3} \zeta_2 \right) + \epsilon \left(-\frac{84433}{972} + \frac{277}{27} \zeta_3 + \frac{481}{36} \zeta_2 \right. \\ & \left. + \frac{73}{60} \zeta_2^2 \right) + \epsilon^2 \left(\frac{1913059}{11664} - \frac{151}{30} \zeta_5 - \frac{2269}{81} \zeta_3 - \frac{1009}{36} \zeta_2 + \frac{5}{2} \zeta_2 \zeta_3 - \frac{131}{45} \zeta_2^2 \right) \\ & + \epsilon^3 \left(-\frac{40845067}{139968} + \frac{559}{45} \zeta_5 + \frac{251461}{3888} \zeta_3 - \frac{343}{108} \zeta_3^2 + \frac{68603}{1296} \zeta_2 - \frac{25}{4} \zeta_2 \zeta_3 + \frac{6911}{864} \zeta_2^2 \right. \\ & \left. + \frac{781}{1680} \zeta_2^3 \right) \bigg\} + C_A^2 \bigg\{ \frac{1}{\epsilon^4} \left(32 \right) + \frac{1}{\epsilon^3} \left(-44 \right) + \frac{1}{\epsilon^2} \left(\frac{226}{3} - 4\zeta_2 \right) + \frac{1}{\epsilon} \left(-81 \right. \\ & + \frac{50}{3} \zeta_3 + \frac{11}{3} \zeta_2 \bigg) + \left(\frac{5249}{108} - 11\zeta_3 - \frac{67}{18} \zeta_2 - \frac{21}{5} \zeta_2^2 \right) + \epsilon \left(\frac{59009}{1296} - \frac{71}{10} \zeta_5 + \frac{433}{18} \zeta_3 \right. \\ & - \frac{337}{108} \zeta_2 - \frac{23}{6} \zeta_2 \zeta_3 + \frac{99}{40} \zeta_2^2 \bigg) + \epsilon^2 \left(-\frac{1233397}{5184} + \frac{759}{20} \zeta_5 - \frac{8855}{216} \zeta_3 + \frac{901}{36} \zeta_3^2 \right. \\ & + \frac{12551}{648} \zeta_2 + \frac{77}{36} \zeta_2 \zeta_3 - \frac{4843}{720} \zeta_2^2 + \frac{2313}{280} \zeta_2^3 \bigg) + \epsilon^3 \left(\frac{108841321}{186624} - \frac{3169}{28} \zeta_7 - \frac{4691}{60} \zeta_5 \right. \\ & + \frac{22231}{216} \zeta_3 - \frac{2365}{72} \zeta_3^2 - \frac{813499}{15552} \zeta_2 + \frac{313}{40} \zeta_2 \zeta_5 - \frac{1609}{216} \zeta_2 \zeta_3 + \frac{21901}{1440} \zeta_2^2 - \frac{1291}{80} \zeta_2^2 \zeta_3 \\ & \left. \left. - \frac{65659}{3360} \zeta_2^3 \right) \right\}, \quad (11.14) \end{aligned}$$

$$\begin{aligned}
\hat{\mathcal{F}}^{G,g,(3)} = & C_F n_f^2 \left\{ \frac{1}{\epsilon^3} \left(\frac{256}{81} \right) + \frac{1}{\epsilon^2} \left(-\frac{128}{9} \right) + \frac{1}{\epsilon} \left(\frac{30916}{729} - \frac{160}{27} \zeta_2 \right) + \left(-\frac{78268}{729} + \frac{208}{81} \zeta_3 \right. \right. \\
& + \left. \frac{80}{3} \zeta_2 \right) \Big\} + C_F^2 n_f \left\{ \frac{1}{\epsilon^3} \left(\frac{512}{81} \right) + \frac{1}{\epsilon^2} \left(-\frac{1600}{81} \right) + \frac{1}{\epsilon} \left(\frac{20180}{729} + \frac{320}{9} \zeta_3 - \frac{320}{27} \zeta_2 \right) \right. \\
& + \left. \left(\frac{35957}{2430} - \frac{45056}{405} \zeta_3 + \frac{1144}{27} \zeta_2 - \frac{32}{3} \zeta_2^2 \right) \right\} + C_A n_f^2 \left\{ \frac{1}{\epsilon^4} \left(-\frac{128}{81} \right) + \frac{1}{\epsilon^3} \left(\frac{1696}{243} \right) \right. \\
& + \frac{1}{\epsilon^2} \left(-\frac{6328}{243} + \frac{80}{27} \zeta_2 \right) + \frac{1}{\epsilon} \left(\frac{189167}{2187} - \frac{464}{81} \zeta_3 - \frac{1060}{81} \zeta_2 \right) + \left(-\frac{6734887}{26244} \right. \\
& + \frac{5500}{243} \zeta_3 + \frac{3805}{81} \zeta_2 + \frac{293}{135} \zeta_2^2 \Big) \Big\} + C_A C_F n_f \left\{ \frac{1}{\epsilon^4} \left(-\frac{256}{9} \right) + \frac{1}{\epsilon^3} \left(\frac{2032}{27} \right) \right. \\
& + \frac{1}{\epsilon^2} \left(-\frac{10532}{81} - \frac{64}{9} \zeta_3 + \frac{224}{9} \zeta_2 \right) + \frac{1}{\epsilon} \left(\frac{39715}{243} - \frac{944}{27} \zeta_3 - \frac{1490}{27} \zeta_2 + \frac{32}{15} \zeta_2^2 \right) \\
& + \left(-\frac{1315651}{14580} - \frac{112}{9} \zeta_5 + \frac{29818}{405} \zeta_3 + \frac{11719}{162} \zeta_2 + \frac{40}{3} \zeta_2 \zeta_3 + \frac{50}{3} \zeta_2^2 \right) \Big\} \\
& + C_A^2 n_f \left\{ \frac{1}{\epsilon^5} \left(\frac{64}{3} \right) + \frac{1}{\epsilon^4} \left(-\frac{4784}{81} \right) + \frac{1}{\epsilon^3} \left(\frac{35764}{243} - \frac{376}{27} \zeta_2 \right) + \frac{1}{\epsilon^2} \left(-\frac{7435}{27} \right. \right. \\
& + \frac{1208}{27} \zeta_3 + \frac{2458}{81} \zeta_2 \Big) + \frac{1}{\epsilon} \left(\frac{2991329}{8748} - \frac{6634}{81} \zeta_3 - \frac{27059}{486} \zeta_2 - \frac{1493}{90} \zeta_2^2 \right) \\
& + \left. \left(\frac{4440127}{524880} - \frac{3002}{45} \zeta_5 + \frac{219163}{810} \zeta_3 + \frac{229919}{5832} \zeta_2 - \frac{331}{9} \zeta_2 \zeta_3 + \frac{11461}{360} \zeta_2^2 \right) \right\} \\
& + C_A^3 \left\{ \frac{1}{\epsilon^6} \left(-\frac{256}{3} \right) + \frac{1}{\epsilon^5} \left(\frac{352}{3} \right) + \frac{1}{\epsilon^4} \left(-\frac{14744}{81} \right) + \frac{1}{\epsilon^3} \left(\frac{13126}{243} - \frac{176}{3} \zeta_3 \right. \right. \\
& + \frac{484}{27} \zeta_2 \Big) + \frac{1}{\epsilon^2} \left(\frac{149939}{486} - \frac{440}{27} \zeta_3 - \frac{4321}{81} \zeta_2 + \frac{494}{45} \zeta_2^2 \right) + \frac{1}{\epsilon} \left(-\frac{14639165}{17496} \right. \\
& + \frac{1756}{15} \zeta_5 - \frac{634}{9} \zeta_3 + \frac{112633}{972} \zeta_2 + \frac{170}{9} \zeta_2 \zeta_3 + \frac{4213}{180} \zeta_2^2 \Big) + \left(\frac{1056263429}{1049760} + \frac{5014}{45} \zeta_5 \right. \\
& + \frac{539}{2430} \zeta_3 - \frac{1766}{9} \zeta_3^2 - \frac{1988293}{11664} \zeta_2 - \frac{92}{9} \zeta_2 \zeta_3 - \frac{64997}{2160} \zeta_2^2 - \frac{22523}{270} \zeta_2^3 \Big) \Big\}, \quad (11.15)
\end{aligned}$$

$$\hat{\mathcal{F}}^{Q,g,(0)} = 0, \quad (11.16)$$

$$\begin{aligned}
\hat{\mathcal{F}}^{Q,g,(1)} = & n_f \left\{ \frac{1}{\epsilon} \left(-\frac{4}{3} \right) + \left(\frac{35}{18} \right) + \epsilon \left(-\frac{497}{216} + \frac{1}{6} \zeta_2 \right) + \epsilon^2 \left(\frac{6593}{2592} - \frac{7}{18} \zeta_3 - \frac{35}{144} \zeta_2 \right) \right. \\
& + \epsilon^3 \left(-\frac{84797}{31104} + \frac{245}{432} \zeta_3 + \frac{497}{1728} \zeta_2 + \frac{47}{480} \zeta_2^2 \right) + \epsilon^4 \left(\frac{1072433}{373248} - \frac{31}{120} \zeta_5 - \frac{3479}{5184} \zeta_3 \right. \\
& - \frac{6593}{20736} \zeta_2 + \frac{7}{144} \zeta_2 \zeta_3 - \frac{329}{2304} \zeta_2^2 \Big) \Big\}, \quad (11.17)
\end{aligned}$$

$$\begin{aligned}
\hat{\mathcal{F}}^{Q,g,(2)} = & C_F n_f \left\{ \frac{1}{\epsilon^2} \left(-\frac{32}{9} \right) + \frac{1}{\epsilon} \left(\frac{206}{27} \right) + \left(-\frac{695}{81} - 8\zeta_3 + \frac{8}{3} \zeta_2 \right) + \epsilon \left(\frac{149}{243} + \frac{469}{27} \zeta_3 \right. \right. \\
& - \frac{121}{18} \zeta_2 + \frac{12}{5} \zeta_2^2 \Big) + \epsilon^2 \left(\frac{143693}{5832} - 14\zeta_5 - \frac{2554}{81} \zeta_3 + \frac{1219}{108} \zeta_2 + 2\zeta_2 \zeta_3 - \frac{95}{18} \zeta_2^2 \right)
\end{aligned}$$

$$\begin{aligned}
& + \epsilon^3 \left(-\frac{1386569}{17496} + \frac{6037}{180} \zeta_5 + \frac{104639}{1944} \zeta_3 - \frac{23}{3} \zeta_3^2 - \frac{6581}{432} \zeta_2 - \frac{29}{12} \zeta_2 \zeta_3 + \frac{20633}{2160} \zeta_2^2 \right. \\
& \left. + \frac{99}{35} \zeta_3^3 \right) \Big\} + C_A n_f \left\{ \frac{1}{\epsilon^3} \left(\frac{32}{3} \right) + \frac{1}{\epsilon^2} \left(-\frac{184}{9} \right) + \frac{1}{\epsilon} \left(\frac{868}{27} - \frac{8}{3} \zeta_2 \right) + \left(-\frac{15541}{324} \right. \right. \\
& \left. \left. + \frac{128}{9} \zeta_3 + \frac{53}{9} \zeta_2 \right) + \epsilon \left(\frac{273061}{3888} - \frac{823}{27} \zeta_3 - \frac{649}{54} \zeta_2 - \frac{61}{15} \zeta_2^2 \right) + \epsilon^2 \left(-\frac{4764919}{46656} \right. \right. \\
& \left. \left. + \frac{182}{15} \zeta_5 + \frac{37373}{648} \zeta_3 + \frac{14545}{648} \zeta_2 - \frac{44}{9} \zeta_2 \zeta_3 + \frac{541}{60} \zeta_2^2 \right) + \epsilon^3 \left(\frac{83029021}{559872} - \frac{8507}{360} \zeta_5 \right. \right. \\
& \left. \left. - \frac{219191}{1944} \zeta_3 + \frac{454}{27} \zeta_3^2 - \frac{604667}{15552} \zeta_2 + \frac{1307}{108} \zeta_2 \zeta_3 - \frac{4783}{270} \zeta_2^2 + \frac{109}{420} \zeta_2^3 \right) \right\}, \quad (11.18)
\end{aligned}$$

$$\begin{aligned}
\hat{\mathcal{F}}^{Q,g,(3)} = & C_F n_f^2 \left\{ \frac{1}{\epsilon^3} \left(-\frac{256}{81} \right) + \frac{1}{\epsilon^2} \left(\frac{112}{9} \right) + \frac{1}{\epsilon} \left(-\frac{20440}{729} - \frac{32}{3} \zeta_3 + \frac{160}{27} \zeta_2 \right) + \left(\frac{27661}{729} \right. \right. \\
& \left. \left. + \frac{3500}{81} \zeta_3 - 26 \zeta_2 + \frac{16}{5} \zeta_2^2 \right) \right\} + C_F^2 n_f \left\{ \frac{1}{\epsilon^3} \left(-\frac{512}{81} \right) + \frac{1}{\epsilon^2} \left(\frac{1600}{81} \right) + \frac{1}{\epsilon} \left(-\frac{19694}{729} \right. \right. \\
& \left. \left. - \frac{320}{9} \zeta_3 + \frac{320}{27} \zeta_2 \right) + \left(-\frac{34246}{1215} + 80 \zeta_5 + \frac{25076}{405} \zeta_3 - \frac{1144}{27} \zeta_2 + \frac{32}{3} \zeta_2^2 \right) \right\} \\
& + C_A n_f^2 \left\{ \frac{1}{\epsilon^4} \left(\frac{32}{9} \right) + \frac{1}{\epsilon^3} \left(-\frac{1012}{81} \right) + \frac{1}{\epsilon^2} \left(\frac{8029}{243} - \frac{28}{9} \zeta_2 \right) + \frac{1}{\epsilon} \left(-\frac{237197}{2916} + \frac{52}{3} \zeta_3 \right. \right. \\
& \left. \left. + \frac{235}{18} \zeta_2 \right) + \left(\frac{34159189}{174960} - \frac{59047}{810} \zeta_3 - \frac{28457}{648} \zeta_2 - \frac{983}{180} \zeta_2^2 \right) \right\} + C_A C_F n_f \left\{ \frac{1}{\epsilon^4} \left(\frac{256}{9} \right) \right. \\
& \left. + \frac{1}{\epsilon^3} \left(-\frac{1648}{27} \right) + \frac{1}{\epsilon^2} \left(\frac{5396}{81} + 64 \zeta_3 - \frac{224}{9} \zeta_2 \right) + \frac{1}{\epsilon} \left(-\frac{4519}{243} - \frac{472}{9} \zeta_3 + \frac{1418}{27} \zeta_2 \right. \right. \\
& \left. \left. - \frac{96}{5} \zeta_2^2 \right) + \left(-\frac{516221}{14580} + 152 \zeta_5 - \frac{4508}{45} \zeta_3 - \frac{9883}{162} \zeta_2 - \frac{40}{3} \zeta_2 \zeta_3 + \frac{146}{15} \zeta_2^2 \right) \right\} \\
& + C_A^2 n_f \left\{ \frac{1}{\epsilon^5} \left(-\frac{128}{3} \right) + \frac{1}{\epsilon^4} \left(\frac{736}{9} \right) + \frac{1}{\epsilon^3} \left(-\frac{9982}{81} + \frac{32}{3} \zeta_2 \right) + \frac{1}{\epsilon^2} \left(\frac{77047}{486} - \frac{296}{3} \zeta_3 \right. \right. \\
& \left. \left. - \frac{58}{3} \zeta_2 \right) + \frac{1}{\epsilon} \left(-\frac{96755}{648} + \frac{1385}{9} \zeta_3 + \frac{115}{4} \zeta_2 + \frac{147}{5} \zeta_2^2 \right) + \left(-\frac{1027661}{349920} - \frac{2842}{15} \zeta_5 \right. \right. \\
& \left. \left. - \frac{36668}{405} \zeta_3 + \frac{1109}{432} \zeta_2 + 37 \zeta_2 \zeta_3 - \frac{4019}{90} \zeta_2^2 \right) \right\}, \quad (11.19)
\end{aligned}$$

$$\hat{\mathcal{F}}^{G,q,(0)} = 0, \quad (11.20)$$

$$\begin{aligned}
\hat{\mathcal{F}}^{G,q,(1)} = & C_F \left\{ \frac{1}{\epsilon} \left(-\frac{16}{3} \right) + \left(\frac{34}{9} \right) + \epsilon \left(-\frac{79}{27} + \frac{2}{3} \zeta_2 \right) + \epsilon^2 \left(\frac{401}{162} - \frac{14}{9} \zeta_3 - \frac{17}{36} \zeta_2 \right) \right. \\
& \left. + \epsilon^3 \left(-\frac{2179}{972} + \frac{119}{108} \zeta_3 + \frac{79}{216} \zeta_2 + \frac{47}{120} \zeta_2^2 \right) + \epsilon^4 \left(\frac{12377}{5832} - \frac{31}{30} \zeta_5 - \frac{553}{648} \zeta_3 - \frac{401}{1296} \zeta_2 \right. \right. \\
& \left. \left. + \frac{7}{36} \zeta_2 \zeta_3 - \frac{799}{2880} \zeta_2^2 \right) \right\}, \quad (11.21)
\end{aligned}$$

$$\hat{\mathcal{F}}^{G,q,(2)} = C_F n_f \left\{ \frac{1}{\epsilon^2} \left(-\frac{64}{9} \right) + \frac{1}{\epsilon} \left(\frac{376}{27} \right) + \left(-\frac{1798}{81} + \frac{16}{9} \zeta_2 \right) + \epsilon \left(\frac{16259}{486} - \frac{256}{27} \zeta_3 \right. \right.$$

$$\begin{aligned}
& -\frac{94}{27}\zeta_2) + \epsilon^2\left(-\frac{289163}{5832} + \frac{1504}{81}\zeta_3 + \frac{899}{162}\zeta_2 + \frac{38}{15}\zeta_2^2\right) + \epsilon^3\left(\frac{5125571}{69984} - \frac{544}{45}\zeta_5\right. \\
& \left. - \frac{7192}{243}\zeta_3 - \frac{16259}{1944}\zeta_2 + \frac{64}{27}\zeta_2\zeta_3 - \frac{893}{180}\zeta_2^2\right) + C_F^2\left\{\frac{1}{\epsilon^3}\left(\frac{128}{3}\right) + \frac{1}{\epsilon^2}\left(-\frac{688}{9}\right)\right. \\
& \left. + \frac{1}{\epsilon}\left(\frac{3340}{27} - \frac{32}{3}\zeta_2\right) + \left(-\frac{14257}{81} + \frac{224}{9}\zeta_3 + \frac{236}{9}\zeta_2\right) + \epsilon\left(\frac{229261}{972} - \frac{1012}{27}\zeta_3\right.\right. \\
& \left. - \frac{1211}{27}\zeta_2 - \frac{28}{5}\zeta_2^2\right) + \epsilon^2\left(-\frac{3597469}{11664} + \frac{248}{15}\zeta_5 + \frac{5437}{81}\zeta_3 + \frac{21233}{324}\zeta_2 - \frac{56}{9}\zeta_2\zeta_3\right. \\
& \left. + \frac{743}{90}\zeta_2^2\right) + \epsilon^3\left(\frac{56232181}{139968} - \frac{613}{45}\zeta_5 - \frac{51995}{486}\zeta_3 + \frac{196}{27}\zeta_3^2 - \frac{350153}{3888}\zeta_2 + \frac{461}{27}\zeta_2\zeta_3\right. \\
& \left. - \frac{3331}{216}\zeta_2^2 - \frac{31}{21}\zeta_2^3\right) + C_A C_F\left\{\frac{1}{\epsilon^2}\left(\frac{176}{9}\right) + \frac{1}{\epsilon}\left(-\frac{1124}{27}\right) + \left(\frac{5651}{81} - \frac{16}{9}\zeta_2\right)\right. \\
& \left. + \epsilon\left(-\frac{108275}{972} + \frac{356}{27}\zeta_3 - \frac{86}{27}\zeta_2 - \frac{16}{15}\zeta_2^2\right) + \epsilon^2\left(\frac{2055287}{11664} - 24\zeta_5 - \frac{961}{162}\zeta_3 + \frac{986}{81}\zeta_2\right.\right. \\
& \left. - \frac{16}{3}\zeta_2\zeta_3 - \frac{5}{6}\zeta_2^2\right) + \epsilon^3\left(-\frac{38875571}{139968} + \frac{5377}{90}\zeta_5 - \frac{110159}{1944}\zeta_3 + \frac{88}{3}\zeta_3^2 - \frac{47947}{1944}\zeta_2\right. \\
& \left. + \frac{287}{27}\zeta_2\zeta_3 - \frac{5323}{1080}\zeta_2^2 + \frac{484}{35}\zeta_2^3\right)\}, \tag{11.22}
\end{aligned}$$

$$\begin{aligned}
\hat{\mathcal{F}}^{G,q,(3)} = & C_F n_f^2 \left\{ \frac{1}{\epsilon^3} \left(-\frac{256}{27} \right) + \frac{1}{\epsilon^2} \left(\frac{2464}{81} \right) + \frac{1}{\epsilon} \left(-\frac{17216}{243} + \frac{32}{9}\zeta_2 \right) + \left(\frac{107816}{729} - \frac{800}{27}\zeta_3 \right. \right. \\
& \left. \left. - \frac{308}{27}\zeta_2 \right) \right\} + C_F^2 n_f \left\{ \frac{1}{\epsilon^4} \left(\frac{640}{9} \right) + \frac{1}{\epsilon^3} \left(-\frac{18544}{81} \right) + \frac{1}{\epsilon^2} \left(\frac{130696}{243} - \frac{176}{9}\zeta_2 \right) \right. \\
& \left. + \frac{1}{\epsilon} \left(-\frac{776510}{729} + \frac{752}{9}\zeta_3 + \frac{706}{9}\zeta_2 \right) + \left(\frac{8387353}{4374} - \frac{18250}{81}\zeta_3 - \frac{15461}{81}\zeta_2 - \frac{289}{15}\zeta_2^2 \right) \right\} \\
& + C_F^3 \left\{ \frac{1}{\epsilon^5} \left(-\frac{512}{3} \right) + \frac{1}{\epsilon^4} \left(\frac{1472}{3} \right) + \frac{1}{\epsilon^3} \left(-\frac{89312}{81} + 64\zeta_2 \right) + \frac{1}{\epsilon^2} \left(\frac{55964}{27} - \frac{832}{3}\zeta_3 \right. \right. \\
& \left. \left. - \frac{1592}{9}\zeta_2 \right) + \frac{1}{\epsilon} \left(-\frac{2565953}{729} + \frac{2296}{3}\zeta_3 + \frac{8644}{27}\zeta_2 + \frac{1148}{15}\zeta_2^2 \right) + \left(\frac{16239107}{2916} \right. \right. \\
& \left. \left. - \frac{656}{5}\zeta_5 - \frac{162008}{81}\zeta_3 - \frac{65755}{162}\zeta_2 + \frac{440}{3}\zeta_2\zeta_3 - \frac{2451}{10}\zeta_2^2 \right) \right\} + C_A C_F n_f \left\{ \frac{1}{\epsilon^3} \left(\frac{4928}{81} \right) \right. \\
& \left. + \frac{1}{\epsilon^2} \left(-\frac{51592}{243} \right) + \frac{1}{\epsilon} \left(\frac{127238}{243} + \frac{256}{9}\zeta_3 - \frac{280}{27}\zeta_2 \right) + \left(-\frac{2526404}{2187} + \frac{5960}{81}\zeta_3 \right. \right. \\
& \left. \left. - \frac{13}{27}\zeta_2 - \frac{128}{9}\zeta_2^2 \right) \right\} + C_A C_F^2 \left\{ \frac{1}{\epsilon^4} \left(-\frac{704}{3} \right) + \frac{1}{\epsilon^3} \left(\frac{21784}{27} - \frac{64}{3}\zeta_2 \right) \right. \\
& \left. + \frac{1}{\epsilon^2} \left(-\frac{487996}{243} + \frac{416}{3}\zeta_3 + \frac{352}{9}\zeta_2 \right) + \frac{1}{\epsilon} \left(\frac{3102511}{729} - \frac{6092}{9}\zeta_3 - \frac{1321}{27}\zeta_2 - \frac{536}{15}\zeta_2^2 \right) \right. \\
& \left. + \left(-\frac{71606351}{8748} + \frac{1624}{3}\zeta_5 + \frac{13865}{9}\zeta_3 - \frac{7513}{162}\zeta_2 - \frac{52}{3}\zeta_2\zeta_3 + \frac{14549}{90}\zeta_2^2 \right) \right\}
\end{aligned}$$

$$\begin{aligned}
& + C_A^2 C_F \left\{ \frac{1}{\epsilon^3} \left(-\frac{7744}{81} \right) + \frac{1}{\epsilon^2} \left(\frac{87352}{243} \right) + \frac{1}{\epsilon} \left(-\frac{704276}{729} - \frac{128}{9} \zeta_3 - \frac{88}{9} \zeta_2 \right) \right. \\
& \left. + \left(\frac{5045099}{2187} - 240 \zeta_5 + \frac{6098}{81} \zeta_3 + 209 \zeta_2 - \frac{104}{3} \zeta_2 \zeta_3 + \frac{622}{15} \zeta_2^2 \right) \right\}, \quad (11.23)
\end{aligned}$$

$$\hat{\mathcal{F}}^{Q,q,(0)} = 1, \quad (11.24)$$

$$\begin{aligned}
\hat{\mathcal{F}}^{Q,q,(1)} = C_F & \left\{ \frac{1}{\epsilon^2} \left(-8 \right) + \frac{1}{\epsilon} \left(\frac{34}{3} \right) + \left(-\frac{124}{9} + \zeta_2 \right) + \epsilon \left(\frac{403}{27} - \frac{7}{3} \zeta_3 - \frac{17}{12} \zeta_2 \right) \right. \\
& + \epsilon^2 \left(-\frac{2507}{162} + \frac{119}{36} \zeta_3 + \frac{31}{18} \zeta_2 + \frac{47}{80} \zeta_2^2 \right) + \epsilon^3 \left(\frac{15301}{972} - \frac{31}{20} \zeta_5 - \frac{217}{54} \zeta_3 - \frac{403}{216} \zeta_2 \right. \\
& + \frac{7}{24} \zeta_2 \zeta_3 - \frac{799}{960} \zeta_2^2 \left. \right) + \epsilon^4 \left(-\frac{92567}{5832} + \frac{527}{240} \zeta_5 + \frac{2821}{648} \zeta_3 - \frac{49}{144} \zeta_3^2 + \frac{2507}{1296} \zeta_2 \right. \\
& \left. \left. - \frac{119}{288} \zeta_2 \zeta_3 + \frac{1457}{1440} \zeta_2^2 + \frac{949}{4480} \zeta_2^3 \right) \right\}, \quad (11.25)
\end{aligned}$$

$$\begin{aligned}
\hat{\mathcal{F}}^{Q,q,(2)} = C_F n_f & \left\{ \frac{1}{\epsilon^3} \left(-\frac{8}{3} \right) + \frac{1}{\epsilon^2} \left(\frac{40}{3} \right) + \frac{1}{\epsilon} \left(-\frac{89}{3} - \frac{2}{3} \zeta_2 \right) + \left(\frac{1909}{36} - \frac{26}{9} \zeta_3 + \frac{22}{9} \zeta_2 \right) \right. \\
& + \epsilon \left(-\frac{36925}{432} + \frac{86}{9} \zeta_3 - \frac{613}{108} \zeta_2 + \frac{41}{60} \zeta_2^2 \right) + \epsilon^2 \left(\frac{677941}{5184} - \frac{121}{30} \zeta_5 - \frac{2317}{108} \zeta_3 \right. \\
& + \frac{15745}{1296} \zeta_2 - \frac{13}{18} \zeta_2 \zeta_3 - \frac{359}{180} \zeta_2^2 \left. \right) + \epsilon^3 \left(-\frac{12131053}{62208} + \frac{67}{6} \zeta_5 + \frac{52237}{1296} \zeta_3 - \frac{169}{108} \zeta_3^2 \right. \\
& \left. - \frac{364273}{15552} \zeta_2 + \frac{209}{54} \zeta_2 \zeta_3 + \frac{19369}{4320} \zeta_2^2 + \frac{127}{112} \zeta_2^3 \right) \left. \right\} + C_F^2 \left\{ \frac{1}{\epsilon^4} \left(32 \right) + \frac{1}{\epsilon^3} \left(-\frac{272}{3} \right) \right. \\
& + \frac{1}{\epsilon^2} \left(\frac{1570}{9} - 8 \zeta_2 \right) + \frac{1}{\epsilon} \left(-\frac{15023}{54} + \frac{128}{3} \zeta_3 + \frac{32}{3} \zeta_2 \right) + \left(\frac{257615}{648} - \frac{1034}{9} \zeta_3 \right. \\
& \left. - \frac{103}{18} \zeta_2 - 13 \zeta_2^2 \right) + \epsilon \left(-\frac{4112375}{7776} + \frac{92}{5} \zeta_5 + \frac{13967}{54} \zeta_3 - \frac{3767}{216} \zeta_2 - \frac{56}{3} \zeta_2 \zeta_3 \right. \\
& + \frac{1033}{30} \zeta_2^2 \left. \right) + \epsilon^2 \left(\frac{62375663}{93312} - \frac{1429}{30} \zeta_5 - \frac{356111}{648} \zeta_3 + \frac{652}{9} \zeta_3^2 + \frac{177023}{2592} \zeta_2 + \frac{691}{18} \zeta_2 \zeta_3 \right. \\
& \left. - \frac{56369}{720} \zeta_2^2 + \frac{223}{20} \zeta_2^3 \right) + \epsilon^3 \left(-\frac{911224295}{1119744} - \frac{4471}{28} \zeta_7 + \frac{9439}{72} \zeta_5 + \frac{8942747}{7776} \zeta_3 \right. \\
& - \frac{21385}{108} \zeta_3^2 - \frac{5072471}{31104} \zeta_2 - \frac{23}{5} \zeta_2 \zeta_5 - \frac{16141}{216} \zeta_2 \zeta_3 + \frac{488237}{2880} \zeta_2^2 - \frac{686}{15} \zeta_2^2 \zeta_3 \\
& \left. - \frac{3001}{105} \zeta_2^3 \right) \left. \right\} + C_A C_F \left\{ \frac{1}{\epsilon^3} \left(\frac{44}{3} \right) + \frac{1}{\epsilon^2} \left(-\frac{508}{9} + 4 \zeta_2 \right) + \frac{1}{\epsilon} \left(\frac{7169}{54} - 26 \zeta_3 + \frac{11}{3} \zeta_2 \right) \right. \\
& + \left(-\frac{165413}{648} + \frac{755}{9} \zeta_3 - \frac{235}{9} \zeta_2 + \frac{44}{5} \zeta_2^2 \right) + \epsilon \left(\frac{3429125}{7776} - \frac{51}{2} \zeta_5 - \frac{5629}{27} \zeta_3 \right. \\
& + \frac{15449}{216} \zeta_2 + \frac{89}{6} \zeta_2 \zeta_3 - \frac{1057}{40} \zeta_2^2 \left. \right) + \epsilon^2 \left(-\frac{66913709}{93312} + \frac{5411}{60} \zeta_5 + \frac{286661}{648} \zeta_3 \right. \\
& \left. - \frac{569}{12} \zeta_3^2 - \frac{383285}{2592} \zeta_2 - \frac{877}{36} \zeta_2 \zeta_3 + \frac{2527}{40} \zeta_2^2 - \frac{809}{280} \zeta_2^3 \right) + \epsilon^3 \left(\frac{1260896789}{1119744} + \frac{93}{2} \zeta_7 \right.
\end{aligned}$$

$$\begin{aligned}
& -\frac{42157}{180}\zeta_5 - \frac{6822089}{7776}\zeta_3 + \frac{29399}{216}\zeta_3^2 + \frac{8369333}{31104}\zeta_2 + \frac{497}{40}\zeta_2\zeta_5 + \frac{3683}{108}\zeta_2\zeta_3 \\
& - \frac{1142729}{8640}\zeta_2^2 + \frac{7103}{240}\zeta_2^2\zeta_3 - \frac{143}{160}\zeta_2^3 \Bigg\}, \tag{11.26}
\end{aligned}$$

$$\begin{aligned}
\hat{\mathcal{F}}^{Q,q,(3)} = & C_F n_f^2 \left\{ \frac{1}{\epsilon^4} \left(-\frac{128}{81} \right) + \frac{1}{\epsilon^3} \left(\frac{3808}{243} \right) + \frac{1}{\epsilon^2} \left(-\frac{4240}{81} - \frac{16}{9}\zeta_2 \right) \right. \\
& + \frac{1}{\epsilon} \left(\frac{283256}{2187} - \frac{272}{81}\zeta_3 + \frac{284}{27}\zeta_2 \right) + \left(-\frac{1827880}{6561} + \frac{4348}{243}\zeta_3 - \frac{314}{9}\zeta_2 - \frac{83}{135}\zeta_2^2 \right) \Bigg\} \\
& + C_F^2 n_f \left\{ \frac{1}{\epsilon^5} \left(\frac{64}{3} \right) + \frac{1}{\epsilon^4} \left(-\frac{1232}{9} \right) + \frac{1}{\epsilon^3} \left(\frac{33784}{81} + \frac{8}{3}\zeta_2 \right) + \frac{1}{\epsilon^2} \left(-\frac{232876}{243} \right. \right. \\
& + \frac{584}{9}\zeta_3 - \frac{94}{3}\zeta_2 \Bigg) + \frac{1}{\epsilon} \left(\frac{1359371}{729} - \frac{8234}{27}\zeta_3 + \frac{3533}{27}\zeta_2 - \frac{337}{18}\zeta_2^2 \right) + \left(-\frac{28437107}{8748} \right. \\
& + \frac{278}{45}\zeta_5 + \frac{3287}{3}\zeta_3 - \frac{849}{2}\zeta_2 - \frac{343}{9}\zeta_2\zeta_3 + \frac{69809}{1080}\zeta_2^2 \Bigg) \Bigg\} + C_F^3 \left\{ \frac{1}{\epsilon^6} \left(-\frac{256}{3} \right) \right. \\
& + \frac{1}{\epsilon^5} \left(\frac{1088}{3} \right) + \frac{1}{\epsilon^4} \left(-\frac{2864}{3} + 32\zeta_2 \right) + \frac{1}{\epsilon^3} \left(\frac{161240}{81} - \frac{800}{3}\zeta_3 - 40\zeta_2 \right) \\
& + \frac{1}{\epsilon^2} \left(-\frac{97202}{27} + \frac{3256}{3}\zeta_3 - \frac{730}{9}\zeta_2 + \frac{426}{5}\zeta_2^2 \right) + \frac{1}{\epsilon} \left(\frac{8625031}{1458} - \frac{1288}{5}\zeta_5 \right. \\
& - 3050\zeta_3 + \frac{15017}{27}\zeta_2 + \frac{428}{3}\zeta_2\zeta_3 - \frac{633}{2}\zeta_2^2 \Bigg) + \left(-\frac{53150197}{5832} + \frac{14042}{15}\zeta_5 + \frac{590021}{81}\zeta_3 \right. \\
& - \frac{1826}{3}\zeta_3^2 - \frac{576475}{324}\zeta_2 - 267\zeta_2\zeta_3 + \frac{289927}{360}\zeta_2^2 - \frac{9095}{252}\zeta_2^3 \Bigg) \Bigg\} + C_A C_F n_f \left\{ \frac{1}{\epsilon^4} \left(\frac{1408}{81} \right) \right. \\
& + \frac{1}{\epsilon^3} \left(-\frac{32816}{243} + \frac{128}{27}\zeta_2 \right) + \frac{1}{\epsilon^2} \left(\frac{12868}{27} - \frac{1024}{27}\zeta_3 + \frac{1264}{81}\zeta_2 \right) + \frac{1}{\epsilon} \left(-\frac{2758264}{2187} \right. \\
& + \frac{17480}{81}\zeta_3 - \frac{38542}{243}\zeta_2 + \frac{88}{5}\zeta_2^2 \Bigg) + \left(\frac{18919184}{6561} - \frac{128}{3}\zeta_5 - \frac{70690}{81}\zeta_3 + \frac{916919}{1458}\zeta_2 \right. \\
& + \frac{392}{9}\zeta_2\zeta_3 - \frac{1777}{27}\zeta_2^2 \Bigg) \Bigg\} + C_A C_F^2 \left\{ \frac{1}{\epsilon^5} \left(-\frac{352}{3} \right) + \frac{1}{\epsilon^4} \left(\frac{5560}{9} - 32\zeta_2 \right) \right. \\
& + \frac{1}{\epsilon^3} \left(-\frac{51404}{27} + 208\zeta_3 + \frac{92}{3}\zeta_2 \right) + \frac{1}{\epsilon^2} \left(\frac{1110322}{243} - \frac{3704}{3}\zeta_3 + \frac{2119}{9}\zeta_2 - \frac{332}{5}\zeta_2^2 \right) \\
& + \frac{1}{\epsilon} \left(-\frac{13792217}{1458} + 284\zeta_5 + \frac{37901}{9}\zeta_3 - \frac{68459}{54}\zeta_2 - \frac{430}{3}\zeta_2\zeta_3 + \frac{72523}{180}\zeta_2^2 \right) \\
& + \left(\frac{311359573}{17496} - \frac{42634}{45}\zeta_5 - \frac{23739}{2}\zeta_3 + \frac{1616}{3}\zeta_3^2 + \frac{1339027}{324}\zeta_2 + \frac{2026}{9}\zeta_2\zeta_3 \right. \\
& - \frac{2603779}{2160}\zeta_2^2 - \frac{18619}{1260}\zeta_2^3 \Bigg) \Bigg\} + C_A^2 C_F \left\{ \frac{1}{\epsilon^4} \left(-\frac{3872}{81} \right) + \frac{1}{\epsilon^3} \left(\frac{75400}{243} - \frac{704}{27}\zeta_2 \right) \right. \\
& + \frac{1}{\epsilon^2} \left(-\frac{10172}{9} + \frac{6688}{27}\zeta_3 - \frac{2212}{81}\zeta_2 - \frac{352}{45}\zeta_2^2 \right) + \frac{1}{\epsilon} \left(\frac{6969164}{2187} + \frac{272}{3}\zeta_5 - \frac{36500}{27}\zeta_3 \right. \\
& + \frac{123145}{243}\zeta_2 + \frac{176}{9}\zeta_2\zeta_3 - \frac{1604}{15}\zeta_2^2 \Bigg) + \left(-\frac{102217595}{13122} - \frac{428}{9}\zeta_5 + \frac{2427625}{486}\zeta_3 \right.
\end{aligned}$$

$$\left. - \frac{1136}{9} \zeta_3^2 - \frac{1632292}{729} \zeta_2 - \frac{614}{9} \zeta_2 \zeta_3 + \frac{247963}{540} \zeta_2^2 - \frac{6152}{189} \zeta_2^3 \right) \Bigg\}. \quad (11.27)$$

where $C_A = N$ and $C_F = (N^2 - 1)/2N$ are the quadratic Casimir of the $SU(N)$ group. $T_F = 1/2$ and n_f is the number of light active quark flavours. ζ_i is the Riemann Zeta function.

11.4 Results of the partonic cross sections: universal coupling

In this appendix, we present the renormalized and finite partonic coefficient functions involving spin-2 particles, $\Delta_{ab}^{h,(k)}(z, Q^2, \mu_F^2)$ in eq. 4.40, up to NNLO QCD ($k = 0, 1, 2$). We use these results in section 5.3 to investigate the phenomenological impact of higher order QCD corrections. The results at NLO are in agreement with the existing ones [68]. The soft-virtual corrections i.e. the contributions arising from the soft gluon emissions at NNLO were computed in [101]. Our results are also consistent with these ones. Below we present all of our findings after normalising the components of the coefficient functions by the leading order results:

$$\begin{aligned}\Delta_{gg}^{h,(k)} &\equiv \frac{\pi}{2(N^2 - 1)} \bar{\Delta}_{gg}^{h,(k)}, \\ \Delta_{ab}^{h,(k)} &\equiv \frac{\pi}{8N} \bar{\Delta}_{ab}^{h,(k)} \quad \text{for } ab \neq gg\end{aligned}\tag{11.28}$$

and all the $\left(\frac{\log^i(1-z)}{1-z}\right)$ terms should be understood as distributions, \mathcal{D}_i with

$$\mathcal{D}_i \equiv \left[\frac{\log^i(1-z)}{1-z} \right]_+, \quad i = 0, 1, 2, \dots \tag{11.29}$$

The results are obtained as

$$\begin{aligned}\bar{\Delta}_{gg}^{h,(0)} &= \delta(1-z), \\ \bar{\Delta}_{gg}^{h,(1)} &= \mathbf{n}_f \left\{ \delta(1-z) \left(\frac{35}{9} \right) + \log\left(\frac{Q^2}{\mu_F^2}\right) \delta(1-z) \left(-\frac{4}{3} \right) \right\} \\ &\quad + \mathbf{C}_A \left\{ \left(-2 - \frac{22}{3} \frac{1}{z} + 2z + \frac{22}{3} z^2 \right) \right. \\ &\quad \left. + \log(1-z) \left(-32 + 16 \frac{1}{z} + 16 \frac{1}{1-z} + 16z - 16z^2 \right) \right\}\end{aligned}$$

$$\begin{aligned}
& + \log(z) \left(16 - 8 \frac{1}{z} - 8 \frac{1}{1-z} - 8z + 8z^2 \right) + \delta(1-z) \left(-\frac{203}{9} \right) \\
& + \log \left(\frac{Q^2}{\mu_F^2} \right) \left[\left(-16 + 8 \frac{1}{z} + 8 \frac{1}{1-z} + 8z - 8z^2 \right) + \delta(1-z) \left(\frac{22}{3} \right) \right] \\
& + \zeta_2 \delta(1-z) \left(8 \right) \Bigg\}, \\
\bar{\Delta}_{gg}^{h,(2)} = & \mathbf{n}_f^2 \left\{ \delta(1-z) \left(\frac{1225}{324} \right) + \log \left(\frac{Q^2}{\mu_F^2} \right) \delta(1-z) \left(-\frac{70}{27} \right) \right. \\
& + \log^2 \left(\frac{Q^2}{\mu_F^2} \right) \delta(1-z) \left(\frac{4}{9} \right) + \zeta_2 \delta(1-z) \left(\frac{8}{3} \right) \Bigg\} \\
& + \mathbf{C}_F \mathbf{n}_f \left\{ \left(-\frac{664}{9} + \frac{1748}{27} \frac{1}{z} - \frac{389}{9} z + \frac{1411}{27} z^2 \right) \right. \\
& + S_{1,2}(1-z) \left(60 - 16 \frac{1}{z} - 24z - 28z^2 \right) + S_{1,2}(-z) \left(-72 - 32 \frac{1}{z} - 48z - 8z^2 \right) \\
& + \text{Li}_3(1-z) \left(-72 + 8 \frac{1}{z} - 16z + 32z^2 \right) + \text{Li}_3(-z) \left(-36 - 80 \frac{1}{z} - 56z + 4z^2 \right) \\
& + \text{Li}_2(1-z) \left(-2 + \frac{8}{3} \frac{1}{z} - 16z + \frac{116}{3} z^2 \right) + \text{Li}_2(-z) \left(20 - 16 \frac{1}{z} + 36z \right) \\
& + \log(1+z) \text{Li}_2(-z) \left(-72 - 32 \frac{1}{z} - 48z - 8z^2 \right) \\
& + \log(1-z) \left(-\frac{235}{3} - \frac{256}{9} \frac{1}{z} + \frac{436}{3} z - \frac{347}{9} z^2 \right) \\
& + \log(1-z) \text{Li}_2(1-z) \left(56 + 32z - 32z^2 \right) + \log^2(1-z) \left(8 + \frac{64}{3} \frac{1}{z} - 32z + \frac{8}{3} z^2 \right) \\
& + \log(z) \left(\frac{25}{2} + \frac{200}{9} \frac{1}{z} - 144z + \frac{433}{18} z^2 \right) \\
& + \log(z) \text{Li}_2(1-z) \left(-2 - 8 \frac{1}{z} - 40z - 8z^2 \right) \\
& + \log(z) \text{Li}_2(-z) \left(72 + 64 \frac{1}{z} + 64z + 4z^2 \right) + \log(z) \log(1+z) \left(20 - 16 \frac{1}{z} + 36z \right) \\
& + \log(z) \log^2(1+z) \left(-36 - 16 \frac{1}{z} - 24z - 4z^2 \right) \\
& + \log(z) \log(1-z) \left(-30 - \frac{64}{3} \frac{1}{z} + 32z + \frac{104}{3} z^2 \right) \\
& + \log(z) \log^2(1-z) \left(28 + 16z - 16z^2 \right) + \log^2(z) \left(-9 + \frac{16}{3} \frac{1}{z} - 37z - 20z^2 \right) \\
& + \log^2(z) \log(1+z) \left(54 + 24 \frac{1}{z} + 36z + 6z^2 \right)
\end{aligned}$$

$$\begin{aligned}
& + \log^2(z) \log(1-z) \left(-30 - 24z + 8z^2 \right) \\
& + \log^3(z) \left(\frac{17}{3} - \frac{4}{3}z - \frac{8}{3}z^2 \right) + \delta(1-z) \left(\frac{61}{3} \right) \\
& + \log \left(\frac{Q^2}{\mu_F^2} \right) \left[\left(-\frac{235}{6} - \frac{128}{9} \frac{1}{z} + \frac{218}{3}z - \frac{347}{18}z^2 \right) \right. \\
& + \text{Li}_2(1-z) \left(28 + 16z - 16z^2 \right) + \log(1-z) \left(8 + \frac{64}{3} \frac{1}{z} - 32z + \frac{8}{3}z^2 \right) \\
& + \log(z) \left(-15 - \frac{32}{3} \frac{1}{z} + 16z + \frac{52}{3}z^2 \right) + \log(z) \log(1-z) \left(28 + 16z - 16z^2 \right) \\
& + \log^2(z) \left(-15 - 12z + 4z^2 \right) + \delta(1-z) \left(-4 \right) \Big] \\
& + \log^2 \left(\frac{Q^2}{\mu_F^2} \right) \left[\left(2 + \frac{16}{3} \frac{1}{z} - 8z + \frac{2}{3}z^2 \right) + \log(z) \left(7 + 4z - 4z^2 \right) \right] \\
& + \zeta_3 \left(-18 - 56 \frac{1}{z} - 36z + 4z^2 \right) + \zeta_3 \delta(1-z) \left(-16 \right) \\
& + \zeta_2 \left(2 - \frac{88}{3} \frac{1}{z} + 50z - \frac{8}{3}z^2 \right) + \zeta_2 \log(1+z) \left(-36 - 16 \frac{1}{z} - 24z - 4z^2 \right) \\
& + \zeta_2 \log(z) \left(-10 - 8 \frac{1}{z} - 12z + 20z^2 \right) \Big\} \\
& + \mathbf{C_A n_f} \left\{ \left(\frac{41}{108} - \frac{226}{27} \frac{1}{z} + \frac{224}{27} \frac{1}{1-z} - \frac{196}{27}z + \frac{751}{108}z^2 \right) \right. \\
& + S_{1,2}(1-z) \left(-50 + 40 \frac{1}{z} + 28z - 2z^2 \right) + S_{1,2}(-z) \left(36 + 16 \frac{1}{z} + 24z + 4z^2 \right) \\
& + \text{Li}_3(1-z) \left(16 - 16 \frac{1}{z} - 8z \right) + \text{Li}_3(-z) \left(54 + 24 \frac{1}{z} + 36z + 6z^2 \right) \\
& + \text{Li}_2(1-z) \left(-8 + \frac{16}{3} \frac{1}{z} + \frac{8}{3} \frac{1}{1-z} - 12z + \frac{8}{3}z^2 \right) \\
& + \text{Li}_2(-z) \left(-20 - \frac{16}{3} \frac{1}{z} - 24z - \frac{28}{3}z^2 \right) \\
& + \log(1+z) \text{Li}_2(-z) \left(36 + 16 \frac{1}{z} + 24z + 4z^2 \right) \\
& + \log(1-z) \left(-\frac{176}{9} - \frac{142}{9} \frac{1}{z} + \frac{400}{9} \frac{1}{1-z} - \frac{110}{9}z + \frac{16}{9}z^2 \right) \\
& + \log(1-z) \text{Li}_2(1-z) \left(-16 + 16 \frac{1}{z} + 8z \right) \\
& + \log^2(1-z) \left(-\frac{40}{3} + 8 \frac{1}{z} + \frac{32}{3} \frac{1}{1-z} + \frac{8}{3}z - 8z^2 \right) \Big\}
\end{aligned}$$

$$\begin{aligned}
& + \log(z) \left(-\frac{187}{9} + \frac{2}{9} \frac{1}{z} - \frac{200}{9} \frac{1}{1-z} + \frac{53}{9} z - \frac{625}{18} z^2 \right) \\
& + \log(z) \text{Li}_2(-z) \left(-54 - 24 \frac{1}{z} - 36z - 6z^2 \right) \\
& + \log(z) \log(1+z) \left(-20 - \frac{16}{3} \frac{1}{z} - 24z - \frac{28}{3} z^2 \right) \\
& + \log(z) \log^2(1+z) \left(18 + 8 \frac{1}{z} + 12z + 2z^2 \right) \\
& + \log(z) \log(1-z) \left(-16 - \frac{32}{3} \frac{1}{1-z} + 4z + \frac{16}{3} z^2 \right) \\
& + \log^2(z) \left(37 - \frac{8}{3} \frac{1}{z} + \frac{4}{3} \frac{1}{1-z} + 3z + \frac{27}{2} z^2 \right) \\
& + \log^2(z) \log(1+z) \left(-27 - 12 \frac{1}{z} - 18z - 3z^2 \right) + \delta(1-z) \left(-\frac{2983}{162} \right) \\
& + \log \left(\frac{Q^2}{\mu_F^2} \right) \left[\left(-\frac{316}{9} + \frac{140}{9} \frac{1}{z} + \frac{200}{9} \frac{1}{1-z} + \frac{116}{9} z - \frac{140}{9} z^2 \right) \right. \\
& + \log(1-z) \left(\frac{64}{3} - \frac{32}{3} \frac{1}{z} - \frac{32}{3} \frac{1}{1-z} - \frac{32}{3} z + \frac{32}{3} z^2 \right) \\
& + \log(z) \left(-16 + \frac{16}{3} \frac{1}{z} + \frac{16}{3} \frac{1}{1-z} - \frac{16}{3} z^2 \right) + \delta(1-z) \left(\frac{647}{27} \right) \Big] \\
& + \log^2 \left(\frac{Q^2}{\mu_F^2} \right) \left[\left(16 - 8 \frac{1}{z} - 8 \frac{1}{1-z} - 8z + 8z^2 \right) + \delta(1-z) \left(-\frac{44}{9} \right) \right] \\
& + \zeta_3 \left(36 + 16 \frac{1}{z} + 24z + 4z^2 \right) + \zeta_3 \delta(1-z) \left(\frac{64}{3} \right) \\
& + \zeta_2 \left(-\frac{86}{3} - \frac{32}{3} \frac{1}{1-z} + \frac{52}{3} z - \frac{22}{3} z^2 \right) + \zeta_2 \log(1+z) \left(18 + 8 \frac{1}{z} + 12z + 2z^2 \right) \\
& + \zeta_2 \delta(1-z) \left(-\frac{94}{9} \right) + \zeta_2 \log \left(\frac{Q^2}{\mu_F^2} \right) \delta(1-z) \left(-\frac{16}{3} \right) \Big\} \\
& + \mathbf{C}_A^2 \left\{ \left(\frac{20137}{27} - \frac{21595}{27} \frac{1}{z} - \frac{1616}{27} \frac{1}{1-z} - \frac{6605}{27} z + \frac{9679}{27} z^2 \right) \right. \\
& + S_{1,2}(1-z) \left(64 \frac{1}{z^2} - 112 \frac{1}{z} - 144 \frac{1}{1-z} + 64 \frac{1}{1+z} - 528z + 112z^2 \right) \\
& + S_{1,2}(-z) \left(-480 - 192 \frac{1}{z^2} - 320 \frac{1}{z} - 32 \frac{1}{1+z} - 288z - 64z^2 \right) \\
& + \text{Li}_3 \left(\frac{1-z}{1+z} \right) \left(-128 - 64 \frac{1}{z} + 64 \frac{1}{1+z} - 64z - 64z^2 \right) \\
& + \text{Li}_3 \left(-\frac{1-z}{1+z} \right) \left(128 + 64 \frac{1}{z} - 64 \frac{1}{1+z} + 64z + 64z^2 \right) \Big\}
\end{aligned}$$

$$\begin{aligned}
& + \operatorname{Li}_3(1-z) \left(744 + 32 \frac{1}{z^2} - 16 \frac{1}{z} - 8 \frac{1}{1-z} - 64 \frac{1}{1+z} + 536z + 88z^2 \right) \\
& + \operatorname{Li}_3(-z) \left(-272 - 160 \frac{1}{z^2} + 320 \frac{1}{z} - 16 \frac{1}{1+z} + 304z - 64z^2 \right) \\
& + \operatorname{Li}_2(1-z) \left(-376 - \frac{748}{3} \frac{1}{z} - \frac{44}{3} \frac{1}{1-z} - 400z - \frac{704}{3} z^2 \right) \\
& + \operatorname{Li}_2(-z) \left(296 + 264 \frac{1}{z} + 120z + 88z^2 \right) \\
& + \log(1+z) \operatorname{Li}_2(-z) \left(-480 - 192 \frac{1}{z^2} - 320 \frac{1}{z} - 32 \frac{1}{1+z} - 288z - 64z^2 \right) \\
& + \log(1-z) \left(-\frac{1492}{9} + \frac{4396}{9} \frac{1}{z} - \frac{2176}{9} \frac{1}{1-z} + \frac{4040}{9} z - \frac{4756}{9} z^2 \right) \\
& + \log(1-z) \operatorname{Li}_2(1-z) \left(-496 - 16 \frac{1}{z} - 544z \right) \\
& + \log(1-z) \operatorname{Li}_2(-z) \left(128 + 64 \frac{1}{z} - 64 \frac{1}{1+z} + 64z + 64z^2 \right) \\
& + \log^2(1-z) \left(\frac{1324}{3} - 572 \frac{1}{z} - \frac{176}{3} \frac{1}{1-z} - \frac{1148}{3} z + 572z^2 \right) \\
& + \log^3(1-z) \left(-256 + 128 \frac{1}{z} + 128 \frac{1}{1-z} + 128z - 128z^2 \right) \\
& + \log(z) \left(\frac{946}{9} - \frac{1264}{3} \frac{1}{z} + \frac{1088}{9} \frac{1}{1-z} - \frac{2582}{9} z + \frac{5740}{9} z^2 \right) \\
& + \log(z) \operatorname{Li}_2(1-z) \left(8 + 48 \frac{1}{z} - 56 \frac{1}{1-z} + 48 \frac{1}{1+z} + 24z + 8z^2 \right) \\
& + \log(z) \operatorname{Li}_2(-z) \left(256 + 160 \frac{1}{z^2} - 64 \frac{1}{z} + 64 \frac{1}{1+z} - 64z + 16z^2 \right) \\
& + \log(z) \log(1+z) \left(296 + 264 \frac{1}{z} + 120z + 88z^2 \right) \\
& + \log(z) \log^2(1+z) \left(-240 - 96 \frac{1}{z^2} - 160 \frac{1}{z} - 16 \frac{1}{1+z} - 144z - 32z^2 \right) \\
& + \log(z) \log(1-z) \left(-832 + \frac{1232}{3} \frac{1}{z} + \frac{176}{3} \frac{1}{1-z} + 72z - 968z^2 \right) \\
& + \log(z) \log(1-z) \log(1+z) \left(128 + 64 \frac{1}{z} - 64 \frac{1}{1+z} + 64z + 64z^2 \right) \\
& + \log(z) \log^2(1-z) \left(240 - 248 \frac{1}{z} - 248 \frac{1}{1-z} - 504z + 248z^2 \right) \\
& + \log^2(z) \left(28 - \frac{220}{3} \frac{1}{z} - \frac{22}{3} \frac{1}{1-z} + 44z + \frac{550}{3} z^2 \right)
\end{aligned}$$

$$\begin{aligned}
& + \log^2(z) \log(1+z) \left(120 + 80 \frac{1}{z^2} + 96 \frac{1}{z} + 56 \frac{1}{1+z} + 88z - 16z^2 \right) \\
& + \log^2(z) \log(1-z) \left(-96 + 112 \frac{1}{z} + 128 \frac{1}{1-z} + 16 \frac{1}{1+z} + 304z - 144z^2 \right) \\
& + \log^3(z) \left(-\frac{16}{3} - 16 \frac{1}{z} - \frac{56}{3} \frac{1}{1-z} - \frac{16}{3} \frac{1}{1+z} - \frac{184}{3} z + 24z^2 \right) \\
& + \delta(1-z) \left(\frac{7801}{324} \right) \\
& + \log \left(\frac{Q^2}{\mu_F^2} \right) \left[\left(-\frac{518}{9} + 150 \frac{1}{z} - \frac{1088}{9} \frac{1}{1-z} + \frac{1606}{9} z - 150z^2 \right) \right. \\
& + \text{Li}_2(1-z) \left(-256 - 256z \right) + \text{Li}_2(-z) \left(64 + 32 \frac{1}{z} - 32 \frac{1}{1+z} + 32z + 32z^2 \right) \\
& + \log(1-z) \left(\frac{752}{3} - \frac{1408}{3} \frac{1}{z} + \frac{176}{3} \frac{1}{1-z} - \frac{928}{3} z + \frac{1408}{3} z^2 \right) \\
& + \log^2(1-z) \left(-384 + 192 \frac{1}{z} + 192 \frac{1}{1-z} + 192z - 192z^2 \right) \\
& + \log(z) \left(-376 + \frac{440}{3} \frac{1}{z} - \frac{88}{3} \frac{1}{1-z} - 440z^2 \right) \\
& + \log(z) \log(1+z) \left(64 + 32 \frac{1}{z} - 32 \frac{1}{1+z} + 32z + 32z^2 \right) \\
& + \log(z) \log(1-z) \left(192 - 224 \frac{1}{z} - 224 \frac{1}{1-z} - 480z + 224z^2 \right) \\
& + \log^2(z) \left(32 \frac{1}{z} + 40 \frac{1}{1-z} + 8 \frac{1}{1+z} + 128z - 48z^2 \right) + \delta(1-z) \left(-\frac{1657}{27} \right) \Big] \\
& + \log^2 \left(\frac{Q^2}{\mu_F^2} \right) \left[\left(8 - \frac{220}{3} \frac{1}{z} + 44 \frac{1}{1-z} - 52z + \frac{220}{3} z^2 \right) \right. \\
& + \log(1-z) \left(-128 + 64 \frac{1}{z} + 64 \frac{1}{1-z} + 64z - 64z^2 \right) \\
& + \log(z) \left(-32 \frac{1}{z} - 32 \frac{1}{1-z} - 96z + 32z^2 \right) + \delta(1-z) \left(\frac{121}{9} \right) \Big] \\
& + \zeta_3 \left(-768 - 96 \frac{1}{z^2} + 592 \frac{1}{z} + 312 \frac{1}{1-z} - 8 \frac{1}{1+z} + 576z - 352z^2 \right) \\
& + \zeta_3 \delta(1-z) \left(-\frac{88}{3} \right) + \zeta_3 \log \left(\frac{Q^2}{\mu_F^2} \right) \delta(1-z) \left(152 \right) \\
& + \zeta_2 \left(-\frac{436}{3} + \frac{1628}{3} \frac{1}{z} + \frac{176}{3} \frac{1}{1-z} + \frac{884}{3} z - \frac{1100}{3} z^2 \right) \\
& + \zeta_2 \log(1+z) \left(-240 - 96 \frac{1}{z^2} - 160 \frac{1}{z} - 16 \frac{1}{1+z} - 144z - 32z^2 \right)
\end{aligned}$$

$$\begin{aligned}
& + \zeta_2 \log(1-z) \left(384 - 128 \frac{1}{z} - 160 \frac{1}{1-z} - 32 \frac{1}{1+z} - 128z + 192z^2 \right) \\
& + \zeta_2 \log(z) \left(-40 + 272 \frac{1}{z} + 144 \frac{1}{1-z} + 24 \frac{1}{1+z} + 520z - 168z^2 \right) \\
& + \zeta_2 \delta(1-z) \left(-\frac{224}{9} \right) \\
& + \zeta_2 \log \left(\frac{Q^2}{\mu_F^2} \right) \left(192 - 64 \frac{1}{z} - 80 \frac{1}{1-z} - 16 \frac{1}{1+z} - 64z + 96z^2 \right) \\
& + \zeta_2 \log \left(\frac{Q^2}{\mu_F^2} \right) \delta(1-z) \left(\frac{88}{3} \right) + \zeta_2 \log^2 \left(\frac{Q^2}{\mu_F^2} \right) \delta(1-z) \left(-32 \right) \\
& + \zeta_2^2 \delta(1-z) \left(-\frac{4}{5} \right) \Bigg\}, \\
\bar{A}_{gq}^{h,(1)} &= \left(\frac{9}{2} - 6 \frac{1}{z} + 9z - \frac{7}{2} z^2 \right) + \log(1-z) \left(-14 + 16 \frac{1}{z} + 4z + 4z^2 \right) \\
& + \log(z) \left(7 - 8 \frac{1}{z} - 2z - 2z^2 \right) + \log \left(\frac{Q^2}{\mu_F^2} \right) \left(-7 + 8 \frac{1}{z} + 2z + 2z^2 \right), \\
\bar{A}_{gq}^{h,(2)} &= \mathbf{n}_f \left\{ \left(-\frac{160}{27} + \frac{304}{27} \frac{1}{z} + \frac{380}{27} z \right) + \text{Li}_2(1-z) \left(-\frac{32}{3} + \frac{32}{3} \frac{1}{z} + \frac{4}{3} z \right) \right. \\
& + \log(1-z) \left(-\frac{200}{9} + \frac{200}{9} \frac{1}{z} + \frac{88}{9} z + \frac{16}{3} z^2 \right) \\
& + \log^2(1-z) \left(-\frac{8}{3} + \frac{8}{3} \frac{1}{z} + \frac{4}{3} z \right) + \log(z) \left(-\frac{4}{3} z - \frac{16}{3} z^2 \right) \\
& + \log(z) \log(1-z) \left(-4z \right) + \log^2(z) \left(2z \right) \\
& + \log \left(\frac{Q^2}{\mu_F^2} \right) \left[\left(-\frac{40}{3} + \frac{40}{3} \frac{1}{z} + \frac{4}{3} z \right) + \log(1-z) \left(\frac{32}{3} - \frac{32}{3} \frac{1}{z} - \frac{16}{3} z \right) \right] \\
& + \log^2 \left(\frac{Q^2}{\mu_F^2} \right) \left(\frac{16}{3} - \frac{16}{3} \frac{1}{z} - \frac{8}{3} z \right) \Bigg\} \\
& + \mathbf{C}_F \left\{ \left(\frac{1507}{36} - \frac{4057}{27} \frac{1}{z} + \frac{2935}{18} z - \frac{4499}{108} z^2 \right) \right. \\
& + S_{1,2}(1-z) \left(-118 + 64 \frac{1}{z} + 92z - 68z^2 \right) \\
& + \text{Li}_3(1-z) \left(30 - 80 \frac{1}{z} + 4z + 36z^2 \right) + \text{Li}_3(-z) \left(144 - 64 \frac{1}{z} - 160z + 32z^2 \right) \\
& + \text{Li}_2(1-z) \left(167 - \frac{392}{3} \frac{1}{z} - 52z + \frac{248}{3} z^2 \right) \\
& + \text{Li}_2(-z) \left(40 - \frac{160}{3} \frac{1}{z} + 48z - \frac{136}{3} z^2 \right) \Bigg\}
\end{aligned}$$

$$\begin{aligned}
& + \log(1-z) \left(-\frac{346}{3} + \frac{1360}{9} \frac{1}{z} - \frac{593}{3} z + \frac{728}{9} z^2 \right) \\
& + \log(1-z) \text{Li}_2(1-z) \left(-70 + 96 \frac{1}{z} + 44z - 52z^2 \right) \\
& + \log^2(1-z) \left(133 - \frac{392}{3} \frac{1}{z} + 22z - \frac{157}{3} z^2 \right) \\
& + \log^3(1-z) \left(-23 + \frac{104}{3} \frac{1}{z} - 6z + \frac{70}{3} z^2 \right) \\
& + \log(z) \left(-\frac{19}{2} - \frac{284}{9} \frac{1}{z} + \frac{667}{6} z - \frac{919}{9} z^2 \right) \\
& + \log(z) \text{Li}_2(1-z) \left(50 - 48 \frac{1}{z} - 44z \right) \\
& + \log(z) \text{Li}_2(-z) \left(-72 + 32 \frac{1}{z} + 80z - 16z^2 \right) \\
& + \log(z) \log(1+z) \left(40 - \frac{160}{3} \frac{1}{z} + 48z - \frac{136}{3} z^2 \right) \\
& + \log(z) \log(1-z) \left(-130 + 72 \frac{1}{z} + 32z + 96z^2 \right) \\
& + \log(z) \log^2(1-z) \left(59 - 48 \frac{1}{z} + 2z - 66z^2 \right) + \log^2(z) \left(\frac{325}{4} - 92z + \frac{61}{3} z^2 \right) \\
& + \log^2(z) \log(1-z) \left(-36 + 16 \frac{1}{z} + 40z^2 \right) + \log^3(z) \left(\frac{23}{6} + \frac{7}{3} z - \frac{26}{3} z^2 \right) \\
& + \log \left(\frac{Q^2}{\mu_F^2} \right) \left[\left(-40 + \frac{212}{9} \frac{1}{z} - 26z - \frac{77}{9} z^2 \right) + \text{Li}_2(1-z) \left(32 \frac{1}{z} - 24z^2 \right) \right. \\
& + \log(1-z) \left(80 - 72 \frac{1}{z} + 44z - 46z^2 \right) \\
& + \log^2(1-z) \left(-30 + 48 \frac{1}{z} - 12z + 36z^2 \right) + \log(z) \left(-11 - 12z + \frac{170}{3} z^2 \right) \\
& + \log(z) \log(1-z) \left(44 - 32 \frac{1}{z} + 8z - 64z^2 \right) + \log^2(z) \left(-12 + 16z^2 \right) \Big] \\
& + \log^2 \left(\frac{Q^2}{\mu_F^2} \right) \left[\left(\frac{13}{2} + 4z \right) + \log(1-z) \left(-10 + 16 \frac{1}{z} - 4z + 12z^2 \right) \right. \\
& + \log(z) \left(5 + 2z - 12z^2 \right) \Big] \\
& + \zeta_3 \left(82 + 16 \frac{1}{z} - 164z + 100z^2 \right) + \zeta_2 \left(-214 + \frac{512}{3} \frac{1}{z} + 156z - 88z^2 \right) \\
& + \zeta_2 \log(1-z) \left(120 - 128 \frac{1}{z} - 48z - 16z^2 \right) + \zeta_2 \log(z) \left(-52 + 48 \frac{1}{z} - 8z + 48z^2 \right)
\end{aligned}$$

$$\begin{aligned}
& + \zeta_2 \log\left(\frac{Q^2}{\mu_F^2}\right) \left(60 - 64\frac{1}{z} - 24z - 8z^2\right) \Big\} \\
& + \mathbf{C}_A \left\{ \left(\frac{42329}{54} - \frac{21895}{27} \frac{1}{z} - \frac{2474}{27} z - \frac{137}{18} z^2 \right) \right. \\
& + S_{1,2}(1-z) \left(20 + 128\frac{1}{z^2} - 144\frac{1}{z} - 200z + 16z^2 \right) \\
& + S_{1,2}(-z) \left(-448 - 384\frac{1}{z^2} - 640\frac{1}{z} - 128z \right) \\
& + \text{Li}_3\left(\frac{1-z}{1+z}\right) \left(-56 - 64\frac{1}{z} - 16z + 16z^2 \right) \\
& + \text{Li}_3\left(-\frac{1-z}{1+z}\right) \left(56 + 64\frac{1}{z} + 16z - 16z^2 \right) \\
& + \text{Li}_3(1-z) \left(722 + 64\frac{1}{z^2} + 112\frac{1}{z} + 220z - 24z^2 \right) \\
& + \text{Li}_3(-z) \left(-324 - 320\frac{1}{z^2} + 608\frac{1}{z} + 136z - 8z^2 \right) \\
& + \text{Li}_2(1-z) \left(-\frac{1822}{3} - \frac{28}{3} \frac{1}{z} - \frac{532}{3} z - \frac{88}{3} z^2 \right) \\
& + \text{Li}_2(-z) \left(516 + 504\frac{1}{z} + 68z + 48z^2 \right) \\
& + \log(1+z) \text{Li}_2(-z) \left(-448 - 384\frac{1}{z^2} - 640\frac{1}{z} - 128z \right) \\
& + \log(1-z) \left(-\frac{4618}{9} + \frac{3952}{9} \frac{1}{z} + \frac{143}{9} z - \frac{10}{3} z^2 \right) \\
& + \log(1-z) \text{Li}_2(1-z) \left(-500 - 224\frac{1}{z} - 272z + 20z^2 \right) \\
& + \log(1-z) \text{Li}_2(-z) \left(56 + 64\frac{1}{z} + 16z - 16z^2 \right) \\
& + \log^2(1-z) \left(\frac{1112}{3} - \frac{1484}{3} \frac{1}{z} + \frac{452}{3} z + 2z^2 \right) \\
& + \log^3(1-z) \left(-89 + \frac{280}{3} \frac{1}{z} + 38z + \frac{26}{3} z^2 \right) \\
& + \log(z) \left(\frac{1174}{3} - \frac{1544}{3} \frac{1}{z} - 98z - \frac{11}{3} z^2 \right) \\
& + \log(z) \text{Li}_2(1-z) \left(-48 + 192\frac{1}{z} + 68z - 8z^2 \right) \\
& + \log(z) \text{Li}_2(-z) \left(328 + 320\frac{1}{z^2} - 64\frac{1}{z} - 16z + 16z^2 \right)
\end{aligned}$$

$$\begin{aligned}
& + \log(z) \log(1+z) \left(516 + 504 \frac{1}{z} + 68z + 48z^2 \right) \\
& + \log(z) \log^2(1+z) \left(-224 - 192 \frac{1}{z^2} - 320 \frac{1}{z} - 64z \right) \\
& + \log(z) \log(1-z) \left(-838 + \frac{1208}{3} \frac{1}{z} - 416z + \frac{70}{3} z^2 \right) \\
& + \log(z) \log(1-z) \log(1+z) \left(56 + 64 \frac{1}{z} + 16z - 16z^2 \right) \\
& + \log(z) \log^2(1-z) \left(-118 - 264 \frac{1}{z} - 184z - 12z^2 \right) \\
& + \log^2(z) \left(-\frac{341}{2} - \frac{284}{3} \frac{1}{z} + 130z - \frac{181}{3} z^2 \right) \\
& + \log^2(z) \log(1+z) \left(166 + 160 \frac{1}{z^2} + 240 \frac{1}{z} + 52z + 12z^2 \right) \\
& + \log^2(z) \log(1-z) \left(90 + 128 \frac{1}{z} + 100z + 4z^2 \right) + \log^3(z) \left(-\frac{95}{3} - \frac{80}{3} \frac{1}{z} - \frac{28}{3} z \right) \\
& + \log \left(\frac{Q^2}{\mu_F^2} \right) \left[\left(-\frac{709}{3} + \frac{620}{3} \frac{1}{z} + \frac{64}{3} z + 17z^2 \right) \right. \\
& + \text{Li}_2(1-z) \left(-276 - 96 \frac{1}{z} - 120z + 8z^2 \right) + \text{Li}_2(-z) \left(28 + 32 \frac{1}{z} + 8z - 8z^2 \right) \\
& + \log(1-z) \left(\frac{1042}{3} - 456 \frac{1}{z} + \frac{460}{3} z + \frac{50}{3} z^2 \right) \\
& + \log^2(1-z) \left(-138 + 144 \frac{1}{z} + 60z + 12z^2 \right) \\
& + \log(z) \left(-458 + \frac{568}{3} \frac{1}{z} - 188z - 8z^2 \right) \\
& + \log(z) \log(1+z) \left(28 + 32 \frac{1}{z} + 8z - 8z^2 \right) \\
& + \log(z) \log(1-z) \left(-124 - 256 \frac{1}{z} - 184z - 8z^2 \right) + \log^2(z) \left(60 + 48 \frac{1}{z} + 44z \right) \Big] \\
& + \log^2 \left(\frac{Q^2}{\mu_F^2} \right) \left[\left(\frac{203}{3} - \frac{280}{3} \frac{1}{z} + \frac{104}{3} z + \frac{17}{3} z^2 \right) \right. \\
& + \log(1-z) \left(-46 + 48 \frac{1}{z} + 20z + 4z^2 \right) + \log(z) \left(-46 - 48 \frac{1}{z} - 40z \right) \Big] \\
& + \zeta_3 \left(-434 - 192 \frac{1}{z^2} + 784 \frac{1}{z} + 240z - 4z^2 \right) \\
& + \zeta_2 \left(138 + \frac{1636}{3} \frac{1}{z} - 164z + \frac{230}{3} z^2 \right)
\end{aligned}$$

$$\begin{aligned}
& + \zeta_2 \log(1+z) \left(-224 - 192 \frac{1}{z^2} - 320 \frac{1}{z} - 64z \right) + \zeta_2 \log(1-z) \left(48 + 16z - 32z^2 \right) \\
& + \zeta_2 \log(z) \left(240 + 416 \frac{1}{z} + 184z + 16z^2 \right) + \zeta_2 \log\left(\frac{Q^2}{\mu_F^2}\right) \left(24 + 8z - 16z^2 \right) \Big\},
\end{aligned}$$

$$\bar{A}_{q\bar{q}}^{h,(0)} = \delta(1-z),$$

$$\begin{aligned}
\bar{A}_{q\bar{q}}^{h,(1)} = & \mathbf{C}_F \left\{ \left(\frac{16}{3} \frac{1}{z} - \frac{16}{3} z^2 \right) + \log(1-z) \left(-8 + 16 \frac{1}{1-z} - 8z \right) \right. \\
& + \log(z) \left(4 - 8 \frac{1}{1-z} + 4z \right) + \delta(1-z) (-20) \\
& \left. + \log\left(\frac{Q^2}{\mu_F^2}\right) \left[\left(-4 + 8 \frac{1}{1-z} - 4z \right) + \delta(1-z) (6) \right] + \zeta_2 \delta(1-z) (8) \right\},
\end{aligned}$$

$$\begin{aligned}
\bar{A}_{q\bar{q}}^{h,(2)} = & \mathbf{C}_F \left\{ \left(\frac{5417}{9} - \frac{12304}{27} \frac{1}{z} - \frac{1550}{9} z + \frac{703}{27} z^2 \right) \right. \\
& + S_{1,2}(1-z) \left(144 + 128 \frac{1}{z^2} + 64 \frac{1}{z} + 64z \right) \\
& + S_{1,2}(-z) \left(-288 - 384 \frac{1}{z^2} - 576 \frac{1}{z} - 48z \right) \\
& + \text{Li}_3(1-z) \left(312 + 64 \frac{1}{z^2} + 128 \frac{1}{z} + 12z \right) \\
& + \text{Li}_3(-z) \left(-144 - 320 \frac{1}{z^2} + 672 \frac{1}{z} + 40z \right) \\
& + \text{Li}_2(1-z) \left(-248 + \frac{736}{3} \frac{1}{z} - 108z + \frac{32}{3} z^2 \right) + \text{Li}_2(-z) \left(488 + 448 \frac{1}{z} + 40z \right) \\
& + \log(1+z) \text{Li}_2(-z) \left(-288 - 384 \frac{1}{z^2} - 576 \frac{1}{z} - 48z \right) \\
& + \log(1-z) \left(-\frac{1160}{3} + \frac{3272}{9} \frac{1}{z} + \frac{128}{3} z - \frac{176}{9} z^2 \right) \\
& + \log(1-z) \text{Li}_2(1-z) \left(-224 - 256 \frac{1}{z} - 32z \right) \\
& + \log^2(1-z) \left(136 - \frac{544}{3} \frac{1}{z} + 56z - \frac{32}{3} z^2 \right) \\
& + \log(z) \left(\frac{974}{3} - 284 \frac{1}{z} - \frac{68}{3} z + \frac{40}{9} z^2 \right) + \log(z) \text{Li}_2(1-z) \left(32 + 224 \frac{1}{z} + 52z \right) \\
& + \log(z) \text{Li}_2(-z) \left(192 + 320 \frac{1}{z^2} - 96 \frac{1}{z} \right) + \log(z) \log(1+z) \left(488 + 448 \frac{1}{z} + 40z \right) \\
& + \log(z) \log^2(1+z) \left(-144 - 192 \frac{1}{z^2} - 288 \frac{1}{z} - 24z \right) \\
& \left. + \log(z) \log(1-z) \left(-232 + 192 \frac{1}{z} - 96z + 32z^2 \right) \right\}
\end{aligned}$$

$$\begin{aligned}
& + \log(z) \log^2(1-z) \left(-112 - 128 \frac{1}{z} - 16z \right) \\
& + \log^2(z) \left(-277 - 48 \frac{1}{z} - 35z - \frac{40}{3} z^2 \right) \\
& + \log^2(z) \log(1+z) \left(120 + 160 \frac{1}{z^2} + 240 \frac{1}{z} + 20z \right) \\
& + \log^2(z) \log(1-z) \left(48 + 64 \frac{1}{z} \right) + \log^3(z) \left(-\frac{14}{3} - \frac{64}{3} \frac{1}{z} + \frac{34}{3} z \right) \\
& + \log \left(\frac{Q^2}{\mu_F^2} \right) \left[\left(-\frac{580}{3} + \frac{1636}{9} \frac{1}{z} + \frac{64}{3} z - \frac{88}{9} z^2 \right) \right. \\
& + \text{Li}_2(1-z) \left(-112 - 128 \frac{1}{z} - 16z \right) \\
& + \log(1-z) \left(136 - \frac{544}{3} \frac{1}{z} + 56z - \frac{32}{3} z^2 \right) + \log(z) \left(-116 + 96 \frac{1}{z} - 48z + 16z^2 \right) \\
& + \log(z) \log(1-z) \left(-112 - 128 \frac{1}{z} - 16z \right) + \log^2(z) \left(24 + 32 \frac{1}{z} \right) \Big] \\
& + \log^2 \left(\frac{Q^2}{\mu_F^2} \right) \left[\left(34 - \frac{136}{3} \frac{1}{z} + 14z - \frac{8}{3} z^2 \right) + \log(z) \left(-28 - 32 \frac{1}{z} - 4z \right) \right] \\
& + \zeta_3 \left(-72 - 192 \frac{1}{z^2} + 576 \frac{1}{z} + 36z \right) + \zeta_2 \left(108 + \frac{1216}{3} \frac{1}{z} - 36z + \frac{32}{3} z^2 \right) \\
& + \zeta_2 \log(1+z) \left(-144 - 192 \frac{1}{z^2} - 288 \frac{1}{z} - 24z \right) + \zeta_2 \log(z) \left(136 + 416 \frac{1}{z} + 36z \right) \Big\} \\
& + \mathbf{C}_{\text{F}\mathbf{n}_f} \left\{ \left(\frac{1280}{27} - \frac{8}{9} \frac{1}{z} + \frac{224}{27} \frac{1}{1-z} - \frac{1252}{27} z - \frac{76}{9} z^2 \right) \right. \\
& + \text{Li}_2(1-z) \left(\frac{8}{3} - \frac{32}{3} \frac{1}{z} - \frac{8}{3} \frac{1}{1-z} + \frac{8}{3} z \right) + \text{Li}_2(-z) \left(-48 - \frac{64}{3} \frac{1}{z} - 32z - \frac{16}{3} z^2 \right) \\
& + \log(1-z) \left(-\frac{16}{9} + \frac{64}{9} \frac{1}{z} - \frac{160}{9} \frac{1}{1-z} + \frac{176}{9} z - \frac{64}{9} z^2 \right) \\
& + \log^2(1-z) \left(-\frac{16}{3} + \frac{32}{3} \frac{1}{1-z} - \frac{16}{3} z \right) \\
& + \log(z) \left(\frac{88}{3} - \frac{40}{3} \frac{1}{z} + \frac{40}{3} \frac{1}{1-z} + \frac{52}{3} z + \frac{164}{9} z^2 \right) \\
& + \log(z) \log(1+z) \left(-48 - \frac{64}{3} \frac{1}{z} - 32z - \frac{16}{3} z^2 \right) \\
& + \log(z) \log(1-z) \left(\frac{32}{3} - \frac{64}{3} \frac{1}{1-z} + \frac{32}{3} z \right) \\
& + \log^2(z) \left(\frac{26}{3} + 8 \frac{1}{1-z} + \frac{14}{3} z + \frac{4}{3} z^2 \right) + \delta(1-z) \left(\frac{461}{18} \right) \Big\}
\end{aligned}$$

$$\begin{aligned}
& + \log\left(\frac{Q^2}{\mu_F^2}\right) \left[\left(-\frac{8}{9} + \frac{32}{9} \frac{1}{z} - \frac{80}{9} \frac{1}{1-z} + \frac{88}{9} z - \frac{32}{9} z^2 \right) \right. \\
& + \log(1-z) \left(-\frac{16}{3} + \frac{32}{3} \frac{1}{1-z} - \frac{16}{3} z \right) \\
& + \log(z) \left(\frac{16}{3} - \frac{32}{3} \frac{1}{1-z} + \frac{16}{3} z \right) + \delta(1-z) \left(-14 \right) \Big] \\
& + \log^2\left(\frac{Q^2}{\mu_F^2}\right) \left[\left(-\frac{4}{3} + \frac{8}{3} \frac{1}{1-z} - \frac{4}{3} z \right) + \delta(1-z) \left(2 \right) \right] + \zeta_3 \delta(1-z) \left(8 \right) \\
& + \zeta_2 \left(-\frac{56}{3} - \frac{32}{3} \frac{1}{z} - \frac{32}{3} \frac{1}{1-z} - \frac{32}{3} z - \frac{8}{3} z^2 \right) + \zeta_2 \delta(1-z) \left(-\frac{64}{9} \right) \Big\} \\
& + \mathbf{C_F}^2 \left\{ \left(96 + 136 \frac{1}{z} - 236z + 12z^2 \right) \right. \\
& + S_{1,2}(1-z) \left(696 - 256 \frac{1}{z} - 208 \frac{1}{1-z} + 696z + 64z^2 \right) \\
& + S_{1,2}(-z) \left(-864 - 384 \frac{1}{z} - 576z - 96z^2 \right) \\
& + \text{Li}_3(1-z) \left(-80 + 96 \frac{1}{z} + 48 \frac{1}{1-z} - 48z \right) \\
& + \text{Li}_3(-z) \left(-144 - 192 \frac{1}{z} - 224z - 16z^2 \right) \\
& + \text{Li}_2(1-z) \left(232 + \frac{320}{3} \frac{1}{z} - 24 \frac{1}{1-z} - 392z - \frac{88}{3} z^2 \right) \\
& + \text{Li}_2(-z) \left(688 + \frac{640}{3} \frac{1}{z} + 608z + \frac{400}{3} z^2 \right) \\
& + \log(1+z) \text{Li}_2(-z) \left(-864 - 384 \frac{1}{z} - 576z - 96z^2 \right) \\
& + \log(1-z) \left(-\frac{32}{3} + 96 \frac{1}{z} - 320 \frac{1}{1-z} + \frac{500}{3} z + 64z^2 \right) \\
& + \log(1-z) \text{Li}_2(1-z) \left(56 - 128 \frac{1}{z} - 16 \frac{1}{1-z} + 56z \right) \\
& + \log^2(1-z) \left(-64 + \frac{128}{3} \frac{1}{z} + 64z - \frac{128}{3} z^2 \right) \\
& + \log^3(1-z) \left(-64 + 128 \frac{1}{1-z} - 64z \right) \\
& + \log(z) \left(\frac{1360}{3} - 64 \frac{1}{z} + 192 \frac{1}{1-z} + 12z - 64z^2 \right) \\
& + \log(z) \text{Li}_2(1-z) \left(344 + 32 \frac{1}{z} - 96 \frac{1}{1-z} + 312z + 32z^2 \right)
\end{aligned}$$

$$\begin{aligned}
& + \log(z) \text{Li}_2(-z) \left(432 + 256 \frac{1}{z} + 352z + 48z^2 \right) \\
& + \log(z) \log(1+z) \left(688 + \frac{640}{3} \frac{1}{z} + 608z + \frac{400}{3} z^2 \right) \\
& + \log(z) \log^2(1+z) \left(-432 - 192 \frac{1}{z} - 288z - 48z^2 \right) \\
& + \log(z) \log(1-z) \left(96 - \frac{128}{3} \frac{1}{z} - 48 \frac{1}{1-z} - 144z + 128z^2 \right) \\
& + \log(z) \log^2(1-z) \left(156 - 248 \frac{1}{1-z} + 156z \right) \\
& + \log^2(z) \left(-184 + 30 \frac{1}{1-z} - 384z - \frac{500}{3} z^2 \right) \\
& + \log^2(z) \log(1+z) \left(360 + 160 \frac{1}{z} + 240z + 40z^2 \right) \\
& + \log^2(z) \log(1-z) \left(-80 + 112 \frac{1}{1-z} - 80z \right) \\
& + \log^3(z) \left(\frac{110}{3} - \frac{40}{3} \frac{1}{1-z} + \frac{134}{3} z + \frac{8}{3} z^2 \right) + \delta(1-z) \left(\frac{2293}{12} \right) \\
& + \log \left(\frac{Q^2}{\mu_F^2} \right) \left[\left(\frac{248}{3} - 160 \frac{1}{1-z} + \frac{232}{3} z \right) + \text{Li}_2(1-z) \left(32 + 32z \right) \right. \\
& + \log(1-z) \left(-112 + \frac{128}{3} \frac{1}{z} + 96 \frac{1}{1-z} + 16z - \frac{128}{3} z^2 \right) \\
& + \log^2(1-z) \left(-96 + 192 \frac{1}{1-z} - 96z \right) \\
& + \log(z) \left(40 - 72 \frac{1}{1-z} - 40z + \frac{128}{3} z^2 \right) \\
& + \log(z) \log(1-z) \left(144 - 224 \frac{1}{1-z} + 144z \right) \\
& + \log^2(z) \left(-28 + 32 \frac{1}{1-z} - 28z \right) + \delta(1-z) \left(-117 \right) \Big] \\
& + \log^2 \left(\frac{Q^2}{\mu_F^2} \right) \left[\left(-40 + 48 \frac{1}{1-z} - 8z \right) \right. \\
& + \log(1-z) \left(-32 + 64 \frac{1}{1-z} - 32z \right) \\
& + \log(z) \left(24 - 32 \frac{1}{1-z} + 24z \right) + \delta(1-z) \left(18 \right) \Big] \\
& + \zeta_3 \left(-128 - 96 \frac{1}{z} + 256 \frac{1}{1-z} - 224z \right) + \zeta_3 \delta(1-z) \left(-124 \right)
\end{aligned}$$

$$\begin{aligned}
& + \zeta_3 \log\left(\frac{Q^2}{\mu_F^2}\right) \delta(1-z) \left(176\right) + \zeta_2 \left(408 + \frac{448}{3} \frac{1}{z} + 240z + 24z^2\right) \\
& + \zeta_2 \log(1+z) \left(-432 - 192 \frac{1}{z} - 288z - 48z^2\right) \\
& + \zeta_2 \log(1-z) \left(64 - 128 \frac{1}{1-z} + 64z\right) \\
& + \zeta_2 \log(z) \left(48 + 32 \frac{1}{z} + 128 \frac{1}{1-z} - 32z + 16z^2\right) + \zeta_2 \delta(1-z) \left(-70\right) \\
& + \zeta_2 \log\left(\frac{Q^2}{\mu_F^2}\right) \left(32 - 64 \frac{1}{1-z} + 32z\right) + \zeta_2 \log\left(\frac{Q^2}{\mu_F^2}\right) \delta(1-z) \left(24\right) \\
& + \zeta_2 \log^2\left(\frac{Q^2}{\mu_F^2}\right) \delta(1-z) \left(-32\right) + \zeta_2^2 \delta(1-z) \left(\frac{8}{5}\right) \Big\} \\
& + \mathbf{C}_A \mathbf{C}_F \left\{ \left(-\frac{4154}{27} - \frac{584}{27} \frac{1}{z} - \frac{1616}{27} \frac{1}{1-z} + \frac{7300}{27} z - \frac{1162}{27} z^2 \right) \right. \\
& + S_{1,2}(1-z) \left(-432 + 256 \frac{1}{z} + 64 \frac{1}{1-z} - 240z - 32z^2 \right) \\
& + S_{1,2}(-z) \left(432 + 192 \frac{1}{z} + 288z + 48z^2 \right) \\
& + \text{Li}_3(1-z) \left(88 - 96 \frac{1}{z} - 56 \frac{1}{1-z} - 8z \right) \\
& + \text{Li}_3(-z) \left(72 + 32 \frac{1}{z} + 48z + 8z^2 \right) \\
& + \text{Li}_2(1-z) \left(-\frac{464}{3} - \frac{272}{3} \frac{1}{z} + \frac{44}{3} \frac{1}{1-z} + \frac{340}{3} z + \frac{140}{3} z^2 \right) \\
& + \text{Li}_2(-z) \left(-408 - 160 \frac{1}{z} - 336z - 88z^2 \right) \\
& + \log(1+z) \text{Li}_2(-z) \left(432 + 192 \frac{1}{z} + 288z + 48z^2 \right) \\
& + \log(1-z) \left(\frac{2440}{9} - \frac{664}{3} \frac{1}{z} + \frac{1072}{9} \frac{1}{1-z} - \frac{2252}{9} z + \frac{256}{3} z^2 \right) \\
& + \log(1-z) \text{Li}_2(1-z) \left(-64 + 128 \frac{1}{z} + 16 \frac{1}{1-z} + 32z \right) \\
& + \log^2(1-z) \left(\frac{88}{3} - \frac{176}{3} \frac{1}{1-z} + \frac{88}{3} z \right) \\
& + \log(z) \left(-\frac{1136}{3} + \frac{232}{3} \frac{1}{z} - \frac{280}{3} \frac{1}{1-z} + \frac{296}{3} z - \frac{256}{3} z^2 \right) \\
& + \log(z) \text{Li}_2(1-z) \left(-168 - 32 \frac{1}{z} + 40 \frac{1}{1-z} - 168z - 16z^2 \right)
\end{aligned}$$

$$\begin{aligned}
& + \log(z) \text{Li}_2(-z) \left(-216 - 96 \frac{1}{z} - 144z - 24z^2 \right) \\
& + \log(z) \log(1+z) \left(-408 - 160 \frac{1}{z} - 336z - 88z^2 \right) \\
& + \log(z) \log^2(1+z) \left(216 + 96 \frac{1}{z} + 144z + 24z^2 \right) \\
& + \log(z) \log(1-z) \left(-\frac{512}{3} + \frac{352}{3} \frac{1}{1-z} - \frac{176}{3} z - \frac{128}{3} z^2 \right) \\
& + \log^2(z) \left(\frac{631}{3} - 44 \frac{1}{1-z} + \frac{667}{3} z + \frac{314}{3} z^2 \right) \\
& + \log^2(z) \log(1+z) \left(-180 - 80 \frac{1}{z} - 120z - 20z^2 \right) \\
& + \log^2(z) \log(1-z) \left(-8 + 16 \frac{1}{1-z} - 8z \right) \\
& + \log^3(z) \left(-10 - \frac{16}{3} \frac{1}{1-z} - 14z - \frac{4}{3} z^2 \right) + \delta(1-z) \left(-\frac{5941}{36} \right) \\
& + \log \left(\frac{Q^2}{\mu_F^2} \right) \left[\left(\frac{212}{9} - \frac{176}{9} \frac{1}{z} + \frac{536}{9} \frac{1}{1-z} - \frac{748}{9} z + \frac{176}{9} z^2 \right) \right. \\
& + \log(1-z) \left(\frac{88}{3} - \frac{176}{3} \frac{1}{1-z} + \frac{88}{3} z \right) + \log(z) \left(-\frac{64}{3} + \frac{176}{3} \frac{1}{1-z} - \frac{64}{3} z \right) \\
& \left. + \log^2(z) \left(-4 + 8 \frac{1}{1-z} - 4z \right) + \delta(1-z) (79) \right] \\
& + \log^2 \left(\frac{Q^2}{\mu_F^2} \right) \left[\left(\frac{22}{3} - \frac{44}{3} \frac{1}{1-z} + \frac{22}{3} z \right) + \delta(1-z) (-11) \right] \\
& + \zeta_3 \left(-28 + 56 \frac{1}{1-z} - 28z \right) + \zeta_3 \delta(1-z) (92) \\
& + \zeta_3 \log \left(\frac{Q^2}{\mu_F^2} \right) \delta(1-z) (-24) \\
& + \zeta_2 \left(-\frac{688}{3} - \frac{272}{3} \frac{1}{z} + \frac{176}{3} \frac{1}{1-z} - \frac{604}{3} z - \frac{100}{3} z^2 \right) \\
& + \zeta_2 \log(1+z) \left(216 + 96 \frac{1}{z} + 144z + 24z^2 \right) + \zeta_2 \log(1-z) \left(16 - 32 \frac{1}{1-z} + 16z \right) \\
& + \zeta_2 \log(z) \left(-80 - 32 \frac{1}{z} + 16 \frac{1}{1-z} - 56z - 8z^2 \right) + \zeta_2 \delta(1-z) \left(\frac{328}{9} \right) \\
& + \zeta_2 \log \left(\frac{Q^2}{\mu_F^2} \right) \left(8 - 16 \frac{1}{1-z} + 8z \right) + \zeta_2^2 \delta(1-z) \left(-\frac{12}{5} \right) \Big\}, \\
\bar{\mathcal{A}}_{qq}^{h,(2)} = \mathbf{C}_F & \left\{ \left(\frac{5417}{9} - \frac{12304}{27} \frac{1}{z} - \frac{1550}{9} z + \frac{703}{27} z^2 \right) \right.
\end{aligned}$$

$$\begin{aligned}
& + S_{1,2}(1-z) \left(144 + 128 \frac{1}{z^2} + 64 \frac{1}{z} + 64z \right) \\
& + S_{1,2}(-z) \left(-288 - 384 \frac{1}{z^2} - 576 \frac{1}{z} - 48z \right) \\
& + \text{Li}_3(1-z) \left(312 + 64 \frac{1}{z^2} + 128 \frac{1}{z} + 12z \right) \\
& + \text{Li}_3(-z) \left(-144 - 320 \frac{1}{z^2} + 672 \frac{1}{z} + 40z \right) \\
& + \text{Li}_2(1-z) \left(-248 + \frac{736}{3} \frac{1}{z} - 108z + \frac{32}{3} z^2 \right) + \text{Li}_2(-z) \left(488 + 448 \frac{1}{z} + 40z \right) \\
& + \log(1+z) \text{Li}_2(-z) \left(-288 - 384 \frac{1}{z^2} - 576 \frac{1}{z} - 48z \right) \\
& + \log(1-z) \left(-\frac{1160}{3} + \frac{3272}{9} \frac{1}{z} + \frac{128}{3} z - \frac{176}{9} z^2 \right) \\
& + \log(1-z) \text{Li}_2(1-z) \left(-224 - 256 \frac{1}{z} - 32z \right) \\
& + \log^2(1-z) \left(136 - \frac{544}{3} \frac{1}{z} + 56z - \frac{32}{3} z^2 \right) \\
& + \log(z) \left(\frac{974}{3} - 284 \frac{1}{z} - \frac{68}{3} z + \frac{40}{9} z^2 \right) + \log(z) \text{Li}_2(1-z) \left(32 + 224 \frac{1}{z} + 52z \right) \\
& + \log(z) \text{Li}_2(-z) \left(192 + 320 \frac{1}{z^2} - 96 \frac{1}{z} \right) + \log(z) \log(1+z) \left(488 + 448 \frac{1}{z} + 40z \right) \\
& + \log(z) \log^2(1+z) \left(-144 - 192 \frac{1}{z^2} - 288 \frac{1}{z} - 24z \right) \\
& + \log(z) \log(1-z) \left(-232 + 192 \frac{1}{z} - 96z + 32z^2 \right) \\
& + \log(z) \log^2(1-z) \left(-112 - 128 \frac{1}{z} - 16z \right) \\
& + \log^2(z) \left(-277 - 48 \frac{1}{z} - 35z - \frac{40}{3} z^2 \right) \\
& + \log^2(z) \log(1+z) \left(120 + 160 \frac{1}{z^2} + 240 \frac{1}{z} + 20z \right) \\
& + \log^2(z) \log(1-z) \left(48 + 64 \frac{1}{z} \right) + \log^3(z) \left(-\frac{14}{3} - \frac{64}{3} \frac{1}{z} + \frac{34}{3} z \right) \\
& + \log \left(\frac{Q^2}{\mu_F^2} \right) \left[\left(-\frac{580}{3} + \frac{1636}{9} \frac{1}{z} + \frac{64}{3} z - \frac{88}{9} z^2 \right) \right. \\
& \left. + \text{Li}_2(1-z) \left(-112 - 128 \frac{1}{z} - 16z \right) + \log(1-z) \left(136 - \frac{544}{3} \frac{1}{z} + 56z - \frac{32}{3} z^2 \right) \right]
\end{aligned}$$

$$\begin{aligned}
& + \log(z) \left(-116 + 96 \frac{1}{z} - 48z + 16z^2 \right) \\
& + \log(z) \log(1-z) \left(-112 - 128 \frac{1}{z} - 16z \right) + \log^2(z) \left(24 + 32 \frac{1}{z} \right) \Bigg] \\
& + \log^2 \left(\frac{Q^2}{\mu_F^2} \right) \left[\left(34 - \frac{136}{3} \frac{1}{z} + 14z - \frac{8}{3} z^2 \right) + \log(z) \left(-28 - 32 \frac{1}{z} - 4z \right) \right] \\
& + \zeta_3 \left(-72 - 192 \frac{1}{z^2} + 576 \frac{1}{z} + 36z \right) + \zeta_2 \left(108 + \frac{1216}{3} \frac{1}{z} - 36z + \frac{32}{3} z^2 \right) \\
& + \zeta_2 \log(1+z) \left(-144 - 192 \frac{1}{z^2} - 288 \frac{1}{z} - 24z \right) + \zeta_2 \log(z) \left(136 + 416 \frac{1}{z} + 36z \right) \Bigg\} \\
& + \mathbf{C_F}^2 \left\{ \left(-194 + 72 \frac{1}{z} + 148z - 26z^2 \right) \right. \\
& + S_{1,2}(1-z) \left(-208 - 192 \frac{1}{z} + 128 \frac{1}{1+z} + 160z - 16z^2 \right) \\
& + S_{1,2}(-z) \left(256 \frac{1}{z} - 64 \frac{1}{1+z} \right) + \text{Li}_3 \left(\frac{1-z}{1+z} \right) \left(-64 + 128 \frac{1}{1+z} + 64z \right) \\
& + \text{Li}_3 \left(-\frac{1-z}{1+z} \right) \left(64 - 128 \frac{1}{1+z} - 64z \right) \\
& + \text{Li}_3(1-z) \left(208 - 64 \frac{1}{z} - 128 \frac{1}{1+z} - 160z + 16z^2 \right) \\
& + \text{Li}_3(-z) \left(32 - 128 \frac{1}{z} - 32 \frac{1}{1+z} - 32z \right) \\
& + \text{Li}_2(1-z) \left(88 - 96 \frac{1}{z} + 96z - 24z^2 \right) + \text{Li}_2(-z) \left(-112 - 192 \frac{1}{z} + 80z \right) \\
& + \log(1+z) \text{Li}_2(-z) \left(256 \frac{1}{z} - 64 \frac{1}{1+z} \right) + \log(1-z) \left(64 - 64z \right) \\
& + \log(1-z) \text{Li}_2(-z) \left(64 - 128 \frac{1}{1+z} - 64z \right) + \log(z) \left(-32 + 68z \right) \\
& + \log(z) \text{Li}_2(1-z) \left(-192 - 64 \frac{1}{z} + 96 \frac{1}{1+z} + 144z - 16z^2 \right) \\
& + \log(z) \text{Li}_2(-z) \left(-64 + 128 \frac{1}{1+z} + 64z \right) \\
& + \log(z) \log(1+z) \left(-112 - 192 \frac{1}{z} + 80z \right) \\
& + \log(z) \log^2(1+z) \left(128 \frac{1}{z} - 32 \frac{1}{1+z} \right) + \log(z) \log(1-z) \left(32 + 32z \right) \\
& + \log(z) \log(1-z) \log(1+z) \left(64 - 128 \frac{1}{1+z} - 64z \right) + \log^2(z) \left(44 - 12z^2 \right)
\end{aligned}$$

$$\begin{aligned}
& + \log^2(z) \log(1+z) \left(-48 - 64 \frac{1}{z} + 112 \frac{1}{1+z} + 48z \right) \\
& + \log^2(z) \log(1-z) \left(-16 + 32 \frac{1}{1+z} + 16z \right) \\
& + \log^3(z) \left(-20 - \frac{32}{3} \frac{1}{1+z} + 12z - \frac{8}{3} z^2 \right) \\
& + \log \left(\frac{Q^2}{\mu_F^2} \right) \left[\left(32 - 32z \right) + \text{Li}_2(-z) \left(32 - 64 \frac{1}{1+z} - 32z \right) \right. \\
& + \log(z) \left(16 + 16z \right) + \log(z) \log(1+z) \left(32 - 64 \frac{1}{1+z} - 32z \right) \\
& + \log^2(z) \left(-8 + 16 \frac{1}{1+z} + 8z \right) \left. \right] \\
& + \zeta_3 \left(24 - 128 \frac{1}{z} - 16 \frac{1}{1+z} - 24z \right) + \zeta_2 \left(-56 - 96 \frac{1}{z} + 40z \right) \\
& + \zeta_2 \log(1+z) \left(128 \frac{1}{z} - 32 \frac{1}{1+z} \right) + \zeta_2 \log(1-z) \left(32 - 64 \frac{1}{1+z} - 32z \right) \\
& + \zeta_2 \log(z) \left(-16 - 64 \frac{1}{z} + 48 \frac{1}{1+z} + 16z \right) \\
& + \zeta_2 \log \left(\frac{Q^2}{\mu_F^2} \right) \left(16 - 32 \frac{1}{1+z} - 16z \right) \left. \right\} \\
& + \mathbf{C}_A \mathbf{C}_F \left\{ \left(97 - 36 \frac{1}{z} - 74z + 13z^2 \right) \right. \\
& + S_{1,2}(1-z) \left(104 + 96 \frac{1}{z} - 64 \frac{1}{1+z} - 80z + 8z^2 \right) \\
& + S_{1,2}(-z) \left(-128 \frac{1}{z} + 32 \frac{1}{1+z} \right) + \text{Li}_3 \left(\frac{1-z}{1+z} \right) \left(32 - 64 \frac{1}{1+z} - 32z \right) \\
& + \text{Li}_3 \left(-\frac{1-z}{1+z} \right) \left(-32 + 64 \frac{1}{1+z} + 32z \right) \\
& + \text{Li}_3(1-z) \left(-104 + 32 \frac{1}{z} + 64 \frac{1}{1+z} + 80z - 8z^2 \right) \\
& + \text{Li}_3(-z) \left(-16 + 64 \frac{1}{z} + 16 \frac{1}{1+z} + 16z \right) \\
& + \text{Li}_2(1-z) \left(-44 + 48 \frac{1}{z} - 48z + 12z^2 \right) + \text{Li}_2(-z) \left(56 + 96 \frac{1}{z} - 40z \right) \\
& + \log(1+z) \text{Li}_2(-z) \left(-128 \frac{1}{z} + 32 \frac{1}{1+z} \right) + \log(1-z) \left(-32 + 32z \right) \\
& + \log(1-z) \text{Li}_2(-z) \left(-32 + 64 \frac{1}{1+z} + 32z \right) + \log(z) \left(16 - 34z \right)
\end{aligned}$$

$$\begin{aligned}
& + \log(z) \text{Li}_2(1-z) \left(96 + 32 \frac{1}{z} - 48 \frac{1}{1+z} - 72z + 8z^2 \right) \\
& + \log(z) \text{Li}_2(-z) \left(32 - 64 \frac{1}{1+z} - 32z \right) + \log(z) \log(1+z) \left(56 + 96 \frac{1}{z} - 40z \right) \\
& + \log(z) \log^2(1+z) \left(-64 \frac{1}{z} + 16 \frac{1}{1+z} \right) + \log(z) \log(1-z) \left(-16 - 16z \right) \\
& + \log(z) \log(1-z) \log(1+z) \left(-32 + 64 \frac{1}{1+z} + 32z \right) + \log^2(z) \left(-22 + 6z^2 \right) \\
& + \log^2(z) \log(1+z) \left(24 + 32 \frac{1}{z} - 56 \frac{1}{1+z} - 24z \right) \\
& + \log^2(z) \log(1-z) \left(8 - 16 \frac{1}{1+z} - 8z \right) + \log^3(z) \left(10 + \frac{16}{3} \frac{1}{1+z} - 6z + \frac{4}{3} z^2 \right) \\
& + \log \left(\frac{Q^2}{\mu_F^2} \right) \left[\left(-16 + 16z \right) + \text{Li}_2(-z) \left(-16 + 32 \frac{1}{1+z} + 16z \right) \right. \\
& + \log(z) \left(-8 - 8z \right) + \log(z) \log(1+z) \left(-16 + 32 \frac{1}{1+z} + 16z \right) \\
& \left. + \log^2(z) \left(4 - 8 \frac{1}{1+z} - 4z \right) \right] \\
& + \zeta_3 \left(-12 + 64 \frac{1}{z} + 8 \frac{1}{1+z} + 12z \right) + \zeta_2 \left(28 + 48 \frac{1}{z} - 20z \right) \\
& + \zeta_2 \log(1+z) \left(-64 \frac{1}{z} + 16 \frac{1}{1+z} \right) + \zeta_2 \log(1-z) \left(-16 + 32 \frac{1}{1+z} + 16z \right) \\
& + \zeta_2 \log(z) \left(8 + 32 \frac{1}{z} - 24 \frac{1}{1+z} - 8z \right) + \zeta_2 \log \left(\frac{Q^2}{\mu_F^2} \right) \left(-8 + 16 \frac{1}{1+z} + 8z \right) \Big\}, \\
\bar{A}_{q_1 q_2}^{h,(2)} = & \mathbf{C_F} \left\{ \left(\frac{5417}{9} - \frac{12304}{27} \frac{1}{z} - \frac{1550}{9} z + \frac{703}{27} z^2 \right) \right. \\
& + S_{1,2}(1-z) \left(144 + 128 \frac{1}{z^2} + 64 \frac{1}{z} + 64z \right) \\
& + S_{1,2}(-z) \left(-288 - 384 \frac{1}{z^2} - 576 \frac{1}{z} - 48z \right) \\
& + \text{Li}_3(1-z) \left(312 + 64 \frac{1}{z^2} + 128 \frac{1}{z} + 12z \right) \\
& + \text{Li}_3(-z) \left(-144 - 320 \frac{1}{z^2} + 672 \frac{1}{z} + 40z \right) \\
& + \text{Li}_2(1-z) \left(-248 + \frac{736}{3} \frac{1}{z} - 108z + \frac{32}{3} z^2 \right) + \text{Li}_2(-z) \left(488 + 448 \frac{1}{z} + 40z \right) \\
& \left. + \log(1+z) \text{Li}_2(-z) \left(-288 - 384 \frac{1}{z^2} - 576 \frac{1}{z} - 48z \right) \right\}
\end{aligned}$$

$$\begin{aligned}
& + \log(1-z) \left(-\frac{1160}{3} + \frac{3272}{9} \frac{1}{z} + \frac{128}{3} z - \frac{176}{9} z^2 \right) \\
& + \log(1-z) \text{Li}_2(1-z) \left(-224 - 256 \frac{1}{z} - 32z \right) \\
& + \log^2(1-z) \left(136 - \frac{544}{3} \frac{1}{z} + 56z - \frac{32}{3} z^2 \right) + \log(z) \left(\frac{974}{3} - 284 \frac{1}{z} - \frac{68}{3} z + \frac{40}{9} z^2 \right) \\
& + \log(z) \text{Li}_2(1-z) \left(32 + 224 \frac{1}{z} + 52z \right) + \log(z) \text{Li}_2(-z) \left(192 + 320 \frac{1}{z^2} - 96 \frac{1}{z} \right) \\
& + \log(z) \log(1+z) \left(488 + 448 \frac{1}{z} + 40z \right) \\
& + \log(z) \log^2(1+z) \left(-144 - 192 \frac{1}{z^2} - 288 \frac{1}{z} - 24z \right) \\
& + \log(z) \log(1-z) \left(-232 + 192 \frac{1}{z} - 96z + 32z^2 \right) \\
& + \log(z) \log^2(1-z) \left(-112 - 128 \frac{1}{z} - 16z \right) + \log^2(z) \left(-277 - 48 \frac{1}{z} - 35z - \frac{40}{3} z^2 \right) \\
& + \log^2(z) \log(1+z) \left(120 + 160 \frac{1}{z^2} + 240 \frac{1}{z} + 20z \right) \\
& + \log^2(z) \log(1-z) \left(48 + 64 \frac{1}{z} \right) + \log^3(z) \left(-\frac{14}{3} - \frac{64}{3} \frac{1}{z} + \frac{34}{3} z \right) \\
& + \log \left(\frac{Q^2}{\mu_F^2} \right) \left[\left(-\frac{580}{3} + \frac{1636}{9} \frac{1}{z} + \frac{64}{3} z - \frac{88}{9} z^2 \right) \right. \\
& + \text{Li}_2(1-z) \left(-112 - 128 \frac{1}{z} - 16z \right) + \log(1-z) \left(136 - \frac{544}{3} \frac{1}{z} + 56z - \frac{32}{3} z^2 \right) \\
& + \log(z) \left(-116 + 96 \frac{1}{z} - 48z + 16z^2 \right) \\
& + \log(z) \log(1-z) \left(-112 - 128 \frac{1}{z} - 16z \right) + \log^2(z) \left(24 + 32 \frac{1}{z} \right) \Big] \\
& + \log^2 \left(\frac{Q^2}{\mu_F^2} \right) \left[\left(34 - \frac{136}{3} \frac{1}{z} + 14z - \frac{8}{3} z^2 \right) + \log(z) \left(-28 - 32 \frac{1}{z} - 4z \right) \right] \\
& + \zeta_3 \left(-72 - 192 \frac{1}{z^2} + 576 \frac{1}{z} + 36z \right) + \zeta_2 \left(108 + \frac{1216}{3} \frac{1}{z} - 36z + \frac{32}{3} z^2 \right) \\
& + \zeta_2 \log(1+z) \left(-144 - 192 \frac{1}{z^2} - 288 \frac{1}{z} - 24z \right) \\
& + \zeta_2 \log(z) \left(136 + 416 \frac{1}{z} + 36z \right) \Big\},
\end{aligned}$$

$$\bar{A}_{q_1 \bar{q}_2}^{h,(2)} = \bar{A}_{q_1 q_2}^{h,(2)}. \quad (11.30)$$

11.5 Results of the partonic cross sections: nonuniversal coupling

In the following we present the mass factorised partonic cross section. We use these results in section 7.2 to investigate the phenomenological impact of higher order QCD corrections. We set $\mu_R = \mu_F$ and present the results. For the gluon initiated processes, we obtain

$$\Delta_{gg}^{h,(0)} = \kappa_G^2 \delta(1-z) \left(1 \right), \quad (11.31)$$

$$\begin{aligned} \Delta_{gg}^{h,(1)} = & n_f \kappa_G \kappa_Q \left[\delta(1-z) \left(\frac{35}{9} \right) + \log \left(\frac{Q^2}{\mu_F^2} \right) \delta(1-z) \left(-\frac{4}{3} \right) \right] + C_A \kappa_G^2 \left[\left(-2 - \frac{22}{3} \frac{1}{z} \right. \right. \\ & + 2z + \frac{22}{3} z^2 \Big) + \log(1-z) \left(-32 + 16 \frac{1}{z} + 16 \frac{1}{1-z} + 16z - 16z^2 \right) + \log(z) \left(16 \right. \\ & - 8 \frac{1}{z} - 8 \frac{1}{1-z} - 8z + 8z^2 \Big) + \delta(1-z) \left(-\frac{203}{9} \right) + \log \left(\frac{Q^2}{\mu_F^2} \right) \left(-16 + 8 \frac{1}{z} \right. \\ & \left. \left. + 8 \frac{1}{1-z} + 8z - 8z^2 \right) + \log \left(\frac{Q^2}{\mu_F^2} \right) \delta(1-z) \left(\frac{22}{3} \right) + \zeta_2 \delta(1-z) \left(8 \right) \right], \quad (11.32) \end{aligned}$$

$$\begin{aligned} \Delta_{gg}^{h,(2)} = & n_f^2 \kappa_Q^2 \left[\delta(1-z) \left(\frac{1225}{324} \right) + \log \left(\frac{Q^2}{\mu_F^2} \right) \delta(1-z) \left(-\frac{70}{27} \right) + \log^2 \left(\frac{Q^2}{\mu_F^2} \right) \delta(1-z) \left(\frac{4}{9} \right) \right. \\ & \left. + \zeta_2 \delta(1-z) \left(\frac{8}{3} \right) \right] + C_F n_f \kappa_Q^2 \left[\left(-\frac{12566}{405} - \frac{686}{2025} \frac{1}{z^3} - \frac{4238}{405} \frac{1}{z^2} + \frac{36}{5} \frac{1}{z} - \frac{1447}{405} z \right. \right. \\ & + \frac{25787}{675} z^2 \Big) + S_{1,2}(1-z) \left(28 - 16 \frac{1}{z} - 56z - 28z^2 \right) + S_{1,2}(-z) \left(-72 - 32 \frac{1}{z} \right. \\ & - 48z - 8z^2 \Big) + \text{Li}_3(1-z) \left(8 + 32z + 32z^2 \right) + \text{Li}_3(-z) \left(-36 - 16 \frac{1}{z} + 8z \right. \\ & + 4z^2 \Big) + \text{Li}_2(1-z) \left(-\frac{226}{9} - \frac{212}{9} z + 28z^2 \right) + \text{Li}_2(-z) \left(20 + 16 \frac{1}{z} + 4z \right) \\ & + \log(1+z) \text{Li}_2(-z) \left(-72 - 32 \frac{1}{z} - 48z - 8z^2 \right) + \log(1-z) \left(-\frac{35}{27} + \frac{49}{135} \frac{1}{z^3} \right. \\ & + \frac{112}{27} \frac{1}{z^2} - \frac{128}{9} \frac{1}{z} + \frac{1895}{27} z - \frac{2663}{45} z^2 \Big) + \log(1-z) \text{Li}_2(1-z) \left(-8 - 32z - 32z^2 \right) \\ & \left. + \log^2(1-z) \left(-8 - 16z + 24z^2 \right) + \log(z) \left(-\frac{577}{54} - \frac{49}{270} \frac{1}{z^3} - \frac{56}{27} \frac{1}{z^2} - \frac{329}{9} \frac{1}{z} \right) \right] \end{aligned}$$

$$\begin{aligned}
& -\frac{2129}{54}z + \frac{4021}{90}z^2 \Big) + \log(z)\text{Li}_2(1-z) \Big(-2 - 8z - 8z^2 \Big) + \log(z)\text{Li}_2(-z) \Big(72 \\
& + 32\frac{1}{z} + 32z + 4z^2 \Big) + \log(z)\log(1+z) \Big(20 + 16\frac{1}{z} + 4z \Big) + \log(z)\log^2(1+z) \\
& \times \Big(-36 - 16\frac{1}{z} - 24z - 4z^2 \Big) + \log(z)\log(1-z) \Big(-\frac{118}{9} + \frac{4}{9}z - 8z^2 \Big) \\
& + \log(z)\log^2(1-z) \Big(-4 - 16z - 16z^2 \Big) + \log^2(z) \Big(-\frac{325}{9} - \frac{31}{3}\frac{1}{z} + \frac{7}{9}z - 4z^2 \Big) \\
& + \log^2(z)\log(1+z) \Big(54 + 24\frac{1}{z} + 36z + 6z^2 \Big) + \log^2(z)\log(1-z) \Big(2 + 8z + 8z^2 \Big) \\
& + \log^3(z) \Big(-\frac{19}{3} - \frac{8}{3}\frac{1}{z} - 8z - \frac{8}{3}z^2 \Big) + \log\left(\frac{Q^2}{\mu_F^2}\right) \Big(-\frac{35}{54} + \frac{49}{270}\frac{1}{z^3} + \frac{56}{27}\frac{1}{z^2} \\
& - \frac{64}{9}\frac{1}{z} + \frac{1895}{54}z - \frac{2663}{90}z^2 \Big) + \log\left(\frac{Q^2}{\mu_F^2}\right)\text{Li}_2(1-z) \Big(-4 - 16z - 16z^2 \Big) \\
& + \log\left(\frac{Q^2}{\mu_F^2}\right)\log(1-z) \Big(-8 - 16z + 24z^2 \Big) + \log\left(\frac{Q^2}{\mu_F^2}\right)\log(z) \Big(-\frac{59}{9} + \frac{2}{9}z - 4z^2 \Big) \\
& + \log\left(\frac{Q^2}{\mu_F^2}\right)\log(z)\log(1-z) \Big(-4 - 16z - 16z^2 \Big) + \log\left(\frac{Q^2}{\mu_F^2}\right)\log^2(z) \Big(1 + 4z + 4z^2 \Big) \\
& + \log^2\left(\frac{Q^2}{\mu_F^2}\right) \Big(-2 - 4z + 6z^2 \Big) + \log^2\left(\frac{Q^2}{\mu_F^2}\right)\log(z) \Big(-1 - 4z - 4z^2 \Big) + \zeta_3 \Big(-18 \\
& - 8\frac{1}{z} + 12z + 4z^2 \Big) + \zeta_2 \Big(18 + 8\frac{1}{z} + 18z - 24z^2 \Big) + \zeta_2\log(1+z) \Big(-36 - 16\frac{1}{z} \\
& - 24z - 4z^2 \Big) + \zeta_2\log(z) \Big(22 + 8\frac{1}{z} + 36z + 20z^2 \Big) \Big] \\
& + C_F n_f K_G K_Q \Big[\Big(-\frac{99068}{405} + \frac{1372}{2025} + \frac{8476}{405}\frac{1}{z^2} + \frac{1517}{45}\frac{1}{z} + \frac{57839}{405}z + \frac{31376}{675}z^2 \Big) \\
& + \text{Li}_3(-z) \Big(-64\frac{1}{z} - 64z \Big) + \text{Li}_2(1-z) \Big(\frac{560}{9} + \frac{712}{9}z \Big) + \text{Li}_2(-z) \Big(-32\frac{1}{z} + 32z \Big) \\
& + \log(1-z) \Big(\frac{1744}{27} - \frac{98}{135} - \frac{224}{27}\frac{1}{z^2} + \frac{304}{9}\frac{1}{z} - \frac{1414}{27}z - \frac{1664}{45}z^2 \Big) + \log(z) \Big(-\frac{2636}{27} \\
& + \frac{49}{135} + \frac{112}{27}\frac{1}{z^2} + \frac{526}{9}\frac{1}{z} - \frac{517}{27}z + \frac{1664}{45}z^2 \Big) + \log(z)\text{Li}_2(-z) \Big(32\frac{1}{z} + 32z \Big) \\
& + \log(z)\log(1+z) \Big(-32\frac{1}{z} + 32z \Big) + \log(z)\log(1-z) \Big(\frac{560}{9} + \frac{712}{9}z \Big) + \log^2(z) \\
& \times \Big(-\frac{124}{9} + \frac{68}{3}\frac{1}{z} - \frac{500}{9}z \Big) + \log^3(z) \Big(\frac{16}{3}\frac{1}{z} + \frac{16}{3}z \Big) + \delta(1-z) \Big(\frac{598}{81} \Big) \\
& + \log\left(\frac{Q^2}{\mu_F^2}\right) \Big(\frac{872}{27} - \frac{49}{135}\frac{1}{z^3} - \frac{112}{27}\frac{1}{z^2} + \frac{152}{9}\frac{1}{z} - \frac{707}{27}z - \frac{832}{45}z^2 \Big)
\end{aligned}$$

$$\begin{aligned}
& + \log\left(\frac{Q^2}{\mu_F^2}\right) \log(z) \left(\frac{280}{9} + \frac{356}{9}z\right) + \log\left(\frac{Q^2}{\mu_F^2}\right) \delta(1-z) \left(\frac{44}{9}\right) + \log^2\left(\frac{Q^2}{\mu_F^2}\right) \\
& \times \delta(1-z) \left(-\frac{16}{9}\right) + \zeta_3 \left(-48\frac{1}{z} - 48z\right) + \zeta_3 \delta(1-z) \left(-16\right) + \zeta_2 \left(-16\frac{1}{z} + 16z\right) \\
& + \zeta_2 \log(z) \left(-16\frac{1}{z} - 16z\right) + \zeta_2 \delta(1-z) \left(\frac{128}{9}\right) \Bigg] \\
& + C_F n_f \kappa_G^2 \left[\left(\frac{81754}{405} - \frac{686}{2025} \frac{1}{z^3} - \frac{4238}{405} \frac{1}{z^2} + \frac{3217}{135} \frac{1}{z} - \frac{73897}{405} z - \frac{2432}{75} z^2 \right) \right. \\
& + S_{1,2}(1-z) \left(32 + 32z \right) + \text{Li}_3(1-z) \left(-80 + 8\frac{1}{z} - 48z \right) + \text{Li}_2(1-z) \left(-\frac{352}{9} \right. \\
& + \frac{8}{3} \frac{1}{z} - \frac{644}{9} z + \frac{32}{3} z^2 \Bigg) + \log(1-z) \left(-\frac{3824}{27} + \frac{49}{135} \frac{1}{z^3} + \frac{112}{27} \frac{1}{z^2} - 48\frac{1}{z} + \frac{3443}{27} z \right. \\
& + \frac{288}{5} z^2 \Bigg) + \log(1-z) \text{Li}_2(1-z) \left(64 + 64z \right) + \log^2(1-z) \left(16 + \frac{64}{3} \frac{1}{z} - 16z - \frac{64}{3} z^2 \right) \\
& + \log(z) \left(\frac{3262}{27} - \frac{49}{270} \frac{1}{z^3} - \frac{56}{27} \frac{1}{z^2} + \frac{1}{3} \frac{1}{z} - \frac{4613}{54} z - \frac{288}{5} z^2 \right) + \log(z) \text{Li}_2(1-z) \\
& \times \left(-8\frac{1}{z} - 32z \right) + \log(z) \log(1-z) \left(-\frac{712}{9} - \frac{64}{3} \frac{1}{z} - \frac{428}{9} z + \frac{128}{3} z^2 \right) \\
& + \log(z) \log^2(1-z) \left(32 + 32z \right) + \log^2(z) \left(\frac{368}{9} - 7\frac{1}{z} + \frac{160}{9} z - 16z^2 \right) \\
& + \log^2(z) \log(1-z) \left(-32 - 32z \right) + \log^3(z) \left(12 - \frac{8}{3} \frac{1}{z} + \frac{4}{3} z \right) + \delta(1-z) \left(\frac{1049}{81} \right) \\
& + \log\left(\frac{Q^2}{\mu_F^2}\right) \left(-\frac{1912}{27} + \frac{49}{270} \frac{1}{z^3} + \frac{56}{27} \frac{1}{z^2} - 24\frac{1}{z} + \frac{3443}{54} z + \frac{144}{5} z^2 \right) + \log\left(\frac{Q^2}{\mu_F^2}\right) \\
& \times \text{Li}_2(1-z) \left(32 + 32z \right) + \log\left(\frac{Q^2}{\mu_F^2}\right) \log(1-z) \left(16 + \frac{64}{3} \frac{1}{z} - 16z - \frac{64}{3} z^2 \right) \\
& + \log\left(\frac{Q^2}{\mu_F^2}\right) \log(z) \left(-\frac{356}{9} - \frac{32}{3} \frac{1}{z} - \frac{214}{9} z + \frac{64}{3} z^2 \right) + \log\left(\frac{Q^2}{\mu_F^2}\right) \log(z) \log(1-z) \\
& \times \left(32 + 32z \right) + \log\left(\frac{Q^2}{\mu_F^2}\right) \log^2(z) \left(-16 - 16z \right) + \log\left(\frac{Q^2}{\mu_F^2}\right) \delta(1-z) \left(-\frac{80}{9} \right) \\
& + \log^2\left(\frac{Q^2}{\mu_F^2}\right) \left(4 + \frac{16}{3} \frac{1}{z} - 4z - \frac{16}{3} z^2 \right) + \log^2\left(\frac{Q^2}{\mu_F^2}\right) \log(z) \left(8 + 8z \right) \\
& + \log^2\left(\frac{Q^2}{\mu_F^2}\right) \delta(1-z) \left(\frac{16}{9} \right) + \zeta_2 \left(-16 - \frac{64}{3} \frac{1}{z} + 16z + \frac{64}{3} z^2 \right) + \zeta_2 \log(z) \left(-32 \right. \\
& - 32z \Bigg) + \zeta_2 \delta(1-z) \left(-\frac{128}{9} \right) \Bigg] \\
& + C_A n_f \kappa_Q^2 \left[\left(\frac{217}{108} - \frac{473}{5400} \frac{1}{z^3} + \frac{17}{27} \frac{1}{z^2} - \frac{82}{3} \frac{1}{z} + \frac{2753}{216} z + \frac{3611}{300} z^2 \right) + S_{1,2}(1-z) \right.
\end{aligned}$$

$$\begin{aligned}
& \times \left(-18 + 8\frac{1}{z} + 12z - 2z^2 \right) + S_{1,2}(-z) \left(36 + 16\frac{1}{z} + 24z + 4z^2 \right) + \text{Li}_3(-z) \left(54 \right. \\
& + 24\frac{1}{z} + 36z + 6z^2 \left. \right) + \text{Li}_2(-z) \left(12 + \frac{16}{3}\frac{1}{z} + 8z + \frac{4}{3}z^2 \right) + \log(1+z)\text{Li}_2(-z) \left(36 \right. \\
& + 16\frac{1}{z} + 24z + 4z^2 \left. \right) + \log(z) \left(-\frac{271}{9} - \frac{20}{9}\frac{1}{z} - \frac{365}{18}z - \frac{949}{90}z^2 \right) + \log(z)\text{Li}_2(-z) \\
& \times \left(-54 - 24\frac{1}{z} - 36z - 6z^2 \right) + \log(z)\log(1+z) \left(12 + \frac{16}{3}\frac{1}{z} + 8z + \frac{4}{3}z^2 \right) \\
& + \log(z)\log^2(1+z) \left(18 + 8\frac{1}{z} + 12z + 2z^2 \right) + \log^2(z) \left(9 - \frac{4}{3}\frac{1}{z} + 3z + \frac{25}{6}z^2 \right) \\
& + \log^2(z)\log(1+z) \left(-27 - 12\frac{1}{z} - 18z - 3z^2 \right) + \zeta_3 \left(36 + 16\frac{1}{z} + 24z \right. \\
& + 4z^2 \left. \right) + \zeta_2 \left(6 + \frac{8}{3}\frac{1}{z} + 4z + \frac{2}{3}z^2 \right) + \zeta_2 \log(1+z) \left(18 + 8\frac{1}{z} + 12z \right. \\
& + 2z^2 \left. \right) \Big] \\
& + C_{An_f K_G K_Q} \left[\left(\frac{820}{27} + \frac{473}{2700}\frac{1}{z^3} - \frac{34}{27}\frac{1}{z^2} - \frac{1049}{27}\frac{1}{z} - \frac{4469}{108}z + \frac{34388}{675}z^2 \right) \right. \\
& + S_{1,2}(1-z) \left(-32 + 32\frac{1}{z} + 16z \right) + \text{Li}_3(1-z) \left(16 - 16\frac{1}{z} - 8z \right) \\
& + \text{Li}_2(1-z) \left(\frac{40}{3} + \frac{8}{3}\frac{1}{z} - \frac{20}{3}z + 8z^2 \right) + \text{Li}_2(-z) \left(-32 - \frac{32}{3}\frac{1}{z} - 32z - \frac{32}{3}z^2 \right) \\
& + \log(1-z) \left(-\frac{616}{9} + \frac{314}{9}\frac{1}{z} + \frac{560}{9}\frac{1}{1-z} + \frac{182}{9}z - \frac{440}{9}z^2 \right) + \log(1-z)\text{Li}_2(1-z) \\
& \times \left(-16 + 16\frac{1}{z} + 8z \right) + \log^2(1-z) \left(8 - \frac{8}{3}\frac{1}{z} - 8z + \frac{8}{3}z^2 \right) + \log(z) \left(\frac{274}{9} - \frac{52}{3}\frac{1}{z} \right. \\
& - \frac{280}{9}\frac{1}{1-z} + \frac{49}{9}z + \frac{128}{15}z^2 \left. \right) + \log(z)\log(1+z) \left(-32 - \frac{32}{3}\frac{1}{z} - 32z - \frac{32}{3}z^2 \right) \\
& + \log(z)\log(1-z) \left(-\frac{80}{3} + \frac{32}{3}\frac{1}{z} + \frac{76}{3}z - \frac{16}{3}z^2 \right) + \log^2(z) \left(\frac{88}{3} - \frac{8}{3}\frac{1}{z} - \frac{20}{3}z \right. \\
& + 12z^2 \left. \right) + \delta(1-z) \left(-\frac{10295}{162} \right) + \log\left(\frac{Q^2}{\mu_F^2}\right) \left(-\frac{536}{9} + \frac{368}{9}\frac{1}{z} + \frac{280}{9}\frac{1}{1-z} \right. \\
& + \frac{256}{9}z - \frac{368}{9}z^2 \left. \right) + \log\left(\frac{Q^2}{\mu_F^2}\right)\log(1-z) \left(\frac{128}{3} - \frac{64}{3}\frac{1}{z} - \frac{64}{3}\frac{1}{1-z} - \frac{64}{3}z + \frac{64}{3}z^2 \right) \\
& + \log\left(\frac{Q^2}{\mu_F^2}\right)\log(z) \left(-\frac{64}{3} + \frac{32}{3}\frac{1}{z} + \frac{32}{3}\frac{1}{1-z} + \frac{32}{3}z - \frac{32}{3}z^2 \right) + \log\left(\frac{Q^2}{\mu_F^2}\right)\delta(1-z) \\
& \times \left(\frac{1127}{27} \right) + \log^2\left(\frac{Q^2}{\mu_F^2}\right) \left(\frac{64}{3} - \frac{32}{3}\frac{1}{z} - \frac{32}{3}\frac{1}{1-z} - \frac{32}{3}z + \frac{32}{3}z^2 \right)
\end{aligned}$$

$$\begin{aligned}
& + \log^2\left(\frac{Q^2}{\mu_F^2}\right) \delta(1-z) \left(-\frac{22}{3}\right) + \zeta_3 \delta(1-z) \left(16\right) + \zeta_2 \left(-56 + 8\frac{1}{z} + 24z - \frac{56}{3}z^2\right) \\
& + \zeta_2 \delta(1-z) \left(18\right) + \zeta_2 \log\left(\frac{Q^2}{\mu_F^2}\right) \delta(1-z) \left(-\frac{32}{3}\right) \Big] \\
& + C_A n_f \kappa_G^2 \Bigg[\left(-32 - \frac{473}{5400} \frac{1}{z^3} + \frac{17}{27} \frac{1}{z^2} + \frac{1561}{27} \frac{1}{z} + \frac{224}{27} \frac{1}{1-z} + \frac{171}{8} z - \frac{37819}{675} z^2\right) \\
& + \text{Li}_2(1-z) \left(-\frac{64}{3} + \frac{8}{3} \frac{1}{z} + \frac{8}{3} \frac{1}{1-z} - \frac{16}{3} z - \frac{16}{3} z^2\right) + \log(1-z) \left(\frac{440}{9} - \frac{152}{3} \frac{1}{z} \right. \\
& - \left. \frac{160}{9} \frac{1}{1-z} - \frac{292}{9} z + \frac{152}{3} z^2\right) + \log^2(1-z) \left(-\frac{64}{3} + \frac{32}{3} \frac{1}{z} + \frac{32}{3} \frac{1}{1-z} + \frac{32}{3} z - \frac{32}{3} z^2\right) \\
& + \log(z) \left(-\frac{190}{9} + \frac{178}{9} \frac{1}{z} + \frac{80}{9} \frac{1}{1-z} + \frac{373}{18} z - \frac{1472}{45} z^2\right) + \log(z) \log(1-z) \left(\frac{32}{3} \right. \\
& - \left. \frac{32}{3} \frac{1}{z} - \frac{32}{3} \frac{1}{1-z} - \frac{64}{3} z + \frac{32}{3} z^2\right) + \log^2(z) \left(-\frac{4}{3} + \frac{4}{3} \frac{1}{z} + \frac{4}{3} \frac{1}{1-z} + \frac{20}{3} z - \frac{8}{3} z^2\right) \\
& + \delta(1-z) \left(\frac{3656}{81}\right) + \log\left(\frac{Q^2}{\mu_F^2}\right) \left(\frac{220}{9} - \frac{76}{3} \frac{1}{z} - \frac{80}{9} \frac{1}{1-z} - \frac{140}{9} z + \frac{76}{3} z^2\right) \\
& + \log\left(\frac{Q^2}{\mu_F^2}\right) \log(1-z) \left(-\frac{64}{3} + \frac{32}{3} \frac{1}{z} + \frac{32}{3} \frac{1}{1-z} + \frac{32}{3} z - \frac{32}{3} z^2\right) \\
& + \log\left(\frac{Q^2}{\mu_F^2}\right) \log(z) \left(\frac{16}{3} - \frac{16}{3} \frac{1}{z} - \frac{16}{3} \frac{1}{1-z} - \frac{32}{3} z + \frac{16}{3} z^2\right) + \log\left(\frac{Q^2}{\mu_F^2}\right) \delta(1-z) \\
& \times \left(-\frac{160}{9}\right) + \log^2\left(\frac{Q^2}{\mu_F^2}\right) \left(-\frac{16}{3} + \frac{8}{3} \frac{1}{z} + \frac{8}{3} \frac{1}{1-z} + \frac{8}{3} z - \frac{8}{3} z^2\right) \\
& + \log^2\left(\frac{Q^2}{\mu_F^2}\right) \delta(1-z) \left(\frac{22}{9}\right) + \zeta_3 \delta(1-z) \left(\frac{16}{3}\right) + \zeta_2 \left(\frac{64}{3} - \frac{32}{3} \frac{1}{z} - \frac{32}{3} \frac{1}{1-z} \right. \\
& - \left. \frac{32}{3} z + \frac{32}{3} z^2\right) + \zeta_2 \delta(1-z) \left(-\frac{256}{9}\right) + \zeta_2 \log\left(\frac{Q^2}{\mu_F^2}\right) \delta(1-z) \left(\frac{16}{3}\right) \Big] \\
& + C_A^2 \kappa_G^2 \Bigg[\left(\frac{20137}{27} - \frac{21595}{27} \frac{1}{z} - \frac{1616}{27} \frac{1}{1-z} - \frac{6605}{27} z + \frac{9679}{27} z^2\right) + S_{1,2}(1-z) \\
& \times \left(64 \frac{1}{z^2} - 112 \frac{1}{z} - 144 \frac{1}{1-z} + 64 \frac{1}{1+z} - 528z + 112z^2\right) + S_{1,2}(-z) \left(-480 \right. \\
& - \left. 192 \frac{1}{z^2} - 320 \frac{1}{z} - 32 \frac{1}{1+z} - 288z - 64z^2\right) + \text{Li}_3\left(\frac{1-z}{1+z}\right) \left(-128 - 64 \frac{1}{z} \right. \\
& + \left. 64 \frac{1}{1+z} - 64z - 64z^2\right) + \text{Li}_3\left(-\frac{1-z}{1+z}\right) \left(128 + 64 \frac{1}{z} - 64 \frac{1}{1+z} + 64z + 64z^2\right) \\
& + \text{Li}_3(1-z) \left(744 + 32 \frac{1}{z^2} - 16 \frac{1}{z} - 8 \frac{1}{1-z} - 64 \frac{1}{1+z} + 536z + 88z^2\right) \\
& + \text{Li}_3(-z) \left(-272 - 160 \frac{1}{z^2} + 320 \frac{1}{z} - 16 \frac{1}{1+z} + 304z - 64z^2\right) + \text{Li}_2(1-z)
\end{aligned}$$

$$\begin{aligned}
& \times \left(-376 - \frac{748}{3} \frac{1}{z} - \frac{44}{3} \frac{1}{1-z} - 400z - \frac{704}{3} z^2 \right) + \text{Li}_2(-z) \left(296 + 264 \frac{1}{z} + 120z \right. \\
& \left. + 88z^2 \right) + \log(1+z) \text{Li}_2(-z) \left(-480 - 192 \frac{1}{z^2} - 320 \frac{1}{z} - 32 \frac{1}{1+z} - 288z - 64z^2 \right) \\
& + \log(1-z) \left(-\frac{1492}{9} + \frac{4396}{9} \frac{1}{z} - \frac{2176}{9} \frac{1}{1-z} + \frac{4040}{9} z - \frac{4756}{9} z^2 \right) \\
& + \log(1-z) \text{Li}_2(1-z) \left(-496 - 16 \frac{1}{z} - 544z \right) + \log(1-z) \text{Li}_2(-z) \left(128 + 64 \frac{1}{z} \right. \\
& \left. - 64 \frac{1}{1+z} + 64z + 64z^2 \right) + \log^2(1-z) \left(\frac{1324}{3} - 572 \frac{1}{z} - \frac{176}{3} \frac{1}{1-z} - \frac{1148}{3} z \right. \\
& \left. + 572z^2 \right) + \log^3(1-z) \left(-256 + 128 \frac{1}{z} + 128 \frac{1}{1-z} + 128z - 128z^2 \right) + \log(z) \\
& \times \left(\frac{946}{9} - \frac{1264}{3} \frac{1}{z} + \frac{1088}{9} \frac{1}{1-z} - \frac{2582}{9} z + \frac{5740}{9} z^2 \right) + \log(z) \text{Li}_2(1-z) \\
& \times \left(8 + 48 \frac{1}{z} - 56 \frac{1}{1-z} + 48 \frac{1}{1+z} + 24z + 8z^2 \right) + \log(z) \text{Li}_2(-z) \\
& \times \left(256 + 160 \frac{1}{z^2} - 64 \frac{1}{z} + 64 \frac{1}{1+z} - 64z + 16z^2 \right) + \log(z) \log(1+z) \left(296 + 264 \frac{1}{z} \right. \\
& \left. + 120z + 88z^2 \right) + \log(z) \log^2(1+z) \left(-240 - 96 \frac{1}{z^2} - 160 \frac{1}{z} - 16 \frac{1}{1+z} - 144z - 32z^2 \right) \\
& + \log(z) \log(1-z) \left(-832 + \frac{1232}{3} \frac{1}{z} + \frac{176}{3} \frac{1}{1-z} + 72z - 968z^2 \right) + \log(z) \log(1-z) \\
& \times \log(1+z) \left(128 + 64 \frac{1}{z} - 64 \frac{1}{1+z} + 64z + 64z^2 \right) + \log(z) \log^2(1-z) \left(240 - 248 \frac{1}{z} \right. \\
& \left. - 248 \frac{1}{1-z} - 504z + 248z^2 \right) + \log^2(z) \left(28 - \frac{220}{3} \frac{1}{z} - \frac{22}{3} \frac{1}{1-z} + 44z + \frac{550}{3} z^2 \right) \\
& + \log^2(z) \log(1+z) \left(120 + 80 \frac{1}{z^2} + 96 \frac{1}{z} + 56 \frac{1}{1+z} + 88z - 16z^2 \right) \\
& + \log^2(z) \log(1-z) \left(-96 + 112 \frac{1}{z} + 128 \frac{1}{1-z} + 16 \frac{1}{1+z} + 304z - 144z^2 \right) + \log^3(z) \\
& \times \left(-\frac{16}{3} - 16 \frac{1}{z} - \frac{56}{3} \frac{1}{1-z} - \frac{16}{3} \frac{1}{1+z} - \frac{184}{3} z + 24z^2 \right) + \delta(1-z) \left(\frac{7801}{324} \right) \\
& + C_A^2 \log \left(\frac{Q^2}{\mu_F^2} \right) \left(-\frac{518}{9} + 150 \frac{1}{z} - \frac{1088}{9} \frac{1}{1-z} + \frac{1606}{9} z - 150z^2 \right) \\
& + \log \left(\frac{Q^2}{\mu_F^2} \right) \text{Li}_2(1-z) \left(-256 - 256z \right) + \log \left(\frac{Q^2}{\mu_F^2} \right) \text{Li}_2(-z) \left(64 + 32 \frac{1}{z} \right. \\
& \left. - 32 \frac{1}{1+z} + 32z + 32z^2 \right) + \log \left(\frac{Q^2}{\mu_F^2} \right) \log(1-z) \left(\frac{752}{3} - \frac{1408}{3} \frac{1}{z} + \frac{176}{3} \frac{1}{1-z} \right)
\end{aligned}$$

$$\begin{aligned}
& -\frac{928}{3}z + \frac{1408}{3}z^2 \Big) + \log\left(\frac{Q^2}{\mu_F^2}\right) \log^2(1-z) \Big(-384 + 192\frac{1}{z} + 192\frac{1}{1-z} \\
& + 192z - 192z^2 \Big) + \log\left(\frac{Q^2}{\mu_F^2}\right) \log(z) \Big(-376 + \frac{440}{3}\frac{1}{z} - \frac{88}{3}\frac{1}{1-z} - 440z^2 \Big) \\
& + \log\left(\frac{Q^2}{\mu_F^2}\right) \log(z) \log(1+z) \Big(64 + 32\frac{1}{z} - 32\frac{1}{1+z} + 32z + 32z^2 \Big) \\
& + \log\left(\frac{Q^2}{\mu_F^2}\right) \log(z) \log(1-z) \Big(192 - 224\frac{1}{z} - 224\frac{1}{1-z} - 480z + 224z^2 \Big) \\
& + \log\left(\frac{Q^2}{\mu_F^2}\right) \log^2(z) \Big(32\frac{1}{z} + 40\frac{1}{1-z} + 8\frac{1}{1+z} + 128z - 48z^2 \Big) \\
& + \log\left(\frac{Q^2}{\mu_F^2}\right) \delta(1-z) \Big(-\frac{1657}{27} \Big) + \log^2\left(\frac{Q^2}{\mu_F^2}\right) \Big(8 - \frac{220}{3}\frac{1}{z} + 44\frac{1}{1-z} - 52z \\
& + \frac{220}{3}z^2 \Big) + \log^2\left(\frac{Q^2}{\mu_F^2}\right) \log(1-z) \Big(-128 + 64\frac{1}{z} + 64\frac{1}{1-z} + 64z - 64z^2 \Big) \\
& + \log^2\left(\frac{Q^2}{\mu_F^2}\right) \log(z) \Big(-32\frac{1}{z} - 32\frac{1}{1-z} - 96z + 32z^2 \Big) \\
& + \log^2\left(\frac{Q^2}{\mu_F^2}\right) \delta(1-z) \Big(\frac{121}{9} \Big) + \zeta_3 \Big(-768 - 96\frac{1}{z^2} + 592\frac{1}{z} + 312\frac{1}{1-z} - 8\frac{1}{1+z} \\
& + 576z - 352z^2 \Big) + \zeta_3 \delta(1-z) \Big(-\frac{88}{3} \Big) + \zeta_3 \log\left(\frac{Q^2}{\mu_F^2}\right) \delta(1-z) \Big(152 \Big) \\
& + \zeta_2 \Big(-\frac{436}{3} + \frac{1628}{3}\frac{1}{z} + \frac{176}{3}\frac{1}{1-z} + \frac{884}{3}z - \frac{1100}{3}z^2 \Big) + \zeta_2 \log(1+z) \Big(-240 \\
& - 96\frac{1}{z^2} - 160\frac{1}{z} - 16\frac{1}{1+z} - 144z - 32z^2 \Big) + \zeta_2 \log(1-z) \Big(384 - 128\frac{1}{z} \\
& - 160\frac{1}{1-z} - 32\frac{1}{1+z} - 128z + 192z^2 \Big) + \zeta_2 \log(z) \Big(-40 + 272\frac{1}{z} \\
& + 144\frac{1}{1-z} + 24\frac{1}{1+z} + 520z - 168z^2 \Big) + \zeta_2 \delta(1-z) \Big(-\frac{224}{9} \Big) \\
& + \zeta_2 \log\left(\frac{Q^2}{\mu_F^2}\right) \Big(192 - 64\frac{1}{z} - 80\frac{1}{1-z} - 16\frac{1}{1+z} - 64z + 96z^2 \Big) \\
& + \zeta_2 \log\left(\frac{Q^2}{\mu_F^2}\right) \delta(1-z) \Big(\frac{88}{3} \Big) + \zeta_2 \log^2\left(\frac{Q^2}{\mu_F^2}\right) \delta(1-z) \Big(-32 \Big) \\
& + \zeta_2^2 \delta(1-z) \Big(-\frac{4}{5} \Big) \Big].
\end{aligned} \tag{11.33}$$

Unlike gluon gluon initiated process, the gluon quark initiated processes start at NLO level. The NLO,NNLO results are found to be

$$\begin{aligned} \Delta_{gq}^{h,(1)} = & \kappa_Q^2 \left[\left(\frac{77}{18} + \frac{7}{18} \frac{1}{z^3} + \frac{28}{9} \frac{1}{z^2} - \frac{16}{3} \frac{1}{z} + \frac{19}{18} z - \frac{7}{2} z^2 \right) + \log(1-z) \left(2 - 4z + 4z^2 \right) \right. \\ & + \log(z) \left(-1 + 2z - 2z^2 \right) + \log \left(\frac{Q^2}{\mu_F^2} \right) \left(1 - 2z + 2z^2 \right) \Big] + \kappa_{GKQ} \left[\left(-\frac{140}{9} \right. \right. \\ & - \frac{7}{9} \frac{1}{z^3} - \frac{56}{9} \frac{1}{z^2} + \frac{38}{3} \frac{1}{z} + \frac{89}{9} z \Big] + \kappa_G^2 \left[\left(\frac{142}{9} + \frac{7}{18} \frac{1}{z^3} + \frac{28}{9} \frac{1}{z^2} - \frac{40}{3} \frac{1}{z} - \frac{35}{18} z \right) \right. \\ & + \log(1-z) \left(-16 + 16 \frac{1}{z} + 8z \right) + \log(z) \left(8 - 8 \frac{1}{z} - 4z \right) \\ & \left. + \log \left(\frac{Q^2}{\mu_F^2} \right) \left(-8 + 8 \frac{1}{z} + 4z \right) \right], \end{aligned} \quad (11.34)$$

$$\begin{aligned} \Delta_{gq}^{h,(2)} = & n_f \kappa_Q^2 \left[\left(-\frac{860}{27} - \frac{7}{6} \frac{1}{z^3} - \frac{46}{3} \frac{1}{z^2} + \frac{760}{27} \frac{1}{z} + \frac{1091}{54} z \right) + \text{Li}_2(1-z) \left(-\frac{8}{3} + \frac{8}{3} \frac{1}{z} + \frac{4}{3} z \right) \right. \\ & + \log(1-z) \left(\frac{388}{27} + \frac{14}{27} \frac{1}{z^3} + \frac{112}{27} \frac{1}{z^2} - \frac{106}{9} \frac{1}{z} - \frac{340}{27} z + \frac{16}{3} z^2 \right) + \log(z) \left(-\frac{388}{27} \right. \\ & - \frac{14}{27} \frac{1}{z^3} - \frac{112}{27} \frac{1}{z^2} + \frac{106}{9} \frac{1}{z} + \frac{340}{27} z - \frac{16}{3} z^2 \Big) + \log(z) \log(1-z) \left(-\frac{8}{3} + \frac{8}{3} \frac{1}{z} + \frac{4}{3} z \right) \\ & + \log^2(z) \left(\frac{4}{3} - \frac{4}{3} \frac{1}{z} - \frac{2}{3} z \right) + \log \left(\frac{Q^2}{\mu_F^2} \right) \left(\frac{280}{27} + \frac{14}{27} \frac{1}{z^3} + \frac{112}{27} \frac{1}{z^2} - \frac{76}{9} \frac{1}{z} - \frac{178}{27} z \right) \Big] \\ & + n_f \kappa_{GKQ} \left[\left(\frac{2806}{27} + \frac{7}{3} \frac{1}{z^3} + \frac{796}{27} \frac{1}{z^2} - \frac{2369}{27} \frac{1}{z} - \frac{292}{9} z \right) + \text{Li}_2(1-z) \left(-8 + 8 \frac{1}{z} \right) \right. \\ & + \log(1-z) \left(-\frac{2276}{27} - \frac{28}{27} \frac{1}{z^3} - \frac{224}{27} \frac{1}{z^2} + \frac{706}{9} \frac{1}{z} + \frac{1250}{27} z \right) + \log(z) \left(\frac{1436}{27} \right. \\ & + \frac{28}{27} \frac{1}{z^3} + \frac{224}{27} \frac{1}{z^2} - \frac{142}{3} \frac{1}{z} - \frac{830}{27} z \Big) + \log(z) \log(1-z) \left(-8 + 8 \frac{1}{z} \right) \\ & + \log^2(z) \left(4 - 4 \frac{1}{z} \right) + \log \left(\frac{Q^2}{\mu_F^2} \right) \left(-\frac{1688}{27} - \frac{28}{27} \frac{1}{z^3} - \frac{224}{27} \frac{1}{z^2} + \frac{172}{3} \frac{1}{z} + \frac{668}{27} z \right) \\ & + \log \left(\frac{Q^2}{\mu_F^2} \right) \log(1-z) \left(\frac{64}{3} - \frac{64}{3} \frac{1}{z} - \frac{32}{3} z \right) + \log \left(\frac{Q^2}{\mu_F^2} \right) \log(z) \left(-\frac{32}{3} + \frac{32}{3} \frac{1}{z} \right. \\ & + \frac{16}{3} z \Big) + \log^2 \left(\frac{Q^2}{\mu_F^2} \right) \left(\frac{32}{3} - \frac{32}{3} \frac{1}{z} - \frac{16}{3} z \right) \Big] + n_f \kappa_G^2 \left[\left(-78 - \frac{7}{6} \frac{1}{z^3} - \frac{382}{27} \frac{1}{z^2} \right. \right. \\ & + \frac{1913}{27} \frac{1}{z} + \frac{1421}{54} z \Big) + \log(1-z) \left(\frac{1288}{27} + \frac{14}{27} \frac{1}{z^3} + \frac{112}{27} \frac{1}{z^2} - \frac{400}{9} \frac{1}{z} - \frac{646}{27} z \right) \\ & \left. + \log^2(1-z) \left(-\frac{8}{3} + \frac{8}{3} \frac{1}{z} + \frac{4}{3} z \right) + \log(z) \left(-\frac{1048}{27} - \frac{14}{27} \frac{1}{z^3} - \frac{112}{27} \frac{1}{z^2} + \frac{320}{9} \frac{1}{z} \right) \right] \end{aligned}$$

$$\begin{aligned}
& + \frac{454}{27}z \Big) + \log(z) \log(1-z) \left(\frac{32}{3} - \frac{32}{3} \frac{1}{z} - \frac{16}{3} z \right) + \log^2(z) \left(-\frac{16}{3} + \frac{16}{3} \frac{1}{z} + \frac{8}{3} z \right) \\
& + \log \left(\frac{Q^2}{\mu_F^2} \right) \left(\frac{1048}{27} + \frac{14}{27} \frac{1}{z^3} + \frac{112}{27} \frac{1}{z^2} - \frac{320}{9} \frac{1}{z} - \frac{454}{27} z \right) \\
& + \log \left(\frac{Q^2}{\mu_F^2} \right) \log(1-z) \left(-\frac{32}{3} + \frac{32}{3} \frac{1}{z} + \frac{16}{3} z \right) + \log \left(\frac{Q^2}{\mu_F^2} \right) \log(z) \left(\frac{32}{3} - \frac{32}{3} \frac{1}{z} \right. \\
& \left. - \frac{16}{3} z \right) + \log^2 \left(\frac{Q^2}{\mu_F^2} \right) \left(-\frac{16}{3} + \frac{16}{3} \frac{1}{z} + \frac{8}{3} z \right) \Big] + C_F \kappa_Q^2 \left[\left(-\frac{4201}{20} - \frac{5953}{5400} \frac{1}{z^3} \right. \right. \\
& \left. \left. + \frac{1813}{405} \frac{1}{z^2} + \frac{8528}{135} \frac{1}{z} + \frac{497971}{3240} z - \frac{41011}{2700} z^2 \right) + S_{1,2}(1-z) \left(-150 + 64 \frac{1}{z} + 108z \right. \right. \\
& \left. \left. - 68z^2 \right) + \text{Li}_3(1-z) \left(62 - 32 \frac{1}{z} - 28z + 36z^2 \right) + \text{Li}_3(-z) \left(144 - 64 \frac{1}{z} - 160z \right. \right. \\
& \left. \left. + 32z^2 \right) + \text{Li}_2(1-z) \left(\frac{583}{9} + \frac{14}{9} \frac{1}{z^3} + \frac{112}{9} \frac{1}{z^2} - \frac{160}{3} \frac{1}{z} - \frac{116}{3} z + \frac{184}{3} z^2 \right) \right. \\
& \left. + \text{Li}_2(-z) \left(40 - \frac{160}{3} \frac{1}{z} + 48z - \frac{136}{3} z^2 \right) + \log(1-z) \left(\frac{256}{3} - \frac{27}{5} \frac{1}{z^3} - \frac{1214}{27} \frac{1}{z^2} \right. \right. \\
& \left. \left. + 53 \frac{1}{z} - \frac{5347}{27} z + \frac{2968}{45} z^2 \right) + \log(1-z) \text{Li}_2(1-z) \left(-70 + 32 \frac{1}{z} + 44z - 52z^2 \right) \right. \\
& \left. + \log^2(1-z) \left(\frac{47}{3} + \frac{7}{3} \frac{1}{z^3} + \frac{56}{3} \frac{1}{z^2} - \frac{116}{3} \frac{1}{z} + \frac{145}{3} z - \frac{157}{3} z^2 \right) + \log^3(1-z) \left(\frac{35}{3} \right. \right. \\
& \left. \left. - \frac{70}{3} z + \frac{70}{3} z^2 \right) + \log(z) \left(-\frac{3985}{54} - \frac{119}{180} \frac{1}{z^3} - \frac{308}{27} \frac{1}{z^2} + 60 \frac{1}{z} + \frac{17041}{108} z \right. \right. \\
& \left. \left. - \frac{4139}{45} z^2 \right) + \log(z) \text{Li}_2(1-z) \left(2 - 4z \right) + \log(z) \text{Li}_2(-z) \left(-72 + 32 \frac{1}{z} + 80z \right. \right. \\
& \left. \left. - 16z^2 \right) + \log(z) \log(1+z) \left(40 - \frac{160}{3} \frac{1}{z} + 48z - \frac{136}{3} z^2 \right) \right. \\
& \left. + \log(z) \log(1-z) \left(-\frac{346}{9} - \frac{14}{9} \frac{1}{z^3} - \frac{112}{9} \frac{1}{z^2} + \frac{68}{3} \frac{1}{z} + \frac{116}{9} z + \frac{224}{3} z^2 \right) \right. \\
& \left. + \log(z) \log^2(1-z) \left(-21 + 42z - 66z^2 \right) + \log^2(z) \left(\frac{383}{12} + \frac{38}{3} \frac{1}{z} - \frac{914}{9} z + 31z^2 \right) \right. \\
& \left. + \log^2(z) \log(1-z) \left(12 - 24z + 40z^2 \right) + \log^3(z) \left(-\frac{27}{2} + \frac{16}{3} \frac{1}{z} + \frac{49}{3} z - \frac{26}{3} z^2 \right) \right. \\
& \left. + \log \left(\frac{Q^2}{\mu_F^2} \right) \left(\frac{244}{9} + \frac{119}{180} \frac{1}{z^3} + \frac{266}{27} \frac{1}{z^2} - \frac{121}{9} \frac{1}{z} - \frac{1301}{108} z - \frac{1561}{45} z^2 \right) \right. \\
& \left. + \log \left(\frac{Q^2}{\mu_F^2} \right) \text{Li}_2(1-z) \left(-24z^2 \right) + \log \left(\frac{Q^2}{\mu_F^2} \right) \log(1-z) \left(\frac{88}{9} + \frac{14}{9} \frac{1}{z^3} + \frac{112}{9} \frac{1}{z^2} \right. \right. \\
& \left. \left. - \frac{64}{3} \frac{1}{z} + \frac{350}{9} z - \frac{74}{3} z^2 \right) + \log \left(\frac{Q^2}{\mu_F^2} \right) \log^2(1-z) \left(18 - 36z + 36z^2 \right) \right.
\end{aligned}$$

$$\begin{aligned}
& + \log\left(\frac{Q^2}{\mu_F^2}\right) \log(z) \left(1 - \frac{133}{9}z + \frac{106}{3}z^2\right) + \log\left(\frac{Q^2}{\mu_F^2}\right) \log(z) \log(1-z) \left(-20\right. \\
& + 40z - 64z^2) + \log\left(\frac{Q^2}{\mu_F^2}\right) \log^2(z) \left(4 - 8z + 16z^2\right) + \log^2\left(\frac{Q^2}{\mu_F^2}\right) \left(\frac{23}{6} - \frac{14}{3}z\right. \\
& + \frac{32}{3}z^2) + \log^2\left(\frac{Q^2}{\mu_F^2}\right) \log(1-z) \left(6 - 12z + 12z^2\right) + \log^2\left(\frac{Q^2}{\mu_F^2}\right) \log(z) \left(-3\right. \\
& + 6z - 12z^2) + \zeta_3 \left(146 - 48\frac{1}{z} - 196z + 100z^2\right) + \zeta_2 \left(-\frac{758}{9} - \frac{28}{9}\frac{1}{z^3} - \frac{224}{9}\frac{1}{z^2}\right. \\
& + \frac{148}{3}\frac{1}{z} + \frac{1364}{9}z - 88z^2) + \zeta_2 \log(1-z) \left(-8 + 16z - 16z^2\right) \\
& + \zeta_2 \log(z) \left(44 - 16\frac{1}{z} - 56z + 48z^2\right) + \zeta_2 \log\left(\frac{Q^2}{\mu_F^2}\right) \left(-4 + 8z - 8z^2\right) \Big] \\
& + C_{FKGKQ} \left[\left(\frac{11522}{45} + \frac{5953}{2700}\frac{1}{z^3} - \frac{3626}{405}\frac{1}{z^2} - \frac{13651}{135}\frac{1}{z} - \frac{54091}{1620}z - \frac{77482}{675}z^2 \right) \right. \\
& + \text{Li}_3(1-z) \left(-32 + 16\frac{1}{z} + 32z\right) + \text{Li}_3(-z) \left(64\frac{1}{z} + 64z\right) + \text{Li}_2(1-z) \left(\frac{424}{9}\right. \\
& - \frac{28}{9}\frac{1}{z^3} - \frac{224}{9}\frac{1}{z^2} - \frac{8}{3}\frac{1}{z} - 116z) + \text{Li}_2(-z) \left(-64 - 16\frac{1}{z} - 48z\right) \\
& + \log(1-z) \left(\frac{1040}{9} + \frac{54}{5}\frac{1}{z^3} + \frac{2428}{27}\frac{1}{z^2} - \frac{548}{3}\frac{1}{z} - \frac{2314}{27}z + \frac{336}{5}z^2\right) \\
& + \log^2(1-z) \left(-\frac{280}{3} - \frac{14}{3}\frac{1}{z^3} - \frac{112}{3}\frac{1}{z^2} + 72\frac{1}{z} + \frac{190}{3}z\right) + \log(z) \left(\frac{1228}{27}\right. \\
& + \frac{119}{90}\frac{1}{z^3} + \frac{616}{27}\frac{1}{z^2} - 102\frac{1}{z} + \frac{2141}{54}z - \frac{168}{5}z^2) + \log(z) \text{Li}_2(1-z) \left(32 - 16\frac{1}{z}\right. \\
& - 32z) + \log(z) \text{Li}_2(-z) \left(-32\frac{1}{z} - 32z\right) + \log(z) \log(1+z) \left(-64 - 16\frac{1}{z} - 48z\right) \\
& + \log(z) \log(1-z) \left(\frac{824}{9} + \frac{28}{9}\frac{1}{z^3} + \frac{224}{9}\frac{1}{z^2} - \frac{172}{3}\frac{1}{z} - \frac{1576}{9}z\right) + \log^2(z) \left(\frac{148}{3}\right. \\
& - \frac{64}{3}\frac{1}{z} + \frac{808}{9}z) + \log^3(z) \left(\frac{32}{3} - \frac{32}{3}\frac{1}{z} - 16z\right) + \log\left(\frac{Q^2}{\mu_F^2}\right) \left(-\frac{652}{9} - \frac{119}{90}\frac{1}{z^3}\right. \\
& - \frac{532}{27}\frac{1}{z^2} + \frac{338}{9}\frac{1}{z} + \frac{605}{54}z + \frac{784}{15}z^2) + \log\left(\frac{Q^2}{\mu_F^2}\right) \log(1-z) \left(-\frac{656}{9} - \frac{28}{9}\frac{1}{z^3}\right. \\
& - \frac{224}{9}\frac{1}{z^2} + \frac{152}{3}\frac{1}{z} + \frac{548}{9}z - \frac{64}{3}z^2) + \log\left(\frac{Q^2}{\mu_F^2}\right) \log(z) \left(\frac{56}{3} - \frac{610}{9}z + \frac{32}{3}z^2\right) \\
& + \log^2\left(\frac{Q^2}{\mu_F^2}\right) \left(-\frac{16}{3} + \frac{32}{3}z - \frac{32}{3}z^2\right) + \zeta_3 \left(48\frac{1}{z} + 48z\right) + \zeta_2 \left(\frac{832}{9} + \frac{56}{9}\frac{1}{z^3}\right. \\
& + \frac{448}{9}\frac{1}{z^2} - \frac{268}{3}\frac{1}{z} - \frac{1108}{9}z) + \zeta_2 \log(z) \left(16\frac{1}{z} + 16z\right) \Big]
\end{aligned}$$

$$\begin{aligned}
& + C_F \kappa_G^2 \left[\left(-\frac{62}{15} - \frac{5953}{5400} \frac{1}{z^3} + \frac{1813}{405} \frac{1}{z^2} - \frac{5054}{45} \frac{1}{z} + \frac{138511}{3240} z + \frac{2208}{25} z^2 \right) \right. \\
& + S_{1,2}(1-z) \left(32 - 16z \right) + \text{Li}_3(1-z) \left(-64 \frac{1}{z} \right) + \text{Li}_3(-z) \left(-64 \frac{1}{z} - 64z \right) \\
& + \text{Li}_2(1-z) \left(\frac{496}{9} + \frac{14}{9} \frac{1}{z^3} + \frac{112}{9} \frac{1}{z^2} - \frac{224}{3} \frac{1}{z} + \frac{308}{3} z + \frac{64}{3} z^2 \right) + \text{Li}_2(-z) \left(64 \right. \\
& + 16 \frac{1}{z} + 48z \left. \right) + \log(1-z) \left(-\frac{2846}{9} - \frac{27}{5} \frac{1}{z^3} - \frac{1214}{27} \frac{1}{z^2} + \frac{2527}{9} \frac{1}{z} + \frac{2324}{27} z \right. \\
& - \left. \frac{784}{15} z^2 \right) + \log(1-z) \text{Li}_2(1-z) \left(64 \frac{1}{z} \right) + \log^2(1-z) \left(\frac{632}{3} + \frac{7}{3} \frac{1}{z^3} + \frac{56}{3} \frac{1}{z^2} \right. \\
& - 164 \frac{1}{z} - \frac{269}{3} z \left. \right) + \log^3(1-z) \left(-\frac{104}{3} + \frac{104}{3} \frac{1}{z} + \frac{52}{3} z \right) + \log(z) \left(\frac{508}{27} - \frac{119}{180} \frac{1}{z^3} \right. \\
& - \frac{308}{27} \frac{1}{z^2} + \frac{94}{9} \frac{1}{z} - \frac{9317}{108} z + \frac{352}{15} z^2 \left. \right) + \log(z) \text{Li}_2(1-z) \left(16 - 32 \frac{1}{z} - 8z \right) \\
& + \log(z) \text{Li}_2(-z) \left(32 \frac{1}{z} + 32z \right) + \log(z) \log(1+z) \left(64 + 16 \frac{1}{z} + 48z \right) \\
& + \log(z) \log(1-z) \left(-\frac{1648}{9} - \frac{14}{9} \frac{1}{z^3} - \frac{112}{9} \frac{1}{z^2} + \frac{320}{3} \frac{1}{z} + \frac{1748}{9} z + \frac{64}{3} z^2 \right) \\
& + \log(z) \log^2(1-z) \left(80 - 48 \frac{1}{z} - 40z \right) + \log^2(z) \left(\frac{26}{3} \frac{1}{z} - \frac{722}{9} z - \frac{32}{3} z^2 \right) \\
& + \log^2(z) \log(1-z) \left(-48 + 16 \frac{1}{z} + 24z \right) + \log^3(z) \left(\frac{20}{3} + \frac{16}{3} \frac{1}{z} + 2z \right) \\
& + \log \left(\frac{Q^2}{\mu_F^2} \right) \left(\frac{16}{3} + \frac{119}{180} \frac{1}{z^3} + \frac{266}{27} \frac{1}{z^2} - \frac{5}{9} \frac{1}{z} - \frac{2717}{108} z - \frac{392}{15} z^2 \right) \\
& + \log \left(\frac{Q^2}{\mu_F^2} \right) \text{Li}_2(1-z) \left(32 \frac{1}{z} \right) + \log \left(\frac{Q^2}{\mu_F^2} \right) \log(1-z) \left(\frac{1288}{9} + \frac{14}{9} \frac{1}{z^3} \right. \\
& + \frac{112}{9} \frac{1}{z^2} - \frac{304}{3} \frac{1}{z} - \frac{502}{9} z \left. \right) + \log \left(\frac{Q^2}{\mu_F^2} \right) \log^2(1-z) \left(-48 + 48 \frac{1}{z} + 24z \right) \\
& + \log \left(\frac{Q^2}{\mu_F^2} \right) \log(z) \left(-\frac{92}{3} + \frac{635}{9} z + \frac{32}{3} z^2 \right) + \log \left(\frac{Q^2}{\mu_F^2} \right) \log(z) \log(1-z) \left(64 \right. \\
& - 32 \frac{1}{z} - 32z \left. \right) + \log \left(\frac{Q^2}{\mu_F^2} \right) \log^2(z) \left(-16 + 8z \right) + \log^2 \left(\frac{Q^2}{\mu_F^2} \right) \left(8 - 2z \right) \\
& + \log^2 \left(\frac{Q^2}{\mu_F^2} \right) \log(1-z) \left(-16 + 16 \frac{1}{z} + 8z \right) + \log^2 \left(\frac{Q^2}{\mu_F^2} \right) \log(z) \left(8 - 4z \right) \\
& + \zeta_3 \left(-64 + 16 \frac{1}{z} - 16z \right) + \zeta_2 \left(-\frac{2000}{9} - \frac{28}{9} \frac{1}{z^3} - \frac{224}{9} \frac{1}{z^2} + \frac{632}{3} \frac{1}{z} + \frac{1148}{9} z \right) \\
& + \zeta_2 \log(1-z) \left(128 - 128 \frac{1}{z} - 64z \right) + \zeta_2 \log(z) \left(-96 + 48 \frac{1}{z} + 32z \right)
\end{aligned}$$

$$\begin{aligned}
& + \zeta_2 \log\left(\frac{Q^2}{\mu_F^2}\right) \left(64 - 64\frac{1}{z} - 32z\right) + C_A \kappa_Q^2 \left[\left(-\frac{32093}{810} + \frac{118543}{16200} \frac{1}{z^3}\right. \right. \\
& + \frac{6683}{405} \frac{1}{z^2} + \frac{14303}{135} \frac{1}{z} - \frac{422299}{3240} z + \frac{5729}{150} z^2 \Big) + S_{1,2}(1-z) \left(228 + 32\frac{1}{z} \right. \\
& + 112z + 16z^2 \Big) + \text{Li}_3\left(\frac{1-z}{1+z}\right) \left(8 + 16z + 16z^2\right) + \text{Li}_3\left(-\frac{1-z}{1+z}\right) \left(-8 \right. \\
& - 16z - 16z^2 \Big) + \text{Li}_3(1-z) \left(-62 + 16\frac{1}{z} - 52z - 24z^2\right) + \text{Li}_3(-z) \left(-4 - 8z \right. \\
& - 8z^2 \Big) + \text{Li}_2(1-z) \left(\frac{110}{9} + \frac{422}{3} \frac{1}{z} + \frac{604}{9} z + \frac{56}{3} z^2\right) + \text{Li}_2(-z) \left(20 + \frac{32}{3} \frac{1}{z} + 36z \right. \\
& + \frac{80}{3} z^2 \Big) + \log(1-z) \left(-\frac{2596}{27} - \frac{784}{135} \frac{1}{z^3} - \frac{430}{27} \frac{1}{z^2} + \frac{910}{9} \frac{1}{z} + \frac{955}{27} z - \frac{78}{5} z^2\right) \\
& + \log(1-z) \text{Li}_2(1-z) \left(60 - 16\frac{1}{z} + 24z + 20z^2\right) + \log(1-z) \text{Li}_2(-z) \left(-8 - 16z \right. \\
& - 16z^2 \Big) + \log^2(1-z) \left(\frac{100}{9} + \frac{14}{9} \frac{1}{z^3} + \frac{112}{9} \frac{1}{z^2} - \frac{38}{3} \frac{1}{z} + \frac{398}{9} z - \frac{170}{3} z^2\right) \\
& + \log^3(1-z) \left(\frac{13}{3} - \frac{26}{3} z + \frac{26}{3} z^2\right) + \log(z) \left(\frac{5462}{27} + \frac{679}{270} \frac{1}{z^3} + \frac{266}{27} \frac{1}{z^2} + \frac{239}{3} \frac{1}{z} \right. \\
& - \frac{239}{27} z - \frac{1213}{45} z^2 \Big) + \log(z) \text{Li}_2(1-z) \left(64 + 32\frac{1}{z} + 68z - 8z^2\right) \\
& + \log(z) \text{Li}_2(-z) \left(8 + 16z + 16z^2\right) + \log(z) \log(1+z) \left(20 + \frac{32}{3} \frac{1}{z} + 36z + \frac{80}{3} z^2\right) \\
& + \log(z) \log(1-z) \left(\frac{370}{9} - \frac{14}{9} \frac{1}{z^3} - \frac{112}{9} \frac{1}{z^2} + 64\frac{1}{z} + \frac{8}{9} z + \frac{422}{3} z^2\right) \\
& + \log(z) \log(1-z) \log(1+z) \left(-8 - 16z - 16z^2\right) + \log(z) \log^2(1-z) \left(2 + 44z \right. \\
& - 12z^2 \Big) + \log^2(z) \left(-\frac{821}{18} + \frac{44}{3} \frac{1}{z} - \frac{248}{9} z - \frac{221}{3} z^2\right) + \log^2(z) \log(1+z) \left(6 \right. \\
& + 12z + 12z^2 \Big) + \log^2(z) \log(1-z) \left(-6 - 28z + 4z^2\right) + \log^3(z) \left(\frac{41}{3} + \frac{16}{3} \frac{1}{z} \right. \\
& + \frac{40}{3} z \Big) + \log\left(\frac{Q^2}{\mu_F^2}\right) \left(-\frac{1043}{27} - \frac{679}{270} \frac{1}{z^3} - \frac{266}{27} \frac{1}{z^2} + \frac{497}{9} \frac{1}{z} - \frac{347}{54} z + \frac{21}{5} z^2\right) \\
& + \log\left(\frac{Q^2}{\mu_F^2}\right) \text{Li}_2(1-z) \left(12 + 24z + 8z^2\right) + \log\left(\frac{Q^2}{\mu_F^2}\right) \text{Li}_2(-z) \left(-4 - 8z - 8z^2\right) \\
& + \log\left(\frac{Q^2}{\mu_F^2}\right) \log(1-z) \left(\frac{190}{9} + \frac{14}{9} \frac{1}{z^3} + \frac{112}{9} \frac{1}{z^2} - 16\frac{1}{z} + \frac{254}{9} z - \frac{142}{3} z^2\right) \\
& + \log\left(\frac{Q^2}{\mu_F^2}\right) \log^2(1-z) \left(6 - 12z + 12z^2\right) + \log\left(\frac{Q^2}{\mu_F^2}\right) \log(z) \left(\frac{190}{9} + \frac{64}{3} \frac{1}{z} \right.
\end{aligned}$$

$$\begin{aligned}
& + \frac{104}{9}z + 56z^2 \Big) + \log\left(\frac{Q^2}{\mu_F^2}\right) \log(z) \log(1+z) \Big(-4 - 8z - 8z^2 \Big) \\
& + \log\left(\frac{Q^2}{\mu_F^2}\right) \log(z) \log(1-z) \Big(4 + 40z - 8z^2 \Big) + \log\left(\frac{Q^2}{\mu_F^2}\right) \log^2(z) \Big(-4 - 12z \Big) \\
& + \log^2\left(\frac{Q^2}{\mu_F^2}\right) \Big(1 + \frac{4}{3}\frac{1}{z} + 8z - \frac{31}{3}z^2 \Big) + \log^2\left(\frac{Q^2}{\mu_F^2}\right) \log(1-z) \Big(2 - 4z + 4z^2 \Big) \\
& + \log^2\left(\frac{Q^2}{\mu_F^2}\right) \log(z) \Big(2 + 8z \Big) + \zeta_3 \Big(-2 - 8z - 4z^2 \Big) + \zeta_2 \Big(\frac{658}{9} + \frac{14}{9}\frac{1}{z^3} \\
& + \frac{112}{9}\frac{1}{z^2} - 38\frac{1}{z} - \frac{952}{9}z + \frac{310}{3}z^2 \Big) + \zeta_2 \log(1-z) \Big(-16 + 16z - 32z^2 \Big) \\
& + \zeta_2 \log(z) \Big(-40z + 16z^2 \Big) + \zeta_2 \log\left(\frac{Q^2}{\mu_F^2}\right) \Big(-8 + 8z - 16z^2 \Big) \Big] \\
& + C_{AKGKQ} \Big[\Big(\frac{198053}{405} - \frac{118543}{8100}\frac{1}{z^3} - \frac{10726}{405}\frac{1}{z^2} - \frac{22192}{45}\frac{1}{z} + \frac{118519}{1620}z \\
& - \frac{18836}{675}z^2 \Big) + S_{1,2}(1-z) \Big(256 + 128\frac{1}{z^2} + 64\frac{1}{z} - 32z \Big) \\
& + S_{1,2}(-z) \Big(-448 - 384\frac{1}{z^2} - 640\frac{1}{z} - 128z \Big) + \text{Li}_3(1-z) \Big(112 + 64\frac{1}{z^2} - 128\frac{1}{z} \\
& - 32z \Big) + \text{Li}_3(-z) \Big(-352 - 320\frac{1}{z^2} + 576\frac{1}{z} + 128z \Big) + \text{Li}_2(1-z) \Big(-\frac{2896}{9} \\
& + \frac{362}{3}\frac{1}{z} - \frac{1148}{9}z - 16z^2 \Big) + \text{Li}_2(-z) \Big(544 + \frac{1552}{3}\frac{1}{z} + 48z + \frac{64}{3}z^2 \Big) \\
& + \log(1+z)\text{Li}_2(-z) \Big(-448 - 384\frac{1}{z^2} - 640\frac{1}{z} - 128z \Big) + \log(1-z) \Big(\frac{1232}{27} \\
& + \frac{1568}{135}\frac{1}{z^3} + \frac{860}{27}\frac{1}{z^2} - \frac{506}{3}\frac{1}{z} + \frac{1510}{27}z + \frac{1064}{45}z^2 \Big) + \log(1-z)\text{Li}_2(1-z) \Big(32 \\
& - 32\frac{1}{z} - 16z \Big) + \log^2(1-z) \Big(-\frac{632}{9} - \frac{28}{9}\frac{1}{z^3} - \frac{224}{9}\frac{1}{z^2} + 58\frac{1}{z} + \frac{410}{9}z - \frac{16}{3}z^2 \Big) \\
& + \log(z) \Big(-\frac{9340}{27} - \frac{679}{135}\frac{1}{z^3} - \frac{532}{27}\frac{1}{z^2} - 362\frac{1}{z} - \frac{2087}{27}z - \frac{1064}{45}z^2 \Big) \\
& + \log(z)\text{Li}_2(1-z) \Big(-48 + 224\frac{1}{z} + 48z \Big) + \log(z)\text{Li}_2(-z) \Big(384 + 320\frac{1}{z^2} \Big) \\
& + \log(z) \log(1+z) \Big(544 + \frac{1552}{3}\frac{1}{z} + 48z + \frac{64}{3}z^2 \Big) + \log(z) \log^2(1+z) \Big(-224 \\
& - 192\frac{1}{z^2} - 320\frac{1}{z} - 64z \Big) + \log(z) \log(1-z) \Big(\frac{184}{9} + \frac{28}{9}\frac{1}{z^3} + \frac{224}{9}\frac{1}{z^2} - \frac{488}{3}\frac{1}{z} \\
& - \frac{1954}{9}z + \frac{32}{3}z^2 \Big) + \log^2(z) \Big(-\frac{3952}{9} - 16\frac{1}{z} + \frac{754}{9}z - 24z^2 \Big)
\end{aligned}$$

$$\begin{aligned}
& + \log^2(z) \log(1+z) \left(208 + 160 \frac{1}{z^2} + 288 \frac{1}{z} + 64z \right) + \log^3(z) \left(-\frac{64}{3} - \frac{64}{3} \frac{1}{z} - \frac{16}{3} z \right) \\
& + \log \left(\frac{Q^2}{\mu_F^2} \right) \left(\frac{1780}{27} + \frac{679}{135} \frac{1}{z^3} + \frac{532}{27} \frac{1}{z^2} - \frac{406}{3} \frac{1}{z} + \frac{707}{27} z + \frac{832}{45} z^2 \right) \\
& + \log \left(\frac{Q^2}{\mu_F^2} \right) \log(1-z) \left(-\frac{560}{9} - \frac{28}{9} \frac{1}{z^3} - \frac{224}{9} \frac{1}{z^2} + \frac{152}{3} \frac{1}{z} + \frac{356}{9} z \right) \\
& + \log \left(\frac{Q^2}{\mu_F^2} \right) \log(z) \left(-\frac{560}{9} - \frac{152}{3} \frac{1}{z} - \frac{712}{9} z \right) + \zeta_3 \left(-208 - 192 \frac{1}{z^2} + 512 \frac{1}{z} \right. \\
& \left. + 112z \right) + \zeta_2 \left(\frac{2248}{9} - \frac{28}{9} \frac{1}{z^3} - \frac{224}{9} \frac{1}{z^2} + \frac{818}{3} \frac{1}{z} + \frac{302}{9} z + \frac{112}{3} z^2 \right) \\
& + \zeta_2 \log(1+z) \left(-224 - 192 \frac{1}{z^2} - 320 \frac{1}{z} - 64z \right) + \zeta_2 \log(z) \left(16 + 288 \frac{1}{z} + 64z \right) \Big] \\
& + C_A \kappa_G^2 \left[\left(\frac{135461}{405} + \frac{118543}{16200} \frac{1}{z^3} + \frac{4043}{405} \frac{1}{z^2} - \frac{57202}{135} \frac{1}{z} - \frac{111619}{3240} z - \frac{12082}{675} z^2 \right) \right. \\
& + S_{1,2}(1-z) \left(-464 - 240 \frac{1}{z} - 280z \right) + \text{Li}_3 \left(\frac{1-z}{1+z} \right) \left(-64 - 64 \frac{1}{z} - 32z \right) \\
& + \text{Li}_3 \left(-\frac{1-z}{1+z} \right) \left(64 + 64 \frac{1}{z} + 32z \right) + \text{Li}_3(1-z) \left(672 + 224 \frac{1}{z} + 304z \right) \\
& + \text{Li}_3(-z) \left(32 + 32 \frac{1}{z} + 16z \right) + \text{Li}_2(1-z) \left(-\frac{2680}{9} - \frac{812}{3} \frac{1}{z} - \frac{1052}{9} z - 32z^2 \right) \\
& + \text{Li}_2(-z) \left(-48 - 24 \frac{1}{z} - 16z \right) + \log(1-z) \left(-\frac{12490}{27} - \frac{784}{135} \frac{1}{z^3} - \frac{430}{27} \frac{1}{z^2} \right. \\
& \left. + \frac{1520}{3} \frac{1}{z} - \frac{2036}{27} z - \frac{512}{45} z^2 \right) + \log(1-z) \text{Li}_2(1-z) \left(-592 - 176 \frac{1}{z} - 280z \right) \\
& + \log(1-z) \text{Li}_2(-z) \left(64 + 64 \frac{1}{z} + 32z \right) + \log^2(1-z) \left(\frac{3868}{9} + \frac{14}{9} \frac{1}{z^3} + \frac{112}{9} \frac{1}{z^2} \right. \\
& \left. - 540 \frac{1}{z} + \frac{548}{9} z + 64z^2 \right) + \log^3(1-z) \left(-\frac{280}{3} + \frac{280}{3} \frac{1}{z} + \frac{140}{3} z \right) \\
& + \log(z) \left(\frac{14444}{27} + \frac{679}{270} \frac{1}{z^3} + \frac{266}{27} \frac{1}{z^2} - \frac{697}{3} \frac{1}{z} - \frac{320}{27} z + \frac{704}{15} z^2 \right) \\
& + \log(z) \text{Li}_2(1-z) \left(-64 - 64 \frac{1}{z} - 48z \right) + \log(z) \text{Li}_2(-z) \left(-64 - 64 \frac{1}{z} - 32z \right) \\
& + \log(z) \log(1+z) \left(-48 - 24 \frac{1}{z} - 16z \right) + \log(z) \log(1-z) \left(-\frac{8096}{9} - \frac{14}{9} \frac{1}{z^3} \right. \\
& \left. - \frac{112}{9} \frac{1}{z^2} + \frac{1504}{3} \frac{1}{z} - \frac{1798}{9} z - 128z^2 \right) + \log(z) \log(1-z) \log(1+z) \left(64 + 64 \frac{1}{z} \right. \\
& \left. + 32z \right) + \log(z) \log^2(1-z) \left(-120 - 264 \frac{1}{z} - 228z \right) + \log^2(z) \left(\frac{2828}{9} - \frac{280}{3} \frac{1}{z} \right.
\end{aligned}$$

$$\begin{aligned}
& + \frac{664}{9}z + \frac{112}{3}z^2 \Big) + \log^2(z) \log(1+z) \Big(-48 - 48\frac{1}{z} - 24z \Big) \\
& + \log^2(z) \log(1-z) \Big(96 + 128\frac{1}{z} + 128z \Big) + \log^3(z) \Big(-24 - \frac{32}{3}\frac{1}{z} - \frac{52}{3}z \Big) \\
& + \log\left(\frac{Q^2}{\mu_F^2}\right) \Big(-\frac{7118}{27} - \frac{679}{270}\frac{1}{z^3} - \frac{266}{27}\frac{1}{z^2} + \frac{2581}{9}\frac{1}{z} + \frac{85}{54}z - \frac{256}{45}z^2 \Big) \\
& + \log\left(\frac{Q^2}{\mu_F^2}\right) \text{Li}_2(1-z) \Big(-288 - 96\frac{1}{z} - 144z \Big) + \log\left(\frac{Q^2}{\mu_F^2}\right) \text{Li}_2(-z) \Big(32 + 32\frac{1}{z} \\
& + 16z \Big) + \log\left(\frac{Q^2}{\mu_F^2}\right) \log(1-z) \Big(\frac{3496}{9} + \frac{14}{9}\frac{1}{z^3} + \frac{112}{9}\frac{1}{z^2} - \frac{1472}{3}\frac{1}{z} + \frac{770}{9}z + 64z^2 \Big) \\
& + \log\left(\frac{Q^2}{\mu_F^2}\right) \log^2(1-z) \Big(-144 + 144\frac{1}{z} + 72z \Big) + \log\left(\frac{Q^2}{\mu_F^2}\right) \log(z) \Big(-\frac{3752}{9} \\
& + \frac{656}{3}\frac{1}{z} - \frac{1084}{9}z - 64z^2 \Big) + \log\left(\frac{Q^2}{\mu_F^2}\right) \log(z) \log(1+z) \Big(32 + 32\frac{1}{z} + 16z \Big) \\
& + \log\left(\frac{Q^2}{\mu_F^2}\right) \log(z) \log(1-z) \Big(-128 - 256\frac{1}{z} - 224z \Big) + \log\left(\frac{Q^2}{\mu_F^2}\right) \log^2(z) \Big(64 \\
& + 48\frac{1}{z} + 56z \Big) + \log^2\left(\frac{Q^2}{\mu_F^2}\right) \Big(\frac{200}{3} - \frac{284}{3}\frac{1}{z} + \frac{80}{3}z + 16z^2 \Big) \\
& + \log^2\left(\frac{Q^2}{\mu_F^2}\right) \log(1-z) \Big(-48 + 48\frac{1}{z} + 24z \Big) + \log^2\left(\frac{Q^2}{\mu_F^2}\right) \log(z) \Big(-48 - 48\frac{1}{z} \\
& - 48z \Big) + \zeta_3 \Big(-224 + 272\frac{1}{z} + 136z \Big) + \zeta_2 \Big(-\frac{1664}{9} + \frac{14}{9}\frac{1}{z^3} + \frac{112}{9}\frac{1}{z^2} + \frac{932}{3}\frac{1}{z} \\
& - \frac{826}{9}z - 64z^2 \Big) + \zeta_2 \log(1-z) \Big(64 \Big) + \zeta_2 \log(z) \Big(224 + 128\frac{1}{z} + 160z \Big) \\
& + \zeta_2 \log\left(\frac{Q^2}{\mu_F^2}\right) \Big(-8 + 8z - 16z^2 \Big) + \zeta_2 \log\left(\frac{Q^2}{\mu_F^2}\right) \Big(32 \Big) \Big], \tag{11.35}
\end{aligned}$$

The quark anti-quark initiated processes start at LO level and the results up to NNLO level are found to be

$$\begin{aligned}
\Delta_{q\bar{q}}^{h,(0)} &= \kappa_Q^2 \delta(1-z) \Big(1 \Big), \\
\Delta_{q\bar{q}}^{h,(1)} &= C_F \kappa_Q^2 \Big[\Big(-\frac{80}{9} + \frac{8}{9}\frac{1}{z^3} + \frac{8}{3}\frac{1}{z} + \frac{16}{3}z \Big) + \log(1-z) \Big(-8 + 16\frac{1}{1-z} - 8z \Big) \\
& + \log(z) \Big(4 - 8\frac{1}{1-z} + 4z \Big) + \delta(1-z) \Big(-\frac{248}{9} \Big) + \log\left(\frac{Q^2}{\mu_F^2}\right) \Big(-4 + 8\frac{1}{1-z} \\
& - 4z \Big) + \log\left(\frac{Q^2}{\mu_F^2}\right) \delta(1-z) \Big(\frac{34}{3} \Big) + \zeta_2 \delta(1-z) \Big(8 \Big) \Big] + C_F \kappa_G \kappa_Q \Big[\Big(\frac{160}{9} - \frac{16}{9}\frac{1}{z^3} \Big)
\end{aligned} \tag{11.36}$$

$$\begin{aligned}
& + \frac{8}{3} \frac{1}{z} - \frac{56}{3} z \Big) + \delta(1-z) \left(\frac{68}{9} \right) + \log \left(\frac{Q^2}{\mu_F^2} \right) \delta(1-z) \left(-\frac{16}{3} \right) \Big] \\
& + C_F K_G^2 \left[\left(-\frac{80}{9} + \frac{8}{9} \frac{1}{z^3} + \frac{40}{3} z - \frac{16}{3} z^2 \right) \right], \tag{11.37}
\end{aligned}$$

$$\begin{aligned}
\Delta_{q\bar{q}}^{h,(2)} = & C_F K_Q^2 \left[\left(\frac{39442}{81} - \frac{163}{81} \frac{1}{z^3} - \frac{5093}{81} \frac{1}{z^2} - \frac{4979}{18} \frac{1}{z} - \frac{27779}{162} z + \frac{703}{27} z^2 \right) \right. \\
& + S_{1,2}(1-z) \left(400 + 128 \frac{1}{z^2} + 320 \frac{1}{z} + 128z \right) + S_{1,2}(-z) \left(-288 - 384 \frac{1}{z^2} \right. \\
& - 576 \frac{1}{z} - 48z \Big) + \text{Li}_3(1-z) \left(56 + 64 \frac{1}{z^2} - 128 \frac{1}{z} - 52z \right) + \text{Li}_3(-z) \left(-144 \right. \\
& - 320 \frac{1}{z^2} + 672 \frac{1}{z} + 40z \Big) + \text{Li}_2(1-z) \left(-\frac{1112}{9} + \frac{1280}{3} \frac{1}{z} - \frac{400}{9} z + \frac{32}{3} z^2 \right) \\
& + \text{Li}_2(-z) \left(488 + 448 \frac{1}{z} + 40z \right) + \log(1+z) \text{Li}_2(-z) \left(-288 - 384 \frac{1}{z^2} \right. \\
& - 576 \frac{1}{z} - 48z \Big) + \log(1-z) \left(-\frac{2488}{27} + \frac{49}{27} \frac{1}{z^3} + \frac{896}{27} \frac{1}{z^2} + \frac{680}{9} \frac{1}{z} + \frac{31}{27} z - \frac{176}{9} z^2 \right) \\
& + \log(1-z) \text{Li}_2(1-z) \left(32 + 32z \right) + \log^2(1-z) \left(8 + \frac{32}{3} \frac{1}{z} - 8z - \frac{32}{3} z^2 \right) \\
& + \log(z) \left(\frac{2174}{27} - \frac{49}{54} \frac{1}{z^3} - \frac{448}{27} \frac{1}{z^2} - \frac{620}{3} \frac{1}{z} + \frac{2243}{54} z + \frac{40}{9} z^2 \right) \\
& + \log(z) \text{Li}_2(1-z) \left(96 + 288 \frac{1}{z} + 68z \right) + \log(z) \text{Li}_2(-z) \left(192 + 320 \frac{1}{z^2} - 96 \frac{1}{z} \right) \\
& + \log(z) \log(1+z) \left(488 + 448 \frac{1}{z} + 40z \right) + \log(z) \log^2(1+z) \left(-144 - 192 \frac{1}{z^2} \right. \\
& - 288 \frac{1}{z} - 24z \Big) + \log(z) \log(1-z) \left(\frac{760}{9} + \frac{256}{3} \frac{1}{z} + \frac{572}{9} z + 32z^2 \right) \\
& + \log(z) \log^2(1-z) \left(16 + 16z \right) + \log^2(z) \left(-\frac{3557}{9} - \frac{64}{3} \frac{1}{z} - \frac{817}{9} z - \frac{40}{3} z^2 \right) \\
& + \log^2(z) \log(1+z) \left(120 + 160 \frac{1}{z^2} + 240 \frac{1}{z} + 20z \right) + \log^2(z) \log(1-z) \left(-16 \right. \\
& - 16z \Big) + \log^3(z) \left(6 - \frac{32}{3} \frac{1}{z} + 14z \right) + \log \left(\frac{Q^2}{\mu_F^2} \right) \left(-\frac{1244}{27} + \frac{49}{54} \frac{1}{z^3} + \frac{448}{27} \frac{1}{z^2} \right. \\
& + \frac{340}{9} \frac{1}{z} + \frac{31}{54} z - \frac{88}{9} z^2 \Big) + \log \left(\frac{Q^2}{\mu_F^2} \right) \text{Li}_2(1-z) \left(16 + 16z \right) \\
& + \log \left(\frac{Q^2}{\mu_F^2} \right) \log(1-z) \left(8 + \frac{32}{3} \frac{1}{z} - 8z - \frac{32}{3} z^2 \right) + \log \left(\frac{Q^2}{\mu_F^2} \right) \log(z) \\
& \times \left(\frac{380}{9} + \frac{128}{3} \frac{1}{z} + \frac{286}{9} z + 16z^2 \right) + \log \left(\frac{Q^2}{\mu_F^2} \right) \log(z) \log(1-z) \left(16 + 16z \right)
\end{aligned}$$

$$\begin{aligned}
& + \log\left(\frac{Q^2}{\mu_F^2}\right) \log^2(z) \left(-8 - 8z\right) + \log^2\left(\frac{Q^2}{\mu_F^2}\right) \left(2 + \frac{8}{3} \frac{1}{z} - 2z - \frac{8}{3} z^2\right) \\
& + \log^2\left(\frac{Q^2}{\mu_F^2}\right) \log(z) \left(4 + 4z\right) + \zeta_3 \left(-72 - 192 \frac{1}{z^2} + 576 \frac{1}{z} + 36z\right) \\
& + \zeta_2 \left(236 + \frac{640}{3} \frac{1}{z} + 28z + \frac{32}{3} z^2\right) + \zeta_2 \log(1+z) \left(-144 - 192 \frac{1}{z^2} - 288 \frac{1}{z} - 24z\right) \\
& + \zeta_2 \log(z) \left(8 + 288 \frac{1}{z} + 4z\right) \Bigg] \\
& + C_F K_G K_Q \left[\left(-\frac{25442}{81} + \frac{326}{81} \frac{1}{z^3} + \frac{10186}{81} \frac{1}{z^2} + \frac{6583}{27} \frac{1}{z} - \frac{4819}{81} z \right) + \text{Li}_2(1-z) \right. \\
& \times \left(-\frac{2240}{9} - \frac{608}{3} \frac{1}{z} - \frac{712}{9} z \right) + \log(1-z) \left(\frac{3104}{27} - \frac{98}{27} \frac{1}{z^3} - \frac{1792}{27} \frac{1}{z^2} - 216 \frac{1}{z} \right. \\
& \left. \left. + \frac{4618}{27} z \right) + \log(z) \left(-\frac{1504}{27} + \frac{49}{27} \frac{1}{z^3} + \frac{896}{27} \frac{1}{z^2} + \frac{724}{3} \frac{1}{z} - \frac{4979}{27} z \right) \right. \\
& \left. + \log(z) \log(1-z) \left(-\frac{2240}{9} - \frac{608}{3} \frac{1}{z} - \frac{712}{9} z \right) + \log^2(z) \left(\frac{832}{9} + \frac{152}{3} \frac{1}{z} + \frac{356}{9} z \right) \right. \\
& \left. + \log\left(\frac{Q^2}{\mu_F^2}\right) \left(\frac{1552}{27} - \frac{49}{27} \frac{1}{z^3} - \frac{896}{27} \frac{1}{z^2} - 108 \frac{1}{z} + \frac{2309}{27} z \right) \right. \\
& \left. + \log\left(\frac{Q^2}{\mu_F^2}\right) \log(z) \left(-\frac{1120}{9} - \frac{304}{3} \frac{1}{z} - \frac{356}{9} z \right) \right] + C_F K_G^2 \left[\left(\frac{34753}{81} - \frac{163}{81} \frac{1}{z^3} \right. \right. \\
& \left. \left. - \frac{5093}{81} \frac{1}{z^2} - \frac{22837}{54} \frac{1}{z} + \frac{9517}{162} z \right) + S_{1,2}(1-z) \left(-256 - 256 \frac{1}{z} - 64z \right) \right. \\
& \left. + \text{Li}_3(1-z) \left(256 + 256 \frac{1}{z} + 64z \right) + \text{Li}_2(1-z) \left(\frac{1120}{9} + \frac{64}{3} \frac{1}{z} + \frac{140}{9} z \right) \right. \\
& \left. + \log(1-z) \left(-\frac{11056}{27} + \frac{49}{27} \frac{1}{z^3} + \frac{896}{27} \frac{1}{z^2} + 504 \frac{1}{z} - \frac{3497}{27} z \right) \right. \\
& \left. + \log(1-z) \text{Li}_2(1-z) \left(-256 - 256 \frac{1}{z} - 64z \right) + \log^2(1-z) \left(128 - 192 \frac{1}{z} + 64z \right) \right. \\
& \left. + \log(z) \left(\frac{8096}{27} - \frac{49}{54} \frac{1}{z^3} - \frac{448}{27} \frac{1}{z^2} - \frac{956}{3} \frac{1}{z} + \frac{6491}{54} z \right) + \log(z) \text{Li}_2(1-z) \left(-64 \right. \right. \\
& \left. \left. - 64 \frac{1}{z} - 16z \right) + \log(z) \log(1-z) \left(-\frac{608}{9} + \frac{928}{3} \frac{1}{z} - \frac{724}{9} z \right) \right. \\
& \left. + \log(z) \log^2(1-z) \left(-128 - 128 \frac{1}{z} - 32z \right) + \log^2(z) \left(\frac{232}{9} - \frac{232}{3} \frac{1}{z} + \frac{146}{9} z \right) \right. \\
& \left. + \log^2(z) \log(1-z) \left(64 + 64 \frac{1}{z} + 16z \right) + \log^3(z) \left(-\frac{32}{3} - \frac{32}{3} \frac{1}{z} - \frac{8}{3} z \right) \right. \\
& \left. + \log\left(\frac{Q^2}{\mu_F^2}\right) \left(-\frac{5528}{27} + \frac{49}{54} \frac{1}{z^3} + \frac{448}{27} \frac{1}{z^2} + 252 \frac{1}{z} - \frac{3497}{54} z \right) \right]
\end{aligned}$$

$$\begin{aligned}
& + \log\left(\frac{Q^2}{\mu_F^2}\right) \text{Li}_2(1-z) \left(-128 - 128\frac{1}{z} - 32z\right) + \log\left(\frac{Q^2}{\mu_F^2}\right) \log(1-z) \left(128\right. \\
& - 192\frac{1}{z} + 64z \left.) + \log\left(\frac{Q^2}{\mu_F^2}\right) \log(z) \left(-\frac{304}{9} + \frac{464}{3}\frac{1}{z} - \frac{362}{9}z\right) \right. \\
& + \log\left(\frac{Q^2}{\mu_F^2}\right) \log(z) \log(1-z) \left(-128 - 128\frac{1}{z} - 32z\right) + \log\left(\frac{Q^2}{\mu_F^2}\right) \log^2(z) \left(32\right. \\
& + 32\frac{1}{z} + 8z \left.) + \log^2\left(\frac{Q^2}{\mu_F^2}\right) \left(32 - 48\frac{1}{z} + 16z\right) + \log^2\left(\frac{Q^2}{\mu_F^2}\right) \log(z) \left(-32\right. \\
& - 32\frac{1}{z} - 8z \left.) + \zeta_2 \left(-128 + 192\frac{1}{z} - 64z\right) + \zeta_2 \log(z) \left(128 + 128\frac{1}{z} + 32z\right) \right] \\
& + C_F n_f K_Q^2 \left[\left(\frac{7264}{81} - \frac{1748}{405}\frac{1}{z^3} + \frac{64}{27}\frac{1}{z^2} + \frac{56}{3}\frac{1}{z} + \frac{224}{27}\frac{1}{1-z} - \frac{328}{3}z - \frac{724}{135}z^2 \right) \right. \\
& + \text{Li}_2(1-z) \left(\frac{8}{3} - \frac{32}{3}\frac{1}{z} - \frac{8}{3}\frac{1}{1-z} + \frac{8}{3}z \right) + \text{Li}_2(-z) \left(-48 - \frac{64}{3}\frac{1}{z} - 32z - \frac{16}{3}z^2 \right) \\
& + \log(1-z) \left(-\frac{368}{27} + \frac{32}{27}\frac{1}{z^3} + \frac{32}{9}\frac{1}{z} - \frac{160}{9}\frac{1}{1-z} + \frac{80}{3}z \right) + \log^2(1-z) \left(-\frac{16}{3} \right. \\
& + \frac{32}{3}\frac{1}{1-z} - \frac{16}{3}z \left.) + \log(z) \left(\frac{1912}{27} - \frac{16}{9}\frac{1}{z^3} - 8\frac{1}{z} + \frac{40}{3}\frac{1}{1-z} - \frac{20}{9}z + 4z^2 \right) \right. \\
& + \log(z) \log(1-z) \left(-48 - \frac{64}{3}\frac{1}{z} - 32z - \frac{16}{3}z^2 \right) + \log(z) \log(1-z) \left(\frac{32}{3} \right. \\
& - \frac{64}{3}\frac{1}{1-z} + \frac{32}{3}z \left.) + \log^2(z) \left(\frac{26}{3} + 8\frac{1}{1-z} + \frac{14}{3}z + \frac{4}{3}z^2 \right) + \delta(1-z) \left(\frac{8813}{162} \right) \right. \\
& + \log\left(\frac{Q^2}{\mu_F^2}\right) \left(-\frac{56}{3} + \frac{16}{9}\frac{1}{z^3} - \frac{80}{9}\frac{1}{1-z} + \frac{232}{9}z \right) + \log\left(\frac{Q^2}{\mu_F^2}\right) \log(1-z) \left(-\frac{16}{3} \right. \\
& + \frac{32}{3}\frac{1}{1-z} - \frac{16}{3}z \left.) + \log\left(\frac{Q^2}{\mu_F^2}\right) \log(z) \left(\frac{16}{3} - \frac{32}{3}\frac{1}{1-z} + \frac{16}{3}z \right) \right. \\
& + \log\left(\frac{Q^2}{\mu_F^2}\right) \delta(1-z) \left(-\frac{286}{9} \right) + \log^2\left(\frac{Q^2}{\mu_F^2}\right) \left(-\frac{4}{3} + \frac{8}{3}\frac{1}{1-z} - \frac{4}{3}z \right) \\
& + \log^2\left(\frac{Q^2}{\mu_F^2}\right) \delta(1-z) \left(\frac{50}{9} \right) + \zeta_3 \delta(1-z) (8) + \zeta_2 \left(-\frac{56}{3} - \frac{32}{3}\frac{1}{z} - \frac{32}{3}\frac{1}{1-z} \right. \\
& - \frac{32}{3}z - \frac{8}{3}z^2 \left.) + \zeta_2 \delta(1-z) \left(-\frac{256}{9} \right) \right] + C_F n_f K_G K_Q \left[\left(-\frac{6416}{81} + \frac{3496}{405}\frac{1}{z^3} \right. \right. \\
& - \frac{32}{9}\frac{1}{z^2} - \frac{784}{27}\frac{1}{z} + \frac{3512}{27}z - \frac{3632}{135}z^2 \left.) + \log(1-z) \left(\frac{640}{27} - \frac{64}{27}\frac{1}{z^3} + \frac{32}{9}\frac{1}{z} - \frac{224}{9}z \right) \right. \\
& + \log(z) \left(-\frac{2240}{27} + \frac{32}{9}\frac{1}{z^3} - \frac{16}{3}\frac{1}{z} + \frac{496}{9}z \right) + \delta(1-z) \left(-\frac{2332}{81} \right) \\
& + \log\left(\frac{Q^2}{\mu_F^2}\right) \left(\frac{320}{9} - \frac{32}{9}\frac{1}{z^3} + \frac{32}{9}\frac{1}{z} - \frac{128}{3}z + \frac{64}{9}z^2 \right) + \log\left(\frac{Q^2}{\mu_F^2}\right) \delta(1-z) \left(\frac{160}{9} \right)
\end{aligned}$$

$$\begin{aligned}
& + \log^2\left(\frac{Q^2}{\mu_F^2}\right) \delta(1-z) \left(-\frac{32}{9}\right) + \zeta_2 \delta(1-z) \left(\frac{64}{3}\right) \Big] + C_F n_f \kappa_G^2 \left[\left(\frac{2992}{81} - \frac{1748}{405} \frac{1}{z^3} \right. \right. \\
& + \frac{32}{27} \frac{1}{z^2} + \frac{256}{27} \frac{1}{z} - \frac{604}{9} z + \frac{1072}{45} z^2 \Big) + \log(1-z) \left(-\frac{320}{27} + \frac{32}{27} \frac{1}{z^3} + \frac{160}{9} z \right. \\
& - \frac{64}{9} z^2 \Big) + \log(z) \left(\frac{1120}{27} - \frac{16}{9} \frac{1}{z^3} - \frac{320}{9} z + \frac{128}{9} z^2 \right) + \log\left(\frac{Q^2}{\mu_F^2}\right) \left(-\frac{160}{9} \right. \\
& + \frac{16}{9} \frac{1}{z^3} + \frac{80}{3} z - \frac{32}{3} z^2 \Big) \Big] + C_F^2 \kappa_Q^2 \left[\left(\frac{56552}{81} + \frac{751}{81} \frac{1}{z^3} - \frac{920}{27} \frac{1}{z^2} + \frac{2206}{27} \frac{1}{z} \right. \right. \\
& - \frac{18767}{27} z - 52 z^2 \Big) + S_{1,2}(1-z) \left(696 - 256 \frac{1}{z} - 208 \frac{1}{1-z} + 696 z + 64 z^2 \right) \\
& + S_{1,2}(-z) \left(-864 - 384 \frac{1}{z} - 576 z - 96 z^2 \right) + \text{Li}_3(1-z) \left(-80 + 96 \frac{1}{z} + 48 \frac{1}{1-z} \right. \\
& - 48 z \Big) + \text{Li}_3(-z) \left(-144 - 64 \frac{1}{z} - 96 z - 16 z^2 \right) + \text{Li}_2(1-z) \left(\frac{3112}{9} + \frac{304}{3} \frac{1}{z} \right. \\
& - 24 \frac{1}{1-z} - 408 z - \frac{344}{3} z^2 \Big) + \text{Li}_2(-z) \left(688 + \frac{832}{3} \frac{1}{z} + 544 z + \frac{400}{3} z^2 \right) \\
& + \log(1+z) \text{Li}_2(-z) \left(-864 - 384 \frac{1}{z} - 576 z - 96 z^2 \right) + \log(1-z) \left(\frac{4928}{27} - \frac{560}{27} \frac{1}{z^3} \right. \\
& + \frac{128}{9} \frac{1}{z^2} + 160 \frac{1}{z} - \frac{3968}{9} \frac{1}{1-z} + \frac{908}{9} z \Big) + \log(1-z) \text{Li}_2(1-z) \left(56 - 128 \frac{1}{z} \right. \\
& - 16 \frac{1}{1-z} + 56 z \Big) + \log^2(1-z) \left(-\frac{1216}{9} + \frac{64}{9} \frac{1}{z^3} + \frac{64}{3} \frac{1}{z} + \frac{320}{3} z \right) \\
& + \log^3(1-z) \left(-64 + 128 \frac{1}{1-z} - 64 z \right) + \log(z) \left(\frac{6112}{9} + \frac{8}{3} \frac{1}{z^3} - \frac{64}{9} \frac{1}{z^2} - \frac{1540}{9} \frac{1}{z} \right. \\
& + \frac{2272}{9} \frac{1}{1-z} + \frac{2120}{9} z \Big) + \log(z) \text{Li}_2(1-z) \left(344 + 32 \frac{1}{z} - 96 \frac{1}{1-z} + 312 z + 32 z^2 \right) \\
& + \log(z) \text{Li}_2(-z) \left(432 + 192 \frac{1}{z} + 288 z + 48 z^2 \right) + \log(z) \log(1+z) \left(688 + \frac{832}{3} \frac{1}{z} \right. \\
& + 544 z + \frac{400}{3} z^2 \Big) + \log(z) \log^2(1+z) \left(-432 - 192 \frac{1}{z} - 288 z - 48 z^2 \right) \\
& + \log(z) \log(1-z) \left(\frac{2528}{9} - \frac{64}{9} \frac{1}{z^3} - \frac{80}{3} \frac{1}{z} - 48 \frac{1}{1-z} - \frac{608}{3} z \right) \\
& + \log(z) \log^2(1-z) \left(156 - 248 \frac{1}{1-z} + 156 z \right) + \log^2(z) \left(-\frac{2168}{9} - \frac{44}{3} \frac{1}{z} \right. \\
& + 30 \frac{1}{1-z} - 368 z - 124 z^2 \Big) + \log^2(z) \log(1+z) \left(360 + 160 \frac{1}{z} + 240 z + 40 z^2 \right) \\
& + \log^2(z) \log(1-z) \left(-80 + 112 \frac{1}{1-z} - 80 z \right) + \log^3(z) \left(\frac{110}{3} - \frac{32}{3} \frac{1}{z} - \frac{40}{3} \frac{1}{1-z} \right)
\end{aligned}$$

$$\begin{aligned}
& + 34z + \frac{8}{3}z^2) + \delta(1-z)\left(\frac{43093}{108}\right) + \log\left(\frac{Q^2}{\mu_F^2}\right)\left(\frac{632}{9} - \frac{8}{3}\frac{1}{z^3} + \frac{64}{9}\frac{1}{z^2} + \frac{160}{9}\frac{1}{z}\right. \\
& - \frac{1984}{9}\frac{1}{1-z} + 128z) + \log\left(\frac{Q^2}{\mu_F^2}\right)\text{Li}_2(1-z)\left(32 + 32z\right) \\
& + \log\left(\frac{Q^2}{\mu_F^2}\right)\log(1-z)\left(-\frac{2032}{9} + \frac{64}{9}\frac{1}{z^3} + \frac{64}{3}\frac{1}{z} + \frac{544}{3}\frac{1}{1-z} + 16z\right) \\
& + \log\left(\frac{Q^2}{\mu_F^2}\right)\log^2(1-z)\left(-96 + 192\frac{1}{1-z} - 96z\right) + \log\left(\frac{Q^2}{\mu_F^2}\right)\log(z)\left(\frac{872}{9}\right. \\
& - \frac{344}{3}\frac{1}{1-z} - 40z) + \log\left(\frac{Q^2}{\mu_F^2}\right)\log(z)\log(1-z)\left(144 - 224\frac{1}{1-z} + 144z\right) \\
& + \log\left(\frac{Q^2}{\mu_F^2}\right)\log^2(z)\left(-28 + 32\frac{1}{1-z} - 28z\right) + \log\left(\frac{Q^2}{\mu_F^2}\right)\delta(1-z)\left(-\frac{8575}{27}\right) \\
& + \log^2\left(\frac{Q^2}{\mu_F^2}\right)\left(-\frac{184}{3} + \frac{272}{3}\frac{1}{1-z} - \frac{88}{3}z\right) + \log^2\left(\frac{Q^2}{\mu_F^2}\right)\log(1-z)\left(-32\right. \\
& + 64\frac{1}{1-z} - 32z) + \log^2\left(\frac{Q^2}{\mu_F^2}\right)\log(z)\left(24 - 32\frac{1}{1-z} + 24z\right) \\
& + \log^2\left(\frac{Q^2}{\mu_F^2}\right)\delta(1-z)\left(\frac{578}{9}\right) + \zeta_3\left(-128 + 256\frac{1}{1-z} - 128z\right) \\
& + \zeta_3\delta(1-z)\left(-124\right) + \zeta_3\log\left(\frac{Q^2}{\mu_F^2}\right)\delta(1-z)\left(176\right) + \zeta_2\left(\frac{3032}{9} + \frac{64}{9}\frac{1}{z^3}\right. \\
& + 160\frac{1}{z} + \frac{752}{3}z + \frac{200}{3}z^2) + \zeta_2\log(1+z)\left(-432 - 192\frac{1}{z} - 288z - 48z^2\right) \\
& + \zeta_2\log(1-z)\left(64 - 128\frac{1}{1-z} + 64z\right) + \zeta_2\log(z)\left(48 + 64\frac{1}{z} + 128\frac{1}{1-z} + 16z^2\right) \\
& + \zeta_2\delta(1-z)\left(-\frac{434}{3}\right) + \zeta_2\log\left(\frac{Q^2}{\mu_F^2}\right)\left(32 - 64\frac{1}{1-z} + 32z\right) \\
& + \zeta_2\log\left(\frac{Q^2}{\mu_F^2}\right)\delta(1-z)\left(\frac{200}{3}\right) + \zeta_2\log^2\left(\frac{Q^2}{\mu_F^2}\right)\delta(1-z)\left(-32\right) \\
& + \zeta_2^2\delta(1-z)\left(\frac{8}{5}\right) + C_F^2\kappa_G\kappa_Q\left[\left(-\frac{41824}{81} - \frac{1502}{81}\frac{1}{z^3} + \frac{1840}{27}\frac{1}{z^2} - \frac{4760}{27}\frac{1}{z}\right.\right. \\
& + \frac{17362}{27}z) + \text{Li}_3(-z)\left(-256\frac{1}{z} - 256z\right) + \text{Li}_2(1-z)\left(-\frac{512}{9} + \frac{80}{3}\frac{1}{z} + \frac{560}{3}z\right) \\
& + \text{Li}_2(-z)\left(-128\frac{1}{z} + 128z\right) + \log(1-z)\left(-\frac{6496}{27} + \frac{1120}{27}\frac{1}{z^3} - \frac{256}{9}\frac{1}{z^2} - \frac{32}{3}\frac{1}{z}\right. \\
& + \frac{1088}{9}\frac{1}{1-z} + \frac{352}{3}z) + \log^2(1-z)\left(\frac{1280}{9} - \frac{128}{9}\frac{1}{z^3} + \frac{64}{3}\frac{1}{z} - \frac{448}{3}z\right) \\
& + \log(z)\left(-\frac{3280}{9} - \frac{16}{3}\frac{1}{z^3} + \frac{128}{9}\frac{1}{z^2} + \frac{440}{9}\frac{1}{z} - \frac{544}{9}\frac{1}{1-z} - \frac{352}{3}z\right)
\end{aligned}$$

$$\begin{aligned}
& + \log(z) \text{Li}_2(-z) \left(128 \frac{1}{z} + 128z \right) + \log(z) \log(1+z) \left(-128 \frac{1}{z} + 128z \right) \\
& + \log(z) \log(1-z) \left(-\frac{1792}{9} + \frac{128}{9} \frac{1}{z^3} + \frac{16}{3} \frac{1}{z} + 336z \right) + \log^2(z) \left(\frac{832}{9} + \frac{16}{3} \frac{1}{z} \right. \\
& \left. - \frac{448}{3} z \right) + \log^3(z) \left(\frac{64}{3} \frac{1}{z} + \frac{64}{3} z \right) + \delta(1-z) \left(-\frac{17998}{81} \right) + \log \left(\frac{Q^2}{\mu_F^2} \right) \left(\frac{304}{9} \right. \\
& + \frac{16}{3} \frac{1}{z^3} - \frac{128}{9} \frac{1}{z^2} - \frac{128}{9} \frac{1}{z} + \frac{544}{9} \frac{1}{1-z} - \frac{640}{9} z \left. \right) + \log \left(\frac{Q^2}{\mu_F^2} \right) \log(1-z) \left(\frac{1664}{9} \right. \\
& \left. - \frac{128}{9} \frac{1}{z^3} + \frac{64}{3} \frac{1}{z} - \frac{256}{3} \frac{1}{1-z} - \frac{320}{3} z \right) + \log \left(\frac{Q^2}{\mu_F^2} \right) \log(z) \left(-\frac{832}{9} + \frac{128}{3} \frac{1}{1-z} \right. \\
& \left. + \frac{160}{3} z \right) + \log \left(\frac{Q^2}{\mu_F^2} \right) \delta(1-z) \left(\frac{5960}{27} \right) + \log^2 \left(\frac{Q^2}{\mu_F^2} \right) \left(\frac{64}{3} - \frac{128}{3} \frac{1}{1-z} + \frac{64}{3} z \right) \\
& + \log^2 \left(\frac{Q^2}{\mu_F^2} \right) \delta(1-z) \left(-\frac{160}{3} \right) + \zeta_3 \left(-192 \frac{1}{z} - 192z \right) + \zeta_2 \left(\frac{1280}{9} - \frac{128}{9} \frac{1}{z^3} \right. \\
& \left. - \frac{128}{3} \frac{1}{z} - \frac{256}{3} z \right) + \zeta_2 \log(z) \left(-64 \frac{1}{z} - 64z \right) + \zeta_2 \delta(1-z) (32) \\
& + \zeta_2 \log \left(\frac{Q^2}{\mu_F^2} \right) \delta(1-z) \left(-\frac{128}{3} \right) \left. \right] + C_F^2 \kappa_G^2 \left[\left(-\frac{6952}{81} + \frac{751}{81} \frac{1}{z^3} - \frac{920}{27} \frac{1}{z^2} \right. \right. \\
& + \frac{6226}{27} \frac{1}{z} - \frac{4967}{27} z + 64z^2 \left. \right) + \text{Li}_3(-z) \left(128 \frac{1}{z} + 128z \right) + \text{Li}_2(1-z) \left(-\frac{512}{9} \right. \\
& \left. - \frac{64}{3} \frac{1}{z} - \frac{512}{3} z + \frac{256}{3} z^2 \right) + \text{Li}_2(-z) \left(64 \frac{1}{z} - 64z \right) + \log(1-z) \left(\frac{1280}{27} - \frac{560}{27} \frac{1}{z^3} \right. \\
& + \frac{128}{9} \frac{1}{z^2} - \frac{160}{3} \frac{1}{z} - \frac{464}{9} z + 64z^2 \left. \right) + \log^2(1-z) \left(-\frac{640}{9} + \frac{64}{9} \frac{1}{z^3} + \frac{320}{3} z \right. \\
& \left. - \frac{128}{3} z^2 \right) + \log(z) \left(\frac{416}{3} + \frac{8}{3} \frac{1}{z^3} - \frac{64}{9} \frac{1}{z^2} + \frac{524}{9} \frac{1}{z} - \frac{956}{9} z - 64z^2 \right) \\
& + \log(z) \text{Li}_2(-z) \left(-64 \frac{1}{z} - 64z \right) + \log(z) \log(1+z) \left(64 \frac{1}{z} - 64z \right) \\
& + \log(z) \log(1-z) \left(\frac{128}{9} - \frac{64}{9} \frac{1}{z^3} - \frac{64}{3} \frac{1}{z} - \frac{832}{3} z + 128z^2 \right) + \log^2(z) \left(-\frac{320}{9} \right. \\
& + \frac{28}{3} \frac{1}{z} + \frac{400}{3} z - \frac{128}{3} z^2 \left. \right) + \log^3(z) \left(-\frac{32}{3} \frac{1}{z} - \frac{32}{3} z \right) + \delta(1-z) \left(\frac{1156}{81} \right) \\
& + \log \left(\frac{Q^2}{\mu_F^2} \right) \left(-\frac{64}{3} - \frac{8}{3} \frac{1}{z^3} + \frac{64}{9} \frac{1}{z^2} - \frac{32}{9} \frac{1}{z} + \frac{184}{9} z \right) \\
& + \log \left(\frac{Q^2}{\mu_F^2} \right) \log(1-z) \left(-\frac{640}{9} + \frac{64}{9} \frac{1}{z^3} + \frac{320}{3} z - \frac{128}{3} z^2 \right) \\
& + \log \left(\frac{Q^2}{\mu_F^2} \right) \log(z) \left(\frac{320}{9} - \frac{160}{3} z + \frac{128}{3} z^2 \right) + \log \left(\frac{Q^2}{\mu_F^2} \right) \delta(1-z) \left(-\frac{544}{27} \right)
\end{aligned}$$

$$\begin{aligned}
& + \log^2\left(\frac{Q^2}{\mu_F^2}\right) \delta(1-z) \left(\frac{64}{9}\right) + \zeta_3 \left(96\frac{1}{z} + 96z\right) + \zeta_2 \left(-\frac{640}{9} + \frac{64}{9}\frac{1}{z^3} + 32\frac{1}{z}\right. \\
& + \left.\frac{224}{3}z - \frac{128}{3}z^2\right) + \zeta_2 \log(z) \left(32\frac{1}{z} + 32z\right) + \zeta_2 \delta(1-z) \left(\frac{128}{3}\right) \Bigg] \\
& + C_A C_F K_Q^2 \left[\left(-\frac{11726}{27} + \frac{59}{6}\frac{1}{z^3} - \frac{130}{9}\frac{1}{z} - \frac{1616}{27}\frac{1}{1-z} + \frac{25097}{54}z + 26z^2 \right) \right. \\
& + S_{1,2}(1-z) \left(-304 + 128\frac{1}{z} + 64\frac{1}{1-z} - 304z - 32z^2 \right) + S_{1,2}(-z) \left(432 + 192\frac{1}{z} \right. \\
& + \left. 288z + 48z^2 \right) + \text{Li}_3(1-z) \left(24 - 32\frac{1}{z} - 56\frac{1}{1-z} + 24z \right) + \text{Li}_3(-z) \left(72 + 32\frac{1}{z} \right. \\
& + \left. 48z + 8z^2 \right) + \text{Li}_2(1-z) \left(-\frac{1712}{9} + \frac{32}{9}\frac{1}{z^3} - \frac{280}{3}\frac{1}{z} + \frac{44}{3}\frac{1}{1-z} + \frac{500}{3}z \right. \\
& + \left. \frac{172}{3}z^2 \right) + \text{Li}_2(-z) \left(-344 - \frac{416}{3}\frac{1}{z} - 272z - \frac{200}{3}z^2 \right) \\
& + \log(1+z) \text{Li}_2(-z) \left(432 + 192\frac{1}{z} + 288z + 48z^2 \right) + \log(1-z) \left(\frac{5152}{27} - \frac{208}{27}\frac{1}{z^3} \right. \\
& + \left. \frac{8}{3}\frac{1}{z^2} - \frac{976}{9}\frac{1}{z} + \frac{1072}{9}\frac{1}{1-z} - \frac{1732}{9}z \right) + \log(1-z) \text{Li}_2(1-z) \left(64\frac{1}{z} + 16\frac{1}{1-z} \right) \\
& + \log^2(1-z) \left(\frac{104}{9} + \frac{16}{9}\frac{1}{z^3} - \frac{8}{3}\frac{1}{z} - \frac{176}{3}\frac{1}{1-z} + 48z \right) + \log(z) \left(-\frac{10960}{27} + \frac{88}{27}\frac{1}{z^3} \right. \\
& - \left. \frac{32}{9}\frac{1}{z^2} + \frac{604}{9}\frac{1}{z} - \frac{280}{3}\frac{1}{1-z} + \frac{358}{9}z \right) + \log(z) \text{Li}_2(1-z) \left(-168 - 32\frac{1}{z} \right. \\
& + \left. 40\frac{1}{1-z} - 168z - 16z^2 \right) + \log(z) \text{Li}_2(-z) \left(-216 - 96\frac{1}{z} - 144z - 24z^2 \right) \\
& + \log(z) \log(1+z) \left(-344 - \frac{416}{3}\frac{1}{z} - 272z - \frac{200}{3}z^2 \right) \\
& + \log(z) \log^2(1+z) \left(216 + 96\frac{1}{z} + 144z + 24z^2 \right) + \log(z) \log(1-z) \left(-\frac{320}{3} \right. \\
& + \left. \frac{352}{3}\frac{1}{1-z} - \frac{248}{3}z \right) + \log^2(z) \left(\frac{391}{3} - \frac{16}{3}\frac{1}{z} - 44\frac{1}{1-z} + \frac{727}{3}z + 62z^2 \right) \\
& + \log^2(z) \log(1+z) \left(-180 - 80\frac{1}{z} - 120z - 20z^2 \right) + \log^2(z) \log(1-z) \left(-8 \right. \\
& + \left. 16\frac{1}{1-z} - 8z \right) + \log^3(z) \left(-10 - \frac{16}{3}\frac{1}{1-z} - 14z - \frac{4}{3}z^2 \right) \\
& + \delta(1-z) \left(-\frac{84773}{324} \right) + \log\left(\frac{Q^2}{\mu_F^2}\right) \left(\frac{1516}{27} - \frac{88}{27}\frac{1}{z^3} - \frac{88}{9}\frac{1}{z} + \frac{536}{9}\frac{1}{1-z} - \frac{308}{3}z \right) \\
& + \log\left(\frac{Q^2}{\mu_F^2}\right) \log(1-z) \left(\frac{88}{3} - \frac{176}{3}\frac{1}{1-z} + \frac{88}{3}z \right) + \log\left(\frac{Q^2}{\mu_F^2}\right) \log(z) \left(-\frac{64}{3} \right.
\end{aligned}$$

$$\begin{aligned}
& + \frac{176}{3} \frac{1}{1-z} - \frac{64}{3} z \Big) + \log \left(\frac{Q^2}{\mu_F^2} \right) \log^2(z) \left(-4 + 8 \frac{1}{1-z} - 4z \right) \\
& + \log \left(\frac{Q^2}{\mu_F^2} \right) \delta(1-z) \left(\frac{1211}{9} \right) + \log^2 \left(\frac{Q^2}{\mu_F^2} \right) \left(\frac{22}{3} - \frac{44}{3} \frac{1}{1-z} + \frac{22}{3} z \right) \\
& + \log^2 \left(\frac{Q^2}{\mu_F^2} \right) \delta(1-z) \left(-\frac{187}{9} \right) + \zeta_3 \left(-28 + 56 \frac{1}{1-z} - 28z \right) + \zeta_3 \delta(1-z) (92) \\
& + \zeta_3 \log \left(\frac{Q^2}{\mu_F^2} \right) \delta(1-z) \left(-24 \right) + \zeta_2 \left(-\frac{272}{3} - \frac{32}{3} \frac{1}{z^3} - \frac{184}{3} \frac{1}{z} + \frac{176}{3} \frac{1}{1-z} \right. \\
& \left. - \frac{820}{3} z - \frac{100}{3} z^2 \right) + \zeta_2 \log(1+z) \left(216 + 96 \frac{1}{z} + 144z + 24z^2 \right) \\
& + \zeta_2 \log(1-z) \left(16 - 32 \frac{1}{1-z} + 16z \right) + \zeta_2 \log(z) \left(-80 - 32 \frac{1}{z} + 16 \frac{1}{1-z} \right. \\
& \left. - 56z - 8z^2 \right) + \zeta_2 \delta(1-z) \left(\frac{800}{9} \right) + \zeta_2 \log \left(\frac{Q^2}{\mu_F^2} \right) \left(8 - 16 \frac{1}{1-z} + 8z \right) \\
& + \zeta_2^2 \delta(1-z) \left(-\frac{12}{5} \right) \Big] + C_A C_F \kappa_G \kappa_Q \left[\left(324 - \frac{59}{3} \frac{1}{z^3} - \frac{176}{27} \frac{1}{z^2} - \frac{158}{3} \frac{1}{z} - \frac{6619}{27} z \right) \right. \\
& + S_{1,2}(1-z) \left(-128 + 128 \frac{1}{z} + 64z \right) + \text{Li}_3(1-z) \left(64 - 64 \frac{1}{z} - 32z \right) \\
& + \text{Li}_2(1-z) \left(\frac{928}{9} - \frac{64}{9} \frac{1}{z^3} + \frac{8}{3} \frac{1}{z} - \frac{128}{3} z + 32z^2 \right) + \text{Li}_2(-z) \left(-128 - \frac{128}{3} \frac{1}{z} \right. \\
& \left. - 128z - \frac{128}{3} z^2 \right) + \log(1-z) \left(\frac{1600}{27} + \frac{416}{27} \frac{1}{z^3} - \frac{16}{3} \frac{1}{z^2} - \frac{880}{9} \frac{1}{z} + \frac{256}{9} z \right) \\
& + \log(1-z) \text{Li}_2(1-z) \left(-64 + 64 \frac{1}{z} + 32z \right) + \log^2(1-z) \left(\frac{320}{9} - \frac{32}{9} \frac{1}{z^3} + \frac{8}{3} \frac{1}{z} \right. \\
& \left. - \frac{136}{3} z + \frac{32}{3} z^2 \right) + \log(z) \left(-\frac{184}{27} - \frac{176}{27} \frac{1}{z^3} + \frac{64}{9} \frac{1}{z^2} - \frac{44}{9} \frac{1}{z} - \frac{320}{9} z \right) \\
& + \log(z) \log(1+z) \left(-128 - \frac{128}{3} \frac{1}{z} - 128z - \frac{128}{3} z^2 \right) + \log(z) \log(1-z) \left(-32 \right. \\
& \left. + 88z - \frac{64}{3} z^2 \right) + \log^2(z) \left(96 + \frac{32}{3} \frac{1}{z} - 20z + 48z^2 \right) + \delta(1-z) \left(\frac{7826}{81} \right) \\
& + \log \left(\frac{Q^2}{\mu_F^2} \right) \left(-\frac{1760}{27} + \frac{176}{27} \frac{1}{z^3} - \frac{88}{9} \frac{1}{z} + \frac{616}{9} z \right) + \log \left(\frac{Q^2}{\mu_F^2} \right) \delta(1-z) \left(-\frac{500}{9} \right) \\
& + \log^2 \left(\frac{Q^2}{\mu_F^2} \right) \delta(1-z) \left(\frac{88}{9} \right) + \zeta_2 \left(-\frac{832}{3} + \frac{64}{3} \frac{1}{z^3} - 40 \frac{1}{z} + 200z - \frac{224}{3} z^2 \right) \\
& + \zeta_2 \delta(1-z) \left(-\frac{472}{9} \right) \Big] + C_A C_F \kappa_G^2 \left[\left(-\frac{392}{9} + \frac{59}{6} \frac{1}{z^3} + \frac{176}{27} \frac{1}{z^2} + \frac{1228}{27} \frac{1}{z} \right. \right. \\
& \left. \left. + \frac{2741}{54} z - \frac{1864}{27} z^2 \right) + \text{Li}_2(1-z) \left(-\frac{608}{9} + \frac{32}{9} \frac{1}{z^3} - \frac{32}{3} z - \frac{128}{3} z^2 \right) \right]
\end{aligned}$$

$$\begin{aligned}
& + \text{Li}_2(-z) \left(64 + \frac{64}{3} \frac{1}{z} + 64z + \frac{64}{3} z^2 \right) + \log(1-z) \left(\frac{568}{27} - \frac{208}{27} \frac{1}{z^3} + \frac{8}{3} \frac{1}{z^2} \right. \\
& - \left. \frac{136}{9} \frac{1}{z} - \frac{776}{9} z + \frac{256}{3} z^2 \right) + \log^2(1-z) \left(-\frac{160}{9} + \frac{16}{9} \frac{1}{z^3} + \frac{80}{3} z - \frac{32}{3} z^2 \right) \\
& + \log(z) \left(\frac{920}{27} + \frac{88}{27} \frac{1}{z^3} - \frac{32}{9} \frac{1}{z^2} + \frac{136}{9} \frac{1}{z} + \frac{850}{9} z - \frac{256}{3} z^2 \right) \\
& + \log(z) \log(1+z) \left(64 + \frac{64}{3} \frac{1}{z} + 64z + \frac{64}{3} z^2 \right) + \log(z) \log(1-z) \left(-32 - 64z \right. \\
& - \left. \frac{64}{3} z^2 \right) + \log^2(z) \left(-16 - \frac{16}{3} \frac{1}{z} - \frac{16}{3} z^2 \right) + \log\left(\frac{Q^2}{\mu_F^2}\right) \left(\frac{880}{27} - \frac{88}{27} \frac{1}{z^3} - \frac{440}{9} z \right. \\
& + \left. \frac{176}{9} z^2 \right) + \zeta_2 \left(\frac{416}{3} - \frac{32}{3} \frac{1}{z^3} + \frac{32}{3} \frac{1}{z} - 128z + \frac{224}{3} z^2 \right) \Bigg], \tag{11.38}
\end{aligned}$$

The identical quark quark initiated processes start at NNLO level and the result is found to be

$$\begin{aligned}
\Delta_{qq}^{h,(2)} = & C_F \kappa_Q^2 \left[\left(\frac{39442}{81} - \frac{163}{81} \frac{1}{z^3} - \frac{5093}{81} \frac{1}{z^2} - \frac{4979}{18} \frac{1}{z} - \frac{27779}{162} z + \frac{703}{27} z^2 \right) \right. \\
& + S_{1,2}(1-z) \left(400 + 128 \frac{1}{z^2} + 320 \frac{1}{z} + 128z \right) + S_{1,2}(-z) \left(-288 - 384 \frac{1}{z^2} - 576 \frac{1}{z} \right. \\
& - \left. 48z \right) + \text{Li}_3(1-z) \left(56 + 64 \frac{1}{z^2} - 128 \frac{1}{z} - 52z \right) + \text{Li}_3(-z) \left(-144 - 320 \frac{1}{z^2} \right. \\
& + \left. 672 \frac{1}{z} + 40z \right) + \text{Li}_2(1-z) \left(-\frac{1112}{9} + \frac{1280}{3} \frac{1}{z} - \frac{400}{9} z + \frac{32}{3} z^2 \right) \\
& + \text{Li}_2(-z) \left(488 + 448 \frac{1}{z} + 40z \right) + \log(1+z) \text{Li}_2(-z) \left(-288 - 384 \frac{1}{z^2} - 576 \frac{1}{z} \right. \\
& - \left. 48z \right) + \log(1-z) \left(-\frac{2488}{27} + \frac{49}{27} \frac{1}{z^3} + \frac{896}{27} \frac{1}{z^2} + \frac{680}{9} \frac{1}{z} + \frac{31}{27} z - \frac{176}{9} z^2 \right) \\
& + \log(1-z) \text{Li}_2(1-z) \left(32 + 32z \right) + \log^2(1-z) \left(8 + \frac{32}{3} \frac{1}{z} - 8z - \frac{32}{3} z^2 \right) \\
& + \log(z) \left(\frac{2174}{27} - \frac{49}{54} \frac{1}{z^3} - \frac{448}{27} \frac{1}{z^2} - \frac{620}{3} \frac{1}{z} + \frac{2243}{54} z + \frac{40}{9} z^2 \right) \\
& + \log(z) \text{Li}_2(1-z) \left(96 + 288 \frac{1}{z} + 68z \right) + \log(z) \text{Li}_2(-z) \left(192 + 320 \frac{1}{z^2} - 96 \frac{1}{z} \right) \\
& + \log(z) \log(1+z) \left(488 + 448 \frac{1}{z} + 40z \right) + \log(z) \log^2(1+z) \left(-144 - 192 \frac{1}{z^2} \right. \\
& - \left. 288 \frac{1}{z} - 24z \right) + \log(z) \log(1-z) \left(\frac{760}{9} + \frac{256}{3} \frac{1}{z} + \frac{572}{9} z + 32z^2 \right) \Bigg]
\end{aligned}$$

$$\begin{aligned}
& + \log(z) \log^2(1-z) \left(16 + 16z \right) + \log^2(z) \left(-\frac{3557}{9} - \frac{64}{3} \frac{1}{z} - \frac{817}{9} z - \frac{40}{3} z^2 \right) \\
& + \log^2(z) \log(1+z) \left(120 + 160 \frac{1}{z^2} + 240 \frac{1}{z} + 20z \right) + \log^2(z) \log(1-z) \left(-16 \right. \\
& \left. - 16z \right) + \log^3(z) \left(6 - \frac{32}{3} \frac{1}{z} + 14z \right) + \log \left(\frac{Q^2}{\mu_F^2} \right) \left(-\frac{1244}{27} + \frac{49}{54} \frac{1}{z^3} + \frac{448}{27} \frac{1}{z^2} \right. \\
& \left. + \frac{340}{9} \frac{1}{z} + \frac{31}{54} z - \frac{88}{9} z^2 \right) + \log \left(\frac{Q^2}{\mu_F^2} \right) \text{Li}_2(1-z) \left(16 + 16z \right) + \log \left(\frac{Q^2}{\mu_F^2} \right) \\
& \times \log(1-z) \left(8 + \frac{32}{3} \frac{1}{z} - 8z - \frac{32}{3} z^2 \right) + \log \left(\frac{Q^2}{\mu_F^2} \right) \log(z) \left(\frac{380}{9} \right. \\
& \left. + \frac{128}{3} \frac{1}{z} + \frac{286}{9} z + 16z^2 \right) + \log \left(\frac{Q^2}{\mu_F^2} \right) \log(z) \log(1-z) \left(16 + 16z \right) \\
& + \log \left(\frac{Q^2}{\mu_F^2} \right) \log^2(z) \left(-8 - 8z \right) + \log^2 \left(\frac{Q^2}{\mu_F^2} \right) \left(2 + \frac{8}{3} \frac{1}{z} - 2z - \frac{8}{3} z^2 \right) \\
& + \log^2 \left(\frac{Q^2}{\mu_F^2} \right) \log(z) \left(4 + 4z \right) + \zeta_3 \left(-72 - 192 \frac{1}{z^2} + 576 \frac{1}{z} + 36z \right) \\
& + \zeta_2 \left(236 + \frac{640}{3} \frac{1}{z} + 28z + \frac{32}{3} z^2 \right) + \zeta_2 \log(1+z) \left(-144 - 192 \frac{1}{z^2} - 288 \frac{1}{z} \right. \\
& \left. - 24z \right) + \zeta_2 \log(z) \left(8 + 288 \frac{1}{z} + 4z \right) \Big] + C_F \kappa_G \kappa_Q \left[\left(-\frac{25442}{81} + \frac{326}{81} \frac{1}{z^3} \right. \right. \\
& \left. + \frac{10186}{81} \frac{1}{z^2} + \frac{6583}{27} \frac{1}{z} - \frac{4819}{81} z \right) + \text{Li}_2(1-z) \left(-\frac{2240}{9} - \frac{608}{3} \frac{1}{z} - \frac{712}{9} z \right) \\
& + \log(1-z) \left(\frac{3104}{27} - \frac{98}{27} \frac{1}{z^3} - \frac{1792}{27} \frac{1}{z^2} - 216 \frac{1}{z} + \frac{4618}{27} z \right) + \log(z) \left(-\frac{1504}{27} \right. \\
& \left. + \frac{49}{27} \frac{1}{z^3} + \frac{896}{27} \frac{1}{z^2} + \frac{724}{3} \frac{1}{z} - \frac{4979}{27} z \right) + \log(z) \log(1-z) \left(-\frac{2240}{9} - \frac{608}{3} \frac{1}{z} \right. \\
& \left. - \frac{712}{9} z \right) + \log^2(z) \left(\frac{832}{9} + \frac{152}{3} \frac{1}{z} + \frac{356}{9} z \right) + \log \left(\frac{Q^2}{\mu_F^2} \right) \left(\frac{1552}{27} - \frac{49}{27} \frac{1}{z^3} - \frac{896}{27} \frac{1}{z^2} \right. \\
& \left. - 108 \frac{1}{z} + \frac{2309}{27} z \right) + \log \left(\frac{Q^2}{\mu_F^2} \right) \log(z) \left(-\frac{1120}{9} - \frac{304}{3} \frac{1}{z} - \frac{356}{9} z \right) \Big] \\
& + C_F \kappa_G^2 \left[\left(\frac{34753}{81} - \frac{163}{81} \frac{1}{z^3} - \frac{5093}{81} \frac{1}{z^2} - \frac{22837}{54} \frac{1}{z} + \frac{9517}{162} z \right) \right. \\
& \left. + S_{1,2}(1-z) \left(-256 - 256 \frac{1}{z} - 64z \right) + \text{Li}_3(1-z) \left(256 + 256 \frac{1}{z} + 64z \right) \right. \\
& \left. + \text{Li}_2(1-z) \left(\frac{1120}{9} + \frac{64}{3} \frac{1}{z} + \frac{140}{9} z \right) + \log(1-z) \left(-\frac{11056}{27} + \frac{49}{27} \frac{1}{z^3} + \frac{896}{27} \frac{1}{z^2} \right. \right. \\
& \left. \left. + 504 \frac{1}{z} - \frac{3497}{27} z \right) + \log(1-z) \text{Li}_2(1-z) \left(-256 - 256 \frac{1}{z} - 64z \right) \right]
\end{aligned}$$

$$\begin{aligned}
& + \log^2(1-z) \left(128 - 192 \frac{1}{z} + 64z \right) + \log(z) \left(\frac{8096}{27} - \frac{49}{54} \frac{1}{z^3} - \frac{448}{27} \frac{1}{z^2} - \frac{956}{3} \frac{1}{z} \right. \\
& + \left. \frac{6491}{54} z \right) + \log(z) \text{Li}_2(1-z) \left(-64 - 64 \frac{1}{z} - 16z \right) + \log(z) \log(1-z) \left(-\frac{608}{9} \right. \\
& + \left. \frac{928}{3} \frac{1}{z} - \frac{724}{9} z \right) + \log(z) \log^2(1-z) \left(-128 - 128 \frac{1}{z} - 32z \right) + \log^2(z) \left(\frac{232}{9} \right. \\
& - \left. \frac{232}{3} \frac{1}{z} + \frac{146}{9} z \right) + \log^2(z) \log(1-z) \left(64 + 64 \frac{1}{z} + 16z \right) + \log^3(z) \left(-\frac{32}{3} - \frac{32}{3} \frac{1}{z} \right. \\
& - \left. \frac{8}{3} z \right) + \log \left(\frac{Q^2}{\mu_F^2} \right) \left(-\frac{5528}{27} + \frac{49}{54} \frac{1}{z^3} + \frac{448}{27} \frac{1}{z^2} + 252 \frac{1}{z} - \frac{3497}{54} z \right) \\
& + \log \left(\frac{Q^2}{\mu_F^2} \right) \text{Li}_2(1-z) \left(-128 - 128 \frac{1}{z} - 32z \right) + \log \left(\frac{Q^2}{\mu_F^2} \right) \log(1-z) \left(128 \right. \\
& - \left. 192 \frac{1}{z} + 64z \right) + \log \left(\frac{Q^2}{\mu_F^2} \right) \log(z) \left(-\frac{304}{9} + \frac{464}{3} \frac{1}{z} - \frac{362}{9} z \right) \\
& + \log \left(\frac{Q^2}{\mu_F^2} \right) \log(z) \log(1-z) \left(-128 - 128 \frac{1}{z} - 32z \right) + \log \left(\frac{Q^2}{\mu_F^2} \right) \log^2(z) \left(32 \right. \\
& + \left. 32 \frac{1}{z} + 8z \right) + \log^2 \left(\frac{Q^2}{\mu_F^2} \right) \left(32 - 48 \frac{1}{z} + 16z \right) + \log^2 \left(\frac{Q^2}{\mu_F^2} \right) \log(z) \left(-32 - 32 \frac{1}{z} \right. \\
& - \left. 8z \right) + \zeta_2 \left(-128 + 192 \frac{1}{z} - 64z \right) + \zeta_2 \log(z) \left(128 + 128 \frac{1}{z} + 32z \right) \Big] \\
& + C_F^2 \kappa_Q^2 \left[\left(-\frac{4646}{27} - \frac{34}{27} \frac{1}{z^3} + \frac{80}{27} \frac{1}{z^2} + \frac{44}{3} \frac{1}{z} + \frac{4906}{27} z - 26z^2 \right) \right. \\
& + S_{1,2}(1-z) \left(-208 - 192 \frac{1}{z} + 128 \frac{1}{1+z} + 160z - 16z^2 \right) + S_{1,2}(-z) \left(256 \frac{1}{z} \right. \\
& - \left. 64 \frac{1}{1+z} \right) + \text{Li}_3 \left(\frac{1-z}{1+z} \right) \left(-64 + 128 \frac{1}{1+z} + 64z \right) + \text{Li}_3 \left(-\frac{1-z}{1+z} \right) \left(64 \right. \\
& - \left. 128 \frac{1}{1+z} - 64z \right) + \text{Li}_3(1-z) \left(208 - 64 \frac{1}{z} - 128 \frac{1}{1+z} - 160z + 16z^2 \right) \\
& + \text{Li}_3(-z) \left(32 - 128 \frac{1}{z} - 32 \frac{1}{1+z} - 32z \right) + \text{Li}_2(1-z) \left(88 - 96 \frac{1}{z} + 96z - 24z^2 \right) \\
& + \text{Li}_2(-z) \left(-112 - 192 \frac{1}{z} + 80z \right) + \log(1+z) \text{Li}_2(-z) \left(256 \frac{1}{z} - 64 \frac{1}{1+z} \right) \\
& + \log(1-z) \left(64 - 64z \right) + \log(1-z) \text{Li}_2(-z) \left(64 - 128 \frac{1}{1+z} - 64z \right) \\
& + \log(z) \left(-\frac{544}{9} - 40 \frac{1}{z} + \frac{428}{9} z \right) + \log(z) \text{Li}_2(1-z) \left(-192 - 64 \frac{1}{z} + 96 \frac{1}{1+z} \right. \\
& + \left. 144z - 16z^2 \right) + \log(z) \text{Li}_2(-z) \left(-64 + 128 \frac{1}{1+z} + 64z \right)
\end{aligned}$$

$$\begin{aligned}
& + \log(z) \log(1+z) \left(-112 - 192 \frac{1}{z} + 80z \right) + \log(z) \log^2(1+z) \left(128 \frac{1}{z} - 32 \frac{1}{1+z} \right) \\
& + \log(z) \log(1-z) \left(32 + 32z \right) + \log(z) \log(1-z) \log(1+z) \left(64 - 128 \frac{1}{1+z} \right. \\
& \left. - 64z \right) + \log^2(z) \left(44 - 8z - 12z^2 \right) + \log^2(z) \log(1+z) \left(-48 - 64 \frac{1}{z} + 112 \frac{1}{1+z} \right. \\
& \left. + 48z \right) + \log^2(z) \log(1-z) \left(-16 + 32 \frac{1}{1+z} + 16z \right) + \log^3(z) \left(-20 - \frac{32}{3} \frac{1}{1+z} \right. \\
& \left. + 12z - \frac{8}{3} z^2 \right) + \log \left(\frac{Q^2}{\mu_F^2} \right) \left(32 - 32z \right) + \log \left(\frac{Q^2}{\mu_F^2} \right) \text{Li}_2(-z) \left(32 - 64 \frac{1}{1+z} \right. \\
& \left. - 32z \right) + \log \left(\frac{Q^2}{\mu_F^2} \right) \log(z) \left(16 + 16z \right) + \log \left(\frac{Q^2}{\mu_F^2} \right) \log(z) \log(1+z) \left(32 \right. \\
& \left. - 64 \frac{1}{1+z} - 32z \right) + \log \left(\frac{Q^2}{\mu_F^2} \right) \log^2(z) \left(-8 + 16 \frac{1}{1+z} + 8z \right) + \zeta_3 \left(24 - 128 \frac{1}{z} \right. \\
& \left. - 16 \frac{1}{1+z} - 24z \right) + \zeta_2 \left(-56 - 96 \frac{1}{z} + 40z \right) + \zeta_2 \log(1+z) \left(128 \frac{1}{z} - 32 \frac{1}{1+z} \right) \\
& + \zeta_2 \log(1-z) \left(32 - 64 \frac{1}{1+z} - 32z \right) + \zeta_2 \log(z) \left(-16 - 64 \frac{1}{z} + 48 \frac{1}{1+z} + 16z \right) \\
& + \zeta_2 \log \left(\frac{Q^2}{\mu_F^2} \right) \left(16 - 32 \frac{1}{1+z} - 16z \right) \Big] + C_F^2 \kappa_G \kappa_Q \left[\left(-\frac{2048}{27} + \frac{68}{27} \frac{1}{z^3} - \frac{160}{27} \frac{1}{z^2} \right. \right. \\
& \left. \left. + \frac{164}{3} \frac{1}{z} + \frac{664}{27} z \right) + \log(z) \left(-\frac{64}{9} + 40 \frac{1}{z} - \frac{64}{9} z \right) + \log^2(z) \left(8z \right) \right] \\
& + C_F^2 \kappa_G^2 \left[\left(\frac{1456}{27} - \frac{34}{27} \frac{1}{z^3} + \frac{80}{27} \frac{1}{z^2} + \frac{8}{3} \frac{1}{z} - \frac{1574}{27} z \right) + \log(z) \left(\frac{320}{9} + \frac{248}{9} z \right) \right] \\
& + C_A C_F \kappa_Q^2 \left[\left(\frac{2323}{27} + \frac{17}{27} \frac{1}{z^3} - \frac{40}{27} \frac{1}{z^2} - \frac{22}{3} \frac{1}{z} - \frac{2453}{27} z + 13z^2 \right) \right. \\
& \left. + S_{1,2}(1-z) \left(104 + 96 \frac{1}{z} - 64 \frac{1}{1+z} - 80z + 8z^2 \right) + S_{1,2}(-z) \left(-128 \frac{1}{z} \right. \right. \\
& \left. \left. + 32 \frac{1}{1+z} \right) + \text{Li}_3 \left(\frac{1-z}{1+z} \right) \left(32 - 64 \frac{1}{1+z} - 32z \right) + \text{Li}_3 \left(-\frac{1-z}{1+z} \right) \left(-32 \right. \right. \\
& \left. \left. + 64 \frac{1}{1+z} + 32z \right) + \text{Li}_3(1-z) \left(-104 + 32 \frac{1}{z} + 64 \frac{1}{1+z} + 80z - 8z^2 \right) \right. \\
& \left. + \text{Li}_3(-z) \left(-16 + 64 \frac{1}{z} + 16 \frac{1}{1+z} + 16z \right) + \text{Li}_2(1-z) \left(-44 + 48 \frac{1}{z} - 48z \right. \right. \\
& \left. \left. + 12z^2 \right) + \text{Li}_2(-z) \left(56 + 96 \frac{1}{z} - 40z \right) + \log(1+z) \text{Li}_2(-z) \left(-128 \frac{1}{z} + 32 \frac{1}{1+z} \right) \right. \\
& \left. + \log(1-z) \left(-32 + 32z \right) + \log(1-z) \text{Li}_2(-z) \left(-32 + 64 \frac{1}{1+z} + 32z \right) \right]
\end{aligned}$$

$$\begin{aligned}
& + \log(z) \left(\frac{272}{9} + 20 \frac{1}{z} - \frac{214}{9} z \right) + \log(z) \text{Li}_2(1-z) \left(96 + 32 \frac{1}{z} - 48 \frac{1}{1+z} - 72z \right. \\
& \left. + 8z^2 \right) + \log(z) \text{Li}_2(-z) \left(32 - 64 \frac{1}{1+z} - 32z \right) + \log(z) \log(1+z) \left(56 + 96 \frac{1}{z} \right. \\
& \left. - 40z \right) + \log(z) \log^2(1+z) \left(-64 \frac{1}{z} + 16 \frac{1}{1+z} \right) + \log(z) \log(1-z) \left(-16 - 16z \right) \\
& + \log(z) \log(1-z) \log(1+z) \left(-32 + 64 \frac{1}{1+z} + 32z \right) + \log^2(z) \left(-22 + 4z \right. \\
& \left. + 6z^2 \right) + \log^2(z) \log(1+z) \left(24 + 32 \frac{1}{z} - 56 \frac{1}{1+z} - 24z \right) \\
& + \log^2(z) \log(1-z) \left(8 - 16 \frac{1}{1+z} - 8z \right) + \log^3(z) \left(10 + \frac{16}{3} \frac{1}{1+z} - 6z + \frac{4}{3} z^2 \right) \\
& + \log \left(\frac{Q^2}{\mu_F^2} \right) \left(-16 + 16z \right) + \log \left(\frac{Q^2}{\mu_F^2} \right) \text{Li}_2(-z) \left(-16 + 32 \frac{1}{1+z} + 16z \right) \\
& + \log \left(\frac{Q^2}{\mu_F^2} \right) \log(z) \left(-8 - 8z \right) + \log \left(\frac{Q^2}{\mu_F^2} \right) \log(z) \log(1+z) \left(-16 + 32 \frac{1}{1+z} \right. \\
& \left. + 16z \right) + \log \left(\frac{Q^2}{\mu_F^2} \right) \log^2(z) \left(4 - 8 \frac{1}{1+z} - 4z \right) + \zeta_3 \left(-12 + 64 \frac{1}{z} + 8 \frac{1}{1+z} \right. \\
& \left. + 12z \right) + \zeta_2 \left(28 + 48 \frac{1}{z} - 20z \right) + \zeta_2 \log(1+z) \left(-64 \frac{1}{z} + 16 \frac{1}{1+z} \right) \\
& + \zeta_2 \log(1-z) \left(-16 + 32 \frac{1}{1+z} + 16z \right) + \zeta_2 \log(z) \left(8 + 32 \frac{1}{z} - 24 \frac{1}{1+z} - 8z \right) \\
& + \zeta_2 \log \left(\frac{Q^2}{\mu_F^2} \right) \left(-8 + 16 \frac{1}{1+z} + 8z \right) \Big] + C_A C_F K_G K_Q \left[\left(\frac{1024}{27} - \frac{34}{27} \frac{1}{z^3} + \frac{80}{27} \frac{1}{z^2} \right. \right. \\
& \left. \left. - \frac{82}{3} \frac{1}{z} - \frac{332}{27} z \right) + \log(z) \left(\frac{32}{9} - 20 \frac{1}{z} + \frac{32}{9} z \right) + \log^2(z) \left(-4z \right) \right] \\
& + C_A C_F K_G^2 \left[\left(-\frac{728}{27} + \frac{17}{27} \frac{1}{z^3} - \frac{40}{27} \frac{1}{z^2} - \frac{4}{3} \frac{1}{z} + \frac{787}{27} z \right) \right. \\
& \left. + \log(z) \left(-\frac{160}{9} - \frac{124}{9} z \right) \right], \tag{11.39}
\end{aligned}$$

The non-identical quark quark initiated processes start at NNLO level and the result is found to be

$$\begin{aligned}
\mathcal{A}_{q_1 q_2}^{h,(2)} = & C_F K_Q^2 \left[\left(\frac{39442}{81} - \frac{163}{81} \frac{1}{z^3} - \frac{5093}{81} \frac{1}{z^2} - \frac{4979}{18} \frac{1}{z} - \frac{27779}{162} z + \frac{703}{27} z^2 \right) \right. \\
& \left. + S_{1,2}(1-z) \left(400 + 128 \frac{1}{z^2} + 320 \frac{1}{z} + 128z \right) + S_{1,2}(-z) \left(-288 - 384 \frac{1}{z^2} \right) \right]
\end{aligned}$$

$$\begin{aligned}
& -576\frac{1}{z} - 48z) + \text{Li}_3(1-z)\left(56 + 64\frac{1}{z^2} - 128\frac{1}{z} - 52z\right) + \text{Li}_3(-z)\left(-144\right. \\
& \left.- 320\frac{1}{z^2} + 672\frac{1}{z} + 40z\right) + \text{Li}_2(1-z)\left(-\frac{1112}{9} + \frac{1280}{3}\frac{1}{z} - \frac{400}{9}z + \frac{32}{3}z^2\right) \\
& + \text{Li}_2(-z)\left(488 + 448\frac{1}{z} + 40z\right) + \log(1+z)\text{Li}_2(-z)\left(-288 - 384\frac{1}{z^2} - 576\frac{1}{z}\right. \\
& \left.- 48z\right) + \log(1-z)\left(-\frac{2488}{27} + \frac{49}{27}\frac{1}{z^3} + \frac{896}{27}\frac{1}{z^2} + \frac{680}{9}\frac{1}{z} + \frac{31}{27}z - \frac{176}{9}z^2\right) \\
& + \log(1-z)\text{Li}_2(1-z)\left(32 + 32z\right) + \log^2(1-z)\left(8 + \frac{32}{3}\frac{1}{z} - 8z - \frac{32}{3}z^2\right) \\
& + \log(z)\left(\frac{2174}{27} - \frac{49}{54}\frac{1}{z^3} - \frac{448}{27}\frac{1}{z^2} - \frac{620}{3}\frac{1}{z} + \frac{2243}{54}z + \frac{40}{9}z^2\right) \\
& + \log(z)\text{Li}_2(1-z)\left(96 + 288\frac{1}{z} + 68z\right) + \log(z)\text{Li}_2(-z)\left(192 + 320\frac{1}{z^2} - 96\frac{1}{z}\right) \\
& + \log(z)\log(1+z)\left(488 + 448\frac{1}{z} + 40z\right) + \log(z)\log^2(1+z)\left(-144 - 192\frac{1}{z^2}\right. \\
& \left.- 288\frac{1}{z} - 24z\right) + \log(z)\log(1-z)\left(\frac{760}{9} + \frac{256}{3}\frac{1}{z} + \frac{572}{9}z + 32z^2\right) \\
& + \log(z)\log^2(1-z)\left(16 + 16z\right) + \log^2(z)\left(-\frac{3557}{9} - \frac{64}{3}\frac{1}{z} - \frac{817}{9}z - \frac{40}{3}z^2\right) \\
& + \log^2(z)\log(1+z)\left(120 + 160\frac{1}{z^2} + 240\frac{1}{z} + 20z\right) + \log^2(z)\log(1-z)\left(-16\right. \\
& \left.- 16z\right) + \log^3(z)\left(6 - \frac{32}{3}\frac{1}{z} + 14z\right) + \log\left(\frac{Q^2}{\mu_F^2}\right)\left(-\frac{1244}{27} + \frac{49}{54}\frac{1}{z^3} + \frac{448}{27}\frac{1}{z^2}\right. \\
& \left.+ \frac{340}{9}\frac{1}{z} + \frac{31}{54}z - \frac{88}{9}z^2\right) + \log\left(\frac{Q^2}{\mu_F^2}\right)\text{Li}_2(1-z)\left(16 + 16z\right) \\
& + \log\left(\frac{Q^2}{\mu_F^2}\right)\log(1-z)\left(8 + \frac{32}{3}\frac{1}{z} - 8z - \frac{32}{3}z^2\right) + \log\left(\frac{Q^2}{\mu_F^2}\right)\log(z)\left(\frac{380}{9} + \frac{128}{3}\frac{1}{z}\right. \\
& \left.+ \frac{286}{9}z + 16z^2\right) + \log\left(\frac{Q^2}{\mu_F^2}\right)\log(z)\log(1-z)\left(16 + 16z\right) \\
& + \log\left(\frac{Q^2}{\mu_F^2}\right)\log^2(z)\left(-8 - 8z\right) + \log^2\left(\frac{Q^2}{\mu_F^2}\right)\left(2 + \frac{8}{3}\frac{1}{z} - 2z - \frac{8}{3}z^2\right) \\
& + \log^2\left(\frac{Q^2}{\mu_F^2}\right)\log(z)\left(4 + 4z\right) + \zeta_3\left(-72 - 192\frac{1}{z^2} + 576\frac{1}{z} + 36z\right) \\
& + \zeta_2\left(236 + \frac{640}{3}\frac{1}{z} + 28z + \frac{32}{3}z^2\right) + \zeta_2\log(1+z)\left(-144 - 192\frac{1}{z^2} - 288\frac{1}{z} - 24z\right) \\
& + \zeta_2\log(z)\left(8 + 288\frac{1}{z} + 4z\right)\Big] + C_{FKGKQ}\left[\left(-\frac{25442}{81} + \frac{326}{81}\frac{1}{z^3} + \frac{10186}{81}\frac{1}{z^2}\right.\right.
\end{aligned}$$

$$\begin{aligned}
& + \frac{6583}{27} \frac{1}{z} - \frac{4819}{81} z \Big) + \text{Li}_2(1-z) \Big(-\frac{2240}{9} - \frac{608}{3} \frac{1}{z} - \frac{712}{9} z \Big) + \log(1-z) \Big(\frac{3104}{27} \\
& - \frac{98}{27} \frac{1}{z^3} - \frac{1792}{27} \frac{1}{z^2} - 216 \frac{1}{z} + \frac{4618}{27} z \Big) + \log(z) \Big(-\frac{1504}{27} + \frac{49}{27} \frac{1}{z^3} + \frac{896}{27} \frac{1}{z^2} \\
& + \frac{724}{3} \frac{1}{z} - \frac{4979}{27} z \Big) + \log(z) \log(1-z) \Big(-\frac{2240}{9} - \frac{608}{3} \frac{1}{z} - \frac{712}{9} z \Big) + \log^2(z) \Big(\frac{832}{9} \\
& + \frac{152}{3} \frac{1}{z} + \frac{356}{9} z \Big) + \log\left(\frac{Q^2}{\mu_F^2}\right) \Big(\frac{1552}{27} - \frac{49}{27} \frac{1}{z^3} - \frac{896}{27} \frac{1}{z^2} - 108 \frac{1}{z} + \frac{2309}{27} z \Big) \\
& + \log\left(\frac{Q^2}{\mu_F^2}\right) \log(z) \Big(-\frac{1120}{9} - \frac{304}{3} \frac{1}{z} - \frac{356}{9} z \Big) \Big] + C_F \kappa_G^2 \Big[\Big(\frac{34753}{81} - \frac{163}{81} \frac{1}{z^3} \\
& - \frac{5093}{81} \frac{1}{z^2} - \frac{22837}{54} \frac{1}{z} + \frac{9517}{162} z \Big) + S_{1,2}(1-z) \Big(-256 - 256 \frac{1}{z} - 64z \Big) \\
& + \text{Li}_3(1-z) \Big(256 + 256 \frac{1}{z} + 64z \Big) + \text{Li}_2(1-z) \Big(\frac{1120}{9} + \frac{64}{3} \frac{1}{z} + \frac{140}{9} z \Big) \\
& + \log(1-z) \Big(-\frac{11056}{27} + \frac{49}{27} \frac{1}{z^3} + \frac{896}{27} \frac{1}{z^2} + 504 \frac{1}{z} - \frac{3497}{27} z \Big) \\
& + \log(1-z) \text{Li}_2(1-z) \Big(-256 - 256 \frac{1}{z} - 64z \Big) + \log^2(1-z) \Big(128 - 192 \frac{1}{z} + 64z \Big) \\
& + \log(z) \Big(\frac{8096}{27} - \frac{49}{54} \frac{1}{z^3} - \frac{448}{27} \frac{1}{z^2} - \frac{956}{3} \frac{1}{z} + \frac{6491}{54} z \Big) + \log(z) \text{Li}_2(1-z) \Big(-64 \\
& - 64 \frac{1}{z} - 16z \Big) + \log(z) \log(1-z) \Big(-\frac{608}{9} + \frac{928}{3} \frac{1}{z} - \frac{724}{9} z \Big) \\
& + \log(z) \log^2(1-z) \Big(-128 - 128 \frac{1}{z} - 32z \Big) + \log^2(z) \Big(\frac{232}{9} - \frac{232}{3} \frac{1}{z} + \frac{146}{9} z \Big) \\
& + \log^2(z) \log(1-z) \Big(64 + 64 \frac{1}{z} + 16z \Big) + \log^3(z) \Big(-\frac{32}{3} - \frac{32}{3} \frac{1}{z} - \frac{8}{3} z \Big) \\
& + \log\left(\frac{Q^2}{\mu_F^2}\right) \Big(-\frac{5528}{27} + \frac{49}{54} \frac{1}{z^3} + \frac{448}{27} \frac{1}{z^2} + 252 \frac{1}{z} - \frac{3497}{54} z \Big) \\
& + \log\left(\frac{Q^2}{\mu_F^2}\right) \text{Li}_2(1-z) \Big(-128 - 128 \frac{1}{z} - 32z \Big) + \log\left(\frac{Q^2}{\mu_F^2}\right) \log(1-z) \Big(128 \\
& - 192 \frac{1}{z} + 64z \Big) + \log\left(\frac{Q^2}{\mu_F^2}\right) \log(z) \Big(-\frac{304}{9} + \frac{464}{3} \frac{1}{z} - \frac{362}{9} z \Big) \\
& + \log\left(\frac{Q^2}{\mu_F^2}\right) \log(z) \log(1-z) \Big(-128 - 128 \frac{1}{z} - 32z \Big) + \log\left(\frac{Q^2}{\mu_F^2}\right) \log^2(z) \Big(32 \\
& + 32 \frac{1}{z} + 8z \Big) + \log^2\left(\frac{Q^2}{\mu_F^2}\right) \Big(32 - 48 \frac{1}{z} + 16z \Big) + \log^2\left(\frac{Q^2}{\mu_F^2}\right) \log(z) \Big(-32 \\
& - 32 \frac{1}{z} - 8z \Big) + \zeta_2 \Big(-128 + 192 \frac{1}{z} - 64z \Big) + \zeta_2 \log(z) \Big(128 + 128 \frac{1}{z} + 32z \Big) \Big].
\end{aligned}$$

(11.40)

Bibliography

- [1] S. D. Drell and T.-M. Yan, *Massive Lepton Pair Production in Hadron-Hadron Collisions at High-Energies*, *Phys. Rev. Lett.* **25** (1970) 316–320. [Erratum: Phys. Rev. Lett.25,902(1970)].
- [2] C. Anastasiou and K. Melnikov, *Higgs boson production at hadron colliders in NNLO QCD*, *Nucl. Phys.* **B646** (2002) 220–256, [arXiv:hep-ph/0207004 \[hep-ph\]](#).
- [3] T. Ahmed, P. Banerjee, P. K. Dhani, M. C. Kumar, P. Mathews, N. Rana, and V. Ravindran, *NNLO QCD corrections to the Drell-Yan cross section in models of TeV-scale gravity*, *Eur. Phys. J.* **C77** no. 1, (2017) 22, [arXiv:1606.08454 \[hep-ph\]](#).
- [4] **D0** Collaboration, V. M. Abazov *et al.*, *Search for Randall-Sundrum gravitons in the dielectron and diphoton final states with 5.4 fb⁻¹ of data from $p\bar{p}$ collisions at $\sqrt{s}=1.96$ TeV*, *Phys. Rev. Lett.* **104** (2010) 241802, [arXiv:1004.1826 \[hep-ex\]](#).
- [5] T. Ahmed, P. Banerjee, P. K. Dhani, P. Mathews, N. Rana, and V. Ravindran, *Three loop form factors of a massive spin-2 particle with nonuniversal coupling*, *Phys. Rev.* **D95** no. 3, (2017) 034035, [arXiv:1612.00024 \[hep-ph\]](#).
- [6] P. Artoisenet *et al.*, *A framework for Higgs characterisation*, *JHEP* **11** (2013) 043, [arXiv:1306.6464 \[hep-ph\]](#).

- [7] P. Banerjee, P. K. Dhani, M. C. Kumar, P. Mathews, and V. Ravindran, *NNLO QCD corrections to production of a spin-2 particle with non-universal couplings in the DY process*, [arXiv:1710.04184 \[hep-ph\]](#).
- [8] V. Ravindran, J. Smith, and W. L. van Neerven, *QCD threshold corrections to di-lepton and Higgs rapidity distributions beyond N^2 LO*, *Nucl. Phys.* **B767** (2007) 100–129, [arXiv:hep-ph/0608308 \[hep-ph\]](#).
- [9] R. P. Feynman and M. Gell-Mann, *Theory of Fermi interaction*, *Phys. Rev.* **109** (1958) 193–198. [,417(1958)].
- [10] E. C. G. Sudarshan and R. e. Marshak, *Chirality invariance and the universal Fermi interaction*, *Phys. Rev.* **109** (1958) 1860–1860.
- [11] J. S. Schwinger, *A Theory of the Fundamental Interactions*, *Annals Phys.* **2** (1957) 407–434.
- [12] S. L. Glashow, *Partial Symmetries of Weak Interactions*, *Nucl. Phys.* **22** (1961) 579–588.
- [13] J. Goldstone, *Field Theories with Superconductor Solutions*, *Nuovo Cim.* **19** (1961) 154–164.
- [14] S. Weinberg, *A Model of Leptons*, *Phys. Rev. Lett.* **19** (1967) 1264–1266.
- [15] UA1 Collaboration, G. Arnison *et al.*, *Experimental Observation of Isolated Large Transverse Energy Electrons with Associated Missing Energy at $s^{*}(1/2) = 540\text{-GeV}$* , *Phys. Lett.* **122B** (1983) 103–116. [,611(1983)].
- [16] UA2 Collaboration, M. Banner *et al.*, *Observation of Single Isolated Electrons of High Transverse Momentum in Events with Missing Transverse Energy at the CERN anti- p p Collider*, *Phys. Lett.* **122B** (1983) 476–485.

- [17] **ATLAS** Collaboration, G. Aad *et al.*, *Observation of a new particle in the search for the Standard Model Higgs boson with the ATLAS detector at the LHC*, *Phys. Lett. B* **716** (2012) 1–29, [arXiv:1207.7214 \[hep-ex\]](#).
- [18] **CMS** Collaboration, S. Chatrchyan *et al.*, *Observation of a new boson at a mass of 125 GeV with the CMS experiment at the LHC*, *Phys. Lett. B* **716** (2012) 30–61, [arXiv:1207.7235 \[hep-ex\]](#).
- [19] S. Dawson, *Radiative corrections to Higgs boson production*, *Nucl. Phys. B* **359** (1991) 283–300.
- [20] A. Djouadi, M. Spira, and P. M. Zerwas, *Production of Higgs bosons in proton colliders: QCD corrections*, *Phys. Lett. B* **264** (1991) 440–446.
- [21] M. Spira, A. Djouadi, D. Graudenz, and P. M. Zerwas, *Higgs boson production at the LHC*, *Nucl. Phys. B* **453** (1995) 17–82, [arXiv:hep-ph/9504378 \[hep-ph\]](#).
- [22] R. V. Harlander and W. B. Kilgore, *Soft and virtual corrections to proton proton $\rightarrow H + x$ at NNLO*, *Phys. Rev. D* **64** (2001) 013015, [arXiv:hep-ph/0102241 \[hep-ph\]](#).
- [23] S. Catani, D. de Florian, and M. Grazzini, *Higgs production in hadron collisions: Soft and virtual QCD corrections at NNLO*, *JHEP* **05** (2001) 025, [arXiv:hep-ph/0102227 \[hep-ph\]](#).
- [24] V. Ravindran, J. Smith, and W. L. van Neerven, *NNLO corrections to the total cross-section for Higgs boson production in hadron hadron collisions*, *Nucl. Phys. B* **665** (2003) 325–366, [arXiv:hep-ph/0302135 \[hep-ph\]](#).
- [25] C. Anastasiou, K. Melnikov, and F. Petriello, *Higgs boson production at hadron colliders: Differential cross sections through next-to-next-to-leading order*, *Phys. Rev. Lett.* **93** (2004) 262002, [arXiv:hep-ph/0409088 \[hep-ph\]](#).

- [26] S. Catani, D. de Florian, M. Grazzini, and P. Nason, *Soft gluon resummation for Higgs boson production at hadron colliders*, *JHEP* **07** (2003) 028, [arXiv:hep-ph/0306211 \[hep-ph\]](#).
- [27] C. Anastasiou, K. Melnikov, and F. Petriello, *Fully differential Higgs boson production and the di-photon signal through next-to-next-to-leading order*, *Nucl. Phys. B* **724** (2005) 197–246, [arXiv:hep-ph/0501130 \[hep-ph\]](#).
- [28] V. Ravindran, J. Smith, and W. L. van Neerven, *Two-loop corrections to Higgs boson production*, *Nucl. Phys. B* **704** (2005) 332–348, [arXiv:hep-ph/0408315 \[hep-ph\]](#).
- [29] C. Anastasiou, C. Duhr, F. Dulat, F. Herzog, and B. Mistlberger, *Higgs Boson Gluon-Fusion Production in QCD at Three Loops*, *Phys. Rev. Lett.* **114** (2015) 212001, [arXiv:1503.06056 \[hep-ph\]](#).
- [30] T. Ahmed, M. K. Mandal, N. Rana, and V. Ravindran, *Rapidity Distributions in Drell-Yan and Higgs Productions at Threshold to Third Order in QCD*, *Phys. Rev. Lett.* **113** (2014) 212003, [arXiv:1404.6504 \[hep-ph\]](#).
- [31] M. Gell-Mann, *The eightfold way: A theory of strong interaction symmetry*, .
- [32] Y. Ne’eman, *Derivation of strong interactions from a gauge invariance*, *Nucl. Phys.* **26** (1961) 222–229.
- [33] M. Gell-Mann, *A Schematic Model of Baryons and Mesons*, *Phys. Lett.* **8** (1964) 214–215.
- [34] G. Zweig, *An SU(3) model for strong interaction symmetry and its breaking. Version 2*, in *DEVELOPMENTS IN THE QUARK THEORY OF HADRONS. VOL. I. 1964 - 1978*, D. Lichtenberg and S. P. Rosen, eds., pp. 22–101. 1964. <http://inspirehep.net/record/4674/files/cern-th-412.pdf>.

- [35] F. Gursey and L. A. Radicati, *Spin and unitary spin independence of strong interactions*, *Phys. Rev. Lett.* **13** (1964) 173–175.
- [36] W. Pauli, *The Connection Between Spin and Statistics*, *Phys. Rev.* **58** (1940) 716–722.
- [37] O. W. Greenberg, *Spin and Unitary Spin Independence in a Paraquark Model of Baryons and Mesons*, *Phys. Rev. Lett.* **13** (1964) 598–602.
- [38] D. J. Gross and F. Wilczek, *Ultraviolet Behavior of Nonabelian Gauge Theories*, *Phys. Rev. Lett.* **30** (1973) 1343–1346. [,271(1973)].
- [39] H. D. Politzer, *Reliable Perturbative Results for Strong Interactions?*, *Phys. Rev. Lett.* **30** (1973) 1346–1349. [,274(1973)].
- [40] M. Gell-Mann, *The Symmetry group of vector and axial vector currents*, *Physics* **1** (1964) 63–75.
- [41] S. L. Adler, *Sum rules giving tests of local current commutation relations in high-energy neutrino reactions*, *Phys. Rev.* **143** (1966) 1144–1155.
- [42] J. D. Bjorken, *AN INEQUALITY FOR ELECTRON AND MUON SCATTERING FROM NUCLEONS*, *Phys. Rev. Lett.* **16** (1966) 408.
- [43] J. D. Bjorken, *Asymptotic Sum Rules at Infinite Momentum*, *Phys. Rev.* **179** (1969) 1547–1553.
- [44] R. P. Feynman, *Very high-energy collisions of hadrons*, *Phys. Rev. Lett.* **23** (1969) 1415–1417.
- [45] J. H. Christenson, G. S. Hicks, L. M. Lederman, P. J. Limon, B. G. Pope, and E. Zavattini, *Observation of muon pairs in high-energy hadron collisions*, *Phys. Rev.* **D8** (1972) 2016–2034.

- [46] **CDF, D0** Collaboration, T. A. Aaltonen *et al.*, *Combination of CDF and D0 W-Boson Mass Measurements*, *Phys. Rev.* **D88** no. 5, (2013) 052018, [arXiv:1307.7627 \[hep-ex\]](#).
- [47] T. Matsuura, *Higher order corrections to the drell-yan process*. PhD thesis, Leiden U., 1989. <http://inspirehep.net/record/278862/files/Thesis-1989-Matsuura.pdf>.
- [48] J. Badier *et al.*, *Experimental Cross-Section for Dimuon Production and the Drell-Yan Model*, .
- [49] G. Altarelli, R. K. Ellis, and G. Martinelli, *Large Perturbative Corrections to the Drell-Yan Process in QCD*, *Nucl. Phys.* **B157** (1979) 461–497.
- [50] J. Abad and B. Humpert, *Perturbative QCD Corrections in Drell-Yan Processes*, *Phys. Lett.* **80B** (1979) 286–289.
- [51] J. Kubar-Andre and F. E. Paige, *Gluon Corrections to the Drell-Yan Model*, *Phys. Rev.* **D19** (1979) 221.
- [52] B. Humpert and W. L. van Neerven, *Infrared and Mass Regularization in Af Field Theories 2. QCD*, *Nucl. Phys.* **B184** (1981) 225–268.
- [53] J. Kubar, M. Le Bellac, J. L. Meunier, and G. Plaut, *QCD Corrections to the Drell-Yan Mechanism and the Pion Structure Function*, *Nucl. Phys.* **B175** (1980) 251–275.
- [54] R. Hamberg, W. L. van Neerven, and T. Matsuura, *A complete calculation of the order $\alpha - s^2$ correction to the Drell-Yan K factor*, *Nucl. Phys.* **B359** (1991) 343–405. [Erratum: Nucl. Phys.B644,403(2002)].
- [55] **UA2** Collaboration, J. Alitti *et al.*, *Measurement of W and Z Production Cross-sections at the CERN $\bar{p}p$ Collider*, *Z. Phys.* **C47** (1990) 11–22.

- [56] A. Vogt, *Next-to-next-to-leading logarithmic threshold resummation for deep inelastic scattering and the Drell-Yan process*, *Phys. Lett. B* **497** (2001) 228–234, [arXiv:hep-ph/0010146 \[hep-ph\]](#).
- [57] T. Ahmed, M. Mahakhud, N. Rana, and V. Ravindran, *Drell-Yan Production at Threshold to Third Order in QCD*, *Phys. Rev. Lett.* **113** no. 11, (2014) 112002, [arXiv:1404.0366 \[hep-ph\]](#).
- [58] S. Catani, L. Cieri, D. de Florian, G. Ferrera, and M. Grazzini, *Threshold resummation at N^3LL accuracy and soft-virtual cross sections at N^3LO* , *Nucl. Phys. B* **888** (2014) 75–91, [arXiv:1405.4827 \[hep-ph\]](#).
- [59] T. Kinoshita, *Mass singularities of Feynman amplitudes*, *J. Math. Phys.* **3** (1962) 650–677.
- [60] T. D. Lee and M. Nauenberg, *Degenerate Systems and Mass Singularities*, *Phys. Rev.* **133** (1964) B1549–B1562. [,25(1964)].
- [61] J. C. Collins, D. E. Soper, and G. F. Sterman, *Factorization for Short Distance Hadron - Hadron Scattering*, *Nucl. Phys. B* **261** (1985) 104–142.
- [62] V. A. Khoze, A. D. Martin, R. Orava, and M. G. Ryskin, *Luminosity monitors at the LHC*, *Eur. Phys. J. C* **19** (2001) 313–322, [arXiv:hep-ph/0010163 \[hep-ph\]](#).
- [63] T. Kaluza, *Zum Unitätsproblem der Physik*, *Sitzungsber. Preuss. Akad. Wiss. Berlin (Math. Phys.)* **1921** (1921) 966–972, [arXiv:1803.08616 \[physics.hist-ph\]](#).
- [64] O. Klein, *Quantum Theory and Five-Dimensional Theory of Relativity*. (In German and English), *Z. Phys.* **37** (1926) 895–906. [,76(1926)].
- [65] H.-C. Cheng, *Introduction to Extra Dimensions*, in *Physics of the large and the small, TASI 09, proceedings of the Theoretical Advanced Study Institute in*

- Elementary Particle Physics, Boulder, Colorado, USA, 1-26 June 2009*, pp. 125–162. 2011. [arXiv:1003.1162 \[hep-ph\]](#).
<https://inspirehep.net/record/847930/files/arXiv:1003.1162.pdf>.
- [66] N. Arkani-Hamed, S. Dimopoulos, and G. R. Dvali, *The Hierarchy problem and new dimensions at a millimeter*, *Phys. Lett.* **B429** (1998) 263–272, [arXiv:hep-ph/9803315 \[hep-ph\]](#).
- [67] T. Han, J. D. Lykken, and R.-J. Zhang, *On Kaluza-Klein states from large extra dimensions*, *Phys. Rev.* **D59** (1999) 105006, [arXiv:hep-ph/9811350 \[hep-ph\]](#).
- [68] P. Mathews, V. Ravindran, K. Sridhar, and W. L. van Neerven, *Next-to-leading order QCD corrections to the Drell-Yan cross section in models of TeV-scale gravity*, *Nucl. Phys.* **B713** (2005) 333–377, [arXiv:hep-ph/0411018 \[hep-ph\]](#).
- [69] W. E. Caswell, *Asymptotic Behavior of Nonabelian Gauge Theories to Two Loop Order*, *Phys. Rev. Lett.* **33** (1974) 244.
- [70] O. V. Tarasov and A. A. Vladimirov, *Three Loop Calculations in Non-Abelian Gauge Theories*, *Phys. Part. Nucl.* **44** (2013) 791–802, [arXiv:1301.5645 \[hep-ph\]](#).
- [71] S. A. Larin and J. A. M. Vermaseren, *The Three loop QCD Beta function and anomalous dimensions*, *Phys. Lett.* **B303** (1993) 334–336, [arXiv:hep-ph/9302208 \[hep-ph\]](#).
- [72] G. Altarelli and G. Parisi, *Asymptotic Freedom in Parton Language*, *Nucl. Phys.* **B126** (1977) 298–318.

- [73] E. G. Floratos, R. Lacaze, and C. Kounnas, *Space and Timelike Cut Vertices in QCD Beyond the Leading Order. 2. The Singlet Sector*, *Phys. Lett.* **B98** (1981) 285–290.
- [74] E. G. Floratos, R. Lacaze, and C. Kounnas, *Space and Timelike Cut Vertices in QCD Beyond the Leading Order. 1. Nonsinglet Sector*, *Phys. Lett.* **B98** (1981) 89–95.
- [75] G. Curci, W. Furmanski, and R. Petronzio, *Evolution of Parton Densities Beyond Leading Order: The Nonsinglet Case*, *Nucl. Phys.* **B175** (1980) 27–92.
- [76] A. Vogt, S. Moch, and J. Vermaseren, *The three-loop splitting functions in QCD*, *Nucl. Phys. Proc. Suppl.* **152** (2006) 110–115, [arXiv:hep-ph/0407321 \[hep-ph\]](#). [[231\(2004\)](#)].
- [77] G. Altarelli, R. K. Ellis, and G. Martinelli, *Leptonproduction and Drell-Yan Processes Beyond the Leading Approximation in Chromodynamics*, *Nucl. Phys.* **B143** (1978) 521. [Erratum: *Nucl. Phys.* **B146**, 544(1978)].
- [78] T. Matsuura and W. L. van Neerven, *Second Order Logarithmic Corrections to the Drell-Yan Cross-section*, *Z. Phys.* **C38** (1988) 623.
- [79] T. Matsuura, S. C. van der Marck, and W. L. van Neerven, *The Calculation of the Second Order Soft and Virtual Contributions to the Drell-Yan Cross-Section*, *Nucl. Phys.* **B319** (1989) 570.
- [80] C. Anastasiou, L. J. Dixon, K. Melnikov, and F. Petriello, *Dilepton rapidity distribution in the Drell-Yan process at NNLO in QCD*, *Phys. Rev. Lett.* **91** (2003) 182002, [arXiv:hep-ph/0306192 \[hep-ph\]](#).
- [81] C. Anastasiou, L. J. Dixon, K. Melnikov, and F. Petriello, *High precision QCD at hadron colliders: Electroweak gauge boson rapidity distributions at NNLO*, *Phys. Rev.* **D69** (2004) 094008, [arXiv:hep-ph/0312266 \[hep-ph\]](#).

- [82] K. Melnikov and F. Petriello, *The W boson production cross section at the LHC through $O(\alpha_s^2)$* , *Phys. Rev. Lett.* **96** (2006) 231803, [arXiv:hep-ph/0603182 \[hep-ph\]](#).
- [83] K. Melnikov and F. Petriello, *Electroweak gauge boson production at hadron colliders through $O(\alpha(s)^2)$* , *Phys. Rev.* **D74** (2006) 114017, [arXiv:hep-ph/0609070 \[hep-ph\]](#).
- [84] S. Catani, L. Cieri, G. Ferrera, D. de Florian, and M. Grazzini, *Vector boson production at hadron colliders: a fully exclusive QCD calculation at NNLO*, *Phys. Rev. Lett.* **103** (2009) 082001, [arXiv:0903.2120 \[hep-ph\]](#).
- [85] Y. Li, A. von Manteuffel, R. M. Schabinger, and H. X. Zhu, *Soft-virtual corrections to Higgs production at N^3LO* , *Phys. Rev.* **D91** (2015) 036008, [arXiv:1412.2771 \[hep-ph\]](#).
- [86] I. Antoniadis, N. Arkani-Hamed, S. Dimopoulos, and G. R. Dvali, *New dimensions at a millimeter to a Fermi and superstrings at a TeV*, *Phys. Lett.* **B436** (1998) 257–263, [arXiv:hep-ph/9804398 \[hep-ph\]](#).
- [87] N. Arkani-Hamed, S. Dimopoulos, and G. R. Dvali, *Phenomenology, astrophysics and cosmology of theories with submillimeter dimensions and TeV scale quantum gravity*, *Phys. Rev.* **D59** (1999) 086004, [arXiv:hep-ph/9807344 \[hep-ph\]](#).
- [88] L. Randall and R. Sundrum, *A Large mass hierarchy from a small extra dimension*, *Phys. Rev. Lett.* **83** (1999) 3370–3373, [arXiv:hep-ph/9905221 \[hep-ph\]](#).
- [89] P. Mathews and V. Ravindran, *Angular distribution of Drell-Yan process at hadron colliders to NLO-QCD in models of TeV scale gravity*, *Nucl. Phys.* **B753** (2006) 1–15, [arXiv:hep-ph/0507250 \[hep-ph\]](#).

- [90] M. C. Kumar, P. Mathews, and V. Ravindran, *PDF and scale uncertainties of various DY distributions in ADD and RS models at hadron colliders*, *Eur. Phys. J. C* **49** (2007) 599–611, [arXiv:hep-ph/0604135 \[hep-ph\]](#).
- [91] M. C. Kumar, P. Mathews, V. Ravindran, and A. Tripathi, *Diphoton signals in theories with large extra dimensions to NLO QCD at hadron colliders*, *Phys. Lett. B* **672** (2009) 45–50, [arXiv:0811.1670 \[hep-ph\]](#).
- [92] M. C. Kumar, P. Mathews, V. Ravindran, and A. Tripathi, *Direct photon pair production at the LHC to order α_s in TeV scale gravity models*, *Nucl. Phys. B* **818** (2009) 28–51, [arXiv:0902.4894 \[hep-ph\]](#).
- [93] N. Agarwal, V. Ravindran, V. K. Tiwari, and A. Tripathi, *Z boson pair production at the LHC to $O(\alpha(s))$ in TeV scale gravity models*, *Nucl. Phys. B* **830** (2010) 248–270, [arXiv:0909.2651 \[hep-ph\]](#).
- [94] N. Agarwal, V. Ravindran, V. K. Tiwari, and A. Tripathi, *Next-to-leading order QCD corrections to the Z boson pair production at the LHC in Randall Sundrum model*, *Phys. Lett. B* **686** (2010) 244–248, [arXiv:0910.1551 \[hep-ph\]](#).
- [95] N. Agarwal, V. Ravindran, V. K. Tiwari, and A. Tripathi, *W^+W^- production in Large extra dimension model at next-to-leading order in QCD at the LHC*, *Phys. Rev. D* **82** (2010) 036001, [arXiv:1003.5450 \[hep-ph\]](#).
- [96] N. Agarwal, V. Ravindran, V. K. Tiwari, and A. Tripathi, *Next-to-leading order QCD corrections to W^+W^- production at the LHC in Randall Sundrum model*, *Phys. Lett. B* **690** (2010) 390–395, [arXiv:1003.5445 \[hep-ph\]](#).
- [97] R. Frederix, M. K. Mandal, P. Mathews, V. Ravindran, S. Seth, P. Torrielli, and M. Zaro, *Diphoton production in the ADD model to NLO+parton shower accuracy at the LHC*, *JHEP* **12** (2012) 102, [arXiv:1209.6527 \[hep-ph\]](#).

- [98] R. Frederix, M. K. Mandal, P. Mathews, V. Ravindran, and S. Seth, *Drell-Yan, ZZ , W^+W^- production in SM & ADD model to NLO+PS accuracy at the LHC*, *Eur. Phys. J.* **C74** no. 2, (2014) 2745, [arXiv:1307.7013 \[hep-ph\]](#).
- [99] G. Das, P. Mathews, V. Ravindran, and S. Seth, *RS resonance in di-final state production at the LHC to NLO+PS accuracy*, *JHEP* **10** (2014) 188, [arXiv:1408.3970 \[hep-ph\]](#).
- [100] G. Das, C. Degrande, V. Hirschi, F. Maltoni, and H.-S. Shao, *NLO predictions for the production of a (750 GeV) spin-two particle at the LHC*, [arXiv:1605.09359 \[hep-ph\]](#).
- [101] D. de Florian, M. Mahakhud, P. Mathews, J. Mazzitelli, and V. Ravindran, *Next-to-Next-to-Leading Order QCD Corrections in Models of TeV-Scale Gravity*, *JHEP* **04** (2014) 028, [arXiv:1312.7173 \[hep-ph\]](#).
- [102] D. de Florian, M. Mahakhud, P. Mathews, J. Mazzitelli, and V. Ravindran, *Quark and gluon spin-2 form factors to two-loops in QCD*, *JHEP* **02** (2014) 035, [arXiv:1312.6528 \[hep-ph\]](#).
- [103] T. Ahmed, G. Das, P. Mathews, N. Rana, and V. Ravindran, *Spin-2 Form Factors at Three Loop in QCD*, *JHEP* **12** (2015) 084, [arXiv:1508.05043 \[hep-ph\]](#).
- [104] T. Ahmed, M. Mahakhud, P. Mathews, N. Rana, and V. Ravindran, *Two-Loop QCD Correction to massive spin-2 resonance $\rightarrow 3$ gluons*, *JHEP* **05** (2014) 107, [arXiv:1404.0028 \[hep-ph\]](#).
- [105] P. Nogueira, *Automatic Feynman graph generation*, *J.Comput.Phys.* **105** (1993) 279–289.
- [106] J. Vermaseren, *New features of FORM*, [arXiv:math-ph/0010025 \[math-ph\]](#).

- [107] M. Tentyukov and J. Vermaseren, *The Multithreaded version of FORM*, *Comput.Phys.Commun.* **181** (2010) 1419–1427, [arXiv:hep-ph/0702279](#) [HEP-PH].
- [108] F. Tkachov, *A Theorem on Analytical Calculability of Four Loop Renormalization Group Functions*, *Phys.Lett.* **B100** (1981) 65–68.
- [109] K. Chetyrkin and F. Tkachov, *Integration by Parts: The Algorithm to Calculate beta Functions in 4 Loops*, *Nucl.Phys.* **B192** (1981) 159–204.
- [110] T. Gehrmann and E. Remiddi, *Differential equations for two loop four point functions*, *Nucl.Phys.* **B580** (2000) 485–518, [arXiv:hep-ph/9912329](#) [hep-ph].
- [111] R. Lee, *Presenting LiteRed: a tool for the Loop InTEgrals REDuction*, [arXiv:1212.2685](#) [hep-ph].
- [112] R. V. Harlander and W. B. Kilgore, *Next-to-next-to-leading order Higgs production at hadron colliders*, *Phys. Rev. Lett.* **88** (2002) 201801, [arXiv:hep-ph/0201206](#) [hep-ph].
- [113] R. E. Cutkosky, *Singularities and discontinuities of Feynman amplitudes*, *J. Math. Phys.* **1** (1960) 429–433.
- [114] C. Anastasiou, S. Buehler, C. Duhr, and F. Herzog, *NNLO phase space master integrals for two-to-one inclusive cross sections in dimensional regularization*, *JHEP* **11** (2012) 062, [arXiv:1208.3130](#) [hep-ph].
- [115] A. Pak, M. Rogal, and M. Steinhauser, *Production of scalar and pseudo-scalar Higgs bosons to next-to-next-to-leading order at hadron colliders*, *JHEP* **09** (2011) 088, [arXiv:1107.3391](#) [hep-ph].
- [116] M. R. Whalley, D. Bourilkov, and R. C. Group, *The Les Houches accord PDFs (LHAPDF) and LHAGLUE*, in *HERA and the LHC: A Workshop on the*

- implications of HERA for LHC physics. Proceedings, Part B.* 2005.
[arXiv:hep-ph/0508110](#) [hep-ph].
- [117] **ATLAS** Collaboration, G. Aad *et al.*, *Search for contact interactions and large extra dimensions in dilepton events from pp collisions at $\sqrt{s} = 7$ TeV with the ATLAS detector*, *Phys. Rev.* **D87** no. 1, (2013) 015010, [arXiv:1211.1150](#) [hep-ex].
- [118] **CMS** Collaboration, S. Chatrchyan *et al.*, *Search for large extra dimensions in dimuon and dielectron events in pp collisions at $\sqrt{s} = 7$ TeV*, *Phys. Lett.* **B711** (2012) 15–34, [arXiv:1202.3827](#) [hep-ex].
- [119] **ATLAS** Collaboration, G. Aad *et al.*, *Search for contact interactions and large extra dimensions in the dilepton channel using proton-proton collisions at $\sqrt{s} = 8$ TeV with the ATLAS detector*, *Eur. Phys. J.* **C74** no. 12, (2014) 3134, [arXiv:1407.2410](#) [hep-ex].
- [120] **CMS** Collaboration, V. Khachatryan *et al.*, *Search for physics beyond the standard model in dilepton mass spectra in proton-proton collisions at $\sqrt{s} = 8$ TeV*, *JHEP* **04** (2015) 025, [arXiv:1412.6302](#) [hep-ex].
- [121] **CMS** Collaboration, V. Khachatryan *et al.*, *Search for narrow resonances in dilepton mass spectra in proton-proton collisions at $\sqrt{s} = 13$ TeV and combination with 8 TeV data*, [arXiv:1609.05391](#) [hep-ex].
- [122] T. Ahmed, M. C. Kumar, P. Mathews, N. Rana, and V. Ravindran, *Pseudo-scalar Higgs Boson Production at Threshold N^3 LO and N^3 LL QCD, To be appeared in EPJC* (2016) , [arXiv:1510.02235](#) [hep-ph].
- [123] J. Ellis, R. Fok, D. S. Hwang, V. Sanz, and T. You, *Distinguishing 'Higgs' spin hypotheses using $\gamma\gamma$ and WW^* decays*, *Eur. Phys. J.* **C73** (2013) 2488, [arXiv:1210.5229](#) [hep-ph].

- [124] J. Ellis, V. Sanz, and T. You, *Prima Facie Evidence against Spin-Two Higgs Impostors*, *Phys. Lett.* **B726** (2013) 244–250, [arXiv:1211.3068 \[hep-ph\]](#).
- [125] J. Ellis, V. Sanz, and T. You, *Associated Production Evidence against Higgs Impostors and Anomalous Couplings*, *Eur. Phys. J.* **C73** (2013) 2507, [arXiv:1303.0208 \[hep-ph\]](#).
- [126] **D0** Collaboration, V. M. Abazov *et al.*, *Search for Randall-Sundrum gravitons in dilepton and diphoton final states*, *Phys. Rev. Lett.* **95** (2005) 091801, [arXiv:hep-ex/0505018 \[hep-ex\]](#).
- [127] **CDF** Collaboration, T. Aaltonen *et al.*, *Search for Randall-Sundrum Gravitons in the Diphoton Channel at CDF*, *Phys. Rev.* **D83** (2011) 011102, [arXiv:1012.2795 \[hep-ex\]](#).
- [128] **ATLAS** Collaboration, G. Aad *et al.*, *Measurement of the isolated di-photon cross-section in pp collisions at $\sqrt{s} = 7$ TeV with the ATLAS detector*, *Phys. Rev.* **D85** (2012) 012003, [arXiv:1107.0581 \[hep-ex\]](#).
- [129] **CDF** Collaboration, T. Aaltonen *et al.*, *Search for New Dielectron Resonances and Randall-Sundrum Gravitons at the Collider Detector at Fermilab*, *Phys. Rev. Lett.* **107** (2011) 051801, [arXiv:1103.4650 \[hep-ex\]](#).
- [130] **CMS** Collaboration, S. Chatrchyan *et al.*, *Search for Resonances in the Dilepton Mass Distribution in pp Collisions at $\sqrt{s} = 7$ TeV*, *JHEP* **05** (2011) 093, [arXiv:1103.0981 \[hep-ex\]](#).
- [131] **CMS** Collaboration, S. Chatrchyan *et al.*, *Search for signatures of extra dimensions in the diphoton mass spectrum at the Large Hadron Collider*, *Phys. Rev. Lett.* **108** (2012) 111801, [arXiv:1112.0688 \[hep-ex\]](#).

- [132] **ATLAS** Collaboration, G. Aad *et al.*, *Search for extra dimensions using diphoton events in 7 TeV proton-proton collisions with the ATLAS detector*, *Phys. Lett. B* **710** (2012) 538–556, [arXiv:1112.2194 \[hep-ex\]](#).
- [133] **ATLAS** Collaboration, G. Aad *et al.*, *Search for Extra Dimensions in diphoton events using proton-proton collisions recorded at $\sqrt{s} = 7$ TeV with the ATLAS detector at the LHC*, *New J. Phys.* **15** (2013) 043007, [arXiv:1210.8389 \[hep-ex\]](#).
- [134] S. Moch, J. A. M. Vermaseren, and A. Vogt, *Three-loop results for quark and gluon form-factors*, *Phys. Lett. B* **625** (2005) 245–252, [arXiv:hep-ph/0508055 \[hep-ph\]](#).
- [135] S. Moch, J. A. M. Vermaseren, and A. Vogt, *The Quark form-factor at higher orders*, *JHEP* **08** (2005) 049, [arXiv:hep-ph/0507039 \[hep-ph\]](#).
- [136] P. A. Baikov, K. G. Chetyrkin, A. V. Smirnov, V. A. Smirnov, and M. Steinhauser, *Quark and gluon form factors to three loops*, *Phys. Rev. Lett.* **102** (2009) 212002, [arXiv:0902.3519 \[hep-ph\]](#).
- [137] T. Gehrmann, E. W. N. Glover, T. Huber, N. Ikizlerli, and C. Studerus, *Calculation of the quark and gluon form factors to three loops in QCD*, *JHEP* **06** (2010) 094.
- [138] T. Gehrmann and D. Kara, *The $Hb\bar{b}$ form factor to three loops in QCD*, *JHEP* **09** (2014) 174, [arXiv:1407.8114 \[hep-ph\]](#).
- [139] T. Ahmed, T. Gehrmann, P. Mathews, N. Rana, and V. Ravindran, *Pseudo-scalar Form Factors at Three Loops in QCD*, *JHEP* **11** (2015) 169, [arXiv:1510.01715 \[hep-ph\]](#).
- [140] N. K. Nielsen, *The Energy Momentum Tensor in a Nonabelian Quark Gluon Theory*, *Nucl. Phys. B* **120** (1977) 212–220.

- [141] S. D. Joglekar and B. W. Lee, *General Theory of Renormalization of Gauge Invariant Operators*, *Annals Phys.* **97** (1976) 160.
- [142] S. Catani, *The Singular behavior of QCD amplitudes at two loop order*, *Phys. Lett.* **B427** (1998) 161–171, [arXiv:hep-ph/9802439](#) [hep-ph].
- [143] G. F. Sterman and M. E. Tejeda-Yeomans, *Multiloop amplitudes and resummation*, *Phys. Lett.* **B552** (2003) 48–56, [arXiv:hep-ph/0210130](#) [hep-ph].
- [144] T. Becher and M. Neubert, *Infrared singularities of scattering amplitudes in perturbative QCD*, *Phys. Rev. Lett.* **102** (2009) 162001, [arXiv:0901.0722](#) [hep-ph]. [Erratum: *Phys. Rev. Lett.* 111, no. 19, 199905 (2013)].
- [145] E. Gardi and L. Magnea, *Factorization constraints for soft anomalous dimensions in QCD scattering amplitudes*, *JHEP* **03** (2009) 079, [arXiv:0901.1091](#) [hep-ph].
- [146] V. Ravindran, *On Sudakov and soft resummations in QCD*, *Nucl. Phys.* **B746** (2006) 58–76, [arXiv:hep-ph/0512249](#) [hep-ph].
- [147] V. V. Sudakov, *Vertex parts at very high-energies in quantum electrodynamics*, *Sov. Phys. JETP* **3** (1956) 65–71. [*Zh. Eksp. Teor. Fiz.* 30, 87 (1956)].
- [148] A. H. Mueller, *On the Asymptotic Behavior of the Sudakov Form-factor*, *Phys. Rev.* **D20** (1979) 2037.
- [149] J. C. Collins, *Algorithm to Compute Corrections to the Sudakov Form-factor*, *Phys. Rev.* **D22** (1980) 1478.
- [150] A. Sen, *Asymptotic Behavior of the Sudakov Form-Factor in QCD*, *Phys. Rev.* **D24** (1981) 3281.
- [151] V. Ravindran, *Higher-order threshold effects to inclusive processes in QCD*, *Nucl. Phys.* **B752** (2006) 173–196, [arXiv:hep-ph/0603041](#) [hep-ph].

- [152] S. Moch, J. A. M. Vermaseren, and A. Vogt, *The Three loop splitting functions in QCD: The Nonsinglet case*, *Nucl. Phys.* **B688** (2004) 101–134, [arXiv:hep-ph/0403192](#) [hep-ph].
- [153] A. Vogt, S. Moch, and J. A. M. Vermaseren, *The Three-loop splitting functions in QCD: The Singlet case*, *Nucl. Phys.* **B691** (2004) 129–181, [arXiv:hep-ph/0404111](#) [hep-ph].
- [154] S. Catani and L. Trentadue, *Resummation of the QCD Perturbative Series for Hard Processes*, *Nucl. Phys.* **B327** (1989) 323–352.
- [155] S. Catani and L. Trentadue, *Comment on QCD exponentiation at large x* , *Nucl. Phys.* **B353** (1991) 183–186.
- [156] T. Ahmed, N. Rana, and V. Ravindran, *Higgs boson production through $b\bar{b}$ annihilation at threshold in N^3LO QCD*, *JHEP* **10** (2014) 139, [arXiv:1408.0787](#) [hep-ph].
- [157] T. Ahmed, P. Banerjee, P. K. Dhani, N. Rana, V. Ravindran, and S. Seth, *Konishi Form Factor at Three Loop in $\mathcal{N} = 4$ SYM*, [arXiv:1610.05317](#) [hep-th].
- [158] S. Laporta, *High precision calculation of multiloop Feynman integrals by difference equations*, *Int. J. Mod. Phys.* **A15** (2000) 5087–5159, [arXiv:hep-ph/0102033](#) [hep-ph].
- [159] C. Anastasiou and A. Lazopoulos, *Automatic integral reduction for higher order perturbative calculations*, *JHEP* **07** (2004) 046.
- [160] A. V. Smirnov, *Algorithm FIRE – Feynman Integral REDuction*, *JHEP* **10** (2008) 107.
- [161] A. von Manteuffel and C. Studerus, *Reduze 2 - Distributed Feynman Integral Reduction*, [arXiv:1201.4330](#) [hep-ph].

- [162] C. Studerus, *Reduze-Feynman Integral Reduction in C++*, *Comput. Phys. Commun.* **181** (2010) 1293–1300.
- [163] R. N. Lee, *LiteRed 1.4: a powerful tool for reduction of multiloop integrals*, *J.Phys.Conf.Ser.* **523** (2014) 012059.
- [164] T. Gehrmann, T. Huber, and D. Maitre, *Two-loop quark and gluon form-factors in dimensional regularisation*, *Phys. Lett.* **B622** (2005) 295–302.
- [165] T. Gehrmann, G. Heinrich, T. Huber, and C. Studerus, *Master integrals for massless three-loop form-factors: One-loop and two-loop insertions*, *Phys. Lett.* **B640** (2006) 252–259.
- [166] G. Heinrich, T. Huber, and D. Maitre, *Master integrals for fermionic contributions to massless three-loop form-factors*, *Phys. Lett.* **B662** (2008) 344–352.
- [167] G. Heinrich, T. Huber, D. A. Kosower, and V. A. Smirnov, *Nine-Propagator Master Integrals for Massless Three-Loop Form Factors*, *Phys. Lett.* **B678** (2009) 359–366.
- [168] R. N. Lee, A. V. Smirnov, and V. A. Smirnov, *Analytic Results for Massless Three-Loop Form Factors*, *JHEP* **04** (2010) 020.
- [169] C. Anastasiou, Z. Bern, L. J. Dixon, and D. A. Kosower, *Planar amplitudes in maximally supersymmetric Yang-Mills theory*, *Phys. Rev. Lett.* **91** (2003) 251602.
- [170] Z. Bern, L. J. Dixon, and V. A. Smirnov, *Iteration of planar amplitudes in maximally supersymmetric Yang-Mills theory at three loops and beyond*, *Phys. Rev.* **D72** (2005) 085001, [arXiv:hep-th/0505205](#) [hep-th].
- [171] A. V. Kotikov, L. N. Lipatov, A. I. Onishchenko, and V. N. Velizhanin, *Three loop universal anomalous dimension of the Wilson operators in $N = 4$ SUSY Yang-Mills model*, *Phys. Lett.* **B595** (2004) 521–529, [arXiv:hep-th/0404092](#) [hep-th]. [Erratum: *Phys. Lett.* **B632**, 754(2006)].

- [172] A. V. Kotikov and L. N. Lipatov, *On the highest transcendentality in $N=4$ SUSY*, *Nucl. Phys.* **B769** (2007) 217–255, [arXiv:hep-th/0611204 \[hep-th\]](#).
- [173] A. V. Kotikov and L. N. Lipatov, *DGLAP and BFKL evolution equations in the $N=4$ supersymmetric gauge theory*, in *35th Annual Winter School on Nuclear and Particle Physics Repino, Russia, February 19-25, 2001*. 2001.
[arXiv:hep-ph/0112346 \[hep-ph\]](#).
<http://alice.cern.ch/format/showfull?sysnb=2289957>.
- [174] A. V. Kotikov and L. N. Lipatov, *NLO corrections to the BFKL equation in QCD and in supersymmetric gauge theories*, *Nucl. Phys.* **B582** (2000) 19–43,
[arXiv:hep-ph/0004008 \[hep-ph\]](#).
- [175] A. V. Kotikov and L. N. Lipatov, *DGLAP and BFKL equations in the $N = 4$ supersymmetric gauge theory*, *Nucl. Phys.* **B661** (2003) 19–61,
[arXiv:hep-ph/0208220 \[hep-ph\]](#). [Erratum: *Nucl. Phys.*B685,405(2004)].
- [176] Z. Bern, M. Czakon, L. J. Dixon, D. A. Kosower, and V. A. Smirnov, *The Four-Loop Planar Amplitude and Cusp Anomalous Dimension in Maximally Supersymmetric Yang-Mills Theory*, *Phys. Rev.* **D75** (2007) 085010,
[arXiv:hep-th/0610248 \[hep-th\]](#).
- [177] S. G. Naculich, H. Nastase, and H. J. Schnitzer, *Subleading-color contributions to gluon-gluon scattering in $N=4$ SYM theory and relations to $N=8$ supergravity*, *JHEP* **11** (2008) 018, [arXiv:0809.0376 \[hep-th\]](#).
- [178] L. V. Bork, D. I. Kazakov, and G. S. Vartanov, *On form factors in $N=4$ sym*, *JHEP* **02** (2011) 063, [arXiv:1011.2440 \[hep-th\]](#).
- [179] A. Brandhuber, G. Travaglini, and G. Yang, *Analytic two-loop form factors in $N=4$ SYM*, *JHEP* **05** (2012) 082, [arXiv:1201.4170 \[hep-th\]](#).

- [180] B. Eden, *Three-loop universal structure constants in $N=4$ susy Yang-Mills theory*, [arXiv:1207.3112 \[hep-th\]](#).
- [181] J. M. Drummond, J. Henn, G. P. Korchemsky, and E. Sokatchev, *On planar gluon amplitudes/Wilson loops duality*, *Nucl. Phys.* **B795** (2008) 52–68, [arXiv:0709.2368 \[hep-th\]](#).
- [182] J. Drummond, C. Duhr, B. Eden, P. Heslop, J. Pennington, and V. A. Smirnov, *Leading singularities and off-shell conformal integrals*, *JHEP* **08** (2013) 133, [arXiv:1303.6909 \[hep-th\]](#).
- [183] T. Gehrmann, J. M. Henn, and T. Huber, *The three-loop form factor in $N=4$ super Yang-Mills*, *JHEP* **03** (2012) 101, [arXiv:1112.4524 \[hep-th\]](#).
- [184] T. Gehrmann, M. Jaquier, E. W. N. Glover, and A. Koukoutsakis, *Two-Loop QCD Corrections to the Helicity Amplitudes for $H \rightarrow 3$ partons*, *JHEP* **02** (2012) 056, [arXiv:1112.3554 \[hep-ph\]](#).
- [185] R. N. Lee and V. A. Smirnov, *Analytic Epsilon Expansions of Master Integrals Corresponding to Massless Three-Loop Form Factors and Three-Loop $g-2$ up to Four-Loop Transcendentality Weight*, *JHEP* **02** (2011) 102, [arXiv:1010.1334 \[hep-ph\]](#).
- [186] G. Degrandi, S. Di Vita, J. Elias-Miro, J. R. Espinosa, G. F. Giudice, G. Isidori, and A. Strumia, *Higgs mass and vacuum stability in the Standard Model at NNLO*, *JHEP* **08** (2012) 098, [arXiv:1205.6497 \[hep-ph\]](#).
- [187] T. Ahmed, G. Das, P. Mathews, N. Rana, and V. Ravindran, *The two-loop QCD correction to massive spin-2 resonance $\rightarrow q\bar{q}g$* , *Eur. Phys. J.* **C76** no. 12, (2016) 667, [arXiv:1608.05906 \[hep-ph\]](#).

- [188] CMS Collaboration, V. Khachatryan *et al.*, *Search for high-mass diphoton resonances in proton–proton collisions at 13 TeV and combination with 8 TeV search*, *Phys. Lett. B* **767** (2017) 147–170, [arXiv:1609.02507 \[hep-ex\]](#).
- [189] ATLAS Collaboration, M. Aaboud *et al.*, *Search for diboson resonances with boson-tagged jets in pp collisions at $\sqrt{s} = 13$ TeV with the ATLAS detector*, [arXiv:1708.04445 \[hep-ex\]](#).
- [190] ATLAS Collaboration, G. Aad *et al.*, *Study of the spin and parity of the Higgs boson in diboson decays with the ATLAS detector*, *Eur. Phys. J. C* **75** no. 10, (2015) 476, [arXiv:1506.05669 \[hep-ex\]](#). [Erratum: *Eur. Phys. J. C* **76**, no. 3, 152 (2016)].
- [191] L. E. Pedersen, *Probing the nature of the Higgs Boson: A study of the Higgs spin and parity through the $ZZ^* \rightarrow 4l$ final state at the ATLAS Experiment*. PhD thesis, Bohr Inst., 2015. http://discoverycenter.nbi.ku.dk/teaching/thesis_page/PhDThesis.pdf.
- [192] A. Falkowski and J. F. Kamenik, *Diphoton portal to warped gravity*, *Phys. Rev. D* **94** no. 1, (2016) 015008, [arXiv:1603.06980 \[hep-ph\]](#).
- [193] J. Davies, A. Vogt, B. Ruijl, T. Ueda, and J. A. M. Vermaseren, *Large- n_f contributions to the four-loop splitting functions in QCD*, *Nucl. Phys. B* **915** (2017) 335–362, [arXiv:1610.07477 \[hep-ph\]](#).
- [194] K. G. Chetyrkin, B. A. Kniehl, and M. Steinhauser, *Decoupling relations to $O(\alpha_s^3)$ and their connection to low-energy theorems*, *Nucl. Phys. B* **510** (1998) 61–87, [arXiv:hep-ph/9708255 \[hep-ph\]](#).
- [195] T. van Ritbergen, J. A. M. Vermaseren, and S. A. Larin, *The Four loop beta function in quantum chromodynamics*, *Phys. Lett. B* **400** (1997) 379–384, [arXiv:hep-ph/9701390 \[hep-ph\]](#).

- [196] O. V. Tarasov, *ANOMALOUS DIMENSIONS OF QUARK MASSES IN THREE LOOP APPROXIMATION*, .
- [197] M. Czakon, *The Four-loop QCD beta-function and anomalous dimensions*, *Nucl. Phys.* **B710** (2005) 485–498, [arXiv:hep-ph/0411261](#) [hep-ph].
- [198] R. V. Harlander and W. B. Kilgore, *Higgs boson production in bottom quark fusion at next-to-next-to leading order*, *Phys. Rev.* **D68** (2003) 013001, [arXiv:hep-ph/0304035](#) [hep-ph].
- [199] Y. Li, A. von Manteuffel, R. M. Schabinger, and H. X. Zhu, *N^3 LO Higgs boson and Drell-Yan production at threshold: The one-loop two-emission contribution*, *Phys. Rev.* **D90** no. 5, (2014) 053006, [arXiv:1404.5839](#) [hep-ph].
- [200] S. Dittmaier and M. Kramer, 1, *Electroweak radiative corrections to W boson production at hadron colliders*, *Phys. Rev.* **D65** (2002) 073007, [arXiv:hep-ph/0109062](#) [hep-ph].
- [201] U. Baur, O. Brein, W. Hollik, C. Schappacher, and D. Wackeroth, *Electroweak radiative corrections to neutral current Drell-Yan processes at hadron colliders*, *Phys. Rev.* **D65** (2002) 033007, [arXiv:hep-ph/0108274](#) [hep-ph].
- [202] R. Gavin, Y. Li, F. Petriello, and S. Quackenbush, *W Physics at the LHC with FEWZ 2.1*, *Comput. Phys. Commun.* **184** (2013) 208–214, [arXiv:1201.5896](#) [hep-ph].
- [203] V. Ravindran and J. Smith, *Threshold corrections to rapidity distributions of Z and W^\pm bosons beyond N^2 LO at hadron colliders*, *Phys. Rev.* **D76** (2007) 114004, [arXiv:0708.1689](#) [hep-ph].
- [204] Y. Li and F. Petriello, *Combining QCD and electroweak corrections to dilepton production in FEWZ*, *Phys. Rev.* **D86** (2012) 094034, [arXiv:1208.5967](#) [hep-ph].

- [205] S. Frixione and B. R. Webber, *Matching NLO QCD computations and parton shower simulations*, *JHEP* **06** (2002) 029, [arXiv:hep-ph/0204244 \[hep-ph\]](#).
- [206] S. Frixione, P. Nason, and C. Oleari, *Matching NLO QCD computations with Parton Shower simulations: the POWHEG method*, *JHEP* **11** (2007) 070, [arXiv:0709.2092 \[hep-ph\]](#).
- [207] J. Alwall, R. Frederix, S. Frixione, V. Hirschi, F. Maltoni, O. Mattelaer, H. S. Shao, T. Stelzer, P. Torrielli, and M. Zaro, *The automated computation of tree-level and next-to-leading order differential cross sections, and their matching to parton shower simulations*, *JHEP* **07** (2014) 079, [arXiv:1405.0301 \[hep-ph\]](#).
- [208] R. K. Ellis, G. Martinelli, and R. Petronzio, *Lepton Pair Production at Large Transverse Momentum in Second Order QCD*, *Nucl. Phys.* **B211** (1983) 106–138.
- [209] P. B. Arnold and M. H. Reno, *The Complete Computation of High p_T W and Z Production in 2nd Order QCD*, *Nucl. Phys.* **B319** (1989) 37–71. [Erratum: Nucl. Phys. B330,284(1990)].
- [210] R. J. Gonsalves, J. Pawlowski, and C.-F. Wai, *QCD Radiative Corrections to Electroweak Boson Production at Large Transverse Momentum in Hadron Collisions*, *Phys. Rev.* **D40** (1989) 2245.
- [211] E. Mirkes, *Angular decay distribution of leptons from W bosons at NLO in hadronic collisions*, *Nucl. Phys.* **B387** (1992) 3–85.
- [212] E. Mirkes and J. Ohnemus, *Angular distributions of Drell-Yan lepton pairs at the Tevatron: Order $\alpha - s^2$ corrections and Monte Carlo studies*, *Phys. Rev.* **D51** (1995) 4891–4904, [arXiv:hep-ph/9412289 \[hep-ph\]](#).
- [213] A. Accardi *et al.*, *A Critical Appraisal and Evaluation of Modern PDFs*, *Eur. Phys. J.* **C76** no. 8, (2016) 471, [arXiv:1603.08906 \[hep-ph\]](#).

- [214] G. F. Sterman, *Summation of Large Corrections to Short Distance Hadronic Cross-Sections*, *Nucl. Phys.* **B281** (1987) 310–364.
- [215] J. C. Collins, D. E. Soper, and G. F. Sterman, *Transverse Momentum Distribution in Drell-Yan Pair and W and Z Boson Production*, *Nucl. Phys.* **B250** (1985) 199–224.
- [216] S. Catani, D. de Florian, and M. Grazzini, *Universality of nonleading logarithmic contributions in transverse momentum distributions*, *Nucl. Phys.* **B596** (2001) 299–312, [arXiv:hep-ph/0008184 \[hep-ph\]](#).
- [217] A. Idilbi and X.-d. Ji, *Threshold resummation for Drell-Yan process in soft-collinear effective theory*, *Phys. Rev.* **D72** (2005) 054016, [arXiv:hep-ph/0501006 \[hep-ph\]](#).
- [218] T. Becher and M. Neubert, *Drell-Yan Production at Small q_T , Transverse Parton Distributions and the Collinear Anomaly*, *Eur. Phys. J.* **C71** (2011) 1665, [arXiv:1007.4005 \[hep-ph\]](#).
- [219] D. Westmark and J. F. Owens, *Enhanced threshold resummation formalism for lepton pair production and its effects in the determination of parton distribution functions*, *Phys. Rev.* **D95** no. 5, (2017) 056024, [arXiv:1701.06716 \[hep-ph\]](#).
- [220] E. Laenen and G. F. Sterman, *Resummation for Drell-Yan differential distributions*, in *The Fermilab Meeting DPF 92. Proceedings, 7th Meeting of the American Physical Society, Division of Particles and Fields, Batavia, USA, November 10-14, 1992. Vol. 1, 2*, pp. 987–989. 1992. http://lss.fnal.gov/cgi-bin/find_paper.pl?conf-92-359.
- [221] G. F. Sterman and W. Vogelsang, *Threshold resummation and rapidity dependence*, *JHEP* **02** (2001) 016, [arXiv:hep-ph/0011289 \[hep-ph\]](#).

- [222] A. Mukherjee and W. Vogelsang, *Threshold resummation for W-boson production at RHIC*, *Phys. Rev.* **D73** (2006) 074005, [arXiv:hep-ph/0601162](#) [hep-ph].
- [223] P. Bolzoni, *Threshold resummation of Drell-Yan rapidity distributions*, *Phys. Lett.* **B643** (2006) 325–330, [arXiv:hep-ph/0609073](#) [hep-ph].
- [224] M. Bonvini, S. Forte, G. Ridolfi, and L. Rottoli, *Resummation prescriptions and ambiguities in SCET vs. direct QCD: Higgs production as a case study*, *JHEP* **01** (2015) 046, [arXiv:1409.0864](#) [hep-ph].
- [225] T. Becher and M. Neubert, *Threshold resummation in momentum space from effective field theory*, *Phys. Rev. Lett.* **97** (2006) 082001, [arXiv:hep-ph/0605050](#) [hep-ph].
- [226] T. Becher, M. Neubert, and G. Xu, *Dynamical Threshold Enhancement and Resummation in Drell-Yan Production*, *JHEP* **07** (2008) 030, [arXiv:0710.0680](#) [hep-ph].
- [227] M. Bonvini, S. Forte, and G. Ridolfi, *Soft gluon resummation of Drell-Yan rapidity distributions: Theory and phenomenology*, *Nucl. Phys.* **B847** (2011) 93–159, [arXiv:1009.5691](#) [hep-ph].
- [228] T. Ahmed, M. K. Mandal, N. Rana, and V. Ravindran, *Higgs Rapidity Distribution in $b\bar{b}$ Annihilation at Threshold in N^3LO QCD*, *JHEP* **02** (2015) 131, [arXiv:1411.5301](#) [hep-ph].
- [229] P. Banerjee, G. Das, P. K. Dhani, and V. Ravindran, *Threshold resummation of the rapidity distribution for Higgs production at NNLO+NNLL*, *Phys. Rev.* **D97** no. 5, (2018) 054024, [arXiv:1708.05706](#) [hep-ph].
- [230] L. A. Harland-Lang, A. D. Martin, P. Motylinski, and R. S. Thorne, *Parton distributions in the LHC era: MMHT 2014 PDFs*, *Eur. Phys. J.* **C75** no. 5, (2015) 204, [arXiv:1412.3989](#) [hep-ph].

- [231] A. Buckley, J. Ferrando, S. Lloyd, K. Nordström, B. Page, M. Rüfenacht, M. Schönherr, and G. Watt, *LHAPDF6: parton density access in the LHC precision era*, *Eur. Phys. J.* **C75** (2015) 132, [arXiv:1412.7420 \[hep-ph\]](#).
- [232] <http://www.slac.stanford.edu/~lance/Vrap>.
- [233] S. Catani, M. L. Mangano, P. Nason, and L. Trentadue, *The Resummation of soft gluons in hadronic collisions*, *Nucl. Phys.* **B478** (1996) 273–310, [arXiv:hep-ph/9604351 \[hep-ph\]](#).
- [234] D. P. Anderle, F. Ringer, and W. Vogelsang, *QCD resummation for semi-inclusive hadron production processes*, *Phys. Rev.* **D87** no. 3, (2013) 034014, [arXiv:1212.2099 \[hep-ph\]](#).
- [235] M. A. Ebert, J. K. L. Michel, and F. J. Tackmann, *Resummation Improved Rapidity Spectrum for Gluon Fusion Higgs Production*, *JHEP* **05** (2017) 088, [arXiv:1702.00794 \[hep-ph\]](#).
- [236] <https://www.ge.infn.it/bonvini/redy>.
- [237] R. D. Ball, L. Del Debbio, S. Forte, A. Guffanti, J. I. Latorre, J. Rojo, and M. Ubiali, *A first unbiased global NLO determination of parton distributions and their uncertainties*, *Nucl. Phys.* **B838** (2010) 136–206, [arXiv:1002.4407 \[hep-ph\]](#).
- [238] S. Alekhin, J. Blümlein, S. Moch, and R. Placakyte, *Parton Distribution Functions, α_s and Heavy-Quark Masses for LHC Run II*, *Phys. Rev.* **D96** no. 1, (2017) 014011, [arXiv:1701.05838 \[hep-ph\]](#).
- [239] NNPDF Collaboration, R. D. Ball *et al.*, *Parton distributions from high-precision collider data*, *Eur. Phys. J.* **C77** no. 10, (2017) 663, [arXiv:1706.00428 \[hep-ph\]](#).

- [240] J. Butterworth *et al.*, *PDF4LHC recommendations for LHC Run II*, *J. Phys.* **G43** (2016) 023001, [arXiv:1510.03865 \[hep-ph\]](#).
- [241] <https://www2.pv.infn.it/~hepcomplex/horace.html>.
- [242] S. Alioli *et al.*, *Precision studies of observables in $pp \rightarrow W \rightarrow lv_l$ and $pp \rightarrow \gamma, Z \rightarrow l^+l^-$ processes at the LHC*, *Eur. Phys. J.* **C77** no. 5, (2017) 280, [arXiv:1606.02330 \[hep-ph\]](#).
- [243] C. M. Carloni Calame, G. Montagna, O. Nicrosini, and A. Vicini, *Precision electroweak calculation of the production of a high transverse-momentum lepton pair at hadron colliders*, *JHEP* **10** (2007) 109, [arXiv:0710.1722 \[hep-ph\]](#).
- [244] C. M. Carloni Calame, G. Montagna, O. Nicrosini, and M. Treccani, *Multiple photon corrections to the neutral-current Drell-Yan process*, *JHEP* **05** (2005) 019, [arXiv:hep-ph/0502218 \[hep-ph\]](#).
- [245] CMS Collaboration, V. Khachatryan *et al.*, *Measurements of differential and double-differential Drell-Yan cross sections in proton-proton collisions at 8 TeV*, *Eur. Phys. J.* **C75** no. 4, (2015) 147, [arXiv:1412.1115 \[hep-ex\]](#).
- [246] CDF Collaboration, T. Affolder *et al.*, *Measurement of $d(\sigma)/dy$ for high mass Drell-Yan e^+e^- pairs from $p\bar{p}$ collisions at $\sqrt{s} = 1.8$ TeV*, *Phys. Rev.* **D63** (2001) 011101, [arXiv:hep-ex/0006025 \[hep-ex\]](#).
- [247] CDF Collaboration, T. A. Aaltonen *et al.*, *Measurement of $d\sigma/dy$ of Drell-Yan e^+e^- pairs in the Z Mass Region from $p\bar{p}$ Collisions at $\sqrt{s} = 1.96$ TeV*, *Phys. Lett.* **B692** (2010) 232–239, [arXiv:0908.3914 \[hep-ex\]](#).
- [248] NuSea Collaboration, R. S. Towell *et al.*, *Improved measurement of the anti-d / anti-u asymmetry in the nucleon sea*, *Phys. Rev.* **D64** (2001) 052002, [arXiv:hep-ex/0103030 \[hep-ex\]](#).

- [249] J. C. Webb, *Measurement of continuum dimuon production in 800-GeV/C proton nucleon collisions*. PhD thesis, New Mexico State U., 2003.
[arXiv:hep-ex/0301031 \[hep-ex\]](#).
http://lss.fnal.gov/cgi-bin/find_paper.pl?thesis-2002-56.
- [250] A. Idilbi, X.-d. Ji, and F. Yuan, *Resummation of threshold logarithms in effective field theory for DIS, Drell-Yan and Higgs production*, *Nucl. Phys.* **B753** (2006) 42–68, [arXiv:hep-ph/0605068 \[hep-ph\]](#).